MARINE INVERTEBRATE AND BACTERIAL EXTRACT LIBRARY SCREENS FOR NOVEL MODULATORS OF THE GLUCAGON-LIKE PEPTIDE-1 AND GLUCOSE-DEPENDENT INSULINOTROPIC POLYPEPTIDE RECEPTORS

by

Catherine Merchant

B.Sc. (Honours), The University of British Columbia, 2009

A THESIS SUBMITTED IN PARTIAL FULFILLMENT OF

THE REQUIREMENTS FOR THE DEGREE OF

MASTER OF SCIENCE

in

THE FACULTY OF GRADUATE STUDIES

(Cell and Developmental Biology)

THE UNIVERSITY OF BRITISH COLUMBIA

(Vancouver)

June 2011

Abstract

Type 2 diabetes is often associated with obesity and is characterized by high blood-glucose levels due to inadequate insulin secretion and/or action. One current treatment for type 2 diabetes and the associated obesity involves multiple daily injections of a peptide-drug targeting the glucagon-like peptide-1 receptor (GLP-1R). GLP-1R activation stimulates glucose-dependent insulin secretion from β-cells, inhibits glucose-dependent glucagon (GCG) secretion from α-cells, slows gastric emptying and suppresses appetite, which normalizes blood-glucose levels and causes weight loss. Another hormone involved in glucose and fat metabolism, glucose-dependent insulinotropic polypeptide (GIP), stimulates glucose-dependent insulin secretion from β-cells and the storage of fat in adipocytes. As such, both GIP receptor (GIPR) agonists and antagonists have been demonstrated to display therapeutic potential to treat diabetes and obesity. However, glucagon-like peptide-1 (GLP-1) and GIP based treatments could be improved if oral drugs were discovered to replace the current injectable medications. In order to discover novel molecules that mimic these effects, we have screened marine invertebrate and bacterial extract compounds, as they generally contain functionally diverse and biologically active small molecules and are a source of many new drugs. A cell-based bioassay capable of measuring GLP-1R or GIPR activity via a luciferase reporter system was used to screen these compounds for receptor activity. Over 2000 compounds were screened in each of four separate bioassays (GLP-1R agonist screen, GLP-1R allosteric modulator screen, GIPR agonist screen and GIPR allosteric modulator/antagonist screen). These screens resulted in the identification of a GIPR antagonist, halistanol sulphate. Halistanol sulphate was demonstrated to be a selective antagonist of the GIPR as it concentration-dependently decreased activity in the GIP bioassay in the presence of GIP, but not in the absence of GIP or in the presence of GLP-1 in the GLP-1 bioassay. In addition, halistanol sulphate was shown to concentration-dependently block ^{125}I-GIP binding to the GIPR, but only block ^{125}I-GLP-1 and ^{125}I-glucagon binding to their respective receptors at very high concentrations. Finally, halistanol sulphate also demonstrated the ability to modulate incretin induced insulin secretion from perifused mouse islets. Thus, halistanol sulphate displays potent antagonistic activity towards the GIPR *in vitro*, but still requires *in vivo* characterization.

Preface

Studies in this thesis have been published in the following articles:

Daoust J, Fontana A, **Merchant CE**, de Voogd NJ, Patrick BO, Kieffer TJ, Andersen RJ. (2010) Ansellone A, a sesterterpenoid isolated from the nudibranch Cadlina luteromarginata and the sponge Phorbas sp., activates the cAMP signalling pathway. *Org. Lett.* 12(14):3208-11.

Studies in this publication are described in Chapter 3. As part of a collaboration with Dr. RJ Andersen's lab, I was responsible for determining the biological activity of a novel compound via a bioassay and writing the relevant sections of the publication (approximately one quarter). None of the material written by the co-authors in the manuscript was included in the production of this thesis.

Forestieri R, **Merchant CE**, de Voogd NJ, Matainaho T, Kieffer TJ, Andersen RJ. (2009) Alotaketals A and B, sesterterpenoids from the marine sponge Hamigera species that activate the cAMP cell signalling pathway. *Org. Lett.* 11(22):5166-9.

Studies in this publication are described in Chapter 3. As part of a collaboration with Dr. RJ Andersen's lab, I was responsible for identifying active sponge extracts, performing bioassays to identify active compounds in the fractionated extracts and writing the relevant sections of the publication (approximately one quarter). None of the material written by the co-authors in the manuscript was included in the production of this thesis.

Material in this thesis has been submitted for publication in the following article:

Cho YM*, **Merchant CE***, Kieffer TJ. Modulation of the Glucagon Receptor Family for Diabetes and Obesity Therapy. Submitted to Pharmacology and Therapeutics.
* Both authors contributed equally

Material in this submission was used to write Chapter 1. I was responsible for half of the writing and the editing of this submission.

Contributions of authors:
Drs. TJ Kieffer, JD Johnson, RJ Andersen and M Roberge provided materials and analysis tools. Mr. T Webber provided technical training. R Forestieri, J Daoust and D Williams performed hit extract fractionation and structure elucidation for the active compounds in Chapter 5. B Hu performed the islet isolation and assisted with the perifusion in Chapter 5. GK Yang performed the perfusion surgeries in Chapter 5.

With the exception of the studies described above, all studies described in Chapters 3 - 6 were performed by CE Merchant and all studies were conceived and designed by CE Merchant and Dr. TJ Kieffer. The writing of this thesis and all publications was performed by CE Merchant with editing provided by Dr. TJ Kieffer.

Certificates of approval:

The animal studies presented in this thesis were performed with ethics approval from the University of British Columbia Animal Care Committee (certificate # A09-0418).

Table of Contents

List of Figures

List of Abbreviations

4H2BH	4-hydroxybenzoic Acid 2-bromobenzylidene Hydrazide
AIB	Aminoisobutyric Acid
AMPK	AMP Activated Protein Kinase
BSA	Bovine Serum Albumin
cAMP	cyclic AMP
cAMP-GEF	cAMP-regulated Guanine Nucleotide Exchange Factors
CMV	Cytomegalovirus
CNS	Central Nervous System
CRE	cAMP Responsive Element
CREB	cAMP Response Element Binding Protein
DIRKO	Double Incretin Receptor Knockout
DMSO	Dimethyl Sulfoxide
DPP-4	Dipeptidy Peptidase 4
EC_{50}	Half Maximal Effective Concentration
ECD	Extracellular Domain
ELISA	Enzyme-linked Immunosorbent Assay
ER	Endoplasmic Reticulum
FBS	Fetal Bovine Serum
GCG	Glucagon
GCGR	Glucagon Receptor
GIP	Glucose-dependent Insulinotropic Polypeptide
GIPR	Glucose-dependent Insulinotropic Polypeptide Receptor
$GIPR^{dn}$	Dominant Negative Glucose-dependent Insulinotropic Polypeptide Receptor
GLI	Glucagon-like Immunoreactivity
GLP-1	Glucagon-like Peptide 1
GLP-1R	Glucagon-like Peptide 1 Receptor
GLUT-1	Glucose Transporter 1
GPCR	G-Protein Coupled Receptor
GWAS	Genome-wide Association Studies
HbA1c	Glycosylated Hemoglobin
HEK	Human Embryonic Kidney
HG-DMEM	High Glucose-Dulbeco's Modified Eagle's Medium
HPLC	High-performance Liquid Chromatography
HS	Halistanol Sulphate

IBMX	3-isobutyl-1-methylxanthine
IC_{50}	Half Maximal Inhibitory Concentration
KRB	Krebs Ringer Bicarbonate
LAR	Long Acting Release
MEK1/2-ERK1/2	ERK kinase-extracellular signal-regulated kinase 1/2
NMR	Nuclear Magnetic Resonance
OGTT	Oral Glucose Tolerance Test
PBS	Phosphate Buffered Saline
PC	Prohormone Convertase
PI3K	Phosphoinositide 3-kinase
PKA	Protein Kinase A
PKB	Protein Kinase B
PKC	Protein Kinase C
RCF	Relative Centrifugal Force
RIA	Radioimmunoassay
SEM	Standard Error of the Mean
SNP	Single Nucleotide Polymorphism
SSTR2	Somatostatin Receptor Subtype 2
SUR1	Sulfonylurea Receptor 1
TORC2	cAMP-responsive CREB Coactivator 2
VDF	Vancouver Diabetic Fatty Zucker
ZDF	Zucker Diabetic Fatty

Acknowledgements

First of all, I would like to thank Dr. Tim Kieffer for the opportunity to work under his supervision as a graduate student. I have learned and grown so much as a person over the past two years, and I owe much of that to you. Thank you for always challenging me to do my best, and for your unconditional support and guidance.

I would also like to thank all of the past and current members of the Kieffer laboratory for their support and friendship. I have never encountered another group of people who work so well together and who are so eager to lend a helping hand. To Travis, thank you for all of the technical support and for keeping me on my toes with your sarcastic humour. To Blair, Frank, Gary, Heather and Jasna, thank you for your exceptional camaraderie and for always making the laboratory an enjoyable place to work. I am humbled to have met so many talented and capable people, and I wish you all success in your careers.

I would also like to thank my family and friends for their endless support. To my sister Laura, thank you for your wonderful companionship and encouragement. To Jimmy, thank you for your unconditional love and for all of the great times we have had over the years. Finally, I owe my upmost gratitude to my mom and dad, who have worked hard to provide me with every opportunity imaginable. Thank you for always supporting and encouraging me, but also allowing me to discover my own ambitions in life. It is with gratitude that I dedicate this thesis to you.

1 Chapter: Introduction

1.1 Introduction to Diabetes

Diabetes is characterized by chronic hyperglycemia as a result of impaired insulin secretion and/or action (DeFronzo, 1988). The incidence of diabetes is on the rise, perhaps in part due to expanding waistlines as obesity is a major risk factor for the development of diabetes. The worldwide prevalence of diabetes in people 20 years or older was estimated to be 4.6% in 2000 and this number is projected to increase to 6.4% by 2030 (Yach et al., 2006). Furthermore, the global prevalence of obesity was estimated to be 5.7% in men and 9.4% in women in 2002 and was predicted to reach 8.0% in men and 12.3% in women by 2010 (Yach et al., 2006). Although more than 80% of patients with type 2 diabetes are obese, only ~10% of obese subjects are diabetic (Harris et al., 1987), signifying the importance of genetic susceptibility and other environmental factors in the development of type 2 diabetes, as well as the remarkable capacity of pancreatic β-cells to typically respond adequately to increasing demands for insulin. The association between obesity and diabetes is often attributed to altered secretion of adipokines, non-esterified fatty acids and pro-inflammatory cytokines, leading to lipotoxicity, the deposition of ectopic fat in β-cells and insulin sensitive tissues and insulin resistance (Kahn et al., 2006; Unger and Scherer, 2010). Chronic hyperglycemia, if not adequately treated, can cause both microvascular complications (e.g., retinopathy, nephropathy and neuropathy) and macrovascular complications (e.g., coronary artery disease, cerebrovascular disease and other peripheral arterial diseases) (Klein, 1995). These complications significantly decrease the quality of life and ultimately reduce the life span of patients with diabetes by an estimated 13 years (Manuel and Schultz, 2004). The costs associated with pre-diabetes and diabetes reached $218 billion in 2007 in the U.S. alone, which included $153 billion in medical costs and $65 billion in reduced productivity (Dall et al., 2010), while the costs associated with obesity were estimated to be $93 billion in the U.S. in 2002 (Finkelstein et al., 2003). Given the serious health consequences and enormous economic burden of diabetes and obesity, it is imperative to rapidly develop better treatments and/or find a cure for both conditions. The receptors for the gastrointestinal hormones, GIP and GLP-1, are emerging as excellent targets to treat both hyperglycemia and obesity.

1.1.1 Incretins and the Enteroinsular Axis

GIP and GLP-1 are incretin hormones, or factors released from the intestine following nutrient ingestion (Figure 1) that potentiate glucose-stimulated insulin secretion (Baggio and Drucker, 2007; Holst, 2007; Kieffer and Habener, 1999). They comprise a major component of the

functional connection between the intestine and pancreatic β-cells, termed the "entero-insular axis" (Kieffer and Habener, 1999; Unger and Eisentraut, 1969). In healthy subjects, intestinal glucose produces a much greater insulin response compared to the same amount of glucose delivered intravenously (McIntyre et al., 1964). Conversely, in patients with diabetes, the oral route fails to substantially increase insulin levels relative to isoglycemic intravenous glucose infusion (Nauck et al., 1986a). The insulinotropic actions of GIP and GLP-1 are estimated to account for ~50-70% of insulin secretion following oral glucose ingestion in healthy individuals (Nauck et al., 1986b). However, the incretin contribution to insulin secretion in response to oral glucose is estimated to be less than 20% in patients with type 2 diabetes (Nauck et al., 1986a). Since the diminished incretin effect associated with type 2 diabetes is not consistently linked to reduced secretion of either GLP-1 or GIP (reviewed in (Meier and Nauck, 2008; Meier and Nauck, 2010)), it is possible that the pancreatic β-cells are less sensitive to the incretins. In this regard, genetic factors may play an important role. Carriers of the major type 2 diabetes risk allele TCF7L2 (rs7903146) display a decreased sensitivity to the insulinotropic effects of GIP and GLP-1 (Lyssenko et al., 2007; Pilgaard et al., 2009; Schafer et al., 2007; Shu et al., 2009; Villareal et al., 2010). In addition, decreased GIPR and GLP-1R expression was observed in islets from patients with type 2 diabetes as well as human islets treated with siRNA against TCF7L2 (Shu et al., 2009). Furthermore, subjects carrying the type 2 diabetes risk allele WFS1 (rs10010131) displayed a decreased insulinotropic response to infused GLP-1 (Schafer et al., 2009). Apart from genetic factors, there is also evidence suggesting that hyperglycemia itself is involved in the diminished incretin effect observed in patients with type 2 diabetes (Gupta et al., 2010; Lynn et al., 2001; Piteau et al., 2007; Xu et al., 2007). It was reported that chronic hyperglycemia decreased the expression of the GIP receptor and GLP-1 receptor in pancreatic islets of 90% pancreatectomized rats; incretin receptor expression was recovered by reducing blood glucose levels with phloridzin, a renal glucose transport inhibitor (Xu et al., 2007). Alternatively, it has been postulated that the decreased incretin effect displayed in patients with type 2 diabetes may be an epi-phenomenon of impaired β-cell function, since reduced incretin activity strongly correlates with decreased β-cell function (Meier and Nauck, 2010). Even though patients with type 2 diabetes generally display a decreased incretin response, exogenous GLP-1 action on insulin secretion is relatively well preserved in these patients and its maximum insulin secretory effect at supraphysiological concentrations is comparable to that of normal subjects (Nauck et al., 1993a). However, the insulinotropic action of exogenous GIP is markedly decreased (by ~50%) in type 2 diabetic patients, even at a supraphysiological doses (Nauck et al., 1993a). Currently, incretin-based therapies such as GLP-1 mimetics and dipeptidyl peptidase-4 (DPP-4, a ubiquitous proteolytic enzyme) inhibitors, which inhibit degradation of GIP and GLP-1, are useful for the treatment of

hyperglycemia in patients with type 2 diabetes (Figure 1) (Chia and Egan, 2008; Lovshin and Drucker, 2009; Tahrani et al., 2010; Verspohl, 2009; Wideman and Kieffer, 2009).
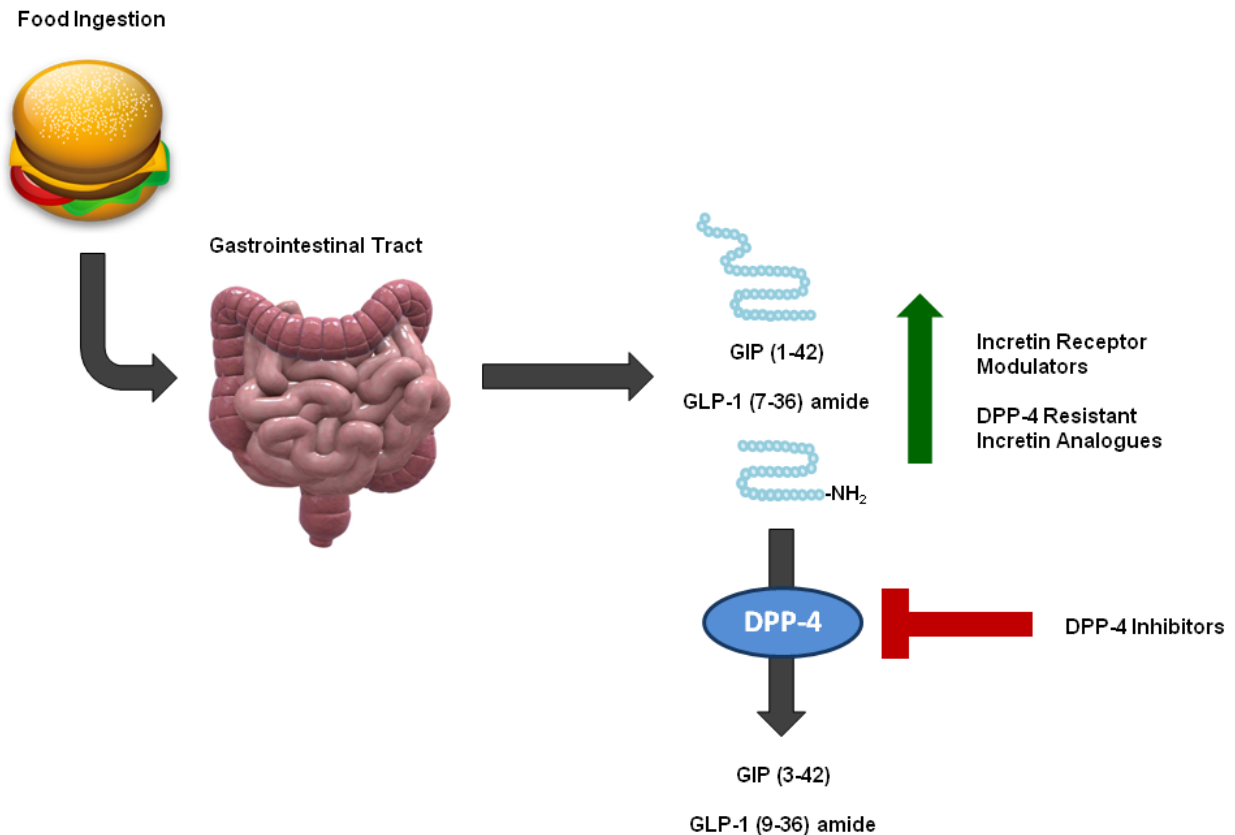
Figure 1.   Therapeutic Strategies to Enhance Incretin Action
Following food ingestion, bioactive GIP(1-42) and GLP-1(7-36) amide are released from the small intestine to stimulate insulin secretion from the pancreatic β-cells. GIP(1-42) and GLP-1(7-36) amide are then rapidly converted to the non-insulinotropic GIP(3-42) and GLP-1(9-36) amide by the proteolytic enzyme DPP-4. Current therapeutic strategies to enhance incretin action include incretin receptor modulators, DPP-4 resistant incretin analogues and DPP-4 inhibitors.

1.1.2   The Importance of α-cell Dysfunction

The pancreatic islet of Langerhans is a micro-organ comprised of glucagon-secreting α-cells, insulin-secreting β-cells, somatostatin-secreting δ-cells, ghrelin-producing ε-cells, and pancreatic polypeptide-secreting PP-cells (Edlund, 2002; Prado et al., 2004). The primary function of pancreatic islets is to maintain glucose homeostasis by coordinated secretion of the glucose lowering hormone insulin and the glucose raising hormone glucagon. Normally, increased blood glucose levels after meals stimulate insulin secretion, while glucagon secretion is suppressed following meals, with reciprocal responses during fasting periods (Dunning and Gerich, 2007). Diabetes has been regarded as a bihormonal disorder, characterized by both insulin deficiency and glucagon

excess (Unger and Orci, 1975). Pancreatic α-cell dysfunction plays an important role in the pathogenesis of type 2 diabetes, with glucagon secretion inappropriately elevated in the presence of hyperglycemia and contributing to the increased basal rate of hepatic glucose production (Baron et al., 1987). In addition, a lack of glucagon suppression contributes to the postprandial hyperglycemia seen in patients with type 2 diabetes (Shah et al., 2000). Therefore, pharmacological interventions that reduce glucagon secretion or block glucagon receptor (GCGR) signalling are theoretically promising treatment options for type 2 diabetes.

1.2 Glucose-Dependent Insulinotropic Polypeptide Receptor

1.2.1 Physiology and Pathophysiology of GIP

GIP was the first incretin hormone to be identified, isolated in the early 70's at the University of British Columbia by John Brown and colleagues (Brown, 1971; Brown and Dryburgh, 1971; Dupre et al., 1973; Jornvall et al., 1981). GIP is a 42 amino acid peptide rapidly released from intestinal K-cells following food intake and circulating levels of GIP typically parallel that of insulin (Buffa et al., 1975; Cataland et al., 1974; Elliott et al., 1993). Perhaps the most important physiological effect of GIP is to stimulate insulin secretion from pancreatic islets (Figure 2) (Brown and Otte, 1978; Dupre et al., 1973; Elahi et al., 1979; Fujimoto et al., 1978; Pederson and Brown, 1976; Schauder et al., 1975; Verdonk et al., 1980). Notably, as the name suggests, the stimulation of insulin secretion by GIP is glucose-dependent (Andersen et al., 1978; Elahi et al., 1979; Pederson and Brown, 1976; Pederson and Brown, 1978). Defective glucose-stimulated insulin secretion and impaired oral glucose tolerance occur in rodents as a result of inhibiting GIPR signalling via targeted genetic inactivation, peptide antagonists and antisera (Baggio et al., 2000b; Gelling et al., 1997a; Lewis et al., 2000; Miyawaki et al., 1999; Tseng et al., 1996). These findings are also supported by recent genome-wide association studies (GWAS) which identified GIP receptor variants that correlate with reduced insulin levels and increased glycemia following oral glucose, but not intravenous glucose (Saxena et al., 2010). In addition, three single nucleotide polymorphisms (SNPs) were recently identified at the 5' gene region of human *GIP* as metabolic modifiers that underlie phenotypic variation in traits associated with diabetes and/or obesity (Chang et al., 2011). These data provide unequivocal support for the role of GIP as an incretin hormone.
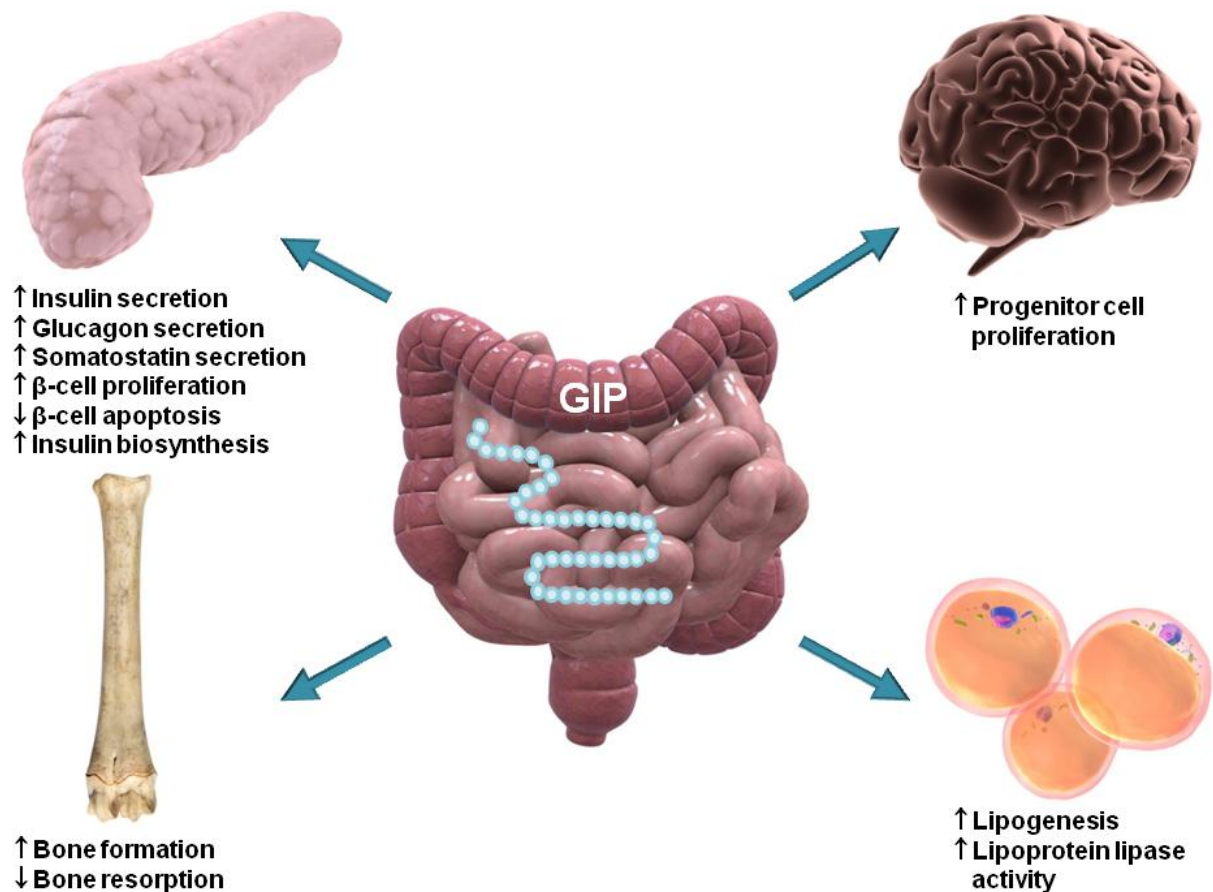
Figure 2. Summary of GIP Actions on Different Tissues
GIP is a 42 amino acid peptide released from intestinal K-cells following food intake. In the pancreas, GIP stimulates glucose-dependent insulin secretion, glucagon secretion, somatostatin secretion and insulin biosynthesis. GIP also increases β–cell proliferation and inhibits β–cell apoptosis. In addition, GIP acts on the adipose tissue to increase lipogenesis and lipoprotein lipase activity, on the bone to stimulate bone formation and reduce bone resorption, and on the brain to induce progenitor cell proliferation.

Beyond its role as an incretin hormone, GIP displays several additional effects on pancreatic β-cells. GIP increases the transcription and biosynthesis of proinsulin (Figure 2) (Drucker, 2007b; Fehmann and Goke, 1995; Schafer and Schatz, 1979; Wang et al., 1996), and the mRNA expression of the β-cell glucose sensor components glucose transporter 1 (GLUT-1) and hexokinase I (Wang et al., 1996). Furthermore, GIP has been shown to display potent prosurvival effects on β-cells (Figure 2) both *in vivo* and *in vitro* (Baggio and Drucker, 2006; Baggio and Drucker, 2007; Drucker, 2006; Ehses et al., 2003; Kim et al., 2005c; Trumper et al., 2002; Trumper et al., 2001). β-cell lines stimulated with GIP display increased proliferation and improved survival (Figure 2) after exposure to streptozotocin (a β-cell toxin), wortmannin (a phosphoinositide 3-kinase (PI3K) inhibitor), glucolipotoxicity, or glucose or serum deprivation (Baggio and Drucker, 2007). In Vancouver diabetic fatty Zucker (VDF) rats, the administration of GIP for two weeks decreases β-cell apoptosis,

5

as evidenced by down-regulation of the pro-apoptotic *bax* gene and increased expression of the anti-apoptotic *bcl-2* gene (Kim et al., 2005c). Finally, GIP decreases endoplasmic reticulum (ER) stress-associated markers in β-cell lines following induction of ER stress (Yusta et al., 2006).

In addition to its effects on β-cells, GIP has actions on other hormone producing cells. In isolated perfused rat pancreas, GIP increases glucagon secretion (Figure 2) below 5.5 mM glucose, while it increases insulin secretion above 5.5 mM (Pederson and Brown, 1978). The stimulation of glucagon secretion by GIP was also observed in rat islets (Fujimoto et al., 1978) and isolated perfused canine pancreas (Adrian et al., 1978), with maximal effects at low glucose concentrations. In patients with type 2 diabetes, supraphysiological concentrations of GIP result in increased glucagon secretion, which offsets the insulinotropic effects of GIP (Chia et al., 2009). Glucagonotropic actions of GIP have also been observed in non-diabetic patients under fasting conditions (Meier et al., 2003), in patients with hyperglucagonemia and cirrhosis of the liver (Dupre et al., 1991) and in perfused human pancreata (Brunicardi et al., 1990). GIP also stimulates pancreatic secretion of pancreatic polypeptide (Adrian et al., 1978; Amland et al., 1985) and somatostatin (Figure 2) (Ipp et al., 1977; McIntosh et al., 1981) in some species. Thus, GIP plays an important role in modulating the secretion of several pancreatic hormones.

In addition to its actions on pancreatic islets, GIP displays potent effects on adipose tissue. Functional GIPRs have been detected on isolated rat adipocytes and differentiated 3T3-L1 adipocytes (Yip et al., 1998). GIP plays an important role in lipid metabolism, enhancing chylomicron-associated triglyceride clearance from blood in dogs (Wasada et al., 1981) and attenuating the plasma triglyceride response to an intraduodenal fat load in rats (Ebert et al., 1991). GIP also enhances the uptake and conversion of glucose into lipids (Hauner et al., 1988), activates fatty acid synthesis (Oben et al., 1991) and enhances free fatty acid re-esterification in rat adipocytes (Figure 2) (Getty-Kaushik et al., 2006). In addition, GIP increases lipoprotein lipase activity (Figure 2) in cultured preadipocytes and mature adipocytes (Eckel et al., 1979; Kim et al., 2007a; Kim et al., 2007b; Knapper et al., 1995b), as well as in subcutaneous human adipocytes (Kim et al., 2007a). Furthermore, GIPR-/- mice fed a high fat diet are protected from developing obesity and use fat as a preferred energy source (Miyawaki et al., 2002). GIP has also been shown to display long-term effects on fat metabolism; subcutaneous injection of GIP 3 times/day for 5 days increased the content and mRNA levels of both pancreatic lipase and colipase (Duan and Erlanson-Albertsson, 1992). GIP has also been shown to stimulate lipolysis (McIntosh et al., 1999), but the significance of the dual lipolytic/lipogenic nature of GIP remains to be determined. Interestingly, differences in GIP function between fed and fasted states may be involved (McIntosh et al., 2009). Although GIP secretion is stimulated by fat ingestion in humans and some obese individuals display elevated GIP plasma levels

(Creutzfeldt et al., 1978; Salera et al., 1982), it is unknown whether a causal relationship between GIP signalling and human obesity exists. However, a recent study on healthy human subjects showed that in combination with a hyperinsulinemic-hyperglycemic clamp, GIP infusion resulted in increased abdominal subcutaneous adipose tissue blood flow and circulating triglyceride hydrolysis and a decreased FFA/glycerol release ratio compared to saline (Asmar et al., 2010). Furthermore, in a recent GWAS performed to identify genetic loci conferring susceptibility to obesity, a *GIPR* variant associated with BMI was identified, suggesting that a link between GIP and body weight regulation exists in humans (Speliotes et al., 2010). Further studies are warranted to investigate the dual lipolytic/lipogenic nature of GIP, as well as the role of GIP in human obesity.

Beyond its actions on the endocrine pancreas and adipose tissue, GIP also displays actions on several other tissues. GIP was initially identified based on its inhibitory effects on gastric acid secretion (Brown, 1971; Brown and Dryburgh, 1971), but this action is only apparent at pharmacological doses in dogs and humans (Nauck et al., 1992; Wolfe et al., 1983). Interestingly, GIPR mRNA and protein has been detected in bone (Bollag et al., 2000), and GIP stimulates responses associated with bone formation in osteoblasts (Figure 2) (Bollag et al., 2000). In addition, GIP has been shown to inhibit the resorptive activity of mature osteoclasts (Figure 2) and demonstrates bone anti-resorptive properties in an *in vitro* organ culture system (Zhong et al., 2007). GIPR-/- mice were also shown to have abnormal bone microarchitecture, altered biochemical properties, impaired bone turnover and reduced bone mass and size (Tsukiyama et al., 2006; Xie et al., 2005). In contrast, GIP-overexpressing mice displayed increased bone mass and bone formation markers and decreased bone resorption markers (Xie et al., 2007). GIPR mRNA has also been detected in multiple brain regions, including the olfactory bulb, hippocampus and cerebral cortex (Usdin et al., 1993). Administration of GIP both *in vivo* and *in vitro* stimulated adult-derived hippocampal progenitor proliferation (Nyberg et al., 2005), suggesting that GIP may be involved in neurogenesis (Figure 2). In support of these findings, GIPR-/- mice exhibited decreased numbers of proliferating cells in the hippocampal dentate gyrus (Nyberg et al., 2005). Furthermore, GIPR overexpressing mice displayed enhanced sensorimotor coordination and memory (Baggio and Drucker, 2007), while GIPR-/- mice had decreased numbers of neuronal progenitor cells in the dentate gyrus and displayed impaired synaptic plasticity and learning (Faivre et al., 2011). The physiological actions of GIP on these tissues warrant further investigation.

1.2.2   Forms of GIP, Tissue Distribution, Regulation of Secretion

The GIP amino acid sequence is well conserved among species, with the human, bovine, porcine, rat and mouse sequences exhibiting greater than 90% amino acid homology (Baggio and

Drucker, 2007). In humans, the *GIP* gene is localized to chromosome 17 and consists of 6 exons and 5 introns (Baggio and Drucker, 2007; Inagaki et al., 1989). The characterization of human cDNA clones encoding *GIP* revealed that the predominant full-length, mature bioactive form of GIP, GIP(1-42) (Figure 3A), is encoded by exons 3 and 4, and is derived by proteolytic processing of a 153-amino acid prohormone precursor (Inagaki et al., 1989). This prohormone precursor encodes a signal peptide, an N-terminal peptide, GIP, and a C-terminal peptide; the N- and C-terminal sequences have no known biological function (Baggio and Drucker, 2007; Takeda et al., 1987). Studies using specific prohormone convertase (PC) null mice and PC overexpressing cell lines demonstrated that PC1/3 co-localizes with GIP in K-cells and is both essential and sufficient to release GIP(1-42) from its prohormone precursor (Ugleholdt et al., 2006). However, proGIP is processed by PC2 in pancreatic α-cells (Fujita et al., 2010b). Based on *in vitro* data (Ugleholdt et al., 2006), PC2 processing of proGIP *in vivo* likely yields GIP(1-31), which can be converted to GIP(1-30) amide by peptidyl-glycine α-amidating monooxygenase (Fujita et al., 2010b). In addition, 5−15% of K-cells express PC2 and likely produce GIP(1-30) amide (Fujita et al., 2010a). Although the insulinotropic and somatostatinotropic actions of GIP(1-30) amide and GIP(1-42) appear to be equipotent (Fehmann and Goke, 1995; Fujita et al., 2010a; Fujita et al., 2010b), GIP(1-30) has been shown to display a reduced ability to increase lipoprotein lipase activity in adipocytes (Widenmaier et al., 2010). Further studies are warranted to investigate the differential actions of GIP isoforms.

The N-terminus and central region of GIP are critical for biological activity, as evidenced from structure-activity studies (Hinke et al., 2003; Hinke et al., 2001). Supporting the results of these structure-activity studies, a high degree of biological activity is retained in truncated forms of GIP, including GIP(1-39) (Sandberg et al., 1986) and GIP(1-30) (Hinke et al., 2003; Hinke et al., 2001; Wheeler et al., 1995). GIP(1-14) and GIP(19-30) are also capable of binding to the GIP receptor and activating adenylyl cyclase (Hinke et al., 2001). On the other hand, even slight alterations to the N-terminal residues Tyr[1] and Ala[2] can severely diminish bioactivity (Hinke et al., 2003). Furthermore, DPP-4 cleaves GIP(1-42) (Figure 3A) *in vivo* to yield GIP(3-42) (Figure 1) (Kieffer et al., 1995; McIntosh, 2008; Mentlein et al., 1993; Pauly et al., 1996), which lacks insulinotropic activity (Schmidt et al., 1987). However, GIP(3-42) may possess some weak antagonistic activity (Deacon et al., 2006; Gault et al., 2002b; Hinke et al., 2002). Another GIP analogue with a single amino acid substitution at the N-terminus, Pro[3]GIP, is a reportedly potent DPP-4 resistant GIPR antagonist (Gault et al., 2002a; Gault et al., 2003). Finally, GIP(6-30) and GIP(7-30) amide have also been reported to act as GIP receptor antagonists (Gelling et al., 1997a; Tseng et al., 1996).
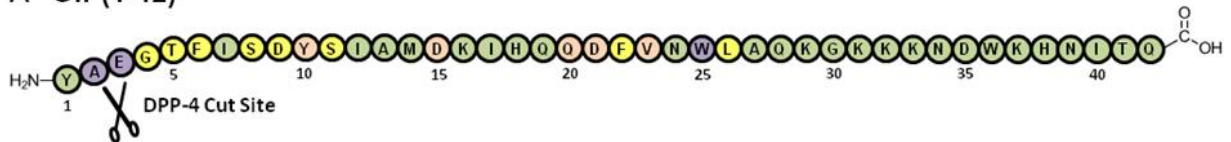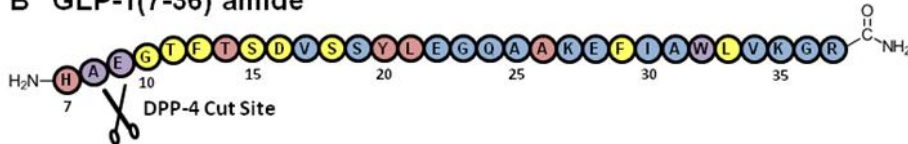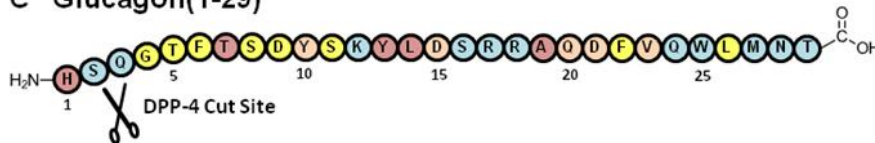
Figure 3. Sequence Comparisons of GIP(1-42), GLP-1(7-36) amide and Glucagon(1-29)
(**A**) GIP(1-42). Residues shown in green are specific to GIP(1-42) and not shared with GLP-1(7-36) amide or glucagon(1-29). (**B**) GLP-1(7-36) amide. Residues shown in blue are specific to GLP-1(7-36) amide and not shared with GIP(1-42) or GCG(1-29). (**C**) Glucagon(1-29). Residues shown in light blue are specific to glucagon(1-29) and not shared with GIP(1-42) or GLP-1(7-36) amide. In addition, residues shown in yellow are conserved between all peptides, residues shown in purple are conserved between GIP(1-42) and GLP-1(7-36) amide, residues shown in red are conserved between GLP-1(7-36) amide and glucagon(1-29) and residues shown in orange are conserved between GIP(1-42) and glucagon(1-29). The cleavage sites of DPP-4 are also shown.

Although GIP can be detected throughout the small intestine, it is most highly concentrated in the duodenum (O'Dorisio et al., 1976). GIP is produced by and secreted from enteroendocrine K-cells, which are mainly located in the duodenum and proximal jejunum (Buchan et al., 1978; Buffa et al., 1975; Polak et al., 1973; Usellini et al., 1984; Van Ginneken and Weyns, 2004). In rodents, the distribution of GIP in the gut extends through to the ileum (Buchan et al., 1982), with the upper small intestine expressing higher levels of GIP than the lower small intestine (Berghofer et al., 1997; Tseng et al., 1993). Interestingly, in many enteroendocrine cells both GIP and GLP-1 immunoreactivity can be detected in the same cells, termed K/L-cells or L/K-cells (Fujita et al., 2008; Mortensen et al., 2003; Theodorakis et al., 2006). GIP mRNA and protein is also co-localized with glucagon in pancreatic α-cells (Alumets et al., 1978; Fujita et al., 2010b; Prasadan et al., 2011; Smith et al., 1977). *Gip* gene expression has also been detected in the submandibular salivary gland (Tseng et al., 1995; Tseng et al., 1993), stomach and brain (Nyberg et al., 2005; Sondhi et al., 2006).

GIP secretion is mainly regulated by nutritional stimuli (Baggio and Drucker, 2007; Kim and Egan, 2008; Krarup, 1988; McIntosh et al., 2009). As such, the morphology of the K-cell is highly specialized to respond to these stimuli. The K-cells are dispersed throughout the gut mucosal lining, account for ~1% of the epithelial cells (Theodorakis et al., 2006), and are typically flask shaped,

passing between adjacent epithelial cells to reach through to the lumen where they can come into direct contact with luminal contents. GIP-containing secretory granules are concentrated at the basal pole of K-cells, and release their contents through the basolateral membrane (Buchan et al., 1978; Sykes et al., 1980) in response to intraluminal nutrients (Baggio and Drucker, 2007; McIntosh et al., 2009). Plasma GIP levels are not affected by intravenous infusion of glucose, fat or protein, whereas intraduodenal or oral administration of these nutrients markedly increases GIP secretion (Andersen et al., 1978; Brown, 1974; Cleator and Gourlay, 1975; Konturek et al., 1986; Kuzio et al., 1974; Morgan, 1979; Pederson et al., 1975; Ross and Dupre, 1978; Varner et al., 1980). In addition, the stimulation of GIP release after intraduodenal or oral nutrient (glucose and/or fat) administration occurs in a dose-dependent manner (Schirra et al., 1996). However, it is the nutrient absorption rate rather than the intestinal presence of nutrients that activates GIP release, since both intestinal malabsorption syndrome and pharmacologic disruption of nutrient absorption decrease GIP secretion (Besterman et al., 1979; Fushiki et al., 1992). Interestingly, the nutritional regulation of GIP release varies by species; fat appears to stimulate GIP secretion the most potently in humans and carbohydrates the most potently in rodents and pigs (Brown et al., 1975; Falko et al., 1975; Knapper et al., 1995a; Yip and Wolfe, 2000). In patients with type 2 diabetes, GIP levels vary between normal and slightly increased (Ross et al., 1977; Vilsboll et al., 2001). Thus, altered regulation of GIP secretion by nutrients does not appear to contribute to diabetes.

Multiple cellular mechanisms are involved in the nutrient-stimulated secretion of GIP from K-cells. Studies on cultured canine endocrine cells have shown that GIP secretion is enhanced by increases in intracellular Ca^{2+} levels, the activation of adenylyl cyclase, K^+-mediated depolarization, gastrin-releasing peptide, glucose and β-adrenergic stimulation (Kieffer et al., 1994). Na^+-coupled glucose transporters, including sodium-dependent glucose cotransporter-1, have been implicated in carbohydrate detection by K-cells and glucose-stimulated GIP secretion (Flatt et al., 1989; Parker et al., 2009; Sykes et al., 1980). In addition, the G-protein coupled receptors (GPCRs) GPR40, GPR120 and GPR119, have also been suggested to play a role in the modulation of incretin release (Chu et al., 2008; Hirasawa et al., 2005); K-cells express high levels of mRNA for GPR40, GPR120 and GPR119 (Parker et al., 2009). Although controversial, the presence of sweet taste receptors has been detected on a small percentage of K-cells, and the activation of these receptors by sugars and sweeteners was shown to stimulate GIP secretion (Egan and Margolskee, 2008; Fujita et al., 2009; Jang et al., 2007). The presence of the ATP-dependent K^+ channel subunits, Kir6.2 and sulfonylurea receptor 1 (SUR1) in K-cells suggest similar glucose-induced response mechanisms to the pancreatic β-cell (Nielsen et al., 2007). However, Kir6.2-/- mice display increased, rather than decreased, plasma levels of GIP after an oral glucose tolerance test (OGTT), suggesting that glucose-stimulated

GIP release is independent of ATP-dependent K$^+$ channels (Miki et al., 2005). Thus, the various cellular mechanisms involved in nutrient-stimulated GIP secretion allow K-cells to effectively respond to different classes of nutrients.

Parallel to the regulation of GIP secretion from K-cells, intraluminal nutrients also regulate *Gip* gene transcription. GIP mRNA and protein levels are elevated upon glucose and lipid administration to the rat gastrointestinal tract, whereas GIP mRNA and protein levels are decreased following prolonged fasting (Higashimoto et al., 1995; Tseng et al., 1994). Consistent with a role of glucose in the modulation of *Gip* gene expression, high glucose levels also increased GIP mRNA concentrations in STC6-14 intestinal cells (Schieldrop et al., 1996). However, the exact mechanisms by which nutrients regulate *Gip* expression are unknown. Specific transcription of *Gip* in rodents can be stimulated by the binding of various transcription factors, including GATA4, Isl1 and Pdx1, to the first 193 bp upstream of the transcription initiation site (Boylan et al., 1997; Jepeal et al., 2008; Jepeal et al., 2003; Jepeal et al., 2005). The importance of Pdx1 as a transcription factor is demonstrated by the fact that Pdx1-/- mice display a 98% decrease in GIP expressing cells (Jepeal et al., 2005). The human *GIP* promoter is also regulated by Pdx1, in addition to Pax6 (Fujita et al., 2008). Interestingly, an essential intronic promoter responsible for cell-specific expression was recently identified in the first intron of the human *GIP* gene (Hoo et al., 2010). Furthermore, a TATA motif, consensus Ap-1, Ap-2, and Sp1 sites, and two 3',5'-cyclic-adenosine monophosphate response elements (Inagaki et al., 1989; Someya et al., 1993) are present in the human *GIP* promoter, indicating protein kinase A (PKA) and protein kinase C (PKC) regulation (McIntosh et al., 2009).

1.2.3   GIP Receptor

1.2.3.1   Structure

The GIPR is a GPCR, belonging to the 7-transmembrane–spanning, heterotrimeric GPCR superfamily (Usdin et al., 1993). The human and rat *GIPR* genes are very similar; the human *GIPR* gene is ~ 13.8 kb (Yamada et al., 1995), contains 14 exons and is localized to chromosome 19q13.3 (Gremlich et al., 1995), while the rat *Gipr* gene spans ~10.2 kb on chromosome 1q21 and contains 13 exons (Boylan et al., 1999). Multiple studies have indicated that alternative mRNA splicing generates GIPR variants of differing lengths in various species and tissues (Boylan et al., 1999; Gremlich et al., 1995; Harada et al., 2008; Volz et al., 1995). Although the functional significance of the majority of these splice variants is unclear, the retention of intron 8 in a mouse variant results in a truncated receptor that effects receptor cell surface expression in a dominant negative manner (Harada et al., 2008). In addition, the N-terminal domain of the GIPR has been shown to contain N-glycosylation consensus sequences, and glycosylation has been suggested to be important for cell

surface expression (McIntosh et al., 2009). Furthermore, threonine and serine residues, which are putative phosphorylation targets, are abundant in the carboxy-terminal tail and third intracellular loop of the GIPR (Bohm et al., 1997; Wheeler et al., 1999). Finally, C-terminal sequences have been shown to play specific roles in regulating binding affinity, adenylyl cyclase coupling and internalization/down-regulation (Tseng and Zhang, 1998a; Tseng and Zhang, 1998b; Wheeler et al., 1999).

In 2007, the first complete atomic level model, built using FTDOCK and refined with a Simulated Annealing procedure, of GIP(1-30) amide complexed with the GIPR was published (Malde et al., 2007). In support of previous studies (Gelling et al., 1997b), the atomic level model suggests that the binding process is initiated by an interaction between the C-terminus of GIP (residues 7-30) and the N-terminus of the GIPR, followed by the interaction of the GIP N-terminus with the juxta-transmembrane domain of the GIPR (Malde et al., 2007). This model provides an explanation for the equipotency of GIP(1-30) amide with GIP(1-42), and also explains why GIP(6–30) amide and GIP(7–30) amide are antagonists of the GIPR (Malde et al., 2007).

Soon after an atomic level model was built, the crystal structure of the human GIP(1-42):GIPR extracellular domain (ECD) complex was determined (Parthier et al., 2007). The crystal structure revealed that GIP, in α-helical conformation, binds in a surface groove of the GIPR ECD while leaving the N-terminal residues of GIP free to interact with different regions of the GIPR (Parthier et al., 2007). This GIP:GIPR complex is held together largely through hydrophobic interactions (Parthier et al., 2007). Adding to previous studies, the crystal structure of the GIP:GIPR ECD provides insight into the mechanism of the ligand-binding step. The crystal structure suggests that the first step in ligand-binding is the capture of GIP by C-terminal hydrophobic residues (Parthier et al., 2007). Binding then induces GIP to change conformation to an α-helix, and restricts the N-terminal conformation of GIP (Parthier et al., 2007). Finally, the N-terminus of GIP is presented to receptor domains involved in further activation and signal transduction (Parthier et al., 2007). Together, these studies reveal the interactions between GIP(1-30) amide and the GIPR, giving insight into the molecular recognition process. This new information can now be exploited for structure-based design of both peptide and nonpeptide GIPR modulators.

1.2.3.2   Distribution

Consistent with the principal function of GIP as an incretin hormone, the pancreatic β-cells appear to express the highest levels of the GIPR in humans (Saxena et al., 2010). In addition, GIPR mRNA transcripts are present in both rat α- and β-cells (Lewis et al., 2000; Moens et al., 1996). However, VDF Zucker rat islets display lower levels of both GIPR mRNA and protein, consistent with the finding that diabetic animals and humans display defective GIP actions (Lynn et al., 2001).

Expression studies have also detected the GIPR in the adipose tissue, stomach, small intestine, heart, bone, lung, kidney, testis, adrenal cortex, pituitary, endothelial cells, trachea, spleen, thymus, thyroid and multiple regions of the central nervous system (CNS) (Baggio and Drucker, 2007; Kim and Egan, 2008; McIntosh et al., 2009; Usdin et al., 1993). Thus, the GIPR is expressed in a wide range of tissues, although the effects of GIPR signalling in several of these tissues are still unknown.

1.2.3.3   Signalling

GIP interacts with its receptor on pancreatic β-cells to potentiate insulin secretion via the cyclic AMP (cAMP)/PKA signalling pathway, increases in intracellular Ca^{2+} concentrations and direct effects on the secretory machinery (Ding and Gromada, 1997; Holst and Gromada, 2004; Wahl et al., 1992; Wheeler et al., 1995). Adenylyl cyclase activation by GIP results in localized increases in cAMP (Seino and Shibasaki, 2005) in β-cell lines (Amiranoff et al., 1984; Ehses et al., 2001; Lu et al., 1993), GIPR transfected cells (Wheeler et al., 1995) and isolated pancreatic islets (Siegel and Creutzfeldt, 1985). Both PKA-dependent (Ding and Gromada, 1997) and -independent pathways (Seino and Shibasaki, 2005) are stimulated by elevated β-cell cAMP. In addition, PKA-dependent pathways are activated by GIP in the α-cell (Ding and Gromada, 1997). GIP enhances Ca^{2+} influx in β-cells and clonal β-cell lines via non-selective ion channels, voltage-dependent Ca^{2+} channels and Ca^{2+}-induced Ca^{2+} release from intracellular stores (Lu et al., 1993; Wahl et al., 1992; Wheeler et al., 1995). GIP also acts directly on the exocytotic machinery, through both PKA-dependent (Ding and Gromada, 1997) and -independent (Seino and Shibasaki, 2005) pathways. PKA-independent activation of the exocytotic machinery involves a cAMP–GEFII–Rim2 complex (Holz, 2004; Holz et al., 2006; Kashima et al., 2001), whereas PKA-dependent activation is stimulated by PKA phosphorylation of proteins associated with exocytosis (Seino and Shibasaki, 2005).

Insulin secretion is also regulated by other GIP-mediated signalling pathways. For instance, MAP kinase is activated by GIP via both wortmannin-sensitive and -insensitive pathways (Kubota et al., 1997; Straub and Sharp, 1996). GIP has also been shown to reduce K_V channel currents, which increases the duration of β-cell action potentials and activates voltage dependent Ca^{2+} channels and Ca^{2+} entry, enhancing glucose-dependent insulin secretion (MacDonald et al., 2002; MacDonald and Wheeler, 2003). Increases in endocytosis of Kv1.4 channels and decreases in ionic peak current amplitude occur as a result of GIP-induced phosphorylation of Kv1.4 channels (Kim et al., 2005b). Thus, GIP-stimulated insulin secretion is a complex process involving multiple cellular processes and signalling pathways.

GIP also displays potent proliferative and prosurvival effects on β-cells (Baggio and Drucker, 2006; Baggio and Drucker, 2007; Drucker, 2006). GIP acts in a glucose-dependent manner to induce the proliferation of INS-1 β-cells (Ehses et al., 2003; Trumper et al., 2002; Trumper et al., 2001),

activating ERK kinase-extracellular signal-regulated kinase 1/2 (MEK1/2-ERK1/2) (Ehses et al., 2002; Kubota et al., 1997; Trumper et al., 2002; Trumper et al., 2001), MKK3/6-p38 (Ehses et al., 2003) and PI3K/protein kinase B (PKB) signalling (Trumper et al., 2002; Trumper et al., 2001). Downstream, enhanced phosphorylation of substrates of ERK1/2 (Ehses et al., 2002), p38 MAPK (Ehses et al., 2002) and PKB (Kim et al., 2005c; Trumper et al., 2001) occur as a result of GIP-activation. Under apoptotic conditions, GIP decreases caspase-3 activation and DNA fragmentation (Ehses et al., 2003; Trumper et al., 2002). These anti-apoptotic effects are regulated by a cAMP-dependent decrease in p38 MAPK phosphorylation (Ehses et al., 2003) and modestly by the MEK1/2-ERK1/2 MAPK pathway (Ehses et al., 2003; Trumper et al., 2002). In addition, GIP regulates β-cell survival at the level of gene expression. The expression of *Bcl-2*, an anti-apoptotic gene, is enhanced by GIP in β-cells via increased nuclear localization of cAMP-responsive CREB coactivator 2 (TORC2) and phosphorylation of cAMP response element binding protein (CREB), as well as decreased phosphorylation of AMP activated protein kinase (AMPK) (Kim et al., 2008). GIP has also been shown to activate PKB/Akt, which results in phosphorylation and nuclear exclusion of the transcription factor Foxo1 (Kim et al., 2005c). Given that the expression of the pro-apoptotic protein Bax requires unphosphorylated Foxo1, the phosphorylation and nuclear exclusion of Foxo1 results in a decrease in Bax levels (Kim et al., 2005c). Further, chronic administration of GIP to VDF Zucker rats resulted in decreased islet apoptosis as well as the up-regulation of Bcl-2 and down-regulation of Bax in β-cells. Thus, the β-cell prosurvival effects of GIP are regulated by the complex interplay between multiple signalling pathways.

In addition to pancreatic islets, adipocytes are also targets of GIP action. Similarly to its actions on β-cells, GIP activates adenylyl cyclase (McIntosh et al., 1999; Yip et al., 1998) and lipolysis (Getty-Kaushik et al., 2006; McIntosh et al., 1999) in rat adipocytes and differentiated 3T3-L1 adipocytes. GIP has also been shown to play a role in the differentiation of preadipocytes to adipocytes via the activation of Akt (Song et al., 2007). In addition, GIP enhances the delivery of triglycerides to adipocytes by activating lipoprotein lipase activity (Eckel et al., 1979; Kim et al., 2007a; Kim et al., 2007b; Knapper et al., 1995b) and potentiates lipogenesis by stimulating glucose and fatty acid uptake (Beck and Max, 1986; Hauner et al., 1988; Oben et al., 1991). The mechanism by which GIP activates lipoprotein lipase activity has been suggested to involve decreased activity of AMP Kinase and elevated release of the adipocytokine resistin (Kim et al., 2007b). These effects are insulin-dependent and regulated via both SAPK/JNK and p38 MAP Kinase signalling pathways (Kim et al., 2007b). However, numerous studies have demonstrated that GIP also has insulin-independent actions on fat metabolism (Beck, 1989; Kim et al., 2007a; Kim et al., 2007b; McIntosh et al., 1999; Morgan, 1996; Yip and Wolfe, 2000). Although the insulin-independent mechanisms by which GIP

elevates adipocyte nutrient uptake are unknown, preliminary evidence suggests that GLUT-4 cell membrane translocation is involved (Song et al., 2007).

1.2.3.4 Regulation of Expression

The expression of the *GIPR* is regulated by the 5'-flanking region, which contains a cAMP response element as well as binding sites for the transcription factors Oct-1, Sp1 and Sp3 (Baldacchino et al., 2005; Boylan et al., 1999). Adipocyte GIPR expression is upregulated via a mechanism involving PPARγ interaction with an acetylated histone region of the *Gipr* promoter (Kim et al., 2011). In addition, the distal 5'-flanking region of the *Gipr* gene contains negative regulatory sequences that modulate cell-specific expression (Boylan et al., 1999). Furthermore, both GIPR mRNA and protein levels are decreased in islets of VDF Zucker rats, consistent with the observation that diabetic animals and humans display defective GIP action (Lynn et al., 2001). Downregulation of the GIPR also correlates with decreased T-cell factor 7-like 2 expression in type 2 diabetes (Shu et al., 2009). Interestingly, the downregulation of the islet GIPR can be reversed by reducing hyperglycemia, suggesting that the downregulation of the GIPR in rodent type 2 diabetes is secondary to chronic hyperglycemia (Piteau et al., 2007). The GIPR has also been shown to undergo homologous desensitization and C-terminal deletion analyses revealed that the C-terminal residues Cys^{411} and Ser^{406} play a role in both desensitization and down-regulation of the rat receptor (Tseng and Zhang, 1998a; Tseng and Zhang, 2000). G protein receptor kinase 2 and β-arrestin 1 have also been implicated in GIPR desensitization (Tseng and Zhang, 2000). Finally, chronic high glucose also results in the desensitization of the islet GIPR (Hinke et al., 2000). Strategies aimed at increasing GIPR expression may be useful in boosting the incretin effect as a means of improving glucose homeostasis in subjects with diabetes.

1.2.4 Consequences of Blocking GIPR Signalling: GIP and Obesity

The disruption of GIPR signalling has revealed some surprising findings. It was discovered that GIPR-/- mice are protected from developing both obesity and insulin resistance when placed on a high fat diet (Miyawaki et al., 2002). Moreover, when crossed with genetically obese, leptin deficient *ob/ob* mice, the lack of GIP signalling significantly reduced weight gain and adiposity (Miyawaki et al., 2002). Probable mechanisms include reducing both GIP- and secondarily insulin-induced uptake and storage of lipids (Irwin and Flatt, 2009). These findings led Miyawaki et al. to conclude that GIP directly links chronic overnutrition to obesity and is a possible target for anti-obesity drugs (Miyawaki et al., 2002). In support of this concept, Flatt and colleagues have reported several studies using a putative peptide-based GIPR antagonist (Pro³GIP) suggesting that GIPR antagonism reverses obesity, insulin resistance and associated metabolic disturbances induced in

mice by the prolonged consumption of a high-fat diet (Gault et al., 2007; Gault et al., 2005; Gault et al., 2002a; Gault et al., 2003; Irwin et al., 2004; Irwin et al., 2007a; Irwin et al., 2007b; McClean et al., 2008a; McClean et al., 2007; McClean et al., 2008b). In an alternative approach, mice in which K-cells are selectively destroyed via the expression of diptheria toxin gained five times less weight than wild-type littermates when placed on a high fat diet and were associated with reduced food intake, increased energy expenditure and improved insulin sensitivity (Althage et al., 2008). Finally, researchers at Cytos Biotechnology generated a vaccine against GIP. That group reported that the vaccination of mice with GIP peptides covalently attached to virus-like particles (VLP-GIP) induced high titers of GIP specific antibodies and efficiently reduced fat accumulation and weight gain in animals fed a high fat diet (Fulurija et al., 2008). Moreover, increased weight loss was observed in obese mice vaccinated with VLP-GIP. Importantly, despite the incretin action of GIP, VLP-GIP-treated mice did not show signs of glucose intolerance (Fulurija et al., 2008). Collectively, these studies support the concept that disrupting GIP signalling represents a promising novel therapeutic strategy for the treatment of obesity. However, while encouraging data have been obtained with Pro^{3}GIP as described above, the utility of this peptide as a therapeutic is hampered by its relatively short circulating half-life and requirement for repeated injections. For anti-obesity therapy, the identification of a novel small molecule GIPR antagonist could lead to the development of an orally active drug.

In order to further investigate the consequences of disrupting GIPR signalling, Herbach et al. developed a transgenic mouse expressing a dominant negative GIPR (GIPR^{dn}) driven by a rat pro-insulin promoter (Herbach et al., 2005). In contrast to GIPR-/- mice which only display mildly impaired glucose tolerance (Miyawaki et al., 1999), GIPR^{dn} mice exhibit a severe phenotype (Herbach et al., 2005). GIPR^{dn} mice are characterized by early-onset diabetes occurring between 14 – 21 days of age in addition to fasting hypoinsulinemia, marked reduction of β-cell mass and structural abnormalities of the pancreatic islets (Herbach et al., 2005). Subsequently, Renner and colleagues developed a transgenic pig expressing a GIPR^{dn} in the pancreatic islets to investigate the effects of impaired GIP function on glucose homeostasis and endocrine pancreas development (Renner et al., 2010). GIPR^{dn} transgenic pigs displayed significantly decreased oral glucose tolerance but not intravenous glucose tolerance (Renner et al., 2010). Interestingly, compared to control pigs, GIPR^{dn} transgenic pigs displayed decreased insulin secretion in response to GIP but an enhanced insulinotropic response to exendin-4, a GLP-1R agonist, suggesting compensatory effects of GLP-1 when GIPR signalling is abolished (Renner et al., 2010); this compensatory mechanism of GLP-1 has also been observed in GIPR-/- mice (Hansotia et al., 2004; Miyawaki et al., 1999). Furthermore, glucose control deteriorated with increasing age in GIPR^{dn} transgenic pigs, as

evidenced by impaired insulin secretion and thus diminished oral and intravenous glucose tolerance (Renner et al., 2010). In addition, β-cell proliferation was decreased by 60% in the pancreata of 11-week-old GIPR^{dn} pigs and this effect was also exaggerated in older pigs (5-month-old compared to 1.25-year-old pigs) (Renner et al., 2010). Notably, body weight was not different between GIPR^{dn} and control pigs (Renner et al., 2010). Thus, these results demonstrate the essential role of GIP in glucose homeostasis and endocrine pancreas development and support the notion that GIPR agonists may be beneficial for the treatment of diabetes. Moreover, due to the similar characteristics between human type 2 diabetic subjects and GIPR^{dn} pigs (glucose intolerance, disrupted GIP activity and decreased pancreatic β-cell mass), GIPR^{dn} pigs may be of interest for the preclinical development of incretin-based therapeutics (Renner et al., 2010).

1.2.5   GIPR Agonists

While there is rationale to block GIP action to treat obesity, the role of GIP in glucose disposal suggests that GIP agonists may also be therapeutic for diabetes (Kieffer, 2003). A series of synthetic N-terminally modified GIP peptides were evaluated for resistance to DPP-4 degradation and affinity for the rat GIPR *in vitro* (Hinke et al., 2002). Based on these *in vitro* experiments, D-Ala^2-GIP(1-42) was determined to possess the greatest resistance to DPP-4 degradation, with minimal effects on GIPR affinity (Hinke et al., 2002). Despite GIP resistance in VDF Zucker rats (Lynn et al., 2001), subcutaneous administration of D-Ala^2-GIP(1-42) effectively reduced glycemic excursion during an OGTT by stimulating insulin release (Hinke et al., 2002). Likewise, D-Ala^2-GIP(1-42) was as effective as dietary intervention in improving glucose homeostasis in high-fat fed mice (Porter et al., 2011). A similar GIPR agonist, D-Ala^2-GIP(1-30), was recently evaluated for its effects on glucose homeostasis and β-cell mass in various rat models of diabetes. Acute administration of D-Ala^2-GIP(1-30) to VDF Zucker rats improved glucose tolerance and insulin secretion, while chronic treatment reduced islet pro-apoptotic protein levels (Widenmaier et al., 2010). In streptozotocin treated rats and Zucker diabetic fatty (ZDF) rats, chronic administration of D-Ala^2-GIP(1-30) preserved β-cell mass, resulting in enhanced insulin secretion and glycemic control, with no change in body weight (Widenmaier et al., 2010). Interestingly, D-Ala^2-GIP(1-30) and GIP(1–42) exhibited equivalent actions *in vitro* on β-cell function and survival, while D-Ala^2-GIP(1-30) displayed markedly reduced effects on lipoprotein lipase activity in 3T3-L1 adipocytes (Widenmaier et al., 2010). Thus, D-Ala^2-GIP(1-30) displays potent anti-diabetic effects and decreased adipogenic actions, with the C-terminus of GIP likely contributing to its lipogenic effects (Widenmaier et al., 2010). In conclusion, GIPR agonists may be beneficial for the treatment of diabetes and it may be possible to develop GIPR agonists that do not promote fat accumulation.

1.3 Glucagon-Like Peptide-1 Receptor

1.3.1 Physiology and Pathophysiology of GLP-1

GLP-1 is a 30 or 31 amino acid proglucagon product (GLP-1(7-36) amide and GLP-1(7-37), respectively) (Figure 3B) that is predominantly released by enteroendocrine L-cells in response to nutrient ingestion (Baggio and Drucker, 2007; Holst, 2007; Kieffer and Habener, 1999). In 1969, L-cells were identified by characteristic "large granules" (hence the name L) in the intestines of cats (Vassallo et al., 1969) and rabbits (Capella et al., 1969). A few years later, L-cells were demonstrated to contain enteroglucagon/glucagon-like immunoreactivity (GLI) in humans, dogs and pigs (Capella and Solcia, 1972). However, it was not until the early 80's that GLP-1 was identified following the discovery of two glucagon-related sequences in angler fish preproglucagon cDNA (Lund, 2005; Lund et al., 1982), and the cloning and sequencing of the mammalian proglucagon gene (Bell et al., 1983a; Bell et al., 1983b; Heinrich et al., 1984; Lopez et al., 1983). After recognizing a GIP-like sequence within GLP-1, GLP-1 was demonstrated to be a potent insulinotropic peptide in rats (Mojsov et al., 1987; Weir et al., 1989), pigs (Holst et al., 1987) and humans (Figure 4) (Kreymann et al., 1987; Nathan et al., 1992). The meal-induced nature of GLP-1 secretion was revealed in humans (Kreymann et al., 1987), which eventually led to the classification of GLP-1 as an additional incretin hormone to GIP.

As an incretin hormone, GLP-1 acts directly on the pancreatic β-cell. GLP-1 potentiates insulin secretion in a glucose-dependent fashion, increases insulin gene transcription and insulin biosynthesis and increases β-cell mass by inducing proliferation and inhibiting apoptosis (Figure 4) (Baggio and Drucker, 2007; Holst, 2007; Kieffer and Habener, 1999). The glucose-dependent nature of GLP-1 action on insulin secretion may contribute to the reduced risk of hypoglycemia observed in clinical trials with GLP-1 based therapeutics (Chia and Egan, 2008; Tahrani et al., 2010; Verspohl, 2009). GLP-1 also reduces plasma glucagon levels (Figure 4) in both healthy subjects and patients with type 1 and type 2 diabetes (Gutniak et al., 1992), which is in contrast to the glucagonotropic action of GIP in perfused rat pancreas (Pederson and Brown, 1978), healthy euglycemic humans (Meier et al., 2003) and patients with type 2 diabetes (Chia et al., 2009). The glucagonostatic action of GLP-1 is also dependent on glucose levels (Nauck et al., 2002). Accordingly, the inhibitory effects of GLP-1 on glucagon secretion are not observed at hypoglycemic plasma glucose concentrations (≤ 3.7 mmol/l) (Nauck et al., 2002). However, the exact mechanism of GLP-1 action on glucagon secretion is controversial. β-cell-specific inactivation of the *Pdx1* gene was demonstrated to abolish exendin-4-induced inhibition of glucagon secretion (Li et al., 2005), indicating that this effect requires β-cell signalling. However, the glucagonostatic effects of GLP-1
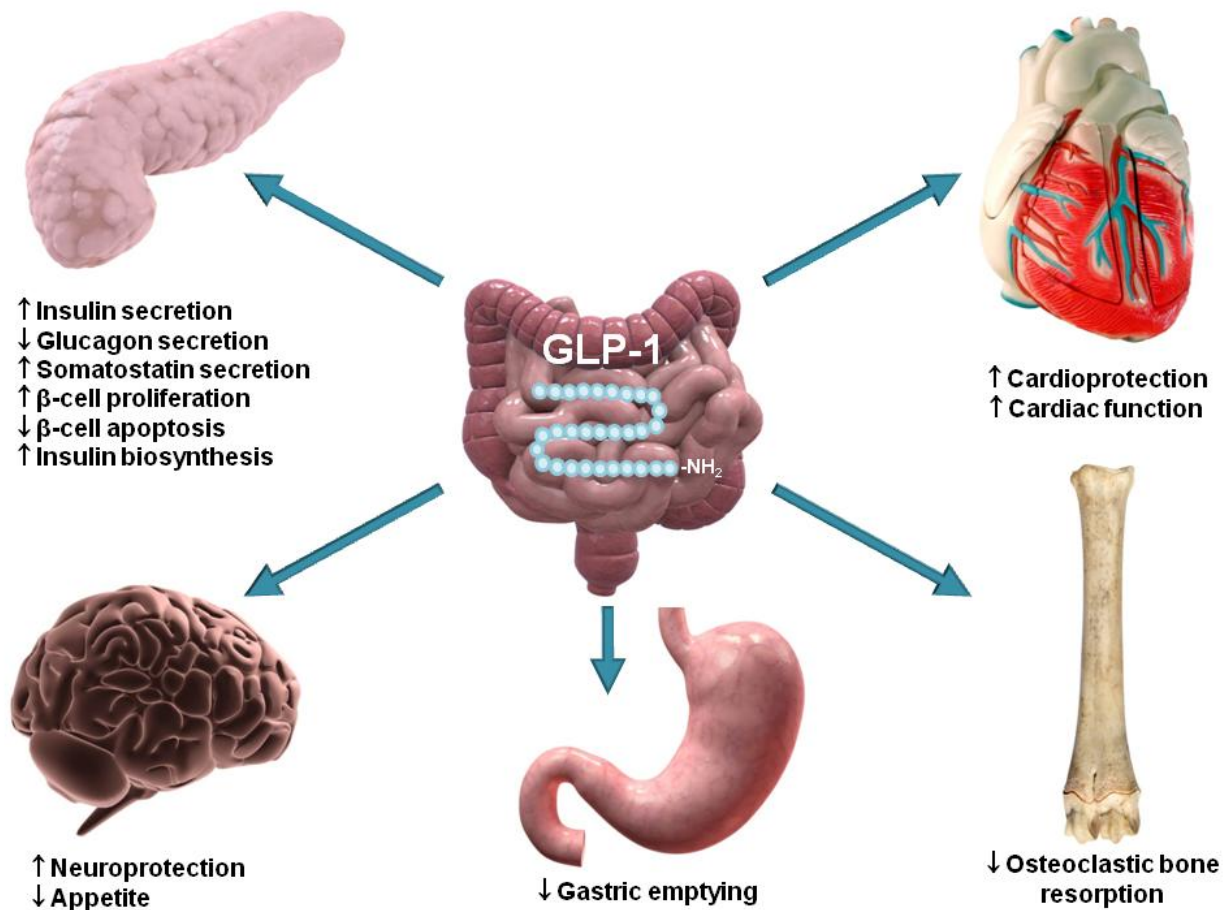
Figure 4.   Summary of GLP-1 Actions on Different Tissues
GLP-1 is a 30 or 31 amino acid proglucagon product released from intestinal L-cells following food intake.   In the pancreas, GLP-1 stimulates glucose-dependent insulin secretion, somatostatin secretion and insulin biosynthesis, and inhibits glucose-dependent glucagon secretion.   GLP-1 also increases β–cell mass by inducing β-cell proliferation and inhibiting β–cell apoptosis.   In addition, GLP-1 acts on the brain to induce neuroprotection and suppress appetite, on the stomach to inhibit gastric emptying, on bone to reduce bone resorption, and on the heart to stimulate cardioprotection and cardiac function.

are still observed in patients with type 1 diabetes who do not display detectable C-peptide responses to glucagon stimulation (Kielgast et al., 2010), suggesting a mechanism independent of β-cells. Since it is well established that GLP-1 stimulates somatostatin secretion from pancreatic islets (Figure 4) (Holst, 2007; Kieffer and Habener, 1999; Kim and Egan, 2008), somatostatin may be acting on the pancreatic islets in a paracrine manner to regulate the actions of GLP-1 on glucagon secretion.   In a recent study using *in situ* pancreas perfusion in rats (de Heer et al., 2008), a highly specific inhibitor of a somatostatin receptor subtype 2 (SSTR2) abolished the glucagonostatic effects of GLP-1 (de Heer et al., 2008).   Therefore, intraislet somatostatin signalling is critical for the glucagonostatic actions of GLP-1.   Interestingly, the glucagonostatic effects of GLP-1 are as important as its insulinotropic effects in improving glucose control in patients with type 2 diabetes

(Hare et al., 2010). Beyond its action on the endocrine pancreas, GLP-1 has pleiotropic extrapancreatic actions including appetite regulation, neuroprotection, inhibition of gastric emptying and gastric acid secretion, regulation of hepatic glucose production, inhibition of osteoclastic bone resorption (likely via the stimulation of calcitonin secretion from thyroid C cells), regulation of cardiac function and cardioprotective effects (Figure 4) (Abu-Hamdah et al., 2009; Baggio and Drucker, 2007; Holst, 2007; Kieffer and Habener, 1999; Kim and Egan, 2008). Collectively, these actions of GLP-1 can provide complementary benefits to patients with diabetes.

Fitting with the role of GLP-1 as an incretin hormone, GLP-1R-/- mice have glucose intolerance and impaired glucose-stimulated insulin secretion (Scrocchi et al., 1996). Inhibition of GLP-1 action leads to impaired postprandial insulin secretion and impaired glucose tolerance. Exendin(9-39), an orthosteric GLP-1R antagonist, reduces postprandial insulin levels, increases glucagon levels and increases glucose levels (D'Alessio et al., 1996; Kolligs et al., 1995; Schirra et al., 1998; Wang et al., 1995). Furthermore, daily administration of Jant-4(9-40)a Lys[40]-C16, a human GLP-1-based peptide that antagonizes the GLP-1R with ~3 fold greater *in vitro* potency than exendin(9-39), for one week to diet-induced obese mice resulted in increased food intake and body weight and decreased glucose tolerance (Patterson et al., 2011).

The first assessments of the clinical potential of GLP-1 in treating diabetes were reported in 1992. GLP-1 administration to type 2 diabetic patients significantly reduced postprandial hyperglycemia (Gutniak et al., 1992; Nathan et al., 1992). The therapeutic potential of GLP-1 was also demonstrated by the efficacy of basal GLP-1 infusion in type 2 diabetic patients with markedly elevated fasting plasma glucose levels despite a regulated diet and sulfonylurea therapy (Nauck et al., 1993b). The ability of GLP-1 to lower blood glucose levels is a result of several complementary mechanisms, including a reduction in glucagon levels, suppression of gastric emptying and reduction in food intake, in addition to the stimulation of glucose-dependent insulin release (Baggio and Drucker, 2007; Holst, 2007; Holst et al., 2009; Kieffer and Habener, 1999; Nauck, 2009). As elaborated upon in subsequent sections, GLP-1 analogues are currently used in clinical practice and there is a plethora of new GLP-1 based drugs in development (Tahrani et al., 2010; Verspohl, 2009).

1.3.2 Forms of GLP-1, Tissue Distribution, Regulation of Secretion

The GLP-1 sequence is remarkably highly conserved, being apparently identical in all mammals. GLP-1 is derived from post-translational processing of proglucagon in the intestinal L-cells, together with GLP-2, oxyntomodulin and glicentin, whereas glucagon is produced from proglucagon in pancreatic α-cells (Mojsov et al., 1986). The proglucagon gene is also expressed in the CNS where it is processed in a similar manner to that seen in the intestinal L-cells, preferentially

producing glicentin, GLP-1 and GLP-2 (Larsen et al., 1997). The differences in the proglucagon products in the pancreatic α-cells, CNS and the intestinal L-cells are due to the tissue-specific posttranslational processing of proglucagon (Mojsov et al., 1986; Orskov et al., 1986). In pancreatic α-cells, proglucagon is processed by PC2 (Rouille et al., 1994). Mice lacking the PC2 gene cannot cleave proglucagon in the α-cells, resulting in deficient circulating glucagon, fasting hypoglycemia and improved glucose tolerance (Furuta et al., 1997). In the intestinal L-cells, proglucagon is processed by PC1/3 to produce glicentin (which may be cleaved further to oxyntomodulin), GLP-1 and GLP-2 (Ugleholdt et al., 2004). GLP-1 can be liberated from proglucagon in α-cells by forced expression of PC1/3, which interestingly results in enhanced glucose-stimulated insulin secretion, improved survival following cytokine treatment and enhanced performance after islet transplantation (Wideman et al., 2006). Interestingly, this same process appears to occur naturally; PC1/3 expression in rodent α-cells has been shown to occur following streptozotocin treatment and chronic hyperglycemia, resulting in GLP-1 production in islets (Hansen et al., 2011; Nie et al., 2000). Mice with a targeted deletion of the PC1/3 gene cannot process proglucagon to GLP-1 and GLP-2 (Ugleholdt et al., 2004; Zhu et al., 2002). However, a patient with multiple endocrinopathies due to severely defective PC1/3 activity displayed near normal postprandial plasma concentrations of fully processed GLP-1 (Jackson et al., 2003), suggesting that the mechanism of proglucagon processing in the intestine may be redundant, at least in humans.

Within L-cells the non-insulinotropic peptides GLP-1(1-37) and GLP-1(1-36) amide are further processed to the potent insulinotropic forms GLP-1(7-37) and GLP-1(7-36) amide (Baggio and Drucker, 2007; Holst, 2007; Kieffer and Habener, 1999). Of the GLP-1 immunoreactivity in the human intestine, it has been estimated that 20% corresponds to GLP-1(7-37) and 80% to GLP-1(7-36) amide (Orskov et al., 1994). The production of GLP-1(7-36) amide from GLP-1(7-37) is presumably achieved by peptidylglycine α-amidating monooxygenase, which catalyzes the two-step formation of bioactive amidated peptides from their glycine-extended precursors (Merkler, 1994; Wettergren et al., 1998). Despite the finding that GLP-1(7-36) amide appears to be more stable than GLP-1(7-37) in plasma (Wettergren et al., 1998), the insulinotropic and glucose lowering actions of these two peptides are largely indistinguishable in humans (Orskov et al., 1993). Thus, GLP-1(7-37) appears to undergo posttranslational processing to GLP-1(7-36) amide in order to increase its stability rather than alter its activity.

Similarly to GIP, both exogenous and endogenous GLP-1 is N-terminally degraded *in vivo* by DPP-4 (Figure 3B), yielding the non-insulinotropic metabolites GLP-1(9-36) amide and GLP-1(9-37) (Figure 1) (Deacon et al., 1995a; Deacon et al., 1995b; Kieffer et al., 1995). Owing to the action of DPP-4, the plasma half-life of exogenously administered intact GLP-1 is less than 2 min and is not

different between diabetic and normal subjects (Vilsboll et al., 2003). It is believed that GLP-1 undergoes substantial N-terminal degradation by DPP-4 before it even leaves the local capillary bed around the L-cells from which it is secreted (Hansen et al., 1999). In addition, 10-15% of GLP-1 is degraded by DPP-4 as it passes through the hepatic-portal system (Deacon et al., 1996; Holst and Deacon, 2005). Thus, it is estimated that only 10-15% of secreted GLP-1 reaches the systemic circulation in its intact form. Since DPP-4 curtails the insulinotropic action of GLP-1 (as well as GIP) (Deacon, 2005), both DPP-4 inhibitors and DPP-4 resistant GLP-1 analogues have been actively developed for therapeutic use (Figure 1) (Chia and Egan, 2008; Tahrani et al., 2010; Verspohl, 2009). Exenatide (marketed under the name Byetta), the synthetic version of exendin-4, is a DPP-4 resistant GLP-1R agonist used for the treatment of type 2 diabetes (Baggio et al., 2000a; Deacon et al., 1998; Drucker et al., 2010; Eng et al., 1992; Greig et al., 1999; Young et al., 1999). In addition, the DPP-4 inhibitors sitagliptin (marketed under the name Januvia) (Herman et al., 2005; Kim et al., 2005a) and saxagliptin (marketed under the name Onglyza) (Augeri et al., 2005) were approved by the U.S. Food and Drug Administration to treat patients with type 2 diabetes in 2006 and 2009, respectively (U.S._Food_and_Drug_Administration, 2006; U.S._Food_and_Drug_Administration, 2009). Another DPP-4 inhibitor, vildagliptin (marketed under the name Galvus) (Brandt et al., 2005; Villhauer et al., 2003), was approved by the European Medicines Agency to treat patients with type 2 diabetes in 2008 (European_Medicines_Agency, 2008). DPP-4 inhibitors, formulated for oral delivery, effectively lower blood glucose levels and are weight neutral in patients with type 2 diabetes (Amori et al., 2007). The weight neutrality may result from an offset of the theoretically sustained satiety effect of GLP-1 by reduced conversion of PYY(1-36) to the appetite suppressing form PYY(3-36) (Unniappan et al., 2006). Since DPP-4 inhibitors only modestly increase plasma GLP-1 and GIP levels, there is controversy regarding whether the glucose-lowering effect of DPP-4 inhibitors is solely mediated by GLP-1 and GIP (Drucker, 2007a; Hucking et al., 2005; Nauck and El-Ouaghlidi, 2005). Moreover, there are numerous potential substrates of DPP-4 and some of them (e.g., PACAP, oxyntomodulin, glucagon and GRP) can modulate glucose homeostasis (Drucker, 2007a). However, DPP-4 inhibitors lower glucose levels and increase plasma insulin levels in wild-type, GLP-1R-/- and GIPR-/- mice, but not in double incretin receptor knockout (DIRKO) mice, suggesting that the effects of DPP-4 inhibitors are solely mediated by GLP-1 and GIP (Hansotia et al., 2004). Thus, GLP-1 and GIP are essential in mediating the glucose lowering action of DPP-4 inhibitors.

It is important to consider that so-called enzymatic degradation products of hormones such as GLP-1 may have as yet unappreciated biological activities. Administration of GLP-1(9-36) amide has been reported to possess glucoregulatory actions in rodents, pigs and humans that complement

the insulinotropic action of GLP-1 (Deacon et al., 2002; Elahi et al., 2008; Meier et al., 2006; Tomas et al., 2011b). Moreover, various positive cardiovascular effects of GLP-1(9-36) amide have been reported, some of which are not shared by insulinotropic forms of GLP-1, raising the possibility that there is another GLP-1 receptor (Tomas and Habener, 2010). GLP-1(9-36) amide and GLP-1(9-37) are further cleaved by neutral endopeptidase 24.11 (a membrane-bound zinc metalloendopeptidase) to produce small C-terminal peptides, including GLP-1(28-36) amide, GLP-1(28-37), GLP-1(32-36) amide and GLP-1(32-37) (Hupe-Sodmann et al., 1997; Hupe-Sodmann et al., 1995; Tomas and Habener, 2010). Interestingly, C-terminal fragments of GLP-1 have recently been hypothesized to act on mitochondria, decreasing oxidative stress, fatty acid oxidation and gluconeogenesis in the liver (Tomas and Habener, 2010). Indeed it was reported that GLP-1(28-36) amide can target mitochondria and inhibit glucose production and oxidative stress in mouse hepatocytes (Tomas et al., 2011a). Whether DPP-4 inhibitors significantly disrupt the downstream actions of various peptide fragments resulting in undesirable effects remains to be determined.

Consistent with the anatomical characteristics of L-cells – open type enteroendocrine cells with long apical processes extending towards the intestinal lumen (Eissele et al., 1992) – GLP-1 is secreted in response to meal ingestion with luminal nutrients including carbohydrate, fat and protein (Baggio and Drucker, 2007; Dube and Brubaker, 2004; Holst, 2007; Kieffer and Habener, 1999; Kim and Egan, 2008; Parker et al., 2010). The rapid increase in blood GLP-1 concentrations following oral glucose ingestion begins within 5 min, which correlates with the time needed for glucose to arrive at the duodenum (Parker et al., 2010; Schirra et al., 1996). This early increase in circulating GLP-1 levels is difficult to explain with the traditional belief that GLP-1 producing L-cells are located predominantly in the distal gut. However, GLP-1 producing cells are also present at a low frequency in the duodenum (Mortensen et al., 2003). Moreover, as previously mentioned, GIP and GLP-1 are frequently colocalized in cells in the mid-small intestine (Mortensen et al., 2003). Therefore, the direct interaction between luminal glucose and L-cells and/or K/L-cells may be the major mechanism of rapid GLP-1 secretion in response to oral glucose ingestion. The exact mechanism of glucose-sensing by L-cells is still being elucidated. Glucokinase (Reimann and Gribble, 2002), K_{ATP} channels (Nielsen et al., 2007; Reimann et al., 2008), sodium-dependent glucose cotransporter-1 (Gribble et al., 2003; Reimann et al., 2008) and sweet taste receptors (Jang et al., 2007) have all been suggested to play a role in L-cell glucose sensing, but the exact molecular mechanisms of glucose sensing are not known (discussed in (Parker et al., 2010)). The fat sensing mechanisms of L-cells are now being elucidated with the recent discovery of fatty acid-sensitive GPCRs (Hirasawa et al., 2008; Ichimura et al., 2009; Lee et al., 2003). GPR40 and GPR120 respond to long-chain fatty acids, GPR84 to medium-chain fatty acids and GPR41 and GPR43 to short-chain

fatty acids (Hirasawa et al., 2008; Ichimura et al., 2009; Lee et al., 2003), with GPR40, GPR41, GPR43, GPR119 and GPR120 being expressed on L-cells (reviewed in (Parker et al., 2010)). Among them, stimulation of GPR119 has been demonstrated to increase GLP-1 secretion *in vivo* and development of an orally active small molecule agonist is being actively pursued (Chu et al., 2007). An atypical protein kinase Cζ has also been suggested as a sensor for long-chain unsaturated fatty acids (such as oleic acid) and a protein kinase Cζ inhibitor abolished GLP-1 secretion stimulated by oleic acid in the murine GLUTag L cell line (Iakoubov et al., 2007). Further elucidating the mechanisms regulating GLP-1 secretion may aid in the design of therapeutic secretagogues of endogenous GLP-1.

1.3.3   GLP-1 Receptor

1.3.3.1   Structure

The *Glp-1r* was first cloned from a rat pancreatic islet cDNA library (Thorens, 1992). Subsequently, the human *GLP-1R* gene was cloned and localized to the short arm of chromosome 6, band 21.1 (Stoffel et al., 1993; Thorens et al., 1993; van Eyll et al., 1994). The *GLP-1R* gene spans 40 kb and consists of at least 7 exons (Lankat-Buttgereit and Goke, 1997). Both rat and human receptors consist of 463 amino acids (63 kDa) and share 90% amino acid sequence identity (Thorens, 1992; van Eyll et al., 1994). The protein contains a large hydrophilic extracellular domain and seven hydrophobic membrane-spanning domains linked together by several hydrophilic intra- and extracellular loops (Doyle and Egan, 2007; Thorens and Widmann, 1996). Regarding signal transduction, specific domains in the intracellular portions of GLP-1R, particularly within the third intracellular loop, couple the receptor to Gα_s. In addition, Gα_q, Gα_i and Gα_o are also coupled to distinct regions within the third intracellular loop of the GLP-1R (Hallbrink et al., 2001; Montrose-Rafizadeh et al., 1999). Furthermore, both glycosylation and palmitoylation of the GLP-1R modulate its function *in vitro* (Goke et al., 1994; Vazquez et al., 2005). However, it is unknown if these posttranslational modifications affect the biological function of the GLP-1R *in vivo*.

The core structure of the N-terminal ligand binding domain of the GLP-1R is characterized by three conserved disulfide bonds, two regions of antiparallel β-sheets and several centrally located conserved amino acid residues, and is similar to that of the corticotropin releasing factor receptor, PACAP receptor and GIPR (Grace et al., 2007; Runge et al., 2008; Sun et al., 2007). Crystal structure analysis of the GLP-1R in complex with exendin(9-39) revealed that the hydrophobic binding site of the GLP-1R is composed of discontinuous segments of α-helix in the N-terminus and a loop between two antiparallel β-strands (Runge et al., 2008). Like other members of the glucagon

receptor family, the GLP-1R contains 6 highly conserved cysteine residues (Thorens et al., 1993). Several discrete amino acid residues in the N-terminal domain (e.g., Thr^{29}-Val^{30}-Ser^{31}-Leu^{32} region, Trp^{39}, Trp^{72}, Trp^{91}, Trp^{110}, and Trp^{120}) and transmembrane domains (e.g., Lys^{197}, Asp^{198}, Lys^{202}, Asp^{215}, Arg^{227}, and Lys^{288}) of the GLP-1R are important for ligand binding, while multiple amino acid residues in the intracellular domains (e.g., Lys^{334}, Lys^{351}, Val^{327}, Ile^{328}, and Val^{331}) are crucial for signal transduction (reviewed in (Doyle and Egan, 2007)). Unlike the *GIPR* (Saxena et al., 2010), polymorphisms of the *GLP-1R* associated with type 2 diabetes risk or glucose homeostasis have not been identified in human genome-wide association studies. However, in a small Japanese study, 5 missense mutations of the *GLP-1R* were identified (Tokuyama et al., 2004). Among these missense mutations, a Thr149Met loss of function mutation was demonstrated to markedly reduce the binding affinity of the GLP-1R to both GLP-1 and exenatide, as well as decrease cAMP production (Beinborn et al., 2005). In addition, in healthy non-diabetic individuals, Gly168Ser and Arg131Gln polymorphisms alter insulin secretion in response to exogenous GLP-1 (Sathananthan et al., 2010). These findings suggest that variations in the *GLP-1R* gene may be responsible for the deterioration of glucose homeostasis in some individuals, although the contribution of *GLP-1R* variants to type 2 diabetes susceptibility may be unremarkable in the general population.

1.3.3.2   Distribution

The GLP-1R is widely expressed in various tissues in several species, explaining the pleiotropic actions of GLP-1. For example, the presence of GLP-1R mRNA was identified in pancreatic islets and ductal cells, lung, brain, stomach, heart and kidney (Bullock et al., 1996; Wei and Mojsov, 1995). Despite the profound effects of GLP-1 on glucose homeostasis, the presence of the GLP-1R in liver, skeletal muscle and adipose tissue is controversial (Bullock et al., 1996; Campos et al., 1994; Egan et al., 1994; Sandhu et al., 1999; Wei and Mojsov, 1995). Consistent with the role of GLP-1 as an incretin hormone, the GLP-1R is abundantly expressed in pancreatic β-cells (Dillon et al., 1993; Thorens et al., 1993; Tornehave et al., 2008). The GLP-1R was also reportedly detected in a subpopulation (~20%) of islet α-cells by single cell RT-PCR and immunostaining (Heller et al., 1997) but was not detected in isolated α-cells by Western blot (Moens et al., 1996), *in situ* hybridization for GLP-1R mRNA or immunocytochemical staining (Tornehave et al., 2008). The reports investigating the presence of the GLP-1R in δ-cells are also inconsistent (Fehmann and Habener, 1991a; Heller et al., 1997; Tornehave et al., 2008). Aside from the physiological distribution of the GLP-1R, insulinomas have also been shown to express high levels of the GLP-1R (Reubi and Waser, 2003). However, the GLP-1R is not overexpressed in pancreatic islets from patients with severe hyperinsulinemic hypoglycemia following gastric bypass (Reubi et al., 2010) .

The expression of high levels of the GLP-1R in insulinomas may be useful in their clinical detection, since insulinomas are typically very small and the diagnostic sensitivity of computed tomography and magnetic resonance imaging is not satisfactory (Chatziioannou et al., 2001). Indeed, a radiolabelled GLP-1R agonist (^{111}In-DOTA-exendin-4) has been successfully used to identify insulinomas in patients (Christ et al., 2009). Furthermore, a radiolabelled GLP-1 analogue decreased the volume of insulinomas in mice by up to 94% (Wicki et al., 2007), suggesting that radiotherapy targeting the GLP-1R can be used to treat medically intractable insulinomas.

1.3.3.3 Signalling

GLP-1R signalling has been extensively studied in pancreatic β-cells in terms of insulin secretion, insulin gene transcription, β-cell proliferation and/or neogenesis and apoptosis. There are distinct domains in the GLP-1R, particularly within the third intracellular loop, that couple the receptor to $G\alpha_s$, $G\alpha_q$, $G\alpha_i$, and $G\alpha_o$ (Hallbrink et al., 2001; Heller et al., 1996; Montrose-Rafizadeh et al., 1999), which in turn couple to various intracellular second messengers including Ca^{2+}, cAMP and phospholipase C. The insulinotropic action of GLP-1 is coupled to production of cAMP via adenylyl cyclase activation, which subsequently activates PKA and the Epac family of cAMP-regulated guanine nucleotide exchange factors (cAMP-GEFs), ultimately resulting in the elevation of intracellular Ca^{2+} levels (de Rooij et al., 1998; Fraser et al., 1998; Gromada et al., 1998; Kawasaki et al., 1998; Lester et al., 1997; Light et al., 2002). PKA plays a key role in the GLP-1 mediated augmentation of insulin secretion by phosphorylating SUR1 of K_{ATP} channels (Light et al., 2002), L-type Ca^{2+} channels (McDonald et al., 1994; Osterrieder et al., 1982) and GLUT2 glucose transporters (Thorens et al., 1996). GLP-1 signalling also inhibits β-cell repolarization by reducing K_V channel currents via the cAMP/PKA-dependent pathway (MacDonald et al., 2002; MacDonald et al., 2003). These same GLP-1 signalling pathways are able to render glucose unresponsive β-cells responsive to glucose, a process referred to as glucose-competence (Holz et al., 1993). Although the mechanism of the glucose-dependent nature of the insulinotropic action of GLP-1 is incompletely understood, it has been noted that GLP-1 requires a threshold ambient glucose concentration to increase intracellular Ca^{2+} levels in β-cells (Lu et al., 1993). Moreover, PKA-mediated K_{ATP} channel closure is ADP-dependent such that GLP-1 may be unable to close K_{ATP} channels in hypo- or euglycemic conditions, when intracellular ADP levels are low (Light et al., 2002). The glucose-dependent nature of GLP-1 provides a clear benefit in reducing the risk of inappropriately high insulin levels and hypoglycemia, as can occur following treatment with other insulin secretagogues, such as sulfonylureas. Therefore, ideally any novel GLP-1 mimetics should retain this important property.

In addition to stimulating insulin secretion, GLP-1 increases insulin biosynthesis by several different mechanisms, thereby replenishing the β-cell insulin reservoirs and preventing β-cell exhaustion. For example, GLP-1 increases insulin mRNA stability via PKA-dependent phosphorylation and the nucleocytoplasmic translocation of polypyrimidine tract binding protein 1 (Knoch et al., 2006). GLP-1 increases insulin gene transcription by activated NFAT (Lawrence et al., 2002), Pdx1 (Buteau et al., 1999; Wang et al., 1999) and CREB (Chepurny et al., 2002; Skoglund et al., 2000). GLP-1 also inhibits FoxO1 through phosphorylation-dependent nuclear exclusion in β-cells and thereby increases Foxa2 and Pdx1 promoter activity, pathways that are also involved in β-cell proliferation and survival, in addition to function (Buteau et al., 2006; Kitamura et al., 2002). Pdx1 is essential in β-cell proliferation, since mice with a β-cell-specific inactivation of Pdx1 do not proliferate in response to exendin-4 treatment (Li et al., 2005). Other pathways implicated in the proliferative effects of GLP-1 on β-cells include up-regulation of cyclin D1 via PKA-dependent activation of CREB (Kim et al., 2006) and activation of β-catenin/ TCF7L2-dependent Wnt signalling (Liu and Habener, 2008), PI3K-mediated EGFR transactivation (Buteau et al., 2003), CREB-mediated IRS2 expression (Jhala et al., 2003) and NFAT (Lawrence et al., 2002). Interestingly, the complete disruption of GLP-1R signalling does not impair the development of islet hyperplasia on the *ob/ob* genetic background (Scrocchi et al., 2000), suggesting that the mechanism of β-cell proliferation in response to insulin resistance is redundant, or compensated following chronic GLP-1R deficient signalling. The signalling pathways mediating the β-cell protective effects of GLP-1 include reduced caspase-3 activation through Akt/PKB (Wang and Brubaker, 2002), reduced ER stress-associated death in a PKA-dependent manner (Yusta et al., 2006), the up-regulation of Bcl-2 and Bcl-xL expression via PKA-and PI3K-dependent pathways (Hui et al., 2003), the up-regulation of Pdx1 following FoxO1 nuclear exclusion via the EGFR- PI3K-Akt/PKB pathway (Buteau et al., 2006) and inhibition of the cytokine-activated JNK pathway (Ferdaoussi et al., 2008). Thus, several different pathways are involved in the growth and survival effects of GLP-1 on β-cells and these actions of GLP-1 could ultimately contribute to restoring a functional β-cell mass in subjects with diabetes.

1.3.3.4 Regulation of Expression

The promoter region of the *GLP-1R* determines its tissue- and cell-specific expression. *GLP-1R* promoter activity is likely regulated by Sp1 and Sp3, and potentially by negatively acting *cis*-regulatory elements upstream of the Sp1-binding sites (Wildhage et al., 1999). Another transcription factor, TCF7L2, modulates *GLP-1R* expression in human islets and regulates GLP-1 sensitivity (Shu et al., 2009; Villareal et al., 2010). Islet GLP-1R expression is down-regulated in response to

dexamethasone (a glucocorticoid) (Abrahamsen and Nishimura, 1995) and high glucose in rats (Xu et al., 2007). In addition, a fast followed by a re-feed was reported to reduce GLP-1R expression in the rat hypothalamus and brainstem (Zhou et al., 2003). GLP-1R expression in rat pancreatic islets was reduced under hyperglycemic conditions induced by 90% pancreatectomy but recovered by the normalization of blood glucose levels by phloridzin treatment (Xu et al., 2007). In rat islets cultured at high glucose concentrations, the overexpression of dominant negative PKCα, which is activated by high glucose in pancreatic islets (Hoy et al., 2003; Kaneto et al., 2002), prevented the decrease of GLP-1 expression (Xu et al., 2007). Further studies will be required to establish the implication of these results.

For the treatment of type 2 diabetes, life-long administration of anti-diabetic drugs is generally required. In this regard, GLP-1R down-regulation may hamper the long-term treatment effects of GLP-1R agonist drugs. Both homologous and heterologous desensitization of the GLP-1R has been reported *in vitro* (Baggio et al., 2004b; Fehmann and Habener, 1991b; Gromada et al., 1996). However, mice overexpressing exendin-4 in multiple tissues, with plasma exendin-4 levels ranging from 5 to 20 pg/ml, do not exhibit a decreased insulinotropic response to exogenous exendin-4 (Baggio et al., 2004b). In addition, the glucose lowering effect of exenatide is generally maintained, even with long-term administration (Blonde et al., 2006; Buse et al., 2007; Gao et al., 2009; Klonoff et al., 2008; Moretto et al., 2008; Ratner et al., 2006; Riddle et al., 2006; Zinman et al., 2007). In an open-label clinical study, patients treated with twice daily exendin-4 for at least 3 years maintained improved glycemic control and showed progressive weight loss (Klonoff et al., 2008). Therefore, these results suggest that clinically meaningful GLP-1R desensitization does not occur with current GLP-1 analogue treatments.

1.3.4   GLP-1R Agonists

Based upon promising results in rodents demonstrating the anti-diabetic potential of GLP-1, studies in patients with diabetes were conducted, and their encouraging findings promoted numerous subsequent trials (Gutniak et al., 1992; Nauck et al., 1993b). A 6-week subcutaneous infusion of GLP-1 to patients with type 2 diabetes decreased fasting and 8 hr mean plasma glucose and glycosylated hemoglobin (HbA1c; an indicator of long term glucose control) levels, normalized fructosamine (an indicator of short term glucose control), decreased body weight and improved both insulin sensitivity and β-cell function (Zander et al., 2002). These results provided a proof of concept that GLP-1 could be used to effectively treat type 2 diabetes. However, the short half-life of GLP-1 was a major obstacle to overcome in order to use GLP-1 in clinical practice without continuous infusion. Since GLP-1 is rapidly degraded to non-insulinotropic fragments *in vivo* by DPP-4 (Kieffer

et al., 1995), DPP-4- resistant GLP-1 analogues and DPP-4 inhibitors have been developed in order to circumvent the short half life of GLP-1 (Brubaker, 2007; Wideman and Kieffer, 2009). In this regard, the discovery of exendin-4, a naturally occurring DPP-4- resistant GLP-1 analogue from the saliva of the Gila monster (*Heloderma suspectum*), was a clinical breakthrough (Eng et al., 1992). In order to develop DPP-4 resistant GLP-1 analogues and/or to increase the biological half-life of native GLP-1, N-terminal modifications (e.g., attachment of chemical groups and substitution of amino acids) and C-terminal modifications (addition of fatty acid or polyethylene glycol [PEG] or fusion to albumin or transferrin) have been extensively tested (Figure 5) (reviewed in (Baggio and Drucker, 2007; Green and Flatt, 2007; Knop et al., 2009; Lovshin and Drucker, 2009; Madsbad et al., 2008)). Although N-terminal modifications of native GLP-1 can prevent DPP-4 degradation and extend its half-life, gradual elimination by the kidney limits its biological activity to approximately 4 hours (Green and Flatt, 2007). Therefore, further measures, such as C-terminal modification, are used to extend the biological half-life of GLP-1R agonists beyond a few hours. As of the first quarter of 2011, there are three generations of GLP-1R agonists on the market and/or in clinical development, classified according to their duration of action (Nauck and Meier, 2010). The first generation of GLP-1 analogues is exemplified by exenatide (a synthetic version of exendin-4), which has a relatively short half-life necessitating twice-daily injection (Buse et al., 2004). The second generation is represented by liraglutide, which maintains its insulinotropic effect for several hours, requiring once daily injection (Chang et al., 2003; Elbrond et al., 2002; Juhl et al., 2002). The third generation of GLP-1R agonists include exenatide-long acting release (LAR) (Drucker et al., 2008), taspoglutide (Retterstol, 2009), albiglutide (St Onge and Miller, 2010) and CJC-1134-PC (Baggio et al., 2008), which display prolonged action and thus only require once-weekly to once-monthly injection. The structures and results of recent clinical trials with GLP-1R agonists are discussed in the subsequent sections.

1.3.4.1 GLP-1R Agonists Based on the Structure of Exendin-4

1.3.4.1.1 Exenatide

Exenatide consists of 39 amino acids (Figure 5Bi) with 53% sequence identity to GLP-1 (Figure 5Ai) (Eng et al., 1992; Goke et al., 1993; Thorens et al., 1993); exenatide has a much longer half-life than GLP-1 as it is not a substrate for DPP-4 (Baggio et al., 2000a; Deacon et al., 1998; Greig et al., 1999; Young et al., 1999). Exenatide is readily absorbed after subcutaneous injection, appearing in the circulation 10-15 min after administration, reaching peak plasma concentrations after ~2 hrs and exhibiting a circulating half life of 3.3-4.0 hrs; exenatide is eliminated predominantly
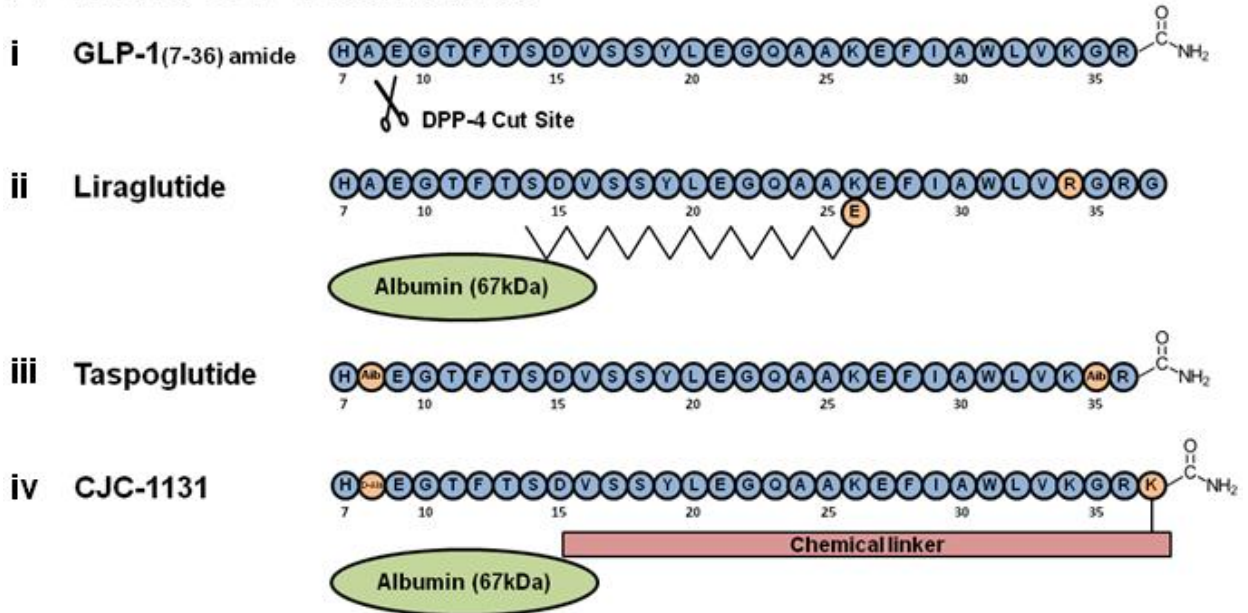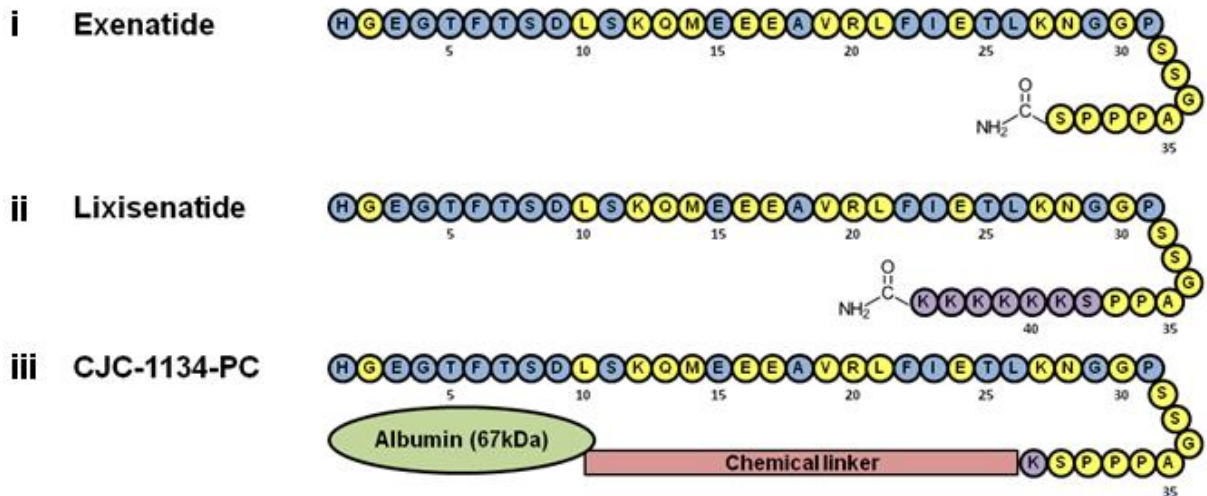
Figure 5. Structures of Peptide-Based GLP-1 Receptor Agonists
(A) Structures of peptide-based GLP-1 receptor agonists based on the sequence of native GLP-1: (i) GLP-1(7-36) amide, (ii) Liraglutide, (iii) CJC-1131 and (iv) Tapsoglutide. **(B)** Structures of peptide-based GLP-1 receptor agonists based on the sequence of exendin-4: (i) Exenatide, (ii) Lixisenatide and (iii) CJC-1134-PC.

by glomerular filtration and subsequent degradation (Fineman et al., 2003; Kolterman et al., 2005; Simonsen et al., 2006). The relatively short half-life of exenatide necessitates twice-daily injections, preferably injected within an hour before morning and evening meals (or before the two main meals of the day, approximately 6 hrs or more apart) (Amylin_Pharmaceuticals, 2010). In patients with type 2 diabetes, exenatide reduces fasting and postprandial glucose levels, restores first-phase insulin

secretion, augments second-phase insulin secretion, decreases glucagon secretion and prolongs gastric emptying time (Chia and Egan, 2008; Tahrani et al., 2010; Verspohl, 2009). Although type 2 diabetes is characterized by progressive and relentless β-cell failure (UKPDS, 1995), exenatide treatment results in sustained improved glycemic control for up to 3 yrs (Klonoff et al., 2008), suggesting that exenatide may actually halt the progression of type 2 diabetes. Exenatide treatment also results in a progressive decrease in body weight for up to 3 yrs in patients with type 2 diabetes (Klonoff et al., 2008; Riddle et al., 2006). Finally, in animal studies, exenatide increases β-cell function and mass by increasing the expression of key β-cell genes and thereby stimulating β-cell proliferation and neogenesis and suppressing β-cell apoptosis (Gedulin et al., 2005; Stoffers et al., 2003; Tourrel et al., 2002; Tourrel et al., 2001; Xu et al., 1999). Whether the same occurs in humans treated with exenatide who typically receive lower doses than those used in animal studies remains to be determined.

Some considerations should be made when prescribing exenatide. The common adverse effects of exenatide are gastrointestinal symptoms such as nausea, vomiting and diarrhea and mild to moderate hypoglycemia (Chia and Egan, 2008; Tahrani et al., 2010; Verspohl, 2009). Nausea is the most common adverse effect, occurring in ~50% of all patients treated with exenatide, and is frequently found during the initial 8 weeks of treatment and lessens over time thereafter (Chia and Egan, 2008; Tahrani et al., 2010; Verspohl, 2009). About 40-50% of patients develop anti-exenatide antibodies with low titer and low binding affinity; however, these antibodies are not likely to affect the glucose lowering efficacy of exenatide (Chia and Egan, 2008; Tahrani et al., 2010; Verspohl, 2009). Although controversial, exenatide may increase the risk or severity of acute pancreatitis in patients with type 2 diabetes (Ahmad and Swann, 2008; Butler et al., 2010; Dore et al., 2009; Drucker et al., 2010). Thus, exenatide should be prescribed with caution to patients with type 2 diabetes according to the label regarding acute pancreatitis (Amylin_Pharmaceuticals, 2010).

1.3.4.1.2   Exenatide LAR

To extend the duration of exenatide action, a LAR preparation has been developed. Exenatide LAR is a poly(D,L-lactic-co-glycolic acid) microsphere suspension with biodegradable microparticles and exenatide (Drucker et al., 2008; Gedulin et al., 2005; Tahrani et al., 2010; Verspohl, 2009). In a 30-week randomized non-inferiority study in 295 drug-naïve patients with type 2 diabetes, compared to twice daily exenatide (10 μg), once weekly exenatide LAR (2 mg) resulted in significantly greater decreases in HbA1c (mean change in HbA1c, −1.9% vs. −1.5%) and fasting plasma glucose levels (mean change in fasting glucose, −2.3 vs. −1.4 mmol/l), with comparable weight loss and without an increased risk of hypoglycemia (Drucker et al., 2008). Exenatide LAR

was associated with a lower rate of nausea than exenatide (26.4% vs. 34.5%), but caused more frequent injection site pruritus (17.6% vs. 1.4%) and a higher titer of anti-exenatide antibodies (Drucker et al., 2008). It is noteworthy that patients who switched from twice daily exenatide to once weekly exenatide LAR reported significant improvements in treatment satisfaction and quality of life (Best et al., 2009), granting additional clinical benefits to the glucose lowering and weight reducing properties of exenatide.

1.3.4.1.3   Lixisenatide

Lixisenatide (formerly known as ZP10A or AVE-0010) is a 44 amino acid exendin-4 analogue with a modified C-terminus with Pro[38] and Ser[39] to Ser[38] and Lys[39] substitutions and 5 additional Lys residues (Figure 5Bii) (Werner et al., 2010). Lixisenatide lowers HbA1c levels in *db/db* mice after 6 weeks of twice-daily intraperitoneal injections (Thorkildsen et al., 2003), and in ZDF rats after 12 weeks of continuous subcutaneous infusion (Werner et al., 2006). In addition, lixisenatide displays β-cell protective properties in INS-1 cells (Tews et al., 2008) and cultured human islets (Werner et al., 2008). Although the pharmacokinetic and pharmacodynamic properties of lixisenatide have not yet been reported in humans, lixisenatide phase 3 clinical trials are underway as of the first quarter of 2011 as a once-daily therapy (Sanofi_Aventis, 2010; Werner et al., 2010).

1.3.4.1.4   CJC-1134-PC

Since exendin-4 is removed from the circulation predominantly by glomerular filtration and subsequent degradation (Kolterman et al., 2005; Tahrani et al., 2010; Verspohl, 2009), increasing the mass of exendin-4 by linking it to large molecules is a conceivable strategy to increase its biological half-life and ultimately decrease its injection frequency. CJC-1134-PC, a modified exendin-4 analogue conjugated to recombinant human albumin (Figure 5Biii), was developed using low-molecular weight chemical linker (cys-$C_{13}H_{19}O_6N_3$-Lys) technology (Christensen and Knop, 2010). In a phase 2 clinical trial, 3-month treatment with CJC-1134-PC reduced HbA1c levels by 0.8% with once weekly (1.5-2.0 mg) administration and 1.4% with twice weekly (1.5 mg) administration, while it decreased body weight by only 1.2 kg with twice weekly (1.5 mg) administration (Wang et al., 2009). The modest weight loss effect of CJC-1134-PC compared to native exenatide may be explained by poor central nervous system penetrance due to its bulky structure (Baggio et al., 2008).

1.3.4.1.5   Other GLP-1R Agonists Based on the Structure of Exendin-4

In a similar strategy to CJC-1134-PC, various other protein-binding techniques have been adopted to increase the half-life and decrease the injection frequency of exendin-4. For example, acylation of exendin-4 with either lauric acid (C12) or palmitic acid (C16) (Chae et al., 2010a) and

subsequent conjugation to a hydrophobic bile acid such as lithocholic acid (Chae et al., 2010b; Son et al., 2009) is a strategy to increase albumin binding and thus the half-life of the drug. In addition, the conjugation of exendin-4 to the N-terminus of non-glycosylated transferrin via a 12-amino acid connecting peptide (two copies of Pro-Glu-Ala-Pro-Thr-Asp) yields an analogue with a prolonged action profile (Kim et al., 2010). In *db/db* mice, transferrin-conjugated exendin-4 exhibits glycemic lowering effects for up to 24 hrs (vs. 8 hrs with exenatide) after a single subcutaneous injection (1 mg/kg) and decreases food intake for up to 48 hrs (vs. 24 hrs with exenatide) after a single intraperitoneal injection (0.3 and 1 mg/kg) (Kim et al., 2010). Finally, the PEGylation of exendin-4 increases its half life, while retaining its biological activity (Zhou et al., 2009).

1.3.4.2 GLP-1R Agonists Based on the Structure of Native GLP-1

1.3.4.2.1 Liraglutide

Liraglutide (also known as NN2211) is a GLP-1 analogue with a Lys^{34} to Arg^{34} substitution and a C16 fatty acid chain attached to Lys^{26} via a Glu spacer (Figure 5Aii) (Knudsen et al., 2000). The fatty acid chain binds to albumin, concealing the DPP-4 cleavage site and dramatically prolonging the half-life of liraglutide in plasma (Knudsen et al., 2000). Compared to exenatide, which reaches peak plasma concentrations after ~2 hrs, liraglutide is absorbed slowly from the injection site and achieves peak plasma concentrations after 9-12 hrs and a half-life of 10-15 hrs, rendering it suitable for once daily injection (Chia and Egan, 2008; Tahrani et al., 2010; Verspohl, 2009). In general, liraglutide reduces fasting and postprandial glucose and HbA1c levels, improves first- and second-phase insulin secretion, suppresses glucose-dependent glucagon secretion and prolongs gastric emptying in patients with type 2 diabetes (Chia and Egan, 2008; Tahrani et al., 2010; Verspohl, 2009). Similar to exenatide, the common adverse effects of liraglutide include nausea, vomiting, diarrhea and hypoglycemia (Chia and Egan, 2008; Tahrani et al., 2010; Verspohl, 2009). However, liraglutide is much less immunogenic than exenatide and low-titers of anti-liraglutide antibodies are only detected in 8.6% of treated patients (Novo_Nordisk, 2010). One potential concern with liraglutide is the risk of developing medullary thyroid cancer originating from calcitonin-secreting thyroid C-cells. In preclinical testing for lifetime carcinogenicity in rats and mice, liraglutide caused thyroid C-cell tumors (Novo_Nordisk, 2010). However, in clinical trials, there were no reported cases of medullary thyroid cancer in patients treated with liraglutide (Novo_Nordisk, 2010). In 2010, the U.S. Food and Drug Administration approved liraglutide for the treatment of type 2 diabetes, with the liraglutide label including a black box warning about potential thyroid C-cell tumors (Novo_Nordisk, 2010).

1.3.4.2.2   Albiglutide

Albiglutide (formerly known as albugon) is a GLP-1R agonist developed via the genetic fusion of recombinant human albumin to two repeats of a DPP-4 resistant human GLP-1(7-36) analogue (containing Gly^8 in the place of Ala^8) (Bush et al., 2009). Since the genetic construct of albiglutide contains the sequences of both the GLP-1 analogue and albumin in the same open reading frame, there is no unbound GLP-1 moiety in the preparation (Baggio et al., 2004a). The structure of albiglutide creates a unique pharmacokinetic profile with slow absorption (T_{max} for albiglutide and exenatide is ~3 days and ~2.1 hrs, respectively) and an extended half-life (~5 days) (Rosenstock et al., 2009), allowing for less frequent dosing. In a double-blind parallel-group trial, various doses and administration schedules of albiglutide (4, 15 or 30 mg weekly, 15, 30 or 50 mg biweekly, 50 or 100 mg monthly) were tested in comparison to twice daily exenatide (5-10 µg) (Rosenstock et al., 2009); dose-dependent reductions in HbA1c levels and similar degrees of weight loss (-1.1 to -1.7 kg) were observed for all dosing schedules (Rosenstock et al., 2009). The incidence of nausea and vomiting was less frequent in subjects receiving weekly albiglutide (30 mg) compared to exenatide, biweekly albiglutide (50 mg) and monthly albiglutide (100 mg) (Rosenstock et al., 2009). The less frequent gastrointestinal side effects of albiglutide compared to exenatide can be explained by its slow absorption kinetics and relative impermeability to the central nervous system due to its bulky structure (Baggio et al., 2004a). Anti-albiglutide antibodies were detected in 2.5% of the subjects receiving albiglutide; however, antibodies were non-neutralizing, low in titer, and largely transient (Rosenstock et al., 2009). As of the first quarter of 2011, albiglutide is in phase 3 clinical trials.

1.3.4.2.3   Taspoglutide

Taspoglutide (also known as R1583 or BIM51077) is a GLP-1 analogue with aminoisobutyric acid (Aib) in place of amino acids 8 and 35 (Figure 5Aiii) with a sustained release formulation suitable for once weekly subcutaneous administration (Nauck et al., 2009). In a phase 2 randomized double-blind study conducted in 306 patients with type 2 diabetes, 8 week treatment with taspoglutide (5, 10 or 20 mg weekly or 10 or 20 mg biweekly) in combination with metformin significantly improved fasting and postprandial glucose levels (by 1.2-2.5 mmol/l) and HbA1c levels (by 0.9-1.2%), and induced weight loss (by 1.9-2.1 kg) (Nauck et al., 2009). The most common adverse effect of taspoglutide was nausea, which was dose-dependent and transient. However, despite the promising results of phase 2 trials, phase 3 clinical trials with taspoglutide were halted in 2010 by the manufacturer due to serious hypersensitivity reactions and gastrointestinal side effects.

1.3.4.2.4   CJC-1131

Similar to CJC-1131-PC, a modified exendin-4 analogue conjugated to recombinant human albumin (Baggio et al., 2008), CJC-1131 is a modified GLP-1 analogue that binds to albumin (Figure 5Aiv) and renders itself DPP-4 resistant (Leger et al., 2004). While CJC-1131-PC is conjugated to recombinant human albumin *in vitro*, CJC-1131 binds to albumin *in vivo* after injection (Baggio et al., 2008; Kim et al., 2003; Leger et al., 2004). The glucose lowering effects of CJC-1131 are maintained for 10-12 hrs after a single injection in *db/db* mice, and twice daily administration for 2 weeks to *db/db* mice significantly reduces glycemic excursion following a glucose challenge (Kim et al., 2003). In addition, CJC-1131 increased insulin transcription as well as the area of pancreatic islets after 4 weeks of twice daily administration (Kim et al., 2003). Nonetheless, CJC-1131 does not appear to be currently in clinical development (Christensen and Knop, 2010; Verspohl, 2009).

1.3.4.2.5   GLP-1/Fc Fusion Proteins

The Fc portion of immunoglobulin can serve as a large carrier moiety for small peptides, thereby improving their pharmacokinetics (Sato et al., 2006). LY2189265 (dulaglutide), a recombinant DPP-4-resistant GLP-1 analogue/ immunoglobulin G (IgG4) Fc fusion protein, displays an increased half-life of up to 1.5-2 days in rats and cynomolgus monkeys (Glaesner et al., 2010). LY2189265 improves glucose tolerance and lowers weight in *db/db* mice (Glaesner et al., 2010). CNTO736, another recombinant DPP-4 resistant GLP-1 analogue/Fc fusion protein (Huang, 2009), displays preserved biological and glucoregulatory activity and has a half-life of ~30 hrs (Picha et al., 2008). Although CNTO736 is too large to easily cross the blood brain barrier, it activates several regions of the brain and decreases food intake following peripheral administration in rats (Picha et al., 2008). In another study, the fusion of native GLP-1 to IgG1 Fc resulted in a compound with potent GLP-1R agonist activity, resistance to DPP-4 degradation and a prolonged half-life *in vitro* (Kim et al., 2009). GLP-1/Fc fusion proteins display prolonged biological half-lives and hence are promising candidates for long-acting GLP-1R agonist therapy.

1.3.4.2.6   Other GLP-1R Agonists Based on the Structure of Native GLP-1

Other strategies to improve GLP-1 therapy involve conjugation to transferrin, the use of prodrugs and PEGylation. Transferrin-conjugated GLP-1 activates the GLP-1R and is resistant to DPP-4 proteolytic activity, extending its half-life to ~2 days (Kim et al., 2010). Furthermore, transferrin-conjugated GLP-1 augments glucose-dependent insulin secretion, reduces blood glucose levels and increases β-cell proliferation in *db/db* mice (Kim et al., 2010). On the other hand, poly-GLP-1 is a prodrug consisting of repeated bioactive GLP-1 sequences coupled together by a linker peptide and expressed as a single 240 amino acid polypeptide chain in *Escherichia coli* (Ma et al.,

2009). Although poly-GLP-1 is an inactive prodrug, it is slowly degraded *in vivo* by endopeptidases, gradually releasing bioactive GLP-1. Six-week poly-GLP-1 treatment in *db/db* mice resulted in improved glycemic control, enhanced insulin sensitivity, increased β-cell mass and proliferation and decreased food intake and body weight gain (Ma et al., 2009). Finally, PEGylation of peptides not only decreases renal clearance by simply increasing their molecular size (Youn et al., 2006), but also decreases enzymatic degradation (Caliceti and Veronese, 2003). A PEGylated GLP-1 residue, Lys[34]-PEG(10k)-GLP-1, reduced postprandial glucose levels in *db/db* mice when administered up to 6 hours before a glucose challenge. Thus, these strategies represent promising new avenues for the development of long-acting GLP-1R agonists.

1.3.4.3   Orally Active GLP-1R Agonists

To overcome the low oral bioavailability of peptide drugs, there have been significant efforts to develop non-peptidyl orally active GLP-1R agonists (Figure 6). Screens with reporter cells expressing the GLP-1R have resulted in the successful discovery of small molecule non-peptidyl agonists of the GLP-1R (Chen et al., 2007; Knudsen et al., 2007; Sloop et al., 2010). In addition, a small molecule non-peptidyl antagonist to the GLP-1R has been reported (Tibaduiza et al., 2001). These studies exemplify the possibility of modifying GLP-1R signalling via small molecules.

1.3.4.3.1   Compound 2

Compound 2 (a substituted quinoxaline: 6,7-dichloro-2-methylsulfonyl-3-N-tertbutylaminoquinoxaline) (Figure 6A) was discovered as a GLP-1R agonist after screening 500,000 compounds and subsequently performing structural modification (Knudsen et al., 2007). Compound 2 significantly increases glucose-stimulated insulin release from mouse islets and the perfused rat pancreas (Knudsen et al., 2007). Interestingly, compound 2 also increases the receptor binding affinity of GLP-1 without changing its potency (Knudsen et al., 2007). In addition, exendin(9-39) does not inhibit cAMP formation by compound 2 (Knudsen et al., 2007). Therefore, compound 2 is regarded as an ago-allosteric modulator of the GLP-1R, acting as both an agonist and an allosteric modulator without binding to the GLP-1R orthosteric site (Knudsen et al., 2007). Although compound 2 displays several beneficial effects, it is cytotoxic at high concentrations (Coopman et al., 2010). Nevertheless, substituted quinoxalines are potent GLP-1R ago-allosteric modulators that can be used to further develop small molecule GLP-1R agonists (Teng et al., 2007).

1.3.4.3.2   Boc5

Boc5, a substituted cyclobutane (Figure 6B), was identified as an orthosteric GLP-1R agonist (binds to the same site of the GLP-1R as native GLP-1) by screening a diverse library of 48,160

synthetic and natural compounds (Chen et al., 2007). The agonistic effects of Boc5 were blocked by exendin(9-39), and were not observed in cells expressing the glucagon or GLP-2 receptors (Chen et al., 2007). Boc5 stimulates insulin secretion both *in vitro* and *in vivo*, and chronic daily injections of Boc5 in *db/db* mice reduce HbA1c levels, blood glucose levels and weight gain (Chen et al., 2007; Su et al., 2008). Notably, Boc5 appears to be orally active, reducing food intake and HbA1c levels in mice following oral administration (Chen et al., 2007; Su et al., 2008). These results provide strong support for the development of orally active small molecule GLP-1R agonists.

1.3.4.3.3 Compound B

Compound B is a pyrimidine-based GLP-1R agonist (Figure 6C) developed by modifying the chemical structure of Compound A (CAS registry number: 870083-94-6), which was initially identified as a putative GLP-1R agonist in a chemical library screening study (Sloop et al., 2010). Compound B increases insulin secretion from islets isolated from both diabetic and non-diabetic subjects . Interestingly, Compound B is not inhibited by exendin(9-39) and does not displace ^{125}I-GLP-1 binding to the human GLP-1R . Thus, Compound B is an allosteric modulator that increases insulin secretion in an additive manner to GLP-1 (Sloop et al., 2010). Unfortunately, unlike intravenous administration, orally administrated Compound B does not display insulinotropic effects (Sloop et al., 2010). Thus, further modification is necessary to improve the pharmacological properties of Compound B in order for it to be administered orally.

1.4 Hybrid Peptides

As GIP and GLP-1 share a high degree of amino acid sequence identity (Figure 3A & 3B), it is conceivable to generate a dual acting peptide capable of modulating both receptors (Figure 7). MAR701, which is in a phase I trial, is a novel GLP-1/GIP co-agonist that Marcadia plans to develop into a once-weekly treatment for type 2 diabetes (Marcadia_Biotech, 2010). Preclinical studies of MAR701 by Marcadia have demonstrated additive efficacy by simultaneous activation of both the GLP-1 and GIP receptors with significant reductions in body weight and blood glucose levels (Marcadia_Biotech, 2010). In addition, no apparent side effects have been reported for MAR701 (Marcadia_Biotech, 2010). Thus, compounds activating both the GLP-1 and GIP receptors represent novel therapeutic options to improve the treatment of type 2 diabetes.

In addition to compounds modulating both the GIP and GLP-1 receptors, the concept of a dual GLP-1/glucagon modulator is also being explored (Figure 7), as GLP-1 and glucagon also display a high level of sequence similarity (Figure 3B & 3C). To obtain a hybrid peptide functioning as both a GLP-1R agonist and a GCGR antagonist, a series of hybrid peptides based on the structures of glucagon and GLP-1 were screened; ANC7K2 was discovered to have potent GLP-1R agonistic
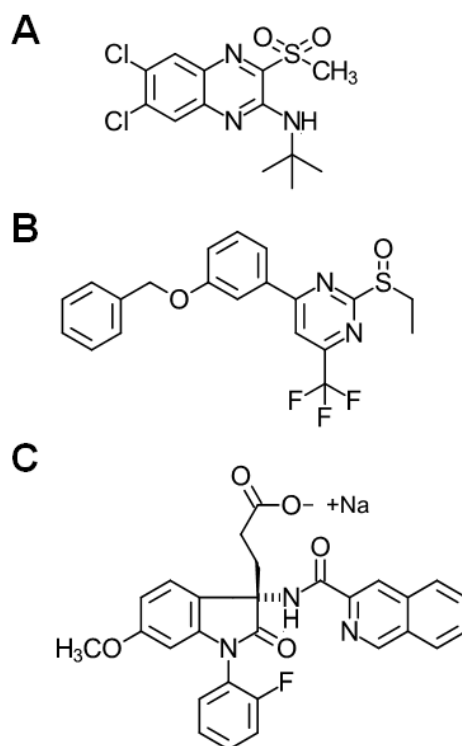
Figure 6. Structures of Non-Peptidyl GLP-1 Receptor Agonists
(A) Compound 2 (a substituted quinoxaline), an ago-allosteric modulator, **(B)** Boc5 (a substituted cyclobutane), an orthosteric agonist and **(C)** Compound B (a pyrimidine-based compound), an allosteric agonist.

activity on a rat insulinoma cell line, RINm5F (EC_{50}, 12.7 nM), and partial GCGR antagonist activity on rat liver membranes (35.6% inhibition of glucagon activity) (Pan et al., 2006). Further, subcutaneous administration of PEGylated ANC7K2 (30 μg/kg) resulted in prolonged *in vivo* activity for up to 65 hrs in rats, and increased insulin levels, improved glucose tolerance and reduced blood glucose levels following a glucagon challenge in mice (Claus et al., 2007). Other strategies have involved the development of dual GLP-1R and GCGR agonists (Figure 7), which have been reported to promote weight loss, improve glucose tolerance and decrease blood lipid levels and hepatic steatosis in rodent models of obesity (Day et al., 2009; Pocai et al., 2009).

Finally, the development of dual acting GIP/glucagon receptor modulators is also being explored, given the sequence similarity between GIP and glucagon (Figure 3A & 3C). The small molecule 4-hydroxybenzoic acid 2-bromobenzylidene hydrazide (4H2BH) was recently discovered as a dual GIPR and GCGR antagonist (Franklin et al., 2011). *In vitro*, 4H2BH inhibited both GIP and glucagon stimulated cAMP generation and insulin secretion (Franklin et al., 2011). In addition, 4H2BH significantly inhibited the glucose lowering and insulin secreting actions of exogenous GIP (Franklin et al., 2011). Furthermore, 4H2BH impaired glucagon stimulated elevations in blood
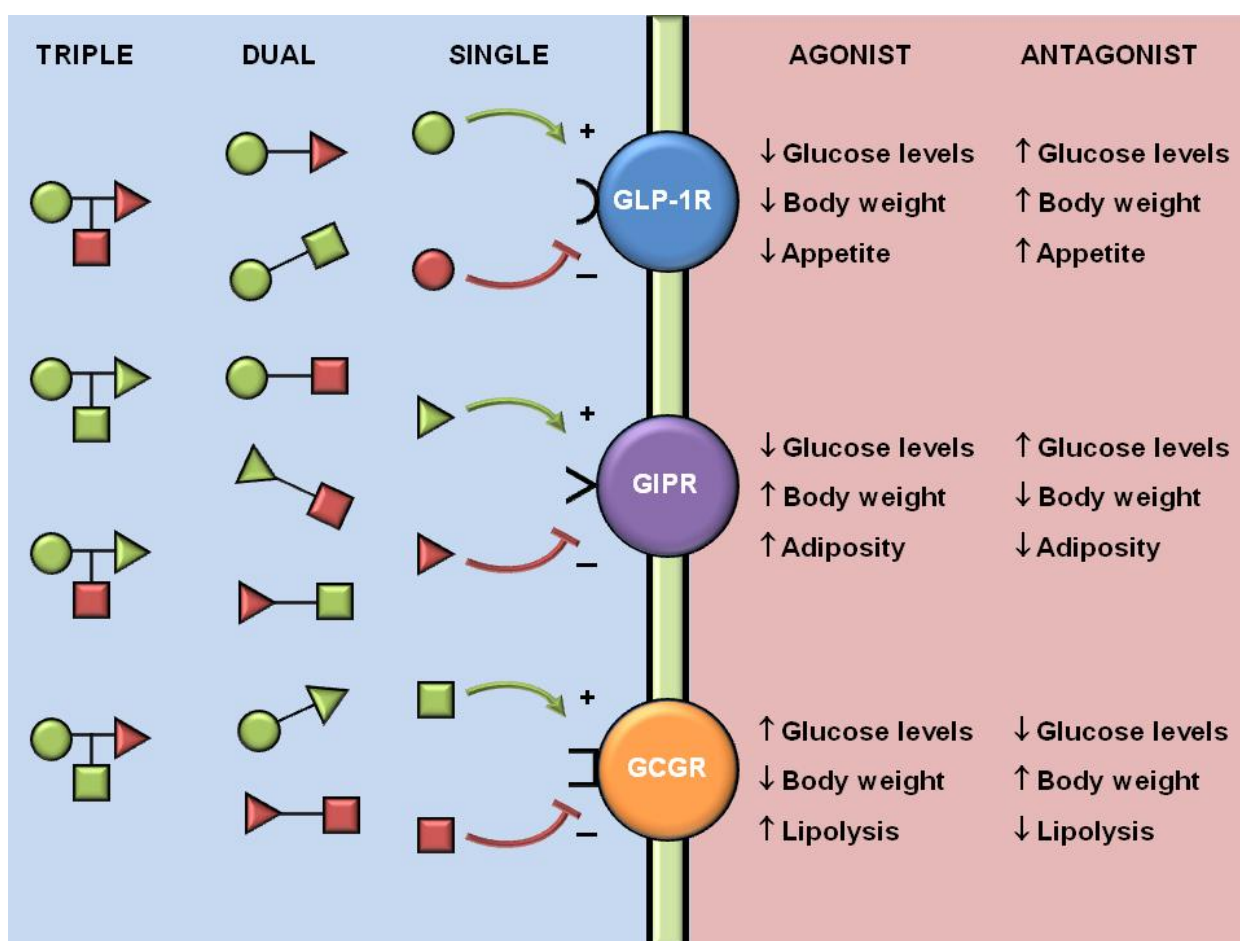
Figure 7. Single, Dual or Triple Acting Modulators of the GLP-1, GIP and GCG Receptors
Given that the sequences of GLP-1, GIP and glucagon are significantly conserved, it is feasible to develop single molecules capable of modulating combinations of these receptors. Dual or triple acting modulators may improve current therapeutics by eliciting additive therapeutic effects while balancing out undesirable effects. Compounds activating the GLP-1 receptor can reduce blood glucose levels, body weight and appetite, while antagonists of the GLP-1 receptor may have the opposite effects. Compounds stimulating the GIP receptor can reduce blood glucose levels, but may increase body weight and adiposity, while antagonists of the GIP receptor may have the opposite effects. Finally, compounds activating the glucagon receptor can increase blood glucose levels and lipolysis, but decrease body weight, while antagonists of the glucagon receptor may have the opposite effects. Shown above are some potential combinations of dual and triple acting GLP-1, GIP and glucagon receptor modulators, and a summary of the predicted basic effects of these modulators.

glucose and insulin levels (Franklin et al., 2011). These studies suggest that 4H2BH and other related compounds warrant further investigation for therapeutic potential in diabetes and obesity (Franklin et al., 2011). In conclusion, the advantage of dual (Habegger et al., 2010), or even triple, acting modulators is that these compounds may elicit additive therapeutic effects, while balancing out undesirable effects at the same time. Furthermore, different combinations of dual or triple acting modulators of the GLP-1, GIP and glucagon receptors represent novel therapeutic avenues to explore for the treatment of diabetes and obesity (Figure 7).

1.5   Thesis Investigation

1.5.1   Rationale

As described above, multiple clinical and preclinical studies have proven that incretin receptor modulators are rational targets for novel therapeutics to treat type 2 diabetes and obesity. However, the incretin receptor modulators currently available for therapeutic use are peptide-based and thus are administered via injection. Since patients generally prefer non-injectable therapeutics over injectable therapeutics (Fallowfield et al., 2006; Freemantle et al., 2005; Hatzichristou et al., 2000), there has been a pursuit to discover small molecule incretin receptor modulators that could potentially be used as oral therapeutics for the treatment of type 2 diabetes and obesity. As such, there are several recent reports of small molecule modulators of the incretin receptors (Chen et al., 2007; Franklin et al., 2011; Knudsen et al., 2007; Sloop et al., 2010; Tibaduiza et al., 2001). Thus, discovering small molecule modulators of the incretin receptors is a reasonable goal with significant implications for type 2 diabetes and obesity therapy.

In order to search for orally active modulators of the incretin receptors, we have obtained marine invertebrate and bacterial extract libraries. Marine invertebrate and bacteria were collected by the Dr. Raymond Andersen (Department of Chemistry, UBC) laboratory from tropical and cold water habitats across the world. We have elected to screen natural product extracts rather than combinatorial libraries since combinatorial libraries are usually limited by the efficiency of chemical synthesis and usually only exploit a limited array of chemical transformations (Cordier et al., 2008). Natural compounds, however, generally contain a wide array of functionally diverse and biologically active structures (Cordier et al., 2008). Many new drugs are now being developed from natural products (Newman et al., 2003). For instance, it has been shown that a considerable proportion of anticancer 'lead' compounds are natural products or their synthetic analogues (Newman et al., 2003). In addition, lengthy investigations have shown that marine invertebrates have potent biological activities and are rich in novel chemotypes (Blunt et al., 2004; Faulkner, 2002). In fact, many anti-cancer agents have been isolated from marine invertebrate metabolites (Jimeno, 2002; Loganzo et al., 2003; Mickel, 2004). However, it is possible that some compounds isolated from marine invertebrates may actually be produced by bacterial symbionts (Konig et al., 2006). An advantage of isolating compounds from bacteria is that the molecule of interest can be produced in large quantities by scaling up the cultures. Thus, it is highly likely that orally active modulators of the incretin receptors can be found in marine invertebrate and/or bacterial extract libraries.

1.5.2   Hypothesis

The overall hypothesis is that modulators of the incretin receptors can be identified in small molecule marine invertebrate and bacterial extract libraries, and that these small molecules may form the basis of novel therapeutic agents.

1.5.3   Objectives

The main objectives were to:

1) characterize the HEK-hGLP-1R-Luc, HEK-hGIPR-Luc, HEK-hGCGR-Luc and HEK-pHTS-CRE cell lines via bioassays and receptor binding assays;

2) screen for GLP-1R activators and GIPR activators and antagonists in marine invertebrate and bacterial extract libraries via the GLP-1 bioassay and the GIP bioassay; and

3) isolate, identify and characterize any hit compounds.

2   Chapter: Methods

2.1   Cell Culture

All cell lines used in this study were cultured in High Glucose-Dulbeco's Modified Eagle's Medium (HG-DMEM, Invitrogen, California, US) supplemented with 10% fetal bovine serum (FBS, GIBCO, Invitrogen, California, US) (100 U/mL) and 1X penicillin-streptomycin (Invitrogen, California, US) (100 ug/mL) at 37 °C in a 10% CO_2 atmosphere. The HEK-hGLP-1R-Luc cells were also cultured in hygromycin B (Invitrogen, California, US) (800 μg/mL) and geneticin/G418 (Invitrogen, California, US) (800 μg/mL), HEK-hGIPR-Luc cells in hygromycin B (200 μg/mL) and geneticin/G418 (500 μg/mL), HEK-hGCGR-Luc cells in hygromycin B (200 μg/mL) and puromycin (0.5 μg/mL), and HEK-pHTS-CRE cells in hygromycin B (200 μg/mL).

2.2   Cell Line Derivation: HEK-hGIPR-Luc

HEK-hGIPR-Luc cells were derived from the transformed human embryonic kidney cell line, HEK293. HEK293 cells were stably transfected with a DNA construct expressing the human GIPR to generate the HEK-GIPR cell line, which was generously donated to the Kieffer lab by Dr. Ted Usdin (National Institute of Mental Health, Maryland, US). HEK-GIPR cells were then transfected by Travis Webber (University of British Columbia) with a DNA construct containing a luciferase gene driven by a cAMP responsive element (pHTS-CRE; Biomyx) to generate the cell line HEK-hGIPR-Luc. A schematic representation of the HEK-hGIPR-Luc cell line derivation is shown in Figure 8A & 8B.

2.3   Cell Line Derivation: HEK-hGLP-1R-Luc

HEK-hGLP-1R-Luc cells were derived from the transformed human embryonic kidney cell line, HEK293. HEK293 cells were stably transfected with a DNA construct expressing the human GLP-1R under the control of the constitutively active cytomegalovirus (CMV) promoter to generate the HEK-hGLP-1R cell line (Gromada et al., 1995), which was generously donated to the Kieffer lab by Dr. Jesper Gromada (Novo Nordisk A/S, Denmark). HEK-hGLP-1R cells were then transfected by Corinna Lee (University of British Columbia) with a DNA construct containing a luciferase gene driven by a cAMP responsive element (pHTS-CRE; Biomyx) to generate the cell line HEK-hGLP-1R-Luc. A schematic representation of the HEK-hGLP-1R-Luc cell line derivation is shown in Figures 8A and 8B.
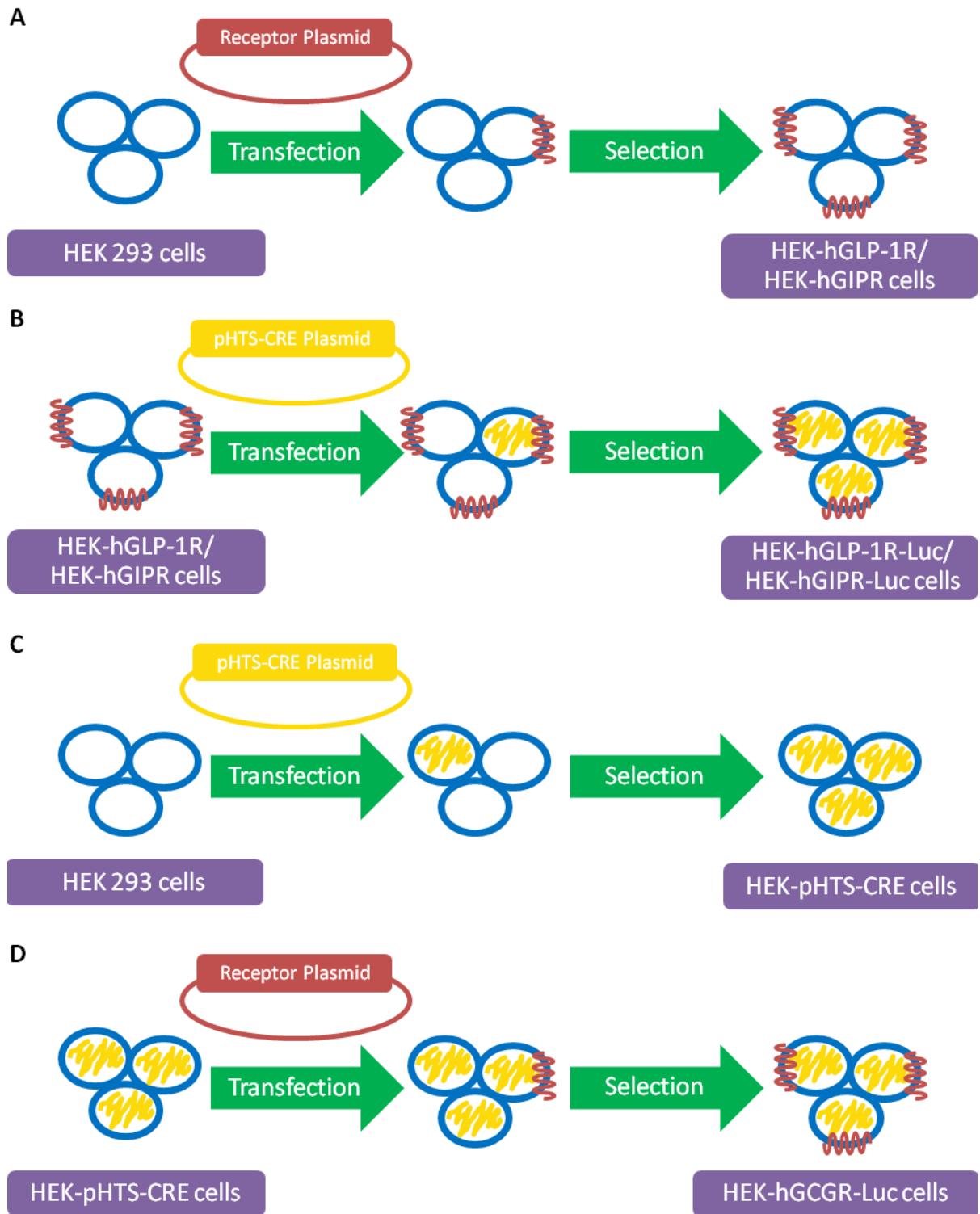
Figure 8.   Cell Line Derivation
The HEK-hGLP-1R-Luc and HEK-hGIPR-Luc cell lines were derived by first transfecting HEK 293 cells with plasmids for the respective receptors and selecting with geneticin/G418 **(A)** and then transfecting these receptor expressing cells with a pHTS-CRE plasmid and selecting with hygromycin B **(B)**. To generate the HEK-pHTS-CRE cell line, HEK 293 cells were transfected with a pHTS-CRE plasmid and then selected for with hygromycin B **(C)**. In order to yield the HEK-hGCGR-Luc cell line, HEK-pHTS-CRE cells were transfected with a plasmid carrying the GCG receptor and then selected for with puromycin **(D)**.

2.4   Cell Line Derivation: HEK-pHTS-CRE

HEK-pHTS-CRE cells were derived from the transformed human embryonic kidney cell line, HEK293, which was generously donated by Western University (Ontario, Canada). HEK293 cells were transfected by Travis Webber with a DNA construct containing a luciferase gene driven by a cAMP responsive element (pHTS-CRE; Biomyx) to generate the cell line HEK-pHTS-CRE. A schematic representation of the HEK-pHTS-CRE cell line derivation is shown in Figure 8C.

2.5   Cell Line Derivation: HEK-hGCGR-Luc

HEK-hGCGR-Luc cells were derived from the HEK-pHTS-CRE cell line. HEK-pHTS-CRE cells were stably transfected by Tahara Bhate (University of British Columbia) with a DNA construct expressing the human GCGR under the control of the constitutively active CMV promoter to generate the HEK-hGCGR-Luc cell line. A schematic representation of the HEK-hGCGR-Luc cell line derivation is shown in Figure 8D.

2.6   GIP Bioassay

HEK-hGIPR-Luc cells were plated in a 96-well flat bottom white polystyrene tissue culture plate (BD Falcon, Mississauga, ON) at a density of 7×10^4 cells/well. The cells were then incubated for 20 - 24 hours at 37 °C in a 10% CO_2 atmosphere. After the incubation period, the medium was removed by blotting the plate on paper towels. Cells were then washed with PBS (137 mM NaCl, 2.7 mM KCl, 10.1 mM Na_2HPO_4, 1.8 mM KH_2PO_4; GIBCO, Invitrogen, California, US) and blotted dry on paper towels. For the agonist screens, 100 μL of Krebs buffer (129mM NaCl, 4.8 mM KCl, 1.2 mM $MgSO_4$, 1.2 mM KH_2PO_4, 2.5 mM $CaCl_2$, 5 mM $NaHCO_3$, 10 mM HEPES, 0.5% bovine serum albumin (BSA); all from Sigma Aldrich, Ontario, Canada) supplemented with 7 mM glucose (Sigma Aldrich, Ontario, Canada) was manually added to cells, followed by the addition of ~200 nL of sponge library extract per well via a 0.4 mm pinning robot needle. For the allosteric modulator/antagonist screens, 100 μL of Krebs buffer supplemented with 7 mM glucose and 1 nM human GIP(1-42) (American Peptide Company, California, US) was manually added to cells, followed by the addition of ~200 nL of sponge library extract per well via a 0.4 mm pinning robot needle (BioRobotics, Cambridge, UK). For the preparation of the standard curves, 100 μL of serially diluted human GIP(1-42) in Krebs buffer supplemented with 7 mM glucose was added to each well. For bioassay-guided fractionation and hit validation studies, 100 μL of diluted sponge extract was manually added to each well; the solvent for these studies was either Krebs buffer supplemented with 7 mM glucose (agonist hits) or Krebs buffer supplemented with 7 mM glucose and 1 nM human GIP(1-42) (allosteric modulator/antagonist hits). After adding solutions to the plates, the cells were

incubated for 5 hours at 37 °C in a 10% CO_2 atmosphere. After the incubation, the solutions were removed and plates washed with PBS, as described above. A luciferase assay was next performed using the Bright-Glo Luciferase Assay Kit (Promega, Wisconsin, US) according to manufacturer's instructions, except that 20 μL of luciferase substrate was added to each well instead of the recommended 100 μL. The reduced volume of luciferase substrate was used in order to save costs, and did not affect the sensitivity of the bioassay (based on GLP-1 standard curves in the GLP-1 bioassay; data not shown). Luminescence was measured using a Tecan Infinite M1000 luminometer (Tecan, Männedorf, Switzerland). A schematic representation of the bioassay procedure can be seen in Figure 9.
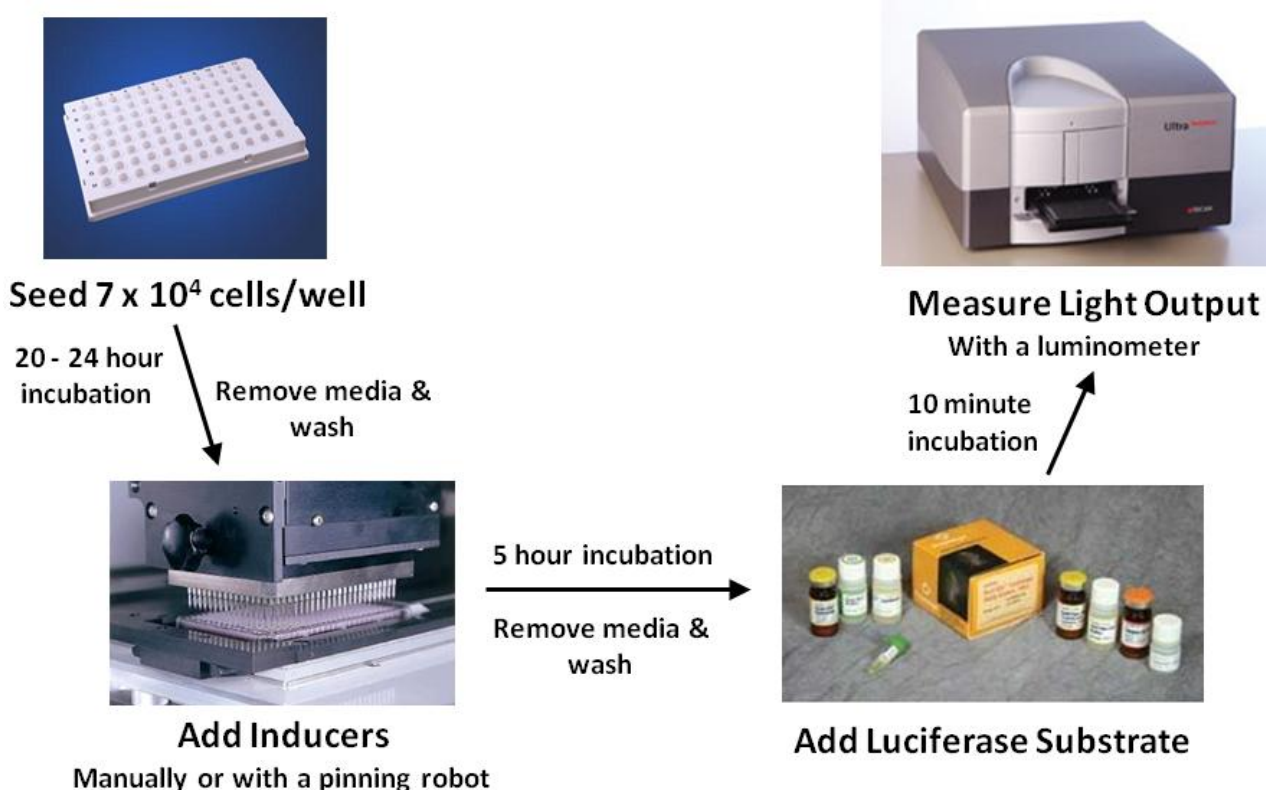
Figure 9. Bioassay Procedure
The general bioassay procedure involves seeding cells at a density of 7 x 10^4 cells/well in 96-well plates and then incubating the cells for 20 - 24 hours at 37 °C in a 10% CO_2 atmosphere. Following the incubation, the media on the cells is removed and replaced with various inducers, either manually or with a pinning robot. The cells are then incubated with the inducers at 37 °C in a 10% CO_2 atmosphere for 5 hours, after which the inducers are removed, cells washed and a luciferase assay performed. Luminescence is then measured using a luminometer.

2.7   GLP-1 Bioassay

HEK-hGLP-1R-Luc cells were plated in a 96-well flat bottom white polystyrene tissue culture plate at a density of 7×10^4 cells/well. The cells were then incubated for 20 - 24 hours at 37 °C in a 10% CO_2 atmosphere. After the incubation period, the medium was removed by blotting the plate on paper towels. Cells were then washed with PBS and blotted dry on paper towels. For the agonist screens, 100 μL of Krebs buffer supplemented with 100 μM 3-Isobutyl-1-methylxanthine (IBMX; a phosphodiesterase inhibitor; Sigma Aldrich, Ontario, Canada) was manually added to cells, followed by the addition of ~200 nL of sponge library extract per well via a 0.4 mm pinning robot needle. For the allosteric modulator screens, 100 μL of Krebs buffer supplemented with 100 μM IBMX and either 10 pM (Plate Series 1) or 3 pM (Plate Series' 2-4) human GLP-1(7-36) amide (American Peptide Company, California, US) was manually added to cells, followed by the addition of ~200 nL of sponge library extract per well via a 0.4 mm pinning robot needle. For the preparation of the standard curves, 100 μL of serially diluted human GLP-1(7-36) amide in Krebs buffer supplemented with 100 μM IBMX was added to each well. For bioassay-guided fractionation and hit validation studies, 100 μL of diluted sponge extract was manually added to each well; the solvent for these studies was either Krebs buffer supplemented with 100 μM IBMX (agonist hits) or Krebs buffer supplemented with 100 μM IBMX and either 10 pM (Plate Series 1) or 3 pM (Plate Series' 2-4) GLP-1(7-36) amide (allosteric modulator hits). After adding solutions to the plates, the cells were incubated for 5 hours at 37 °C in a 10% CO_2 atmosphere. After the incubation, the solutions were removed and plates washed with PBS, as described above. A luciferase assay was next performed using the Bright-Glo Luciferase Assay Kit according to manufacturer's instructions, except that 20 μL of luciferase substrate was added to each well instead of the recommended 100 μL. Luminescence was measured using a Tecan Infinite M1000 luminometer.   A schematic representation of the bioassay procedure can be seen in Figure 9.

2.8   HEK-pHTS-CRE Bioassay

HEK-pHTS-CRE cells were plated in a 96-well flat bottom white polystyrene tissue culture plate at a density of 7×10^4 cells/well. The cells were then incubated for 20 - 24 hours at 37 °C in a 10% CO_2 atmosphere. After the incubation period, the medium was removed by blotting the plate on paper towels. For hit validation studies, diluted sponge extracts were manually added to each well; the solvent for these studies was HG-DMEM supplemented with 10% fetal bovine serum and 1X penicillin-streptomycin. Where noted, 100 μL of forskolin (an adenylyl cyclase activator; Sigma, Missouri, US) diluted in HG-DMEM supplemented with 10% fetal bovine serum and 1X penicillin-streptomycin was included as an induced control. After adding solutions to the plates, the cells were

incubated for 5 hours at 37 °C in a 10% CO_2 atmosphere. After the incubation, the solutions were removed and plates washed with PBS and blotted dry on paper towels. A luciferase assay was next performed using the Bright-Glo Luciferase Assay Kit according to manufacturer's instructions, except that 20 μL of luciferase substrate was added to each well instead of the recommended 100 μL. Luminescence was measured using a Tecan Infinite M1000 luminometer. A schematic representation of the bioassay procedure can be seen in Figure 9.

2.9 GCG Bioassay

HEK-hGCGR-Luc cells were plated in a 96-well flat bottom white polystyrene tissue culture plate at a density of 7×10^4 cells/well. The cells were then incubated for 20 - 24 hours at 37 °C in a 10% CO_2 atmosphere. After the incubation period, the medium was removed by blotting the plate on paper towels. Cells were then washed with PBS and blotted dry on paper towels. For the preparation of the standard curves, 100 μL of serially diluted human GCG(1-29) (American Peptide Company, California, US) in Krebs buffer supplemented with 50 μM IBMX was added to each well. For hit validation studies, 100 μL of diluted sponge extract was manually added to each well; the solvent for these studies was either Krebs buffer supplemented with 50 μM IBMX (agonist hits) or Krebs buffer supplemented with 50 μM IBMX and 3 pM human GCG(1-29) (allosteric modulator/antagonist hits). After adding solutions to the plates, the cells were incubated for 5 hours incubation at 37 °C in a 10% CO_2 atmosphere. After the incubation, the solutions were removed and plates washed with PBS, as described above. A luciferase assay was next performed using the Bright-Glo Luciferase Assay Kit according to manufacturer's instructions, except that 20 μL of luciferase substrate was added to each well instead of the recommended 100 μL. Luminescence was measured using a Tecan Infinite M1000 luminometer. A schematic representation of the bioassay procedure can be seen in Figure 9.

2.10 cAMP Measurements

HEK293 cells were plated on 6 well tissue culture-treated plates (Corning, New York, US) and grown to 100% confluence at 37 °C in a 10% CO_2 atmosphere. On the day of the experiment, the cell culture medium was aspirated and the cells washed with PBS. The cells were then induced with 100 μL of alotaketal B (Dr. Raymond Andersen Laboratory, Department of Chemistry, UBC), forskolin or DMSO diluted in Krebs buffer. After adding the solutions to the wells, the cells were incubated for 30 minutes at 37 °C in a 10% CO_2 atmosphere. Following the incubation, the solutions were aspirated, plates washed three times with ice-cold PBS and 250 μL of cell lysis buffer added to each well. A cell scraper was then used to remove the cells and debris from the bottoms of the wells

and the resultant solutions transferred to Eppendorf tubes. Two freeze/thaw cycles were then carried out and cell lysis confirmed with trypan blue staining. The cells were then centrifuged at 600 relative centrifugal force (rcf) for 10 minutes at 4°C to pellet the cellular debris. The cell lysates were assayed using the R&D Systems Parameter cAMP Assay Kit (R&D Systems, Minnesota, US) according to manufacturer's instuctions.

2.11 Radioligand Binding Assays

To characterize the HEK-hGIPR-Luc, HEK-hGLP-1R-Luc and HEK-hGCGR-Luc cell lines, as well as the ability of halistanol sulphate (HS) to bind to the GIP, GLP-1 and GCG receptors, binding assays were performed. HEK-hGIPR-Luc, HEK-hGLP-1R-Luc or HEK-hGCGR-Luc cells (1×10^6) were resuspended in 800 μL binding buffer (138 mM NaCl, 5.6 mM KCl, 1.2 mM $MgCl_2$, 2.6 mM $CaCl_2$, 10 mM HEPES, 1% BSA, 10 mM glucose [all from Sigma Aldrich, Ontario, Canada] and 1% Trasylol [Bayer, Ontario, Canada]) and transferred into 1.5 mL Eppendorf tubes. Human [^{125}I]GIP(1-42), human [^{125}I]GLP-1(7-36) amide or human [^{125}I]GCG(1-29) (100 μL; ~30,000 counts per minute [cpm]; Pheonix Pharmaceuticals, California, US) was then added to the cells, in addition to various concentrations of cold human GIP(1-42), human GLP-1(7-36) amide, human GCG(1-29) or halistanol sulphate (100 μL) diluted in binding buffer. If the volume of the reaction was less than 1 mL, binding buffer was added to achieve a final volume of 1 mL. The reactions were then incubated for 30 minutes while rotating at room temperature. Following the incubation, cells were centrifuged to pellet the cells (1 min, 10,000 rcf) and the supernatant aspirated. Using a dog nail clipper, the bottoms of the Eppendorf tubes were clipped in order to transfer the pellets to borosillicate glass vials. The radioactivity in the vials was then measured via a 1277 Wallac GammaMaster gamma counter (LKB Wallac, Uppsala, Sweden).

2.12 Perifusions

The surgical isolation of the mouse islets for perifusion studies was performed by Betty Hu (University of British Columbia), as previously described (Salvalaggio et al., 2002). Briefly, islets were isolated from female wild-type mice with a C57BL/6 background using a collagenase and filtration procedure. Isolated islets were purified by hand and cultured in Roswell Park Memorial Institute 1640 media (RPMI 1640, Sigma Aldrich, Ontario, Canada) supplemented with 10 mM glucose overnight at 37 °C in a 5% CO_2 atmosphere. With assistance from Betty Hu, the perifusion experiments were performed on intact islets (~100/chamber) loaded into 300 μL temperature and CO_2 controlled chambers of an Acusyst-S perifusion apparatus (Endotronics, Minnesota, US) surrounded with Cytodex microcarrier beads (Sigma Aldrich, Ontario, Canada) (Figure 10). The

perifusate consisted of Krebs Ringer buffer (129 mM NaCl, 5 mM NaHCO$_3$, 4.8 mM KCl, 2.5 mM CaCl$_2$, 1.2 mM MgSO$_4$, 1.2 mM KH$_2$PO$_4$, 10 mM HEPES, and 5 g/L BSA) containing glucose (3 mM or 10 mM) and/or KCl (30 mM), and was gassed with 95% O$_2$ and 5% CO$_2$ and kept at 37 °C and pH 7.4. Following a 60 minute equilibration period with 3 mM glucose perifusate, sample collection was initiated. Switching between solutions was done manually via valves in the network tubing. In addition, halistanol sulphate (10 µM) and GIP(1-42) (10 nM) were infused at various time intervals. Perifusion was maintained at a rate of 0.35 mL/minute and effluent from the islets collected in 3 minute intervals using an automatic fraction collector and immediately stored at -20 °C. To determine the insulin content in the effluent, an insulin radioimmunoassay (RIA) (RI-13K; Millipore, Massachusetts, US) was performed according to manufacturer's instructions, except that half-volumes of all solutions were used for the reactions.
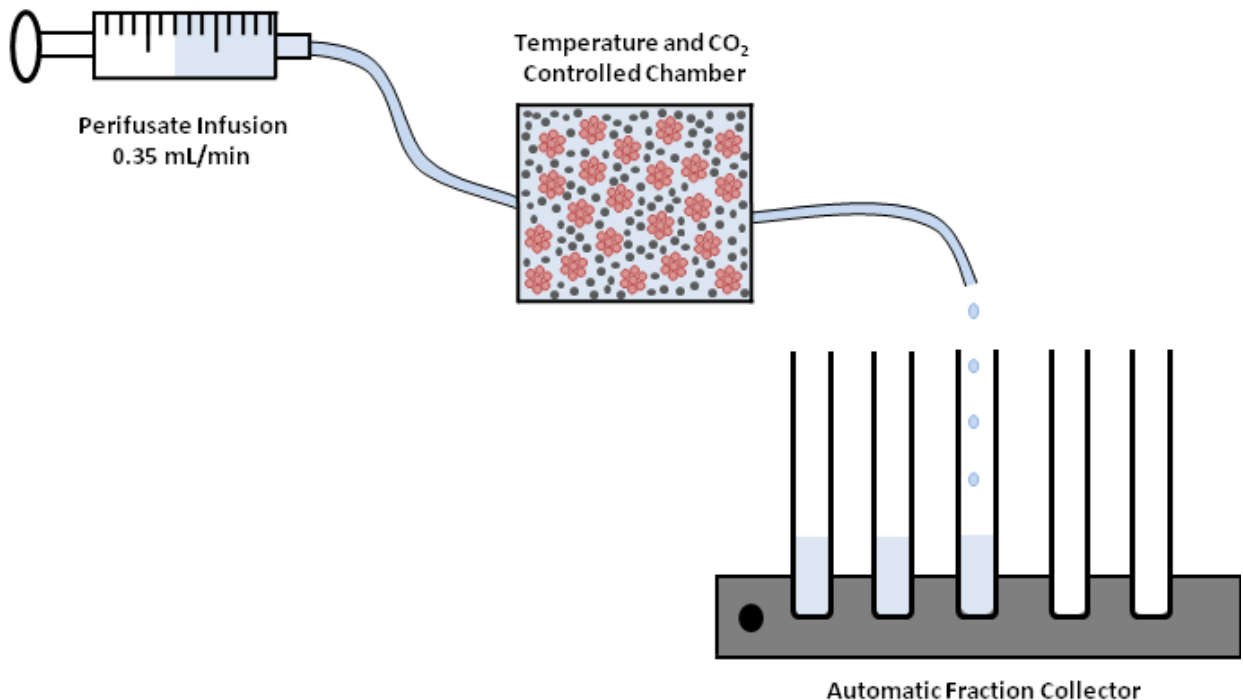
Figure 10. Mouse Islet Perifusion System
The perifusion experiment was performed, with technical assistance from Betty Hu, on intact mouse islets (~100/chamber) loaded into temperature and CO$_2$ controlled chambers of an Acusyst-S perifusion apparatus surrounded with Cytodex microcarrier beads. The perifusate was infused at a rate of 0.35 mL/minute and effluent was collected in 3 minute intervals with an automatic fraction collector.

2.13 Perfusions

The surgical isolation of the mouse pancreas for perfusion studies was performed by Gary Yang (University of British Columbia), as previously described (Fujita et al., 2010b). Briefly, male C57BL/6 mice were fasted for at least 12 but not more than 18 hours and anesthetized with intraperitoneal injections of xylazine (15 mg/kg; Bayer, Ontario, Canada) and ketamine (120 mg/kg; Bioniche Animal Health Canada, Ontario, Canada). The isolation of the mouse pancreas involved ligating the blood vessels supplying the kidneys and the adrenal glands and removing the stomach, spleen and majority of the gut, but leaving the superior mesenteric artery intact. The completed preparation contains a portion of the duodenum that is connected to the pancreas through a vascular network (Figure 11). The perfusate was infused through an aortic cannula and samples were collected via a portal vein cannula. The perfusate consisted of modified Krebs buffer (120 mM NaCl, 4.4 mM KCl, 1.2 mM $MgSO_4$, 1.5 mM KH_2PO_4, 2.5 mM $CaCl_2$, 25 mM $NaHCO_3$ and 5.1 mM dextrose) containing 3% dextran (Sigma Aldrich, Ontario, Canada), 0.2% BSA and glucose (4.4 mM or 16.7 mM), and was gassed with 95% O_2 and 5% CO_2 and kept at 37 °C and pH 7.4. Following a 30 minute equilibration period with 4.4 mM glucose perfusate, sample collection was initiated. Switching between solutions was done manually via valves in the network tubing. In addition, halistanol sulphate (10 μM) and porcine GIP(1-42) (0.2 nM; American Peptide Company, California, US) were infused at various time intervals at a rate of 0.1 mL/minute via a branch of the aortic cannula. Perfusion was maintained at a rate of 1 mL/minute with a peristaltic pump and effluent from the portal vein collected in 3 minute intervals and immediately stored at -20 °C. To determine the insulin content in the portal vein effluent, an insulin RIA (RI-13K; Millipore, Massachusetts, US) was performed according to manufacturer's instructions, except that half-volumes of all solutions were used for the reactions.
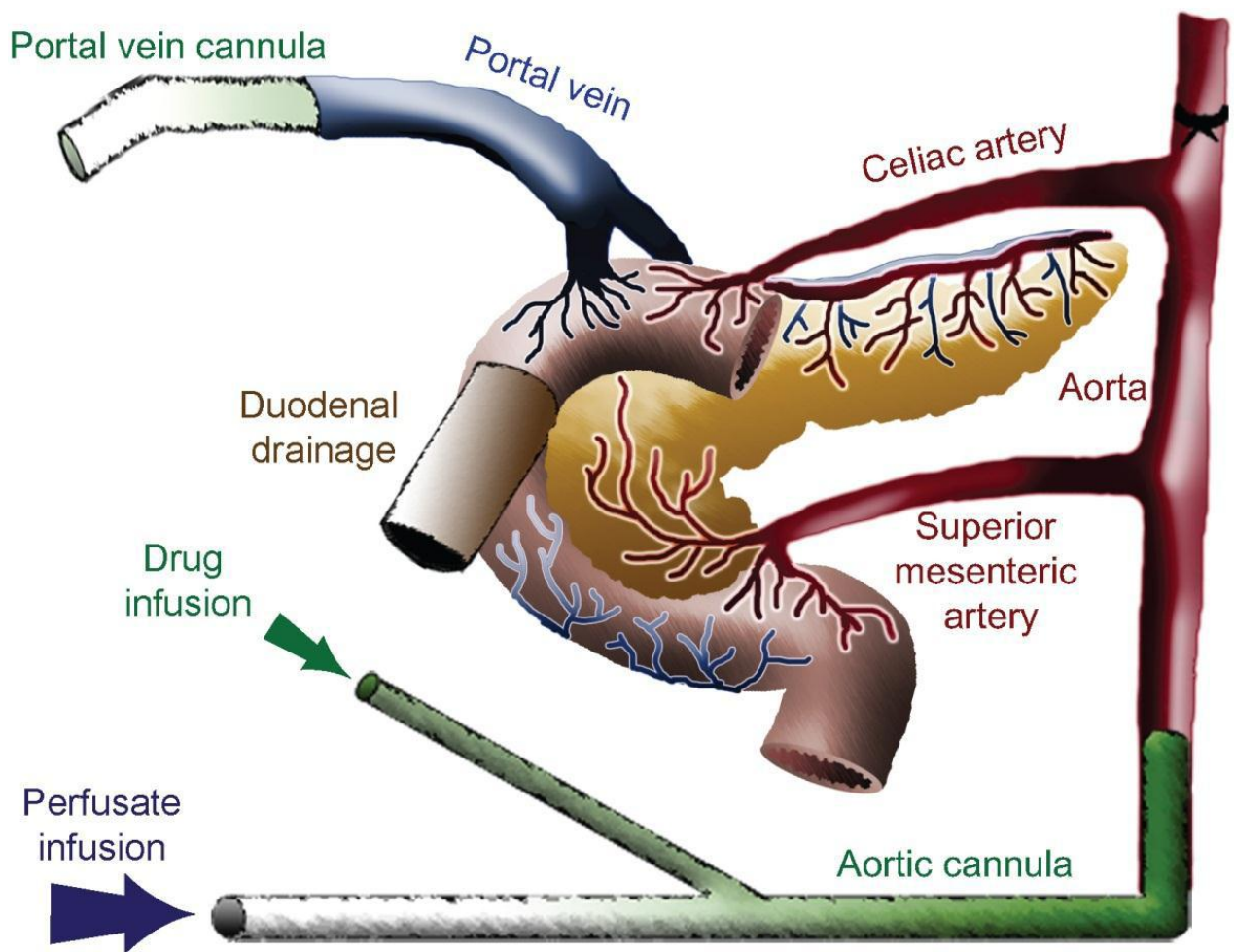
Figure 11. Vascular Perfusion Preparation of the Isolated Mouse Pancreas
The isolation of the mouse pancreas was performed *in situ* by Gary Yang by tying off the blood vessels that branch from the aorta to supply the other peripheral organs. An aortic cannula was used to infuse perfusate and drugs into the system, while a portal vein cannula was used to collect samples. Perfusate was continuously gassed with 95% oxygen and 5% carbon dioxide and kept at 37 °C and pH 7.4. Figure generated by Gary Yang.

2.14 Data Analysis

Data analysis was performed using Sigma Plot 10.01 (Systat Software Inc.; San Jose, USA). Data are presented as mean ± standard error of the mean (SEM) or mean + SEM. Statistical significance was determined using a Student's t-test (unpaired, two-tailed). Statistical significance was defined as $*P < 0.05$.

3 Chapter: Cell Line Characterization

3.1 Bioassay and Receptor Binding Assay Basics

In order to screen marine invertebrate and bacterial libraries for modulators of the GIP and GLP-1 receptors, a functional bioassay was designed. Four different cell lines, HEK-hGIPR-Luc, HEK-hGLP-1R-Luc, HEK-hGCGR-Luc and HEK-pHTS-CRE were developed for this purpose. All cell lines were transfected with a plasmid containing a luciferase gene driven by a cAMP responsive element (Figure 7). In addition, the HEK-hGIPR-Luc, HEK-hGLP-1R-Luc and HEK-hGCGR-Luc cell lines were also transfected with a plasmid containing the respective receptor (Figure 7). However, the HEK-pHTS-CRE cell line was not transfected with a receptor and was used as a negative control cell line (Figure 7). Before screening the libraries, the four cell lines were characterized in both the bioassay and receptor binding assay with respect to natural ligand activity, as well as the activity of related peptides.

The bioassays link receptor activation to luciferase activity. When the GIP, GLP-1 or GCG receptor is activated, a cAMP signalling cascade is initiated, leading to the expression of luciferase (Figure 12). The production of luciferase can also be stimulated via activation of the cAMP signalling pathway downstream of the receptor, or via another signalling pathway that also culminates in the phosphorylation of CREB and/or activation of the cAMP responsive element. In order to determine luciferase activity, luciferase substrate (luciferin) is added to the reaction, resulting in the production of light. Light output is quantified with a luminometer, and is proportional to luciferase activity. Importantly, light output can be correlated to receptor activity when using the necessary controls. The initial characterization of the cell lines in the bioassay led to the determination of the dynamic range and half maximal effective concentration (EC_{50}), and provided a basis for choosing peptide concentrations for allosteric modulator/antagonist screens.

In addition to the bioassay, the cell lines were also characterized in receptor binding assays. The receptor binding assay directly measures the ability of ligands to bind to a receptor, in contrast to the bioassay, which indirectly measures receptor binding and activation via downstream signalling events. In the receptor binding assay, cells are incubated in the presence of the iodinated natural ligand as well as various concentrations of un-labeled ligand. Following incubation, cells are centrifuged and radioactivity measured in the resulting cell pellets. The amount of radioactivity in the cell pellets is negatively related to the amount of un-labeled ligand bound to the receptor. The initial characterization of the cell lines in the receptor binding assays led to the determination of the dynamic range and half maximal inhibitory concentration (IC_{50}), in addition to offering insight into the differences between the binding and signalling capacities of the receptors.
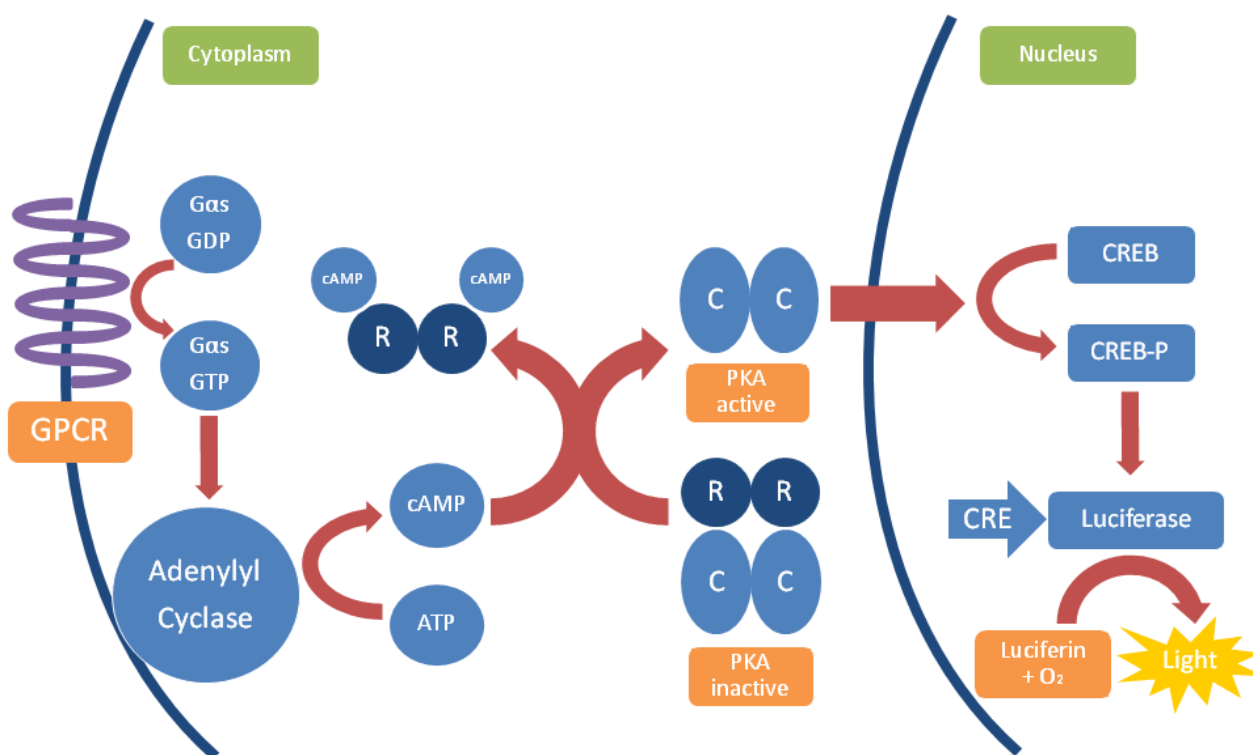
Figure 12.   Bioassay Signalling Pathway
Summary of the key intracellular steps that ultimately result in the production of luciferase in the reporter cell lines. The reporter cell lines stably express the luciferase gene driven by a cAMP responsive element (CRE), as well as the GIP, GLP-1 or GCG receptor. Stimulation of these GPCRs activates adenylyl cyclase, resulting in the formation of cAMP. Binding of cAMP to the regulatory (R) subunit of PKA results in the release of the active catalytic (C) subunit. The active kinase then translocates to the nucleus and phosphorylates the nuclear transcriptional activator, CREB, which binds to the CRE and drives luciferase expression. The addition of luciferase substrate (luciferin) to cells results in the production of light, which can be quantified in a luminometer, and is proportional to receptor activation.

3.2   HEK-hGIPR-Luc Cell Line

The HEK-hGIPR-Luc cell line was first characterized in the bioassay. A standard curve was produced by inducing HEK-hGIPR-Luc cells with varying concentrations (10^{-13} to 10^{-7} M) of human GIP(1-42). The dynamic range of the GIP bioassay was determined to be between 10^{-13} and 10^{-8} M, with the limit of detection (defined as 3 standard deviations above background) being between 10^{-13} and 10^{-12} M (Figure 13A). The EC_{50} value of the GIP bioassay was determined to be 560 pM (Figure 13A). In addition to the initial characterization of the HEK-hGIPR-Luc cell line with a GIP standard curve for the bioassay, a GIP standard curve was also produced as a positive control every time an experiment was done with the HEK-hGIPR-Luc cell line. The GIP standard curve shown is representative of all of the standard curves produced (Figure 13A). Since the bioassay is performed in white-bottom polystyrene plates, the plated cells could not be visualized. Thus, cells were also plated on clear 96-well plates when seeding cells for the bioassay in order to investigate cell density

and health. Cells were visualized in the clear 96-well plates after the initial incubation period and before adding solutions to the cells. The bioassay was only continued if the cells exhibited greater than 80% confluence and appeared healthy. On occasion, the cells did not meet these criteria (due to cell death, contamination, or an inaccurate cell count) and the bioassay was not continued. Therefore, the GIP bioassay was able to detect receptor activation over a wide range of GIP concentrations, and was deemed suitable for screening compounds to identify receptor modulators.

HEK-hGIPR-Luc cells were also characterized in the radioligand binding assay. A standard curve was produced by inducing HEK-hGIPR-Luc cells with varying concentrations (10^{-11} to 10^{-5} M) of human GIP(1-42) in the presence of a set concentration of $[^{125}I]$GIP(1-42). The dynamic range of the GIP receptor binding assay was determined to be between 10^{-11} and 10^{-5} M, with the limit of detection being between 10^{-10} and 10^{-9} M (Figure 13B). In contrast to the bioassay, an IC_{50} value was obtained rather than an EC_{50} value; this is because a higher concentration of un-labeled ligand results in less $[^{125}I]$GIP(1-42) binding. The IC_{50} value of the GIP receptor binding assay was determined to be 3.1 nM (Figure 13B). Compared to the bioassay, the IC_{50} value of the GIP receptor binding assay is slightly higher than the EC_{50} value of the GIP bioassay. This slight discrepancy in half maximal concentrations may be due to the fact that the bioassay allows for amplification of the signal via cAMP signalling and the generation of the luciferase gene product, while the receptor binding assay is solely measuring receptor binding with no allowance for amplification. Thus, the GIP receptor binding assay was able to detect receptor binding over a wide range of GIP concentrations, and was deemed a valuable tool for evaluating ligand binding to the GIP receptor.
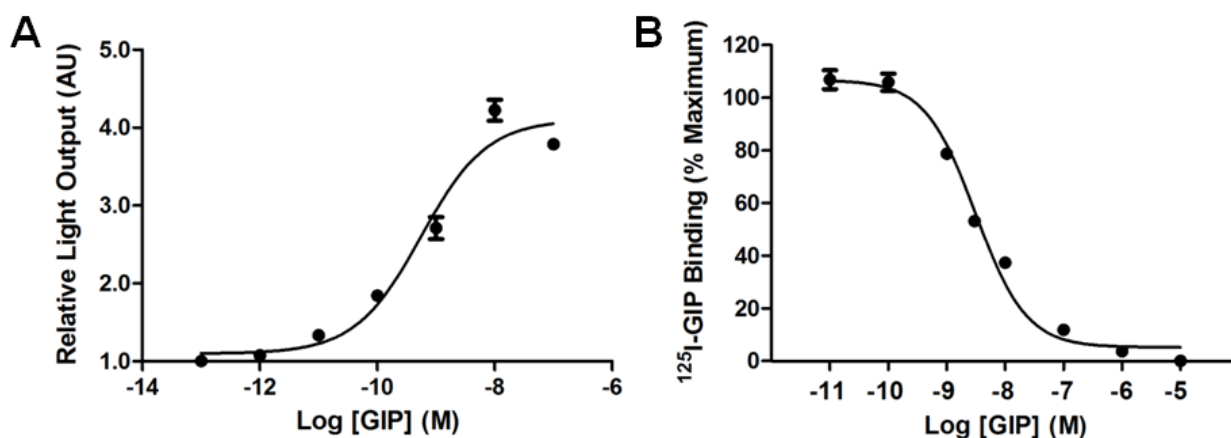
Figure 13. HEK-hGIPR-Luc Cell Line Characterization
(**A**) GIP Bioassay. HEK-hGIPR-Luc cells were induced with GIP and light output measured. The EC_{50} value was determined to be 560 pM. Relative light output was calculated by dividing total light output by background light output. Data are expressed as means ± SEM, n=3. (**B**) GIP Receptor Binding Assay. Competition of ^{125}I-GIP binding was examined with un-labelled GIP in HEK-hGIPR-Luc cells. The IC_{50} value was determined to be 3.1 nM. Values are expressed as a percentage of maximum specific binding and are means ± SEM, n=3.

The HEK-hGIPR-Luc cell line was also evaluated based on the ability of the GIP related peptides, GLP-1 and GCG, to stimulate luciferase production or light output in the bioassay. Since GIP, GLP-1 and GCG display a high level of sequence similarity (Figure 2), it is probable that GLP-1 and GCG may interact with the GIP receptor to stimulate luciferase production in the GIP bioassay. To test this theory, various concentrations (10^{-13} to 10^{-6} M) of human GIP(1-42), GLP-1(7-36) amide and GCG(1-29) were evaluated in the HEK-hGIPR-Luc bioassay. As previously described, GIP displayed an EC_{50} value of 560 pM, with a dynamic range between 10^{-13} and 10^{-8} M (Figure 14A). GCG weakly stimulated luciferase activity in the GIP bioassay at a concentration of 10^{-6} M, but an EC_{50} value was not determined (Figure 14A). However, GLP-1 did not appreciably stimulate luciferase activity in the GIP bioassay between the concentrations of 10^{-13} to 10^{-6} M. Therefore, GCG only displayed a low level of activity in the GIP bioassay, whereas GLP-1 did not display any activity. The low level of cross-reactivity of GCG and GLP-1 in the GIP bioassay demonstrates that the GIP bioassay is highly selective for GIP and is thus a suitable resource to screen for GIPR modulators.

The ability of GLP-1 and GCG to bind to the GIP receptor was also evaluated in the GIP receptor binding assay. HEK-hGIPR-Luc cells were incubated with various concentrations (10^{-11} to 10^{-5} M) of un-labeled human GIP(1-42), GLP-1(7-36) amide and GCG(1-29) in the presence of a set concentration of $[^{125}I]$GIP(1-42). As previously described, the dynamic range of the GIP receptor binding assay was determined to be between 10^{-11} and 10^{-5} M, with an IC_{50} value of 3.1 nM (Figure 14B). Similar to the bioassay, GCG was active at concentrations of 10^{-6} and 10^{-5} M and displayed an IC_{50} value of 3.9 μM (Figure 14B). However, in contrast to the bioassay, GLP-1 was active at concentrations of 10^{-6} and 10^{-5} M in the GIP receptor binding assay, and displayed an IC_{50} value of 530 μM (Figure 14B). This discrepancy may be due to the differential ability of GLP-1 to bind to the GIP receptor vs. activate GIP receptor signalling. Thus, the GIP receptor binding assay is very selective towards GIP, but also displays a low level of cross-reactivity with the related peptides, GLP-1 and GCG.
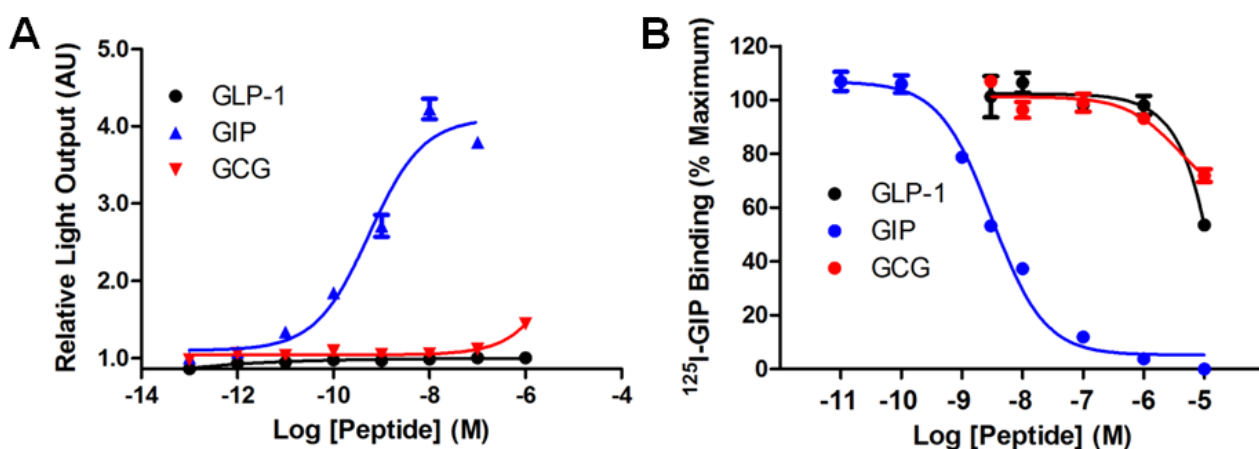
Figure 14. HEK-hGIPR-Luc Cell Line Characterization With Related Peptides
(A) GIP Bioassay. HEK-hGIPR-Luc cells were induced with GIP, GLP-1 or GCG and light output measured. The EC_{50} values were determined to be 560 pM for GIP and undetermined for GLP-1 and GCG. Relative light output was calculated by dividing total light output by background light output. Data are expressed as means ± SEM, n=3. **(B)** GIP Receptor Binding Assay. Competition of ^{125}I-GIP binding was examined with cold GIP, GLP-1 and GCG in HEK-hGIPR-Luc cells. IC_{50} values were determined to be 3.1 nM for GIP, 530 μM for GLP-1 and 3.9 μM for GCG. Values are expressed as a percentage of maximum specific binding and are means ± SEM, n=3.

3.3 HEK-hGLP-1R-Luc Cell Line

In addition to the HEK-hGIPR-Luc cell line, the HEK-hGLP-1R-Luc cell line was also characterized in the bioassay. A standard curve was produced by inducing HEK-hGLP-1R-Luc cells with varying concentrations (10^{-13} to 10^{-9} M) of human GLP-1(7-36) amide. The dynamic range of the GLP-1 bioassay was determined to be between 10^{-13} and 10^{-9} M, with the limit of detection being between 10^{-13} and 10^{-12} M (Figure 15A). In addition, the GLP-1 bioassay displayed an EC_{50} value of 2.8 pM (Figure 15A). Similarly to the GIP bioassay, a GLP-1 standard curve was produced as a positive control every time an experiment was done with the HEK-hGLP-1R-Luc cell line. The GLP-1 standard curve shown is representative of all of the standard curves completed (Figure 15A). HEK-hGLP-1R-Luc cells were also plated on clear 96-well plates and visualized after the incubation period in order to investigate cell confluence and health. As with the GIP bioassay, the GLP-1 bioassay was only continued if the cells exhibited greater than 80% confluence and appeared healthy. Thus, the GLP-1 bioassay allowed the detection of receptor activity over a wide range of GLP-1 concentrations, and was determined to be a suitable resource for the screening studies.

HEK-hGLP-1R-Luc cells were also characterized in the radioligand binding assay. A standard curve was produced by inducing HEK-hGLP-1R-Luc cells with varying concentrations (10^{-11} to 10^{-5} M) of un-labeled human GLP-1(7-36) amide in the presence of a set concentration of [125I]GLP-1(7-36) amide. The dynamic range of the receptor binding assay was determined to be between 10^{-11} and 10^{-5} M, with the limit of detection being between 10^{-10} and 10^{-9} M (Figure 15B).

In addition, the IC_{50} value of the GLP-1 receptor binding assay was determined to be 1.1 nM (Figure 15B). Similar to the results obtained for the GIP bioassay and GIP receptor binding assay, the IC_{50} value of the GLP-1 receptor binding assay is higher than the EC_{50} value of the GLP-1 bioassay. However, this discrepancy in half maximal concentrations is much larger than in the GIP receptor cell line, and is likely due to the fact that IBMX (a phosphodiesterase inhibitor) was used in the GLP-1 bioassay to increase the sensitivity, in addition to the fact that signal amplification occurs in the bioassay but not in the receptor binding assay. Furthermore, the enhanced sensitivity of the GLP-1 bioassay compared to the GIP bioassay may also be attributable to inherent differences in the abilities of the peptides to stimulate cellular signalling via their respective receptors. Thus, the GLP-1 receptor binding assay was able to detect receptor binding over a wide range of GLP-1 concentrations, and was deemed a suitable tool for evaluating ligand binding to the GLP-1 receptor.
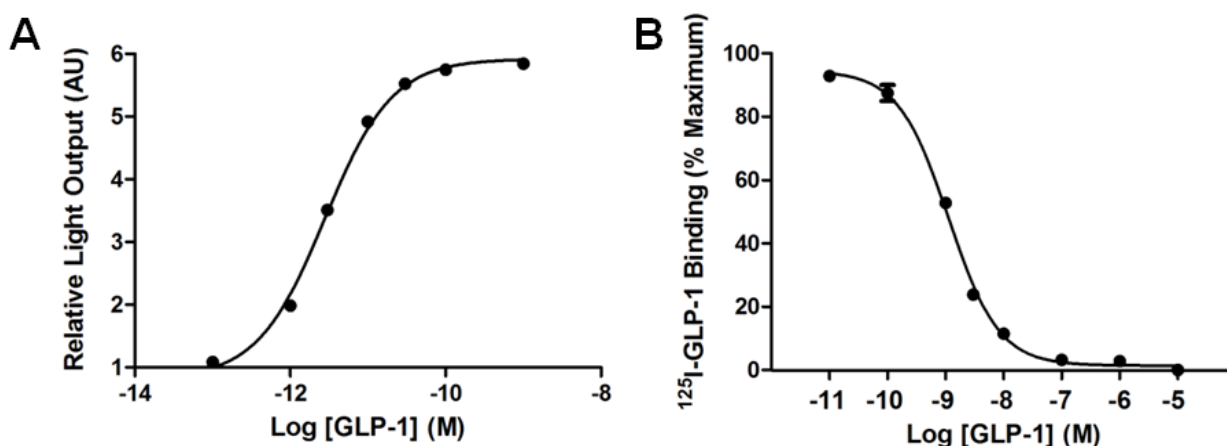
Figure 15. HEK-hGLP-1R-Luc Cell Line Characterization
(A) GLP-1 Bioassay. HEK-hGLP-1R-Luc cells were induced with GLP-1 and light output measured. The EC_{50} value was determined to be 2.8 pM. Relative light output was calculated by dividing total light output by background light output. Data are expressed as means ± SEM, n=3. **(B)** GLP-1 Receptor Binding Assay. Competition of ^{125}I-GLP-1 binding was examined with un-labelled GLP-1 in HEK-hGLP-1R-Luc cells. The IC_{50} value was determined to be 1.1 nM. Values are expressed as a percentage of maximum specific binding and are means ± SEM, n=3.

The HEK-hGLP-1R-Luc cell line was also evaluated based on the ability of the GLP-1 related peptides, GIP and GCG, to stimulate luciferase production in the bioassay. Various concentrations (10^{-13} to 10^{-6} M) of human GIP(1-42), GLP-1(7-36) amide and GCG(1-29) were evaluated in the HEK-hGLP-1R-Luc bioassay. As previously described, GLP-1 displayed an EC_{50} value of 2.8 pM with a dynamic range between 10^{-13} and 10^{-9} M (Figure 16A). GCG strongly stimulated luciferase activity in the GLP-1 bioassay, with a dynamic range between 10^{-12} and 10^{-7} M and an EC_{50} value of 100 pM (Figure 16A). These results demonstrate that the GLP-1 receptor

displays a high level of GCG cross-reactivity. Interestingly, GCG displayed a higher level of maximal luciferase expression or light output in the GLP-1 bioassay than GLP-1 itself. This suggests that GCG is able to activate GLP-1 receptor signalling more strongly than GLP-1. However, the GLP-1 bioassay is ~60 fold more selective for GLP-1 compared to GCG. GIP also displayed activity in the GLP-1 bioassay, but only at concentrations of 10^{-8} to 10^{-6} M and with an EC_{50} value of 36 nM. Therefore, GCG displayed a high level of activity in the GLP-1 bioassay, whereas GIP only displayed a low level of activity. These results demonstrate that the GLP-1 bioassay is highly selective for GLP-1 compared to GIP, but only moderately more selective compared to GCG.

The ability of GIP and GCG to bind to the GLP-1 receptor was also evaluated in the GLP-1 receptor binding assay. HEK-hGLP-1R-Luc cells were incubated with various concentrations (10^{-11} to 10^{-5} M) of un-labeled human GIP(1-42), GLP-1(7-36) amide and GCG(1-29) in the presence of a set concentration of [^{125}I]GLP-1(7-36) amide. As previously described, the dynamic range of the GLP-1 receptor binding assay was determined to be between 10^{-11} and 10^{-5} M, with an IC_{50} value of 1.1 nM (Figure 16B). GCG was active in the GLP-1 receptor binding assay at concentrations of 10^{-8} to 10^{-5} M, and displayed an IC_{50} value of 190 nM (Figure 16B). Similar to the GLP-1 bioassay, the GLP-1 receptor binding assay was ~170 fold more selective for GLP-1 compared to GCG. On the other hand, GIP displayed activity in the GLP-1 receptor binding assay at concentrations of 10^{-6} and 10^{-5} M, with an IC_{50} value of 9.0 μM (Figure 16B). GCG and GIP were both active at higher concentrations in the GLP-1 receptor binding assay compared to the GLP-1 bioassay, in parallel with the general observation that the bioassay is more sensitive than the receptor binding assay due to signal amplification. Thus, the GLP-1 receptor binding assay is selective towards GLP-1, but displays a moderate level of cross-reactivity with GCG and a low level of cross-reactivity with GIP.
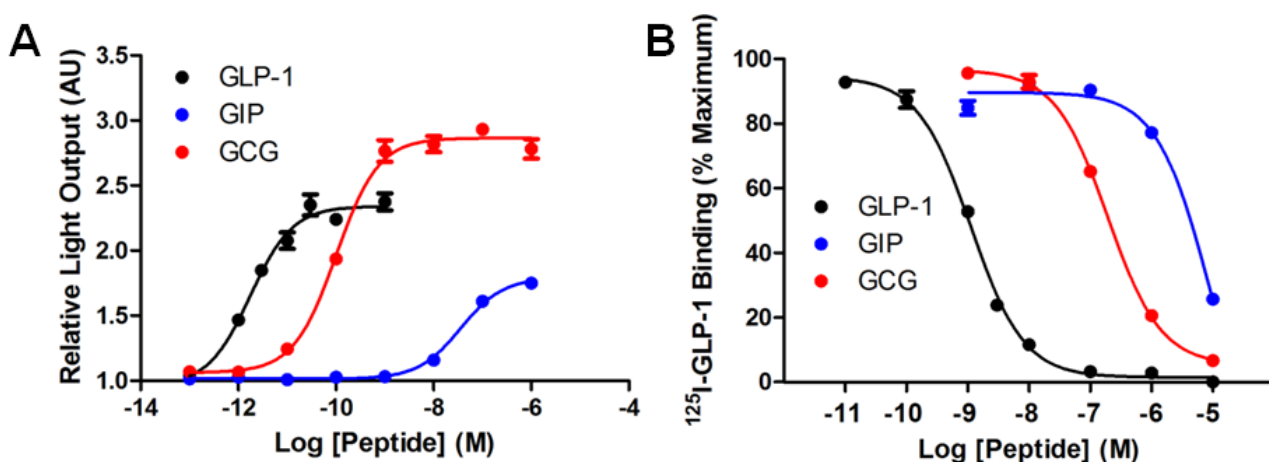
Figure 16.   HEK-hGLP-1R-Luc Cell Line Characterization With Related Peptides
(**A**) GLP-1 Bioassay. HEK-hGLP-1R-Luc cells were induced with GLP-1, GIP or GCG and light output measured. The EC_{50} values were determined to be 1.8 pM for GLP-1, 36 nM for GIP and 100 pM for GCG. Relative light output was calculated by dividing total light output by background light output.   Data are expressed as means ± SEM, n=3.   (**B**) GLP-1 Receptor Binding Assay. Competition of ^{125}I-GLP-1 binding was examined with un-labelled GLP-1, GIP and GCG in HEK-hGLP-1R-Luc cells. The IC_{50} values were determined to be 1.1 nM for GLP-1, 9.0 μM for GIP and 190 nM for GCG. Values are expressed as a percentage of maximum specific binding and are means ± SEM, n=3.

3.4   HEK-hGCGR-Luc Cell Line

In addition to the HEK-hGIPR-Luc and HEK-hGLP-1R-Luc cell lines, the HEK-hGCGR-Luc cell line was also characterized in the bioassay. A standard curve was produced by inducing HEK-hGCGR-Luc cells with varying concentrations (10^{-13} to 10^{-8} M) of human GCG(1-29). The dynamic range of the GCG bioassay was determined to be between 10^{-13} and 10^{-8} M, with the limit of detection being between 10^{-13} and 10^{-12} M (Figure 17A). In addition, the GCG bioassay displayed an EC_{50} value of 2.5 pM (Figure 17A). Similarly to the GIP and GLP-1 bioassays, a GCG standard curve was produced as a positive control every time an experiment was done with the HEK-hGCGR-Luc cell line. Again, the GCG standard curve shown is representative of all of the standard curves produced (Figure 17A). In order to investigate cell density and health, HEK-hGCGR-Luc cells were also plated on clear 96-well plates and visualized after the incubation period. As with the GIP and GLP-1 bioassays, the GCG bioassay was only continued if the cells exhibited greater than 80% confluence and appeared healthy. Thus, the GCG bioassay allowed the detection of receptor activity over a wide range of GCG concentrations, and was determined to be a valuable control cell line.

HEK-hGCGR-Luc cells were also characterized in the radioligand binding assay. A standard curve was produced by inducing HEK-hGCGR-Luc cells with varying concentrations (10^{-11} to 10^{-5} M) of un-labeled human GCG(1-29) in the presence of a set concentration of $[^{125}I]GCG(1-29)$. The dynamic range of the receptor binding assay was determined to be between 10^{-10} and 10^{-5} M, with the

limit of detection being between 10^{-11} and 10^{-10} M (Figure 17B). In addition, the IC_{50} value of the GCG receptor binding assay was determined to be 48 nM (Figure 17B). Similar to the results obtained for the assays in the HEK-hGIPR-Luc and HEK-hGLP-1R-Luc cell lines, the IC_{50} value of the GCG receptor binding assay was much higher than the EC_{50} value of the GCG bioassay. Again, this discrepancy in half maximal concentrations is probably due to the fact that signal amplification occurs in the bioassay, while the receptor binding assay measures a parameter (receptor binding) that is not subject to amplification. Furthermore, similar to the GLP-1 bioassay, the sensitivity of the GCG bioassay was enhanced by IBMX, resulting in a lower half maximal concentration. Thus, the GCG receptor binding assay was able to detect receptor binding over a wide range of GCG concentrations, and was determined to be a suitable tool to investigate the binding of various ligands to the GCG receptor.
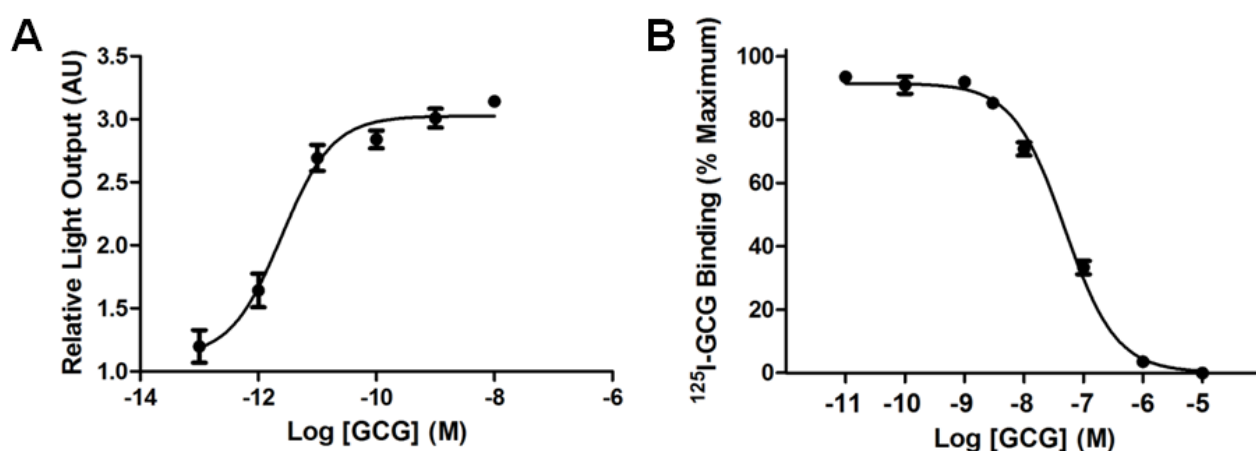
Figure 17.   HEK-hGCGR-Luc Cell Line Characterization
(A) GCG Bioassay. HEK-hGCGR-Luc cells were induced with GCG and light output measured. The EC_{50} value was determined to be 2.5 pM. Relative light output was calculated by dividing total light output by background light output. Data are expressed as means $\pm$ SEM, n=3. **(B)** GCG Receptor Binding Assay. Competition of ^{125}I-GCG binding was examined with un-labelled GCG in HEK-hGCGR-Luc cells. The IC_{50} value was determined to be 48 nM. Values are expressed as a percentage of maximum specific binding and are means $\pm$ SEM, n=3.

The HEK-hGCGR-Luc cell line was also evaluated based on the ability of the GCG related peptides, GIP and GLP-1, to stimulate luciferase production in the bioassay. Various concentrations (10^{-13} to 10^{-6} M) of human GIP(1-42), GLP-1(7-36) amide and GCG(1-29) were evaluated in the HEK-hGCGR-Luc bioassay. As already described, GCG displayed an EC_{50} value of 2.5 pM with a dynamic range between 10^{-13} and 10^{-8} M (Figure 18A). GIP was active in the GCG bioassay between the concentrations of 10^{-8} and 10^{-6} M, and displayed an EC_{50} value of 35 nM (Figure 18A). However, GLP-1 did not appreciably stimulate luciferase activity in the GCG bioassay between the

concentrations of 10^{-13} to 10^{-6} M. Therefore, GIP only displayed a low level of activity in the GCG bioassay, whereas GLP-1 did not display any activity. The low level of cross-reactivity of GIP and GLP-1 in the GCG bioassay demonstrates that the GCG bioassay is highly selective for GCG and is thus a suitable tool to measure GCG receptor bioactivity.

The ability of GIP and GLP-1 to bind to the GCG receptor was also evaluated in the GCG receptor binding assay. HEK-hGCGR-Luc cells were incubated with various concentrations (10^{-11} to 10^{-5} M) of human GIP(1-42), GLP-1(7-36) amide and GCG(1-29) in the presence of a set concentration of $[^{125}I]GCG(1-29)$. As previously discussed, the dynamic range of the GCG receptor binding assay was determined to be between 10^{-10} and 10^{-5} M, with an IC_{50} value of 48 nM (Figure 18B). Similar to the bioassay, GIP was active at concentrations of 10^{-6} and 10^{-5} M and displayed an IC_{50} value of 28 μM (Figure 18B). As with the GIP and GLP-1 assays, the slightly lower activity of GCG in the receptor binding assay compared to the bioassay is probably due to the signal amplification that occurs in the bioassay. On the other hand, similar to the bioassay, GLP-1 was not active in the GCG receptor binding assay between the concentrations of 10^{-13} to 10^{-6} M (Figure 18B). Thus, the GCG receptor binding assay is very selective towards GCG and does not display any cross-reactivity with GLP-1, but does display a low level of cross-reactivity with GIP.
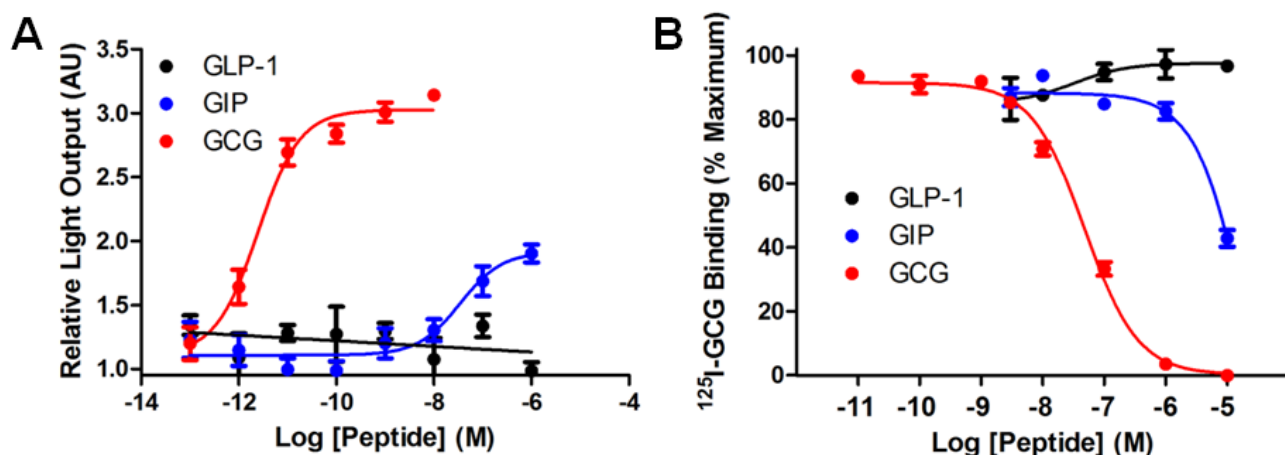
Figure 18. HEK-hGCGR-Luc Cell Line Characterization With Related Peptides
(A) GCG Bioassay. HEK-hGCGR-Luc cells were induced with GCG, GIP or GLP-1 and light output measured. The EC_{50} values were determined to be 2.5 pM for GCG, 35 nM for GIP and undetermined for GLP-1. Relative light output was calculated by dividing total light output by background light output. Data are expressed as means $\pm$ SEM, n=3. **(B)** GCG Receptor Binding Assay. Competition of ^{125}I-GCG binding was examined with un-labelled GCG, GIP and GLP-1 in HEK-hGCGR-Luc cells. The IC_{50} values were determined to be 48 nM for GCG, 28 μM for GIP and undetermined for GLP-1. Values are expressed as a percentage of maximum specific binding and are means $\pm$ SEM, n=3.

3.5   HEK-pHTS-CRE Cell Line

Finally, the HEK-pHTS-CRE cell line was also characterized in the bioassay. A standard curve was produced by inducing HEK-pHTS-CRE cells with varying concentrations (10^{-8} to 10^{-4} M) of forskolin, which activates adenylyl cyclase (the first enzyme in the cAMP signalling pathway) independent of receptor activation.   Forskolin concentration-dependently stimulated luciferase expression, with a dynamic range between 10^{-8} and 10^{-4} M and an EC_{50} value of 2.9 μM (Figure 19A).   The ability of forskolin to induce luciferase production suggests that the cAMP signalling pathway is functioning properly in the HEK-pHTS-CRE cell line.   In order to determine the suitability of HEK-pHTS-CRE as a control cell line, HEK-pHTS-CRE cells were induced with varying concentrations (10^{-13} to 10^{-6} M) of human GIP(1-42), GLP-1(7-36) amide and GCG(1-29). As seen in Figure 19B, GIP, GLP-1 and GCG do not significantly stimulate luciferase production in the HEK-pHTS-CRE cell line.   The inability of GIP, GLP-1 and GCG to stimulate luciferase production in the HEK-pHTS-CRE cell line suggests that either the HEK-pHTS-CRE cell line does not express the receptors for these peptides, or the receptors are expressed at a level so low that their ligands are not able to induce appreciable signalling.   HEK-pHTS-CRE cells were also plated on clear 96-well plates and visualized after the incubation period in order to investigate cell density and health.   As with the GIP, GLP-1 and GCG bioassays, the HEK-pHTS-CRE bioassay was only continued if the cells exhibited greater than 80% confluence and appeared healthy.   Thus, the HEK-pHTS-CRE bioassay was able to detect cAMP signalling over a wide range of forskolin concentrations but was not responsive to GIP, GLP-1 or GCG.   These results deem the HEK-pHTS-CRE cell line a valuable control cell line.
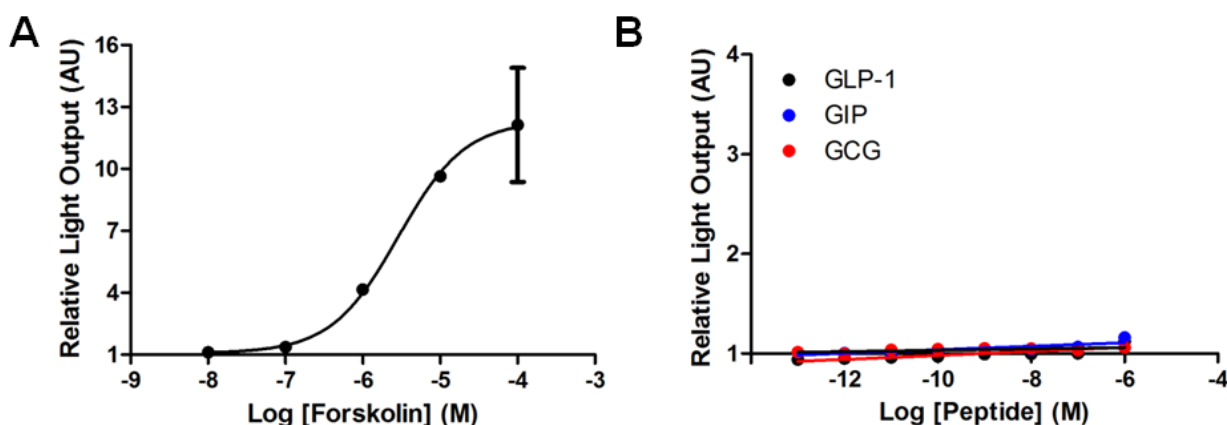
Figure 19.   HEK-pHTS-CRE Cell Line Characterization
(A) Forskolin Standard Curve. HEK-pHTS-CRE cells were induced with forskolin and light output measured. The EC_{50} value was determined to be 2.9 μM. **(B)** HEK-pHTS-CRE Characterization. HEK-pHTS-CRE cells were induced with various peptides and light output measured. The EC_{50} values were undetermined. Relative light output was calculated by dividing total light output by background light output. Data are expressed as means ± SEM, n=3.

4   Chapter: Marine Invertebrate/Bacterial Extract Screens for Incretin Receptor Modulators

4.1   Screening Overview

In this project, I screened over 2000 marine invertebrate and bacterial extracts (14 marine invertebrate extract 96-well plates and 10 bacterial extract 96-well plates) for modulators of the GIP and GLP-1 receptors. Each extract was screened in triplicate in each of four screens: the GIP receptor agonist screen, the GIP receptor allosteric modulator and antagonist screen, the GLP-1 receptor agonist screen and the GLP-1 receptor allosteric modulator screen. In the screens to search for agonists, HEK-hGIPR-Luc or HEK-hGLP-1R-Luc cells were incubated with the marine invertebrate or bacterial extracts and light output measured. To screen for allosteric modulators and antagonists, HEK-hGIPR-Luc or HEK-hGLP-1R-Luc cells were incubated with the marine invertebrate or bacterial extracts in the presence of a half-maximal effective concentration of peptide (GIP or GLP-1, respectively) and light output measured. Light output was expected to increase in the presence of a receptor agonist or allosteric modulator, and decrease in the presence of a receptor antagonist. As previously described, receptor activity is directly proportional to light output when using the necessary controls. DMSO was used as a control in the bioassay since the marine invertebrate and bacterial extracts were dissolved in DMSO. For all screens, several DMSO control wells were included to assess the effect of DMSO on light output in the bioassay. The values obtained in DMSO control wells were compared against the marine invertebrate and bacterial extract light output values to determine hits. In addition, extracts were also tested in the negative control cell line, HEK-pHTS-CRE, to determine if they were acting in a non-specific or receptor-independent manner. Extracts that also modulated light output in the HEK-pHTS-CRE cell line were deemed non-specific. For the agonist screens, hits were identified as those extracts that: (1) displayed a statistically significant increase in light output compared to DMSO controls (t-test, $p < 0.01$), (2) displayed a greater than 25% increase in light output compared to DMSO controls and (3) did not display a statistically significant increase in light output in the negative control cell line, HEK-pHTS-CRE (t-test, $p < 0.05$). For the allosteric modulator screens, hits were identified as those extracts that: (1) displayed a statistically significant increase in light output compared to DMSO controls (t-test, $p < 0.01$), (2) displayed a greater than 15% increase in light output compared to DMSO controls and (3) did not display a statistically significant increase in light output in the negative control cell line, HEK-pHTS-CRE (t-test, $p < 0.05$). For the GIP receptor antagonist screens, hits were identified as those extracts that: (1) displayed a statistically significant decrease in light output compared to DMSO controls (t-test, $p < 0.01$), (2) displayed a greater than 15% decrease in light output compared to DMSO controls and (3) did not display a statistically significant decrease in light output in the

GLP-1 receptor cell line, HEK-hGLP-1R-Luc (t-test, $p < 0.05$). HEK-hGLP-1R-Luc was used as a negative control cell line for the GIP receptor antagonist hit screens since a reduction in light output in this cell line would either indicate that the extract contains a cytotoxic or non-specific compound, or that the compound is a dual GIP/GLP-1 receptor antagonist, both outcomes of which are undesirable. Thus, the bioassay facilitated high throughput screening of marine invertebrate and bacterial extracts to identify modulators of the GIP and GLP-1 receptors.

After identifying hits, fresh aliquots of the extracts were provided by the Andersen lab and concentration-response experiments were performed in both the cell line of interest and the negative control cell line. If the fresh aliquot of the extract of interest displayed a concentration-dependent response in the cell line of interest and was not active in the negative control cell line, fractionation of the extract was initiated. Fractionation was performed by the Andersen laboratory and was bioassay-guided in order to isolate and identify the active compound(s). However, if the fresh aliquot of the extract of interest did not display activity in the cell line of interest, or if it displayed activity in the control cell line, it was ruled out as a hit and not pursued any further. Hit compounds were also tested in the other receptor cell lines (HEK-hGIPR-Luc, HEK-hGLP-1R-Luc and HEK-hGCGR-Luc) in order to determine if the hit compounds also display activity on the other glucagon family receptors. Both the glucagon family peptides and their receptors display a high level of amino acid sequence identity (Brubaker and Drucker, 2002; Irwin, 2009; Kieffer and Habener, 1999), so it is conceivable that hit compounds may exhibit activity at more than one receptor. Thus, the follow-up of hits was performed in a rigorous manner in order to concentrate on hits that might act selectively on the GIP and/or GLP-1 receptors.

4.2 GIP Receptor Agonist Screens

As described above, the GIP receptor agonist screens were performed in triplicate by incubating HEK-hGIPR-Luc cells in the presence of marine invertebrate or bacterial extracts and light output measured. GIP receptor agonist hits were identified as those extracts that: (1) displayed a statistically significant increase in light output in the HEK-hGIPR-Luc cell line compared to DMSO controls (t-test, $p < 0.01$), (2) displayed a greater than 25% increase in light output in the HEK-hGIPR-Luc cell line compared to DMSO controls and (3) did not display a statistically significant increase in light output in the negative control cell line, HEK-pHTS-CRE (t-test, $p < 0.05$). The GIP receptor agonist screen with Plate Series 1 resulted in the identification of several non-specific hits (green bars; hits that passed hit criteria (1) and (2) but not (3)), but no specific hits (Figure 20). However, the GIP receptor agonist screen with Plate Series 2 resulted in the identification of four specific hits (red bars; hits that passed hit criteria (1), (2) and (3)), as well as several non-specific hits (Figure 21). Interestingly, the GIP receptor agonist screen with Plate Series

3 did not result in the identification of any hits, specific or non-specific (Figure 22). Furthermore, the GIP receptor agonist screen with Plate Series 4 only resulted in the identification of one non-specific hit and no specific hits (Figure 23). As Plate Series 3 and 4 were comprised of bacterial extracts, while Plate Series 1 and 2 were comprised of marine invertebrate extracts, these results demonstrate that marine invertebrate extracts display a remarkably greater level of bioactivity than bacterial extracts. In summary, the GIP receptor agonist screens resulted in the identification of four specific hits to pursue.

After identifying four GIP receptor agonist hits in the marine invertebrate and bacterial extracts screens, these hits were subjected to further characterization before beginning the fractionation process. Fresh samples of the hit extracts (RJA PNG 08 100 - Anzia B: Well D6 [PNG 08-134] and RJA 47561β - 47649: Wells B9 [RJA 47582], E9 [RJA 47616] and C11 [RJA 47595]) were then obtained from the Andersen laboratory for subsequent experiments. The four hit extracts were tested at various concentrations in the HEK-hGIPR-Luc cell line; fresh samples of hits PNG 08-134 and RJA 47582 displayed significantly (t-test, $p < 0.05$) increased light output in the HEK-hGIPR-Luc cell line (data not shown), validating these extracts as hits. However, fresh samples of hits RJA 47616 and RJA 47595 did not significantly (t-test, $p < 0.05$) increase light output in the HEK-hGIPR-Luc cell line over several concentrations (data not shown), and thus were ruled out as hits and not pursued further. The fresh samples of hits PNG 08-134 and RJA 47582 were then tested in the HEK-pHTS-CRE cell line at varying concentrations. Both hits (PNG 08-134 and RJA 47582) significantly (t-test, $p < 0.05$) increased light output in the HEK-pHTS-CRE cell line (data not shown), suggesting that the hits were acting in a receptor-independent manner, classifying them as non-specific hits and eliminating them from further investigation. Therefore, the four GIP receptor agonist hits identified in the screens were ruled out as specific hits when tested at multiple concentrations in the HEK-hGIPR-Luc and HEK-pHTS-CRE cell lines.
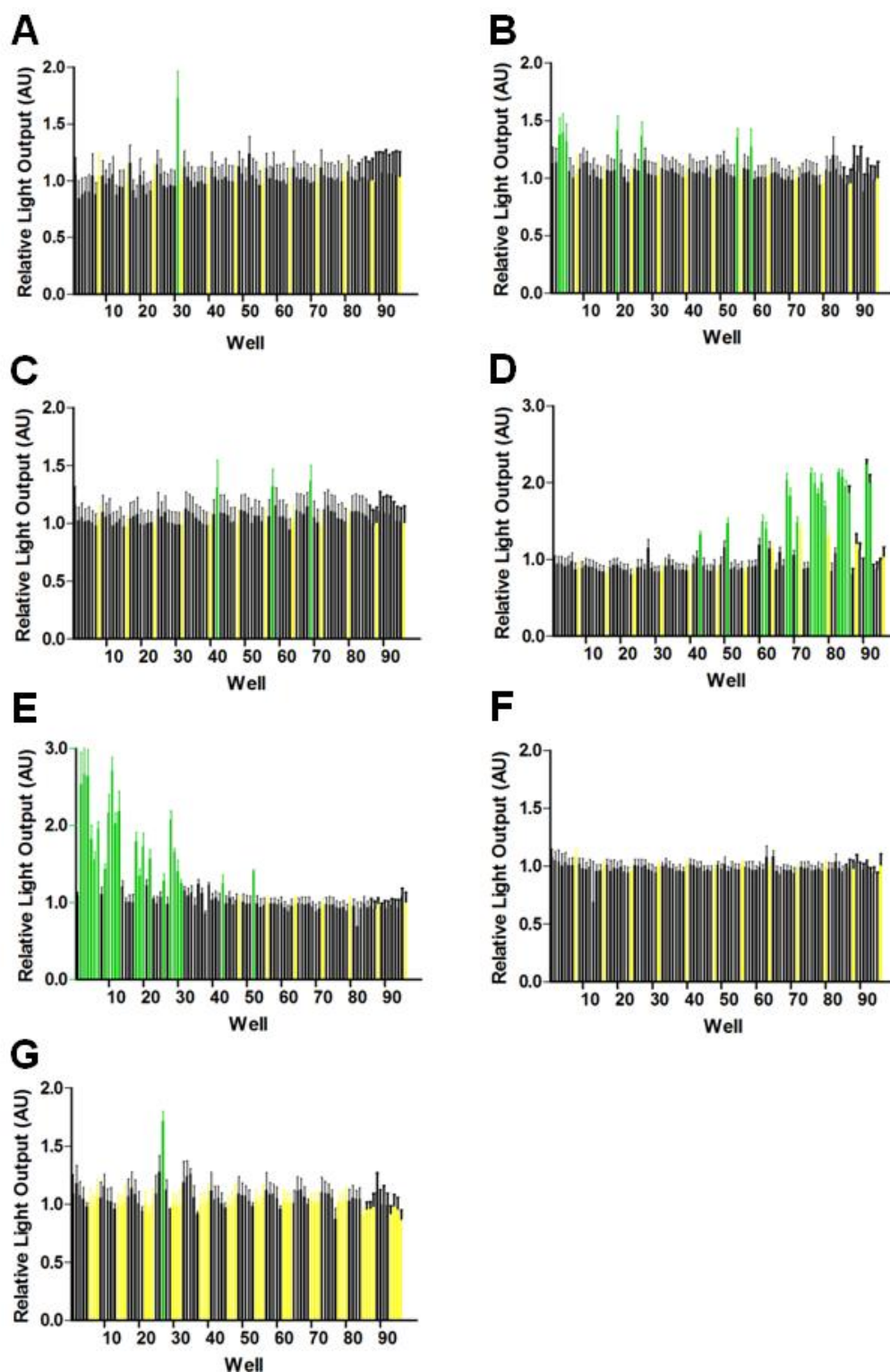
Figure 20. GIP Receptor Agonist Screen With Plate Series 1
(A) RJA 03 37 - 119. **(B)** RJA 03 121 - 204. **(C)** RJA 03 205 - 287. **(D)** RJA 03 289 - 372. **(E)** RJA 03 373 - 500. **(F)** RJA 05 1 - 84. **(G)** RJA 75907. HEK-hGIPR-Luc cells were induced with 200 nl of marine invertebrate extract and light output measured. Yellow bars represent DMSO control wells and green bars represent non-specific hits. Relative light output was calculated by dividing total light output by the average DMSO light output. Data are expressed as means ± SEM, n=3.
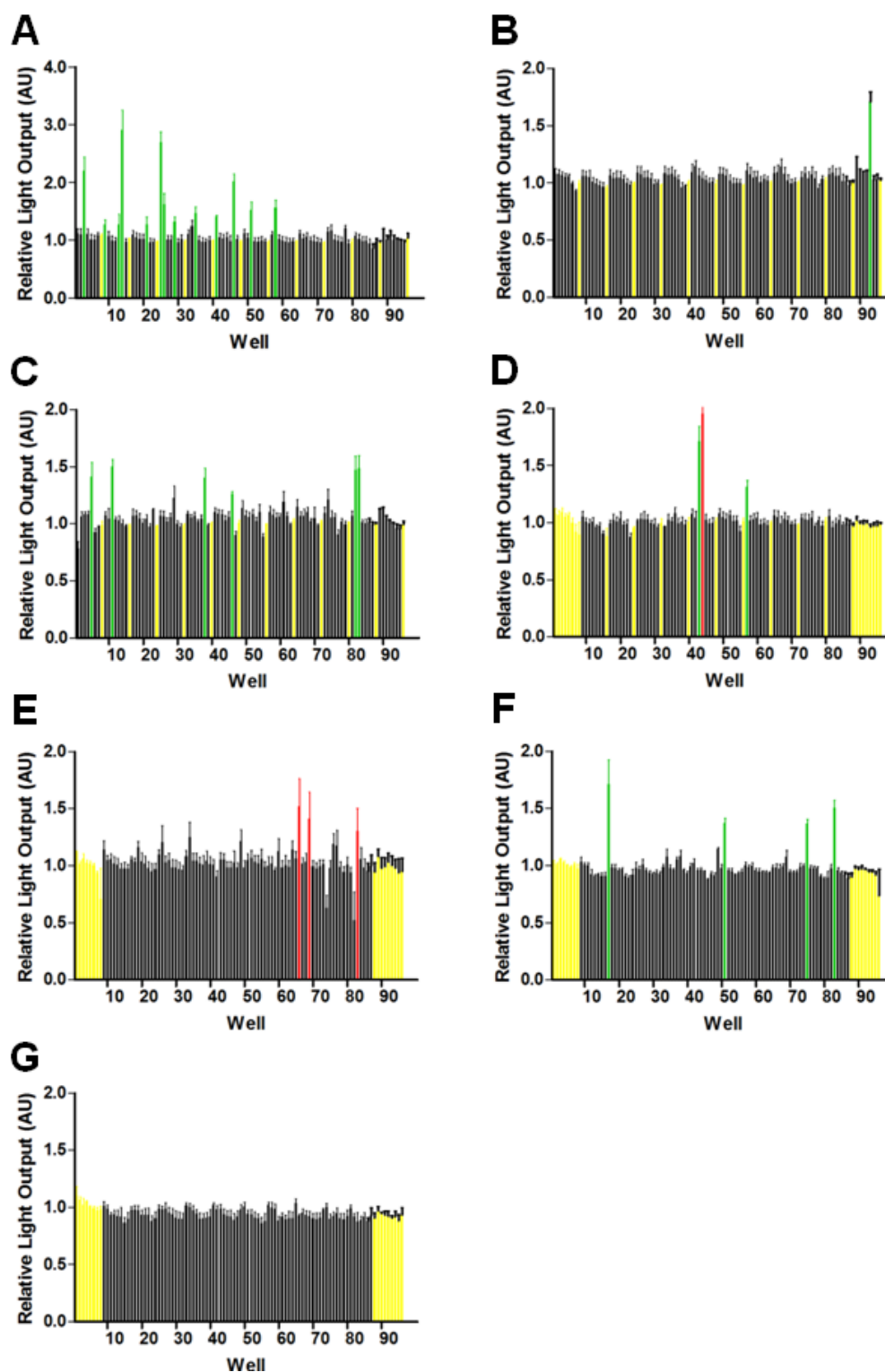
Figure 21.   GIP Receptor Agonist Screen With Plate Series 2
(A) RJA 04 1 - 90. **(B)** RJA 04 91 - 06 114. **(C)** RJA 06 3 - 90. **(D)** RJA PNG 08 100 - Anzia B.
(E) RJA 47561β - 47649. **(F)** RJA 55261β - 55340. **(G)** RJA 76351β - PHP 90 489. HEK-hGIPR-
Luc cells were induced with 200 nl of marine invertebrate extract and light output measured. Yellow
bars represent DMSO control wells, green bars represent non-specific hits and red bars represent
specific hits.   Relative light output was calculated by dividing total light output by the average
DMSO light output. Data are expressed as means ± SEM, n=3.
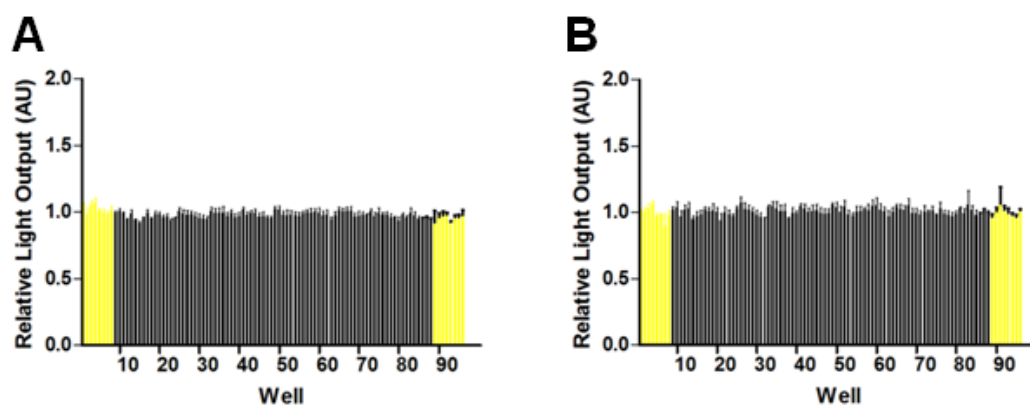
Figure 22. GIP Receptor Agonist Screen With Plate Series 3
(A) RJA CHEM 2891- 2970. **(B)** RJA CHEM 2971 - 3050. HEK-hGIPR-Luc cells were induced with 200 nl of bacterial extract and light output measured. Yellow bars represent DMSO control wells. Relative light output was calculated by dividing total light output by the average DMSO light output. Data are expressed as means ± SEM, n=3.
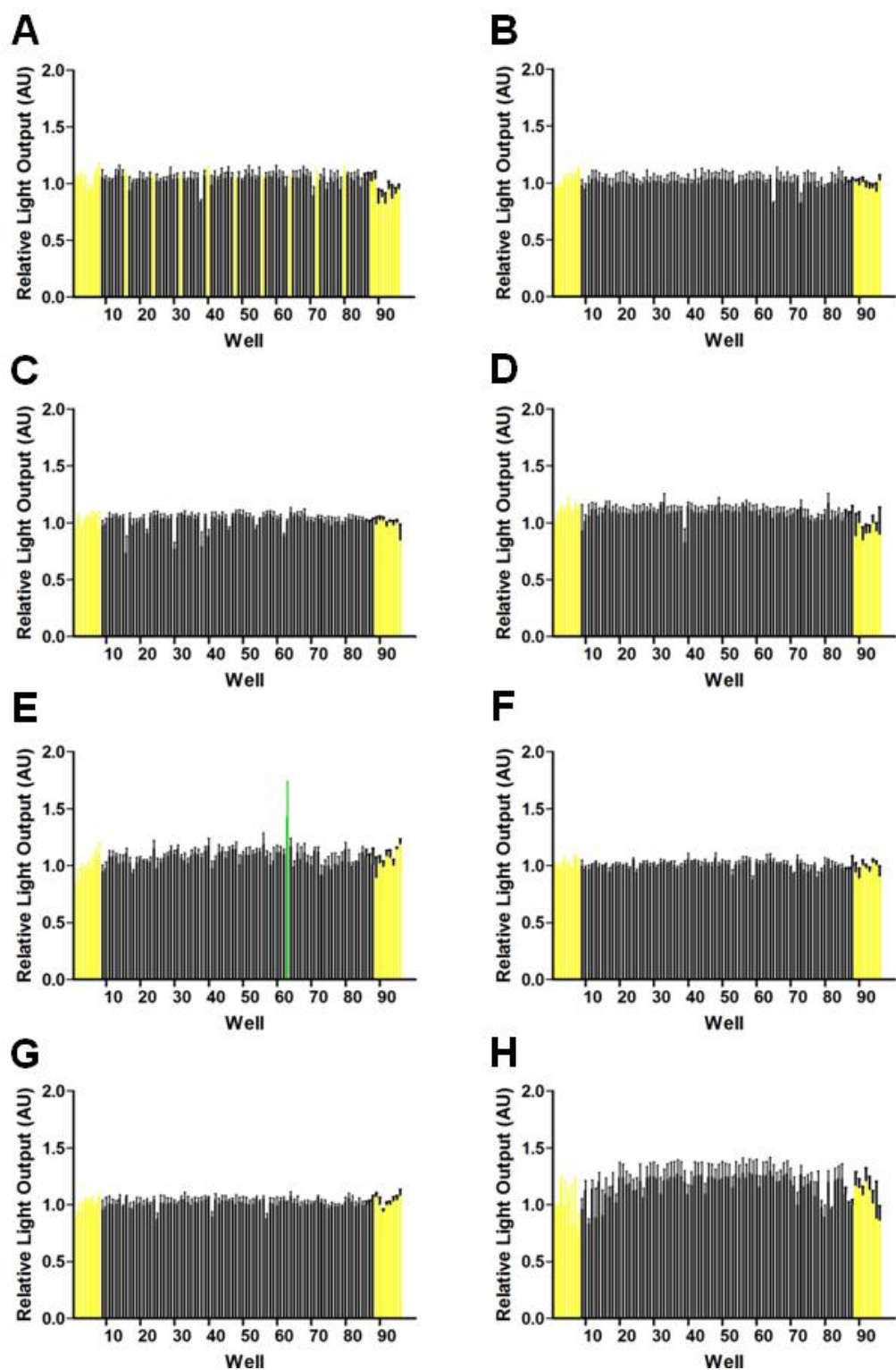
Figure 23. GIP Receptor Agonist Screen With Plate Series 4
(**A**) RJA BACT 3189. (**B**) RJA BACT 3257. (**C**) RJA BACT 3337. (**D**) RJA BACT 3417. (**E**) RJA BACT 3497. (**F**) RJA BACT 3577. (**G**) RJA BACT 3657. (**H**) RJA BACT 3737. HEK-hGIPR-Luc cells were induced with 200 nl of bacterial extract and light output measured. Yellow bars represent DMSO control wells and green bars represent non-specific hits. Relative light output was calculated by dividing total light output by the average DMSO light output. Data are expressed as means ± SEM, n=3.

4.3   GIP Receptor Allosteric Modulator and Antagonist Screens

The GIP receptor allosteric modulator and antagonist screens were performed in triplicate by incubating HEK-hGIPR-Luc cells with marine invertebrate or bacterial extracts in the presence of a half maximal concentration of GIP and light output measured. GIP receptor allosteric modulator hits were identified as those extracts that: (1) displayed a statistically significant increase in light output in the HEK-hGIPR-Luc cell line compared to DMSO controls (t-test, $p < 0.01$), (2) displayed a greater than 15% increase in light output in the HEK-hGIPR-Luc cell line compared to DMSO controls and (3) did not display a statistically significant increase in light output in the HEK-pHTS-CRE cell line (t-test, $p < 0.05$). The GIP receptor allosteric modulator screen with Plate Series 1 resulted in the identification of several non-specific hits (green bars; hits that passed hit criteria (1) and (2) but not (3)) but no specific hits (hits that passed hit criteria (1), (2) and (3)) (Figure 24). Likewise, the GIP receptor allosteric modulator screen with Plate Series 2 resulted in the identification of several non-specific hits but no specific hits (Figure 25). However, the GIP receptor allosteric modulator screen with Plate Series 3 did not result in the identification of any hits, specific or non-specific (Figure 26). Similarly, the GIP receptor allosteric modulator screen with Plate Series 4 did not result in the identification of any hits (Figure 27). As with the GIP receptor agonist screens, the marine invertebrate extracts displayed much more activity than the bacterial extracts. Thus, the GIP receptor allosteric modulator screens did not identify any specific hits to pursue.

Although the GIP receptor allosteric modulator and antagonist screens did not identify any specific GIP receptor allosteric modulator hits to pursue, several specific GIP receptor antagonist hits were identified. GIP receptor antagonist hits were identified as those extracts that: (1) displayed a statistically significant decrease in light output in the HEK-hGIPR-Luc cell line compared to DMSO controls (t-test, $p < 0.01$), (2) displayed a greater than 15% decrease in light output in the HEK-hGIPR-Luc cell line compared to DMSO controls and (3) did not display a statistically significant decrease in light output in the HEK-hGLP-1R-Luc cell line (t-test, $p < 0.05$). The GIP receptor antagonist screen with Plate Series 1 resulted in the identification of ten specific hits (orange bars; hits that passed hit criteria (1), (2) and (3)), as well as several non-specific hits (blue bars; hits that passed hit criteria (1) and (2) but not (3)) (Figure 24). In addition, four specific hits, as well as several non-specific hits, were identified in the GIP receptor antagonist screen with Plate Series 2 (Figure 25). However, the GIP receptor antagonist screen with Plate Series 3 only resulted in the identification of one non-specific hit, and no specific hits (Figure 26). Finally, the GIP receptor antagonist screen with Plate Series 4 resulted in the identification of seven specific hits, in addition to several non-specific hits (Figure 27). Thus, the GIP receptor antagonist screens resulted in the identification of twenty-one specific hits to pursue.

The ten hits identified in the GIP receptor antagonist screens with Plate Series 1 were subjected to further characterization before beginning the fractionation process. Fresh samples of the GIP receptor antagonist hit extracts (RJA 03 121 - 204: Well D8 [RJA 03-164], RJA 03 205 - 287: Wells BI [RJA 03-217], D1 [RJA 03-241], D2 [RJA 03-242] and G8 [RJA 03-284], RJA 03 289 - 372: Wells F3 [RJA 03-351], G3 [RJA 03-363], F4 [RJA 03-352] and G4 [RJA 03-364] and RJA 03 373 - 500: Well G10 [RJA 03-486]) were obtained from the Andersen laboratory for this purpose. The ten hit extracts were tested at various concentrations in the HEK-hGIPR-Luc cell line in the presence of a half maximal concentration of GIP; fresh samples of hits RJA 03-164, RJA 03-217, RJA 03-241, RJA 03-242, RJA 03-284, RJA 03-351, RJA 03-363, RJA 03-352 and RJA 03-486 displayed significantly (t-test, $p<0.05$) decreased light output in the HEK-hGIPR-Luc cell line in the presence of GIP (data not shown), validating these extracts as hits. However, the fresh sample of extract RJA 03-364 did not significantly decrease light output in the HEK-hGIPR-Luc cell line in the presence of GIP (data not shown), and was ruled out as a hit and not further pursued. Fresh samples of the hit extracts were then tested at various concentrations in the HEK-hGLP-1R-Luc cell line in the presence of GLP-1; hit extracts RJA 03-217, RJA 03-241, RJA 03-351, and RJA 03-363 significantly (t-test, $p<0.05$) decreased light output in this experiment (data not shown), resulting in the characterization of these hits as non-specific hit and eliminating them from further investigation. Hit extracts RJA 03-242, RJA 03-284 and RJA 03-352 did not significantly decrease light output in the HEK-hGLP-1R-Luc cell line in the presence of GLP-1 (data not shown), but were not fractionated since the Andersen laboratory did not have enough of these extracts available for further testing. Nonetheless, hit extracts RJA 03-164 and RJA 03-486, which also did not significantly decrease light output in the HEK-hGLP-1R-Luc cell line in the presence of GLP-1 (data not shown), were fractionated in order to identify the active compound(s). After fractionating hit extract RJA 03-164, it was revealed that the active fraction significantly (t-test, $p<0.05$) decreased light output in the HEK-hGLP-1R-Luc cell line in the presence of GLP-1 in a concentration-response experiment (data not shown); extract RJA 03-164 was thus classified as a non-specific hit and was not further pursued. Finally, the fractionation of hit extract RJA 03-486 resulted in the identification of halistanol sulphate (a GIP receptor antagonist and GLP-1 receptor agonist), as described in section 5.2.1. Thus, six of the GIP receptor antagonist hits identified in Plate Series 1 were ruled out as specific hits (1 post-fractionation), three were not pursued due to a lack of material and one was determined to be an actual GIP receptor antagonist.

The four hits identified in the GIPR antagonist screen with Plate Series 2 were also subjected to further characterization before beginning the fractionation process. Fresh samples of the hit extracts (RJA 04 91 - 06 114: Wells F10 [RJA 06-99], G1 [RJA 06-102] and G5 [RJA 06-107] and

RJA 55261β - 55340: Well G10 [RJA 55329]) were obtained from the Andersen laboratory and tested at various concentrations in the HEK-hGIPR-Luc cell line in the presence of GIP. Fresh samples of all four hit extracts significantly (t-test, p<0.05) decreased light output in the HEK-hGIPR-Luc cell line in the presence of GIP, validating these extracts as hits (data not shown). On the other hand, the fresh sample of hit RJA 55329 displayed significantly (t-test, p<0.05) decreased light output in the HEK-hGLP-1R-Luc cell line in the presence of GLP-1 (data not shown), resulting in its characterization as a non-specific hit and eliminating it from further investigation. Hit extracts RJA 06-99, RJA 06-102 and RJA 06-107 did not significantly decrease light output in the HEK-hGLP-1R-Luc cell line in the presence of GLP-1 (data not shown), and were thus fractionated in order to identify the active compound(s). After fractionating hit extracts RJA 06-99 and RJA 06-102, it was revealed that the active fractions of these hits significantly (t-test, p<0.05) decreased light output in the HEK-hGLP-1R-Luc cell line in the presence of GLP-1 in a concentration-response experiment (data not shown); extracts RJA 06-99 and RJA 06-102 were thus classified as non-specific hits and were not further pursued. Fractionated hit extract RJA 06-107 did not significantly decrease light output in the HEK-hGLP-1R-Luc cell line in the presence of GLP-1 at any of the concentrations tested (data not shown). However, the active fraction of hit extract RJA 06-107 significantly (t-test, p<0.05) decreased light output in the HEK-hGIPR-Luc cell line in the absence of GIP in a concentration-response experiment (data not shown), suggesting that the active fraction was acting in a cytotoxic manner and ruling out hit extract RJA 06-107 as a specific hit. Therefore, the four GIP receptor antagonist hits identified in Plate Series 2 were ruled out as specific hits upon further investigation.

Finally, the hits identified in the GIPR antagonist screen with Plate Series 4 were also subjected to further characterization before beginning the fractionation process. However, further characterization of three hit extracts (RJA BACT 3337: Wells F6 [RJA 3391], RJA BACT 3577: Well A4 [RJA 3579] and RJA BACT 3737: Well E6 [RJA 3781]) was not performed since the Andersen laboratory did not have fresh samples of these extracts available for testing. Nonetheless, fresh samples of the other four hit extracts (RJA BACT 3189: Well F5 [RJA 3189], RJA BACT 3337: Well F3 [RJA 3388] and RJA BACT 3737: Wells E7 [RJA 3782] and E8 [RJA 3783]) were obtained from the Andersen laboratory and tested at various concentrations in the HEK-hGIPR-Luc cell line in the presence of GIP. Fresh samples of all four hit extracts significantly (t-test, p<0.05) decreased light output in the HEK-hGIPR-Luc cell line in the presence of GIP, validating these extracts as hits (data not shown). Fresh samples of the hit extracts were then tested at various concentrations in the HEK-hGLP-1R-Luc cell line in the presence of GLP-1; the fresh samples of hit extracts RJA 3388 and RJA 3783 displayed significantly (t-test, p<0.05) decreased light output in

this experiment (data not shown), resulting in their characterization as non-specific hits and eliminating them from further investigation. Hit extracts RJA 3242 and RJA 3782 did not significantly decrease light output in the HEK-hGLP-1R-Luc cell line in the presence of GLP-1 (data not shown), but did significantly (t-test, $p<0.05$) decrease light output in the HEK-hGIPR-Luc cell line in the absence of GIP in a concentration-response experiment (data not shown), suggesting that these extracts were acting in a cytotoxic manner and ruling them out as specific hits. Therefore, four of the GIP receptor antagonist hits identified in Plate Series 4 were ruled out as specific hits upon further investigation, while the other three hits were not pursued due to a lack of material.
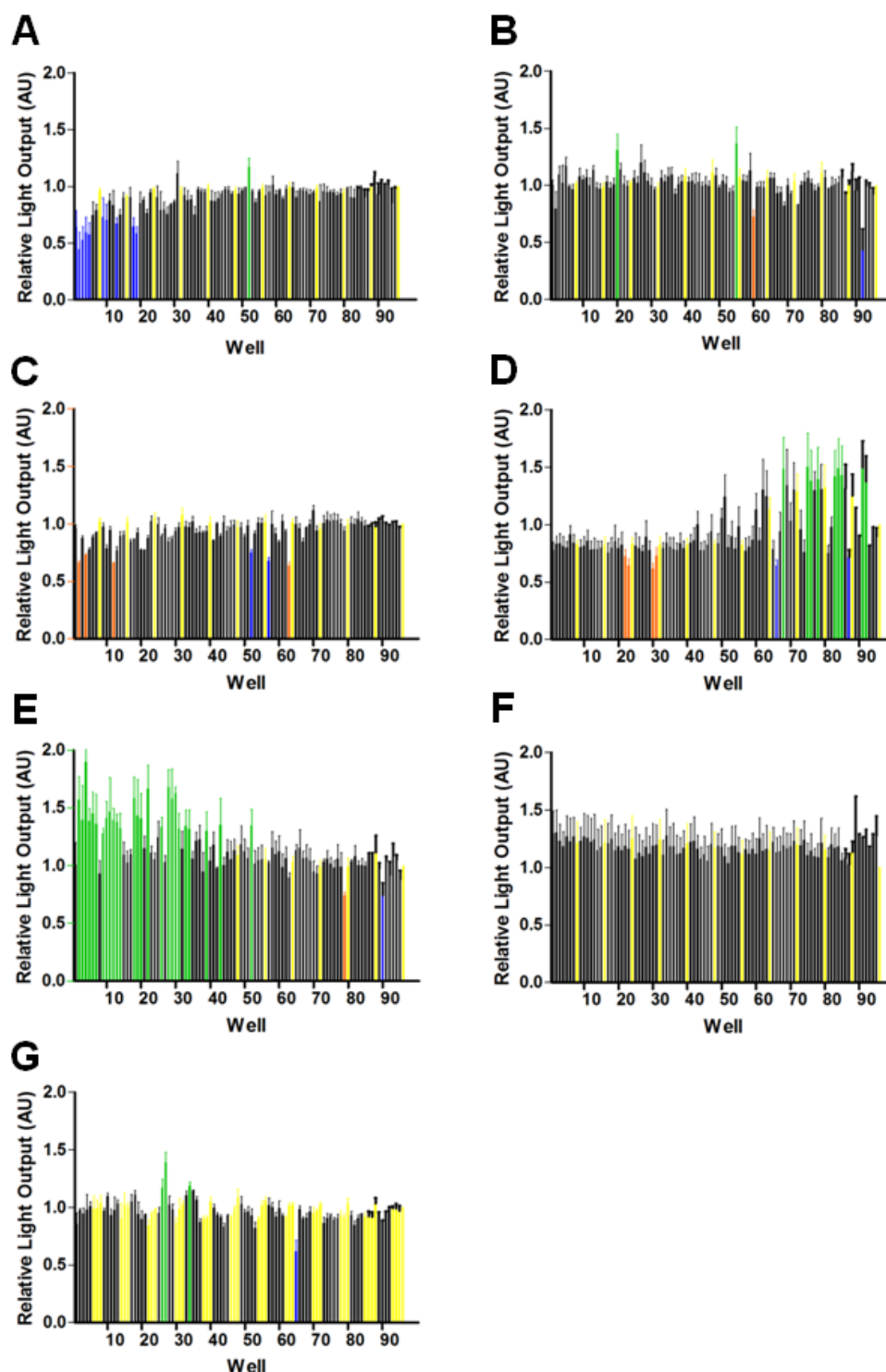
Figure 24.   GIP Receptor Allosteric Modulator and Antagonist Screen With Plate Series 1
(A) RJA 03 37 - 119. **(B)** RJA 03 121 - 204. **(C)** RJA 03 205 - 287. **(D)** RJA 03 289 - 372. **(E)** RJA 03 373 - 500. **(F)** RJA 05 1 - 84. **(G)** RJA 75907. HEK-hGIPR-Luc cells were induced with 200 nl of marine invertebrate extract in the presence of 1 nM GIP and light output measured. Yellow bars represent DMSO control wells, green bars represent non-specific allosteric modulator hits, orange bars represent specific antagonist hits and blue bars represent non-specific antagonist hits. Relative light output was calculated by dividing total light output by the average DMSO light output. Data are expressed as means ± SEM, n=3.

Figure 25. GIP Receptor Allosteric Modulator and Antagonist Screen With Plate Series 2
(A) RJA 04 1 - 90. **(B)** RJA 04 91 - 06 114. **(C)** RJA 06 3 - 90. **(D)** RJA PNG 08 100 - Anzia B.
(E) RJA 47561β - 47649. **(F)** RJA 55261β - 55340. **(G)** RJA 76351β - PHP 90 489. HEK-hGIPR-
Luc cells were induced with 200 nl of marine invertebrate extract in the presence of 1 nM GIP and
light output measured. Yellow bars represent DMSO control wells, green bars represent non-specific
allosteric modulator hits, orange bars represent specific antagonist hits and blue bars represent non-
specific antagonist hits. Relative light output was calculated by dividing total light output by the
average DMSO light output. Data are expressed as means ± SEM, n=3.

Figure 26.   GIP Receptor Allosteric Modulator and Antagonist Screen With Plate Series 3
(A) RJA CHEM 2891- 2970. **(B)** RJA CHEM 2971 - 3050. HEK-hGIPR-Luc cells were induced with 200 nl of bacterial extract in the presence of 1 nM GIP and light output measured. Yellow bars represent DMSO control wells and blue bars represent non-specific antagonist hits. Relative light output was calculated by dividing total light output by the average DMSO light output. Data are expressed as means ± SEM, n=3.
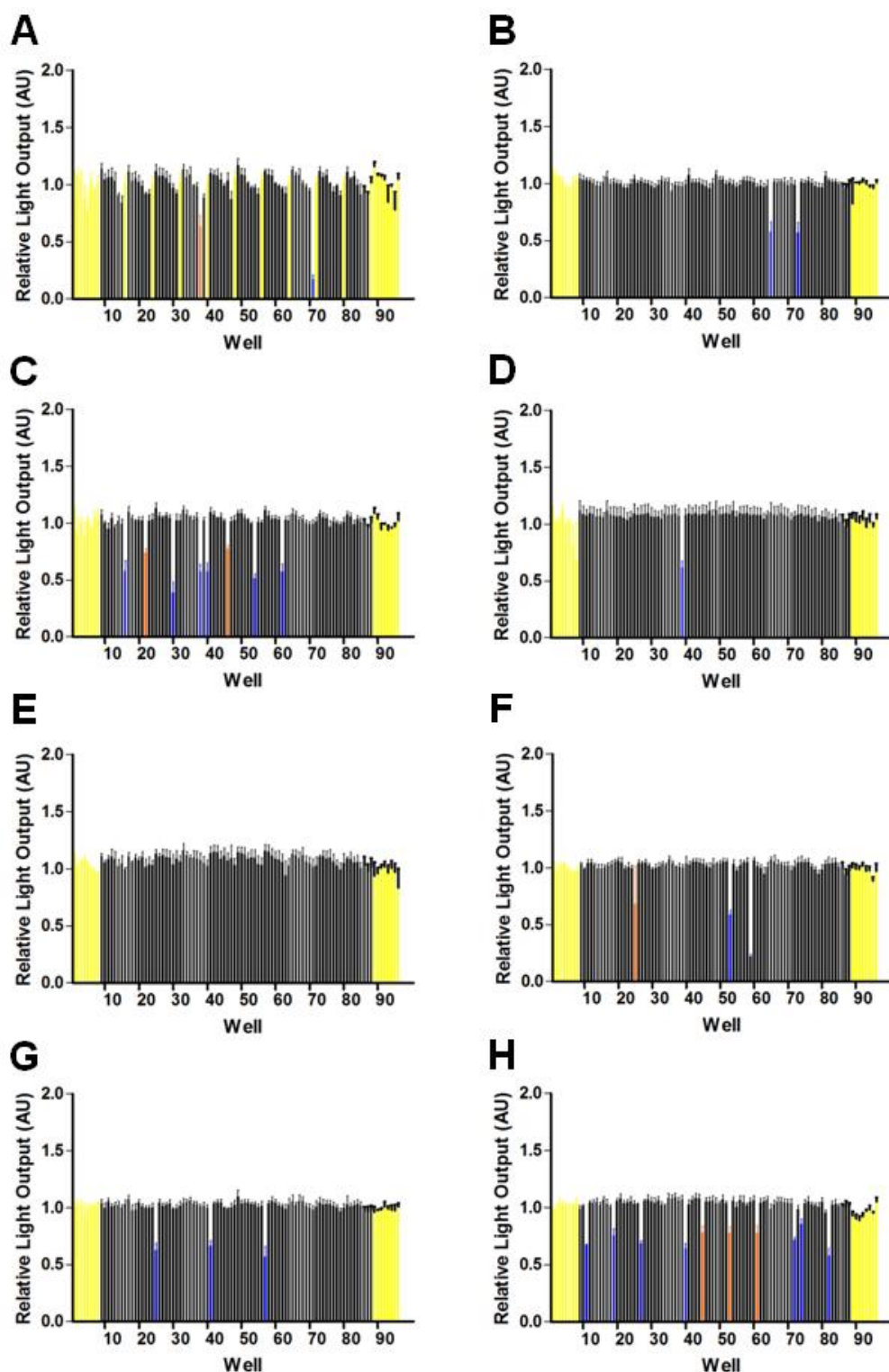
Figure 27.   GIP Receptor Allosteric Modulator and Antagonist Screen With Plate Series 4
(A) RJA BACT 3189. **(B)** RJA BACT 3257. **(C)** RJA BACT 3337. **(D)** RJA BACT 3417. **(E)** RJA BACT 3497. **(F)** RJA BACT 3577. **(G)** RJA BACT 3657. **(H)** RJA BACT 3737. HEK-hGIPR-Luc cells were induced with 200 nl of bacterial extract in the presence of 1 nM GIP and light output measured. Yellow bars represent DMSO control wells, orange bars represent specific antagonist hits and blue bars represent non-specific antagonist hits.   Relative light output was calculated by dividing total light output by the average DMSO light output. Data are expressed as means ± SEM, n=3.

77

4.4 GLP-1 Receptor Agonist Screens

Similar to the GIP receptor agonist screens, the GLP-1 receptor agonist screens were performed in triplicate by incubating HEK-hGLP-1R-Luc cells in the presence of marine invertebrate or bacterial extracts and light output measured. GLP-1 receptor agonist hits were identified as those extracts that: (1) displayed a statistically significant increase in light output in the HEK-hGLP-1R-Luc cell line compared to DMSO controls (t-test, p < 0.01), (2) displayed a greater than 25% increase in light output in the HEK-hGLP-1R-Luc cell line compared to DMSO controls an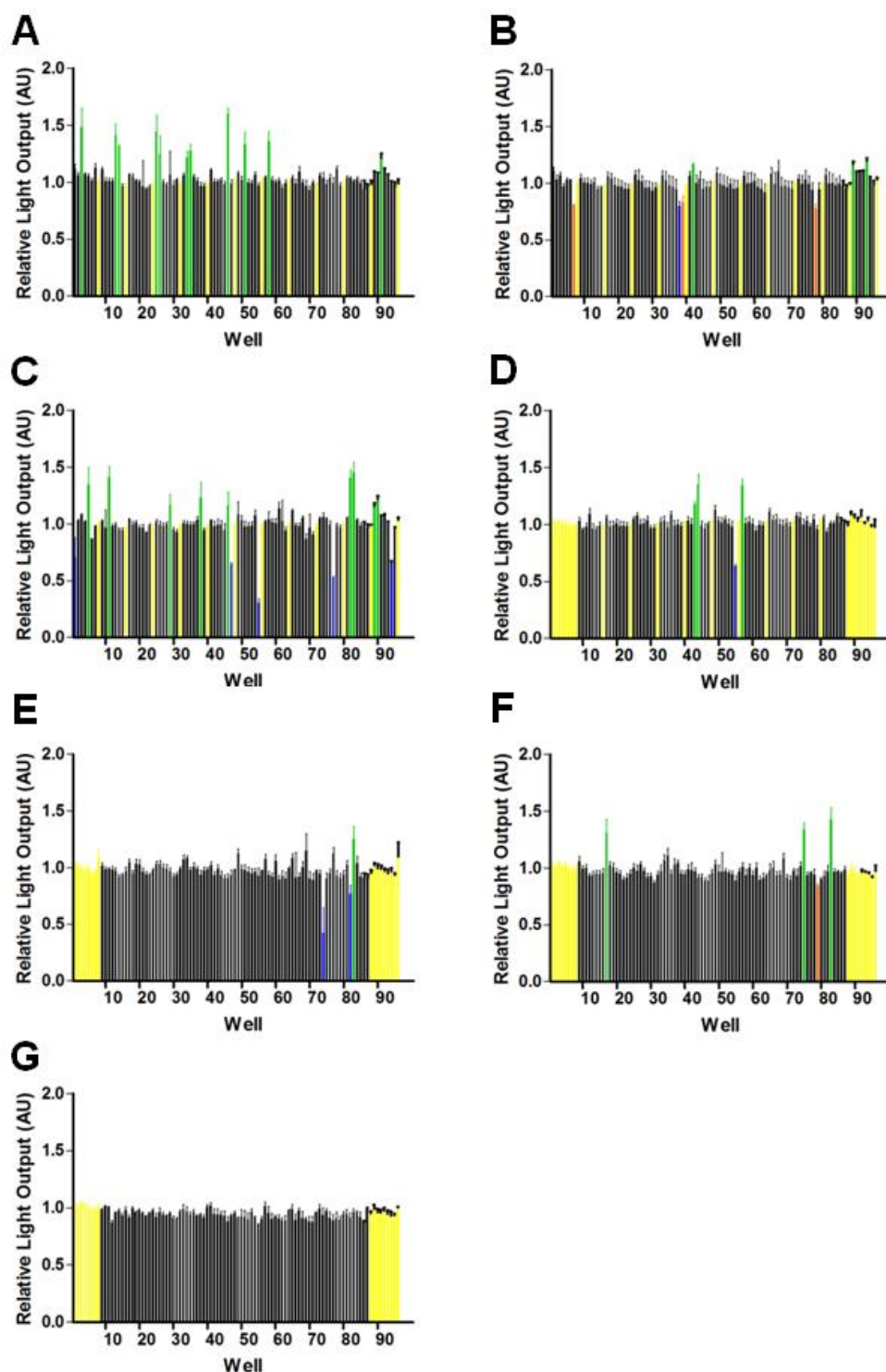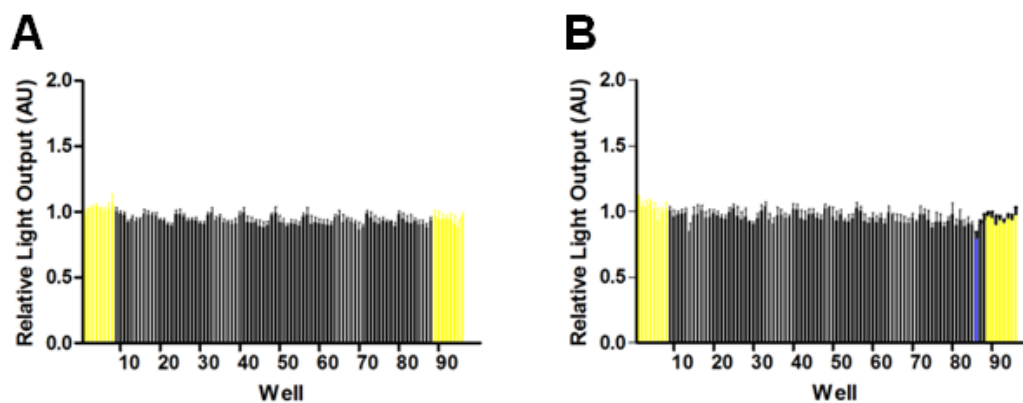d (3) did not display a statistically significant increase in light output in the negative control cell line, HEK-pHTS-CRE (t-test, p < 0.05). The GLP-1 receptor agonist screen with Plate Series 1 resulted in the identification of seven specific hits (red bars; hits that passed hit criteria (1), (2) and (3)), and several non-specific hits (green bars; hits that passed hit criteria (1) and (2) but not (3)) (Figure 28). In addition, two specific hits, as well as several non-specific hits, were identified in the GLP-1 receptor agonist screen with Plate Series 2 (Figure 29). On the other hand, the GLP-1 receptor agonist screen with Plate Series 3 did not result in the identification of any hits, specific or non-specific (Figure 30). Likewise, the GLP-1 receptor agonist screen with Plate Series 4 only resulted in the identification of one non-specific hit and no specific hits (Figure 31). As with the GIP receptor screens, the marine invertebrate extracts displayed much more activity than the bacterial extracts. Thus, the GLP-1 receptor agonist screens resulted in the identification of nine specific hits to pursue.

The seven hits identified in the GLP-1 receptor agonist screens with Plate Series 1 were subjected to further characterization before beginning the fractionation process. Fresh samples of the GLP-1 receptor hit extracts (RJA 03 373 - 500: Wells B1 [RJA 03-385] and C2 [RJA 03-398], RJA 05 1 - 84: Well G3 [RJA 05 - 75] and RJA 75907: Wells D4 [RJA 75947], E4 [RJA 75959], C9 [RJA 75939] and D11 [RJA 75954]) were obtained from the Andersen laboratory for this purpose. The seven hit extracts were tested at various concentrations in the HEK-hGLP-1R-Luc cell line; fresh samples of hits RJA 03-385, RJA 03-398, RJA 05-75, RJA 75959, RJA 75939 and RJA 75954 displayed significantly (t-test, p<0.05) increased light output in the HEK-hGLP-1R-Luc cell line (data not shown), validating these extracts as hits. However, the fresh sample of extract RJA 75947 did not significantly (t-test, p<0.05) stimulate light output in the HEK-hGLP-1R-Luc cell line over multiple concentrations (data not shown), and was ruled out as a hit and not further pursued. Varying concentrations of the fresh samples of hits RJA 03-385, RJA 03-398, RJA 05-75, RJA 75959, RJA 75939 and RJA 75954 were then tested in the HEK-pHTS-CRE cell line. Hit extracts RJA 03-385, RJA 75959, RJA 75939 and RJA 75954 significantly (t-test, p<0.05) stimulated light output in the HEK-pHTS-CRE cell line (data not shown), resulting in the classification of these extracts as non-specific hits and eliminating them from further investigation. Hit extracts RJA 03-398 and RJA 05-

75 did not increase light output in the HEK-pHTS-CRE cell line and were thus fractionated in order to identify the active compound(s). After fractionating hit extract RJA 05-75, it was revealed that the active fraction increased light output in the HEK-pHTS-CRE cell line in a concentration-response experiment (data not shown); extract 05-75 was classified as a non-specific hit and was not further pursued. Finally, the fractionation of hit extract RJA 03-398 resulted in the identification of the alotaketals (compounds that activate the cAMP signalling pathway), as described in section 5.1.1. Thus, the seven GLP-1 receptor agonist hits identified in Plate Series 1 were ruled out as specific hits (2 post-fractionation) when tested at varying concentrations in the HEK-hGLP-1R-Luc and HEK-pHTS-CRE cell lines.

The two hits identified in the GLP-1R agonist screen with Plate Series 2 were also subjected to further characterization before beginning the fractionation process. Fresh samples of the hit extracts (RJA 04 91 - 06 114: Well A6 [RJA 04-96] and RJA 47561β - 47649: Well D10 [RJA 47607]) were obtained from the Andersen laboratory and tested at various concentrations in the HEK-pHTS-CRE cell line. Fresh samples of hits RJA 04-96 and RJA 47607 displayed significantly (t-test, $p < 0.05$) increased light output in the HEK-pHTS-CRE cell line (data not shown), resulting in their characterization as non-specific hits and eliminating them from further investigation. Therefore, the two GLP-1 receptor agonist hits identified in Plate Series 2 were ruled out as specific hits when tested at multiple concentrations in the HEK-pHTS-CRE cell line.

Figure 28.   GLP-1 Receptor Agonist Screen With Plate Series 1
(A) RJA 03 37 - 119. (B) RJA 03 121 - 204. (C) RJA 03 205 - 287. (D) RJA 03 289 - 372. (E) RJA 03 373 - 500. (F) RJA 05 1 - 84. (G) RJA 75907. HEK-hGLP-1R-Luc cells were induced with 200 nl of marine invertebrate extract and light output measured.   Yellow bars represent DMSO control wells, green bars represent non-specific hits and red bars represent specific hits.   Relative light output was calculated by dividing total light output by the average DMSO light output. Data are expressed as means ± SEM, n=3.

Figure 29.   GLP-1 Receptor Agonist Screen With Plate Series 2
(A) RJA 04 1 - 90. **(B)** RJA 04 91 - 06 114. **(C)** RJA 06 3 - 90. **(D)** RJA PNG 08 100 - Anzia B.
(E) RJA 47561β - 47649. **(F)** RJA 55261β - 55340. **(G)** RJA 76351β - PHP 90 489. HEK-hGLP-1R-Luc cells were induced with 200 nl of marine invertebrate extract and light output measured. Yellow bars represent DMSO control wells, green bars represent non-specific hits and red bars represent specific hits.   Relative light output was calculated by dividing total light output by the average DMSO light output. Data are expressed as means ± SEM, n=3.

Figure 30. GLP-1 Receptor Agonist Screen With Plate Series 3
(A) RJA CHEM 2891- 2970. (B) RJA CHEM 2971 - 3050. HEK-hGLP-1R-Luc cells were induced with 200 nl of bacterial extract and light output measured. Yellow bars represent DMSO control wells. Relative light output was calculated by dividing total light output by the average DMSO light output. Data are expressed as means ± SEM, n=3.

Figure 31. GLP-1 Receptor Agonist Screen With Plate Series 4
(A) RJA BACT 3189. **(B)** RJA BACT 3257. **(C)** RJA BACT 3337. **(D)** RJA BACT 3417. **(E)** RJA BACT 3497. **(F)** RJA BACT 3577. **(G)** RJA BACT 3657. **(H)** RJA BACT 3737. HEK-hGLP-1R-Luc cells were induced with 200 nl of bacterial extract and light output measured. Yellow bars represent DMSO control wells and green bars represent non-specific hits. Relative light output was calculated by dividing total light output by the average DMSO light output. Data are expressed as means ± SEM, n=3.

4.5 GLP-1 Receptor Allosteric Modulator Screens

Similar to the GIP receptor allosteric modulator and antagonist screens, the GLP-1 receptor allosteric modulator screens were performed in triplicate by incubating HEK-hGLP-1R-Luc cells with marine invertebrate or bacterial extracts in the presence of a half maximal concentration of GLP-1 and light output measured. GLP-1 receptor allosteric modulator hits were identified as those extracts that: (1) displayed a statistically significant increase in light output in the HEK-hGLP-1R-Luc cell line compared to DMSO controls (t-test, $p < 0.01$), (2) displayed a greater than 15% increase in light output in the HEK-hGLP-1R-Luc cell line compared to DMSO controls and (3) did not display a statistically significant increase in light output in the negative control cell line, HEK-pHTS-CRE (t-test, $p < 0.05$). The GLP-1 receptor allosteric modulator screen with Plate Series 1 resulted in the identification of several non-specific hits (green bars; hits that passed hit criteria (1) and (2) but not (3)), but no specific hits (hits that passed hit criteria (1), (2) and (3)) (Figure 32). Similarly, the GLP-1 receptor allosteric modulator screen with Plate Series 2 resulted in the identification of several non-specific hits, but no specific hits (Figure 33). However, the GLP-1 receptor allosteric modulator screen with Plate Series 3 did not result in the identification of any hits, specific or non-specific (Figure 34). Likewise, the GLP-1 receptor allosteric modulator screen with Plate Series 4 did not result in the identification of any hits (Figure 35). As with the previously described screens, the marine invertebrate extracts displayed much more activity than the bacterial extracts. Thus, the GLP-1 receptor allosteric modulator screens did not identify any specific hits to pursue.
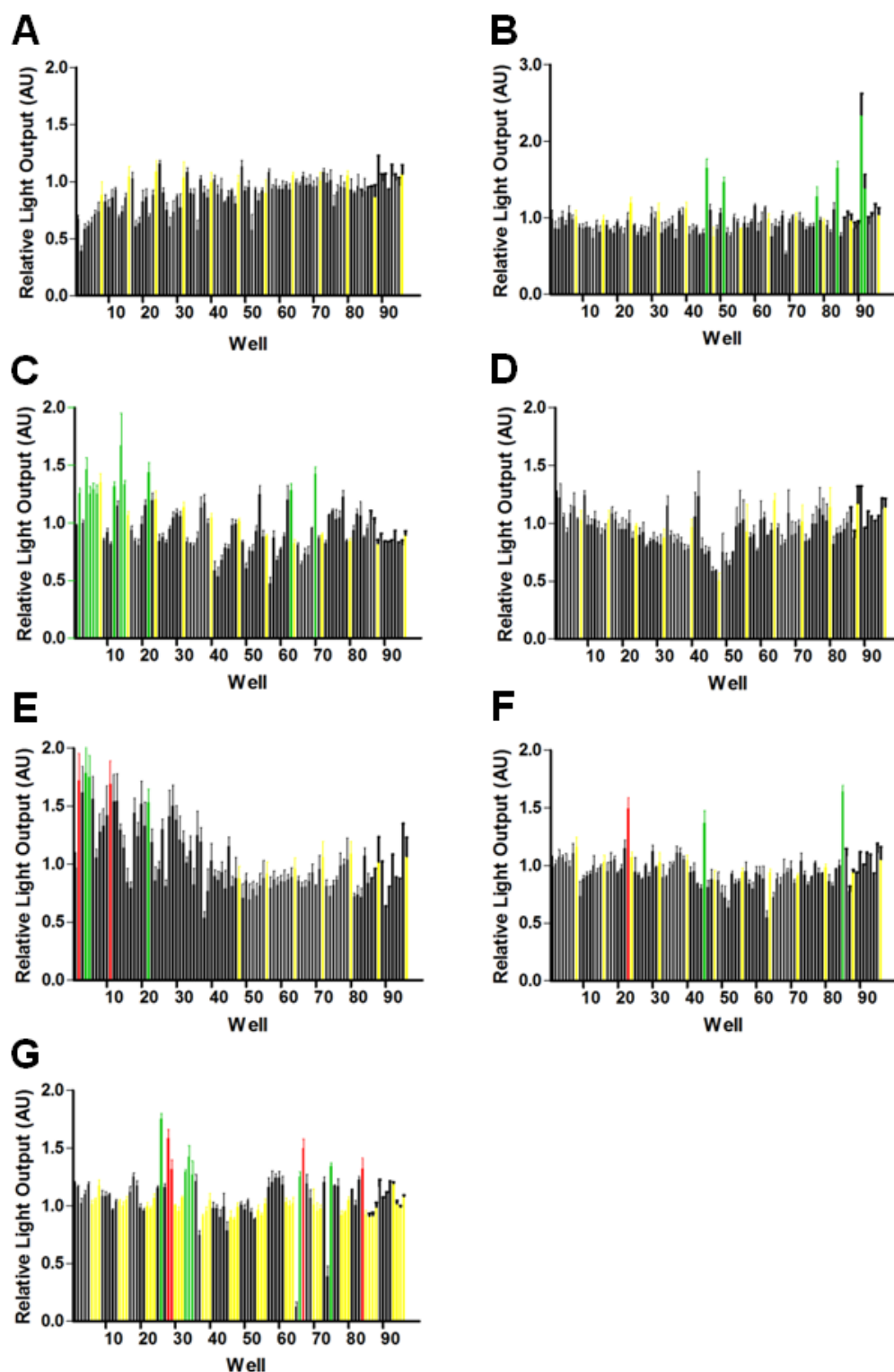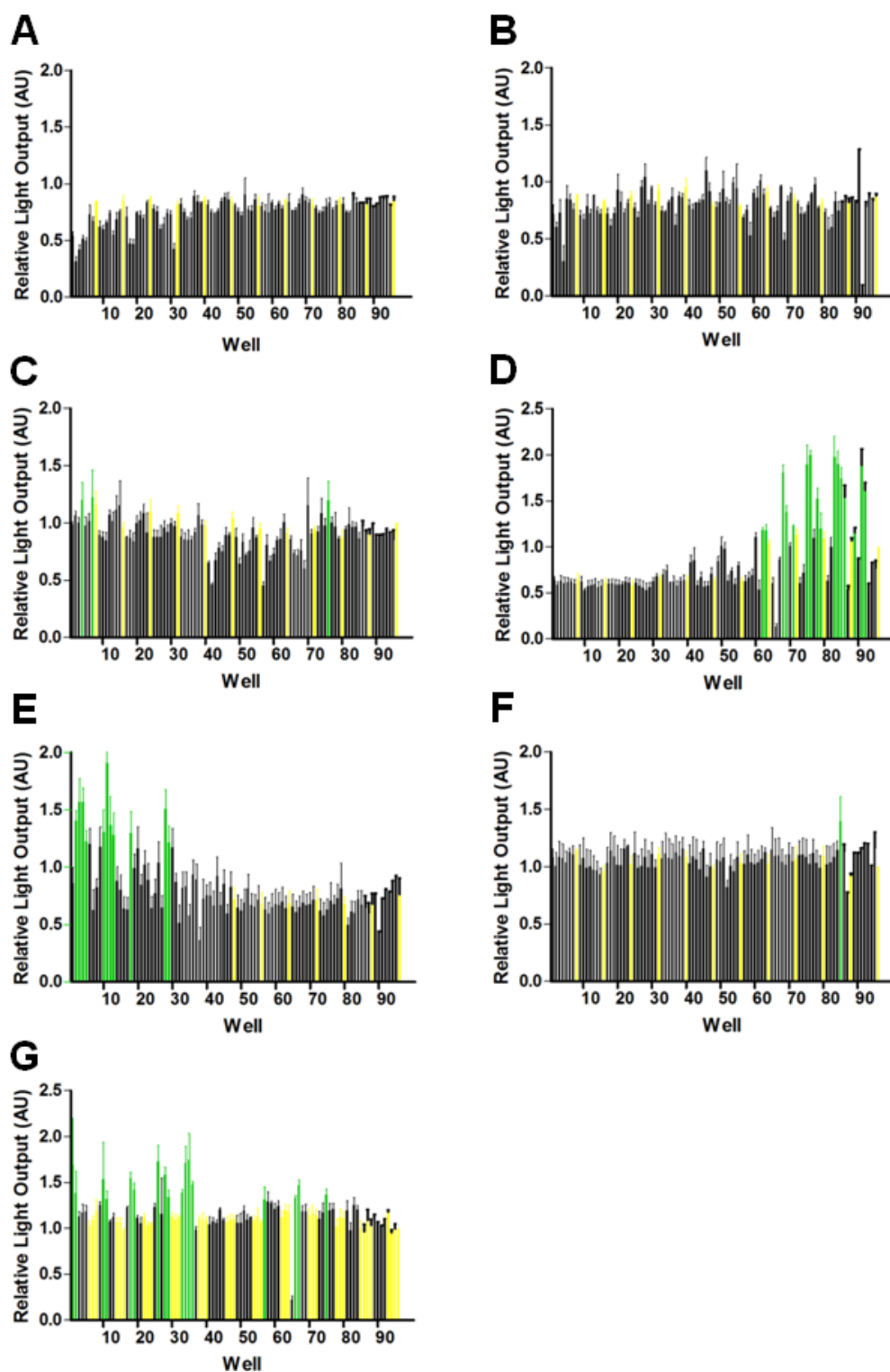
Figure 32. GLP-1 Receptor Allosteric Modulator Screen With Plate Series 1
(A) RJA 03 37 - 119. (B) RJA 03 121 - 204. (C) RJA 03 205 - 287. (D) RJA 03 289 - 372. (E) RJA 03 373 - 500. (F) RJA 05 1 - 84. (G) RJA 75907. HEK-hGLP-1R-Luc cells were induced with 200 nl of marine invertebrate extract in the presence of 10 pM GLP-1 and light output measured. Yellow bars represent DMSO control wells and green bars represent non-specific hits. Relative light output was calculated by dividing total light output by the average DMSO light output. Data are expressed as means ± SEM, n=3.
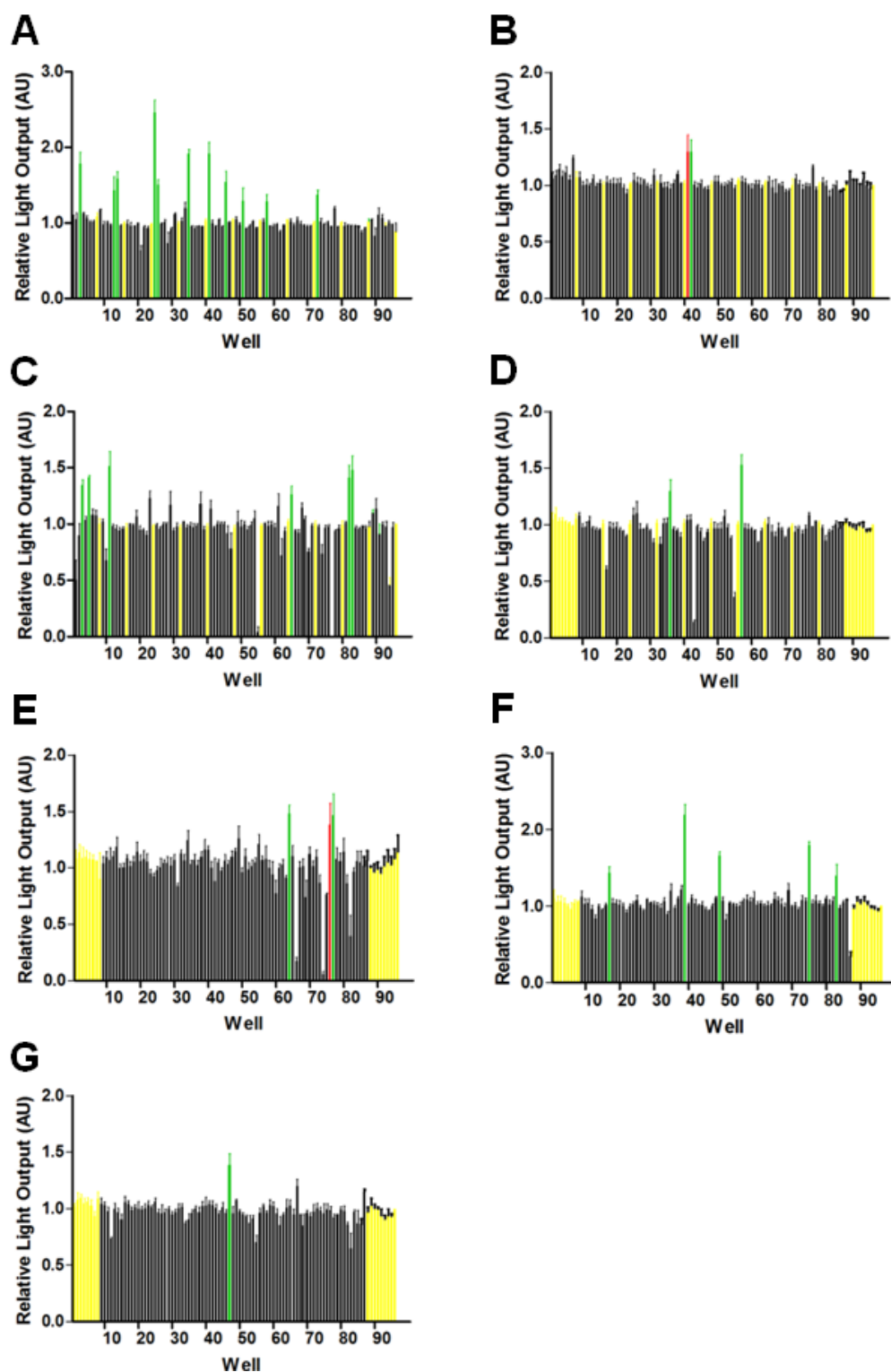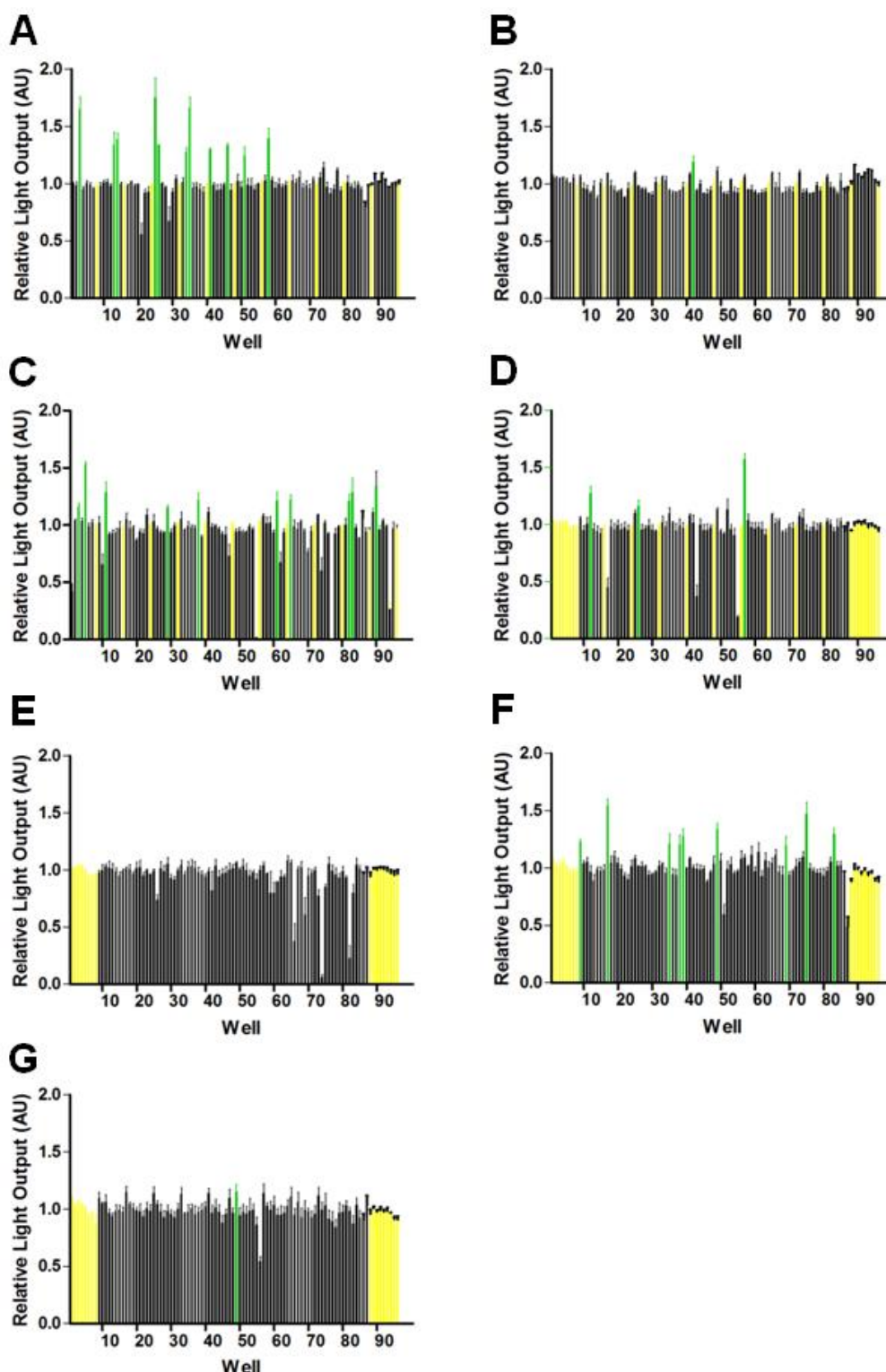
Figure 33. GLP-1 Receptor Allosteric Modulator Screen With Plate Series 2
(**A**) RJA 04 1 - 90. (**B**) RJA 04 91 - 06 114. (**C**) RJA 06 3 - 90. (**D**) RJA PNG 08 100 - Anzia B.
(**E**) RJA 47561β - 47649. (**F**) RJA 55261β - 55340. (**G**) RJA 76351β - PHP 90 489. HEK-hGLP-1R-Luc cells were induced with 200 nl of marine invertebrate extract in the presence of 3 pM GLP-1 and light output measured. Yellow bars represent DMSO control wells and green bars represent non-specific hits. Relative light output was calculated by dividing total light output by the average DMSO light output. Data are expressed as means ± SEM, n=3.
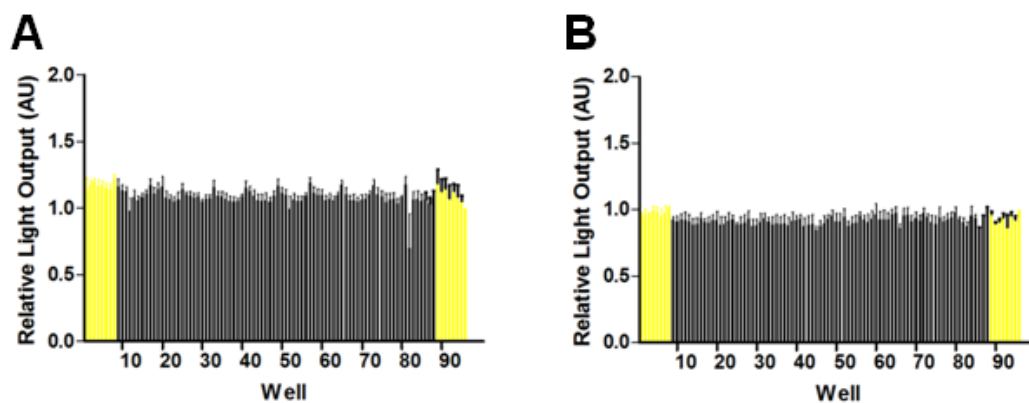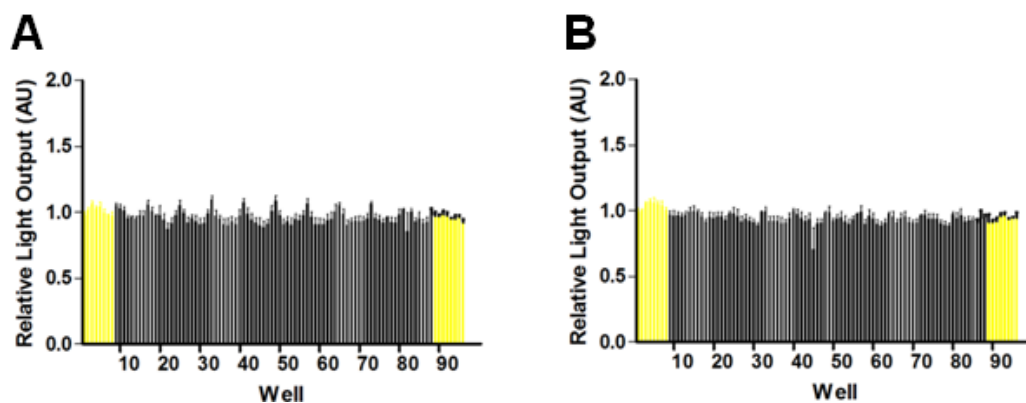
Figure 34.   GLP-1 Receptor Allosteric Modulator Screen With Plate Series 3
(A) RJA CHEM 2891- 2970. **(B)** RJA CHEM 2971 - 3050. HEK-hGLP-1R-Luc cells were induced with 200 nl of bacterial extract in the presence of 3 pM GLP-1 and light output measured. Yellow bars represent DMSO control wells. Relative light output was calculated by dividing total light output by the average DMSO light output. Data are expressed as means ± SEM, n=3.
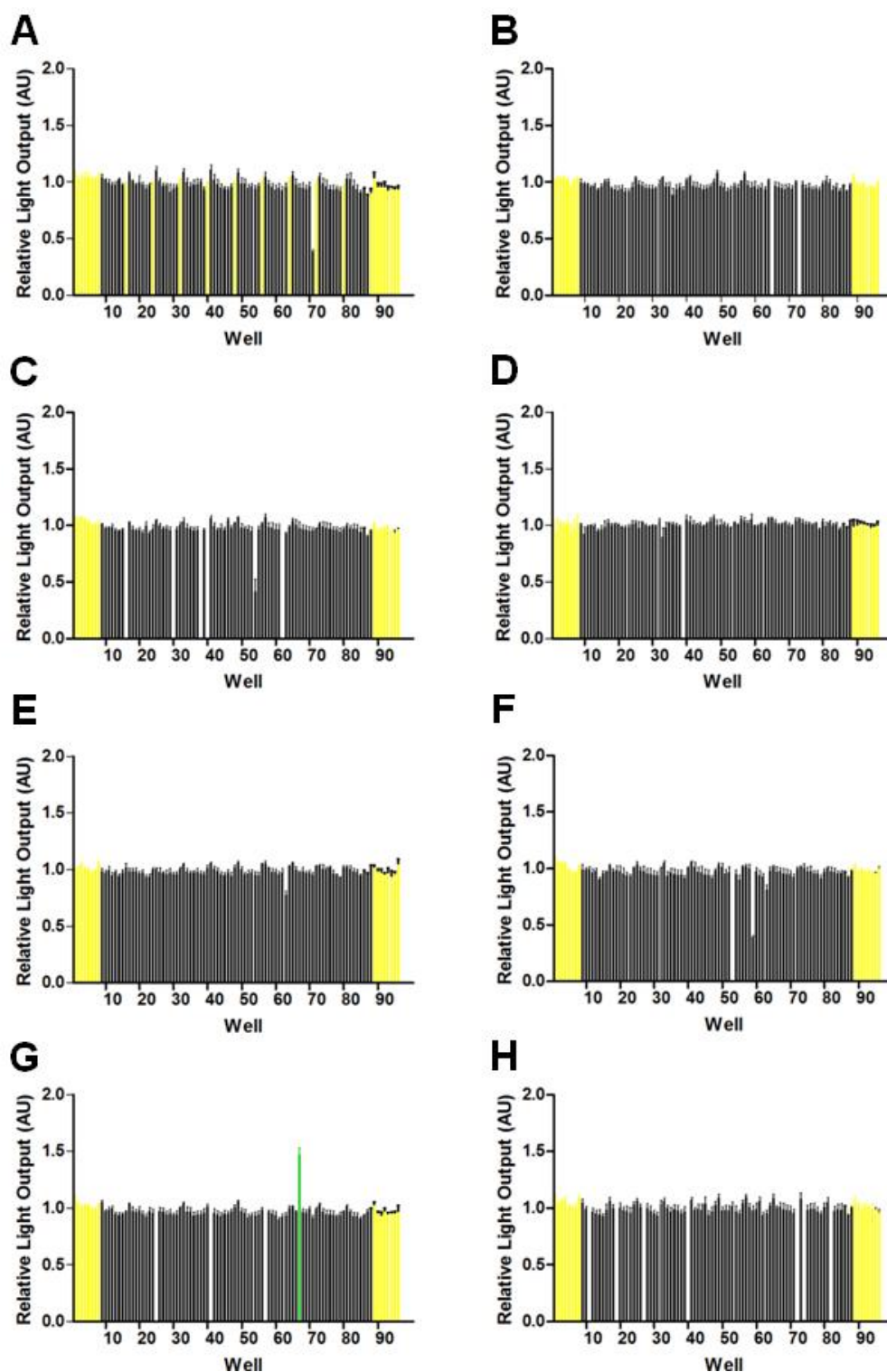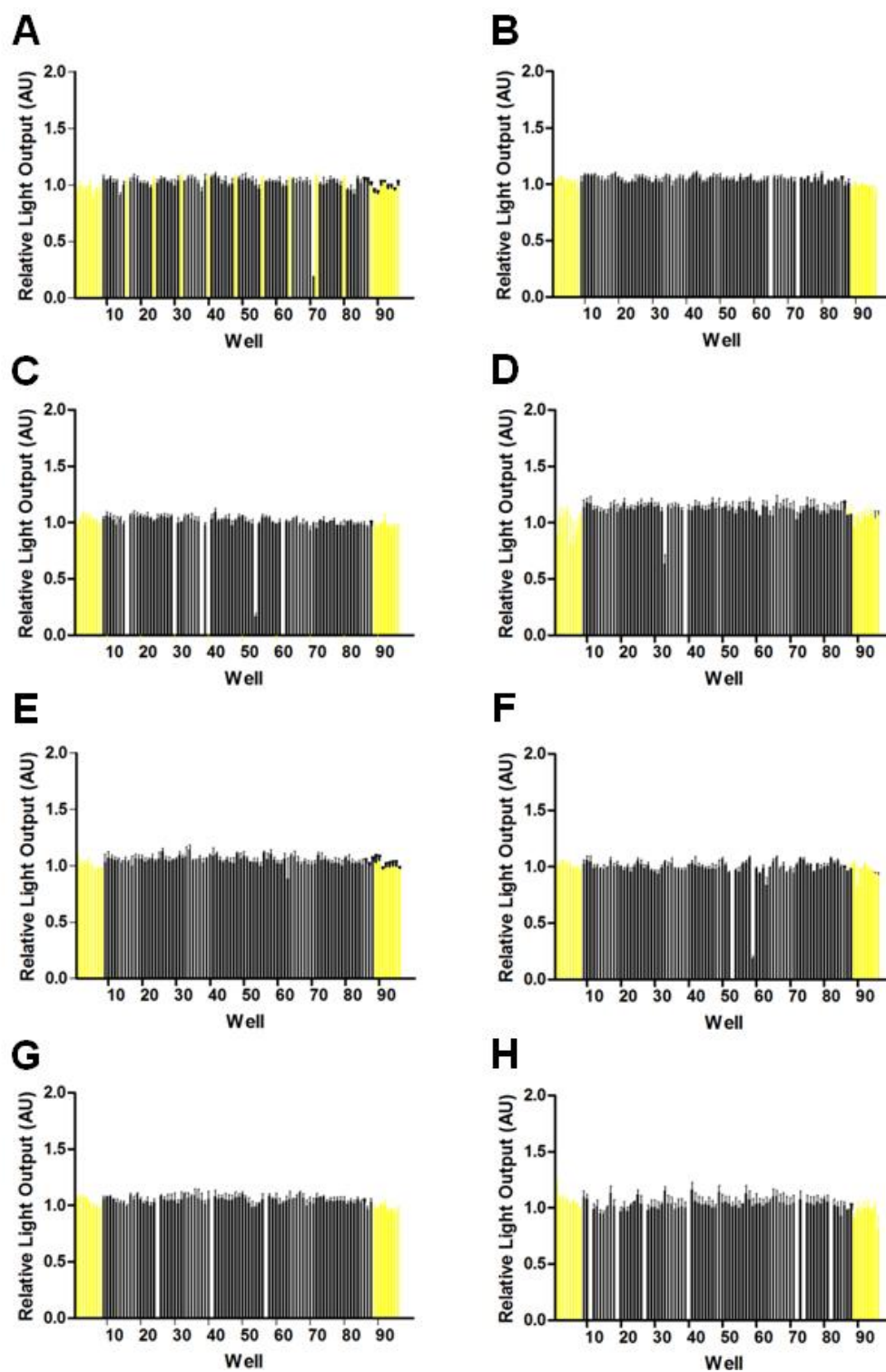
Figure 35. GLP-1 Receptor Allosteric Modulator Screen With Plate Series 4
(**A**) RJA BACT 3189. (**B**) RJA BACT 3257. (**C**) RJA BACT 3337. (**D**) RJA BACT 3417. (**E**) RJA BACT 3497. (**F**) RJA BACT 3577. (**G**) RJA BACT 3657. (**H**) RJA BACT 3737. HEK-hGLP-1R-Luc cells were induced with 200 nl of bacterial extract in the presence of 3 pM GLP-1 and light output measured. Yellow bars represent DMSO control wells. Relative light output was calculated by dividing total light output by the average DMSO light output. Data are expressed as means ± SEM, n=3.

5 Chapter: Isolation, Identification and Characterization of Hits

5.1 Hits That Activate cAMP Signalling

While screening for modulators of the incretin receptors, several compounds that activated cAMP signalling in the absence of receptor activity were identified. These compounds were originally pursued as they were believed to be potential GLP-1 receptor activators, but were subsequently shown to activate cAMP signalling in the absence of GLP-1 receptor activation. Even though compounds capable of modulating cAMP signalling are not of interest as diabetes and/or obesity drugs, these compounds were followed up on due to their novel and interesting chemical structures. In addition, small molecules that selectively modulate cellular signaling are important cell biology research tools. For example, forskolin, a small molecule isolated in India from the plant *Coleus forskohlii*, is a potent activator of adenylyl cyclase (Seamon et al., 1981). Forskolin is commonly used in cell biology research to elevate intracellular cAMP levels, and it has also attracted some attention as a putative drug candidate (Gonzalez-Sanchez et al., 2006). Thus, even though compounds capable of stimulating cAMP signalling are not of interest for diabetes and/or obesity therapy, they may serve as useful tools for cell biology research.

5.1.1 The Alotaketals

While screening Plate Series 1, extract RJA 03-398 was identified as a putative GLP-1 receptor agonist hit as it stimulated light output in HEK-hGLP-1R-Luc cells (Figure 36A; hit extract RJA 03-398 is identified with a # symbol). Extract RJA 03-398 was extracted exhaustively with methanol from the marine sponge *Hamigera* sp., which was collected via SCUBA in Papua New Guinea by Dr. Andersen's laboratory. In order to isolate the active compound(s) in the extract, extract RJA 03-398 was subjected to Sephadex LH20 chromatography with methanol as the eluent to yield the fractions A, B and C (performed by Roberto Forestieri, University of British Columbia). These fractions were then evaluated in the GLP-1 bioassay in order to identify the active fraction(s) (Figure 36B). As seen in Figure 36B, fraction B displayed the strongest activity, significantly stimulating light output across three orders of magnitude at extract concentrations of 0.01X, 0.1X and 1X (an extract concentration of 1X corresponds to the concentration of extract used for screening and is equivalent to 53 mg/L). In addition to fraction B, fractions A and C also significantly stimulated light output at an extract concentration of 1X in the GLP-1 bioassay (Figure 36B). These results demonstrated that the fractionation procedure is able to successfully separate and concentrate compounds, even though some overlap in compound(s) exists between the fractions. Interestingly, a concentration-dependent decrease in light output was apparent between the fraction B concentrations

of 0.1X and 10X (Figure 36B), suggesting that the active compound(s) may also be cytotoxic. Finally, the concentration-dependent decrease in light output seen between the concentrations of 1X and 10X for fractions A and C is probably partially due to DMSO cytotoxicity at the 10X concentration, since the DMSO control also displayed a similar trend (Figure 36 B). Thus, extract RJA 03-398 was identified as a putative GLP-1 receptor agonist, and fractionation of this extract revealed that fraction B contained the relevant bioactivity.
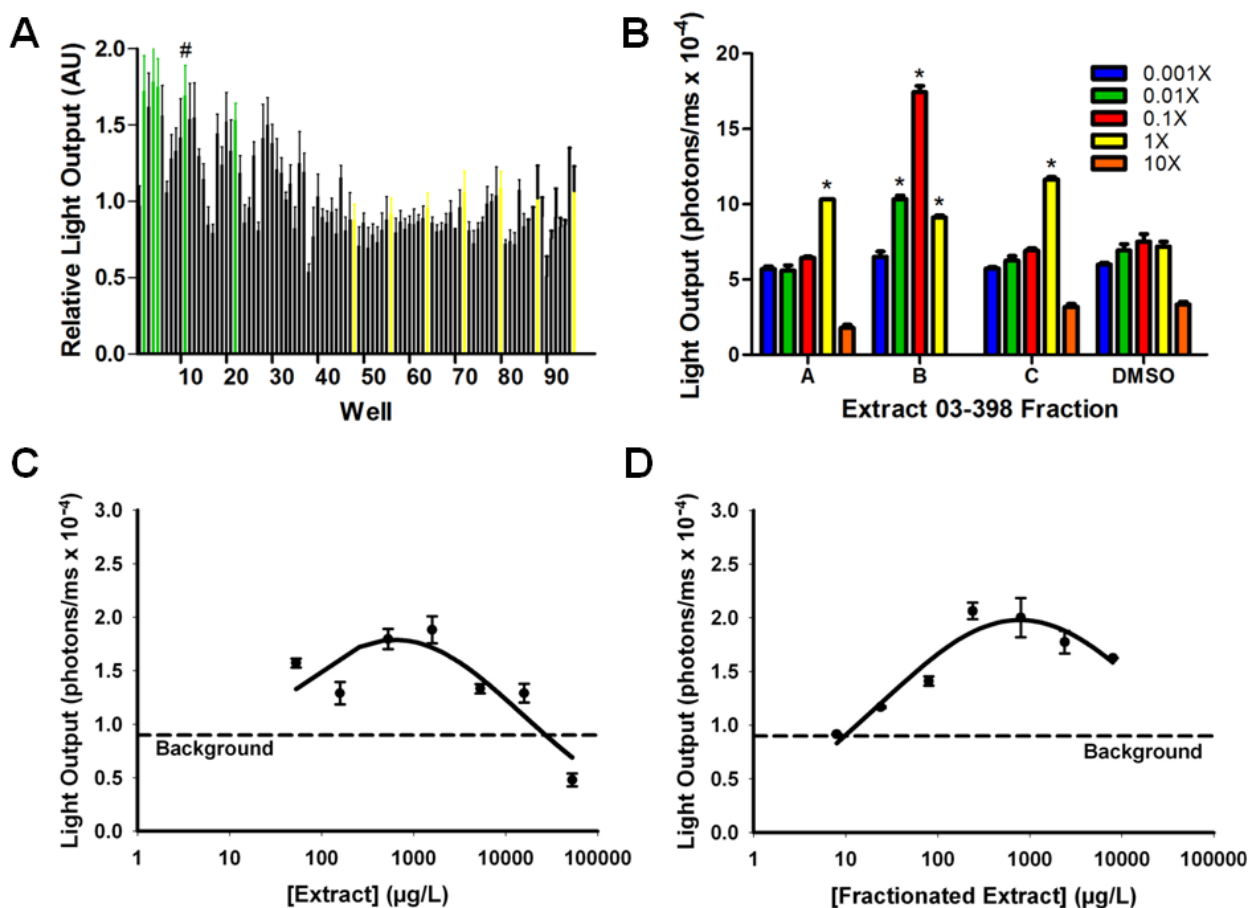
Figure 36. Isolation of Novel Molecules that Stimulate cAMP Signalling
(**A**) GLP-1 Receptor Agonist Screen. HEK-hGLP-1R-Luc cells were induced with 200 nl of marine invertebrate extract and light output measured. Yellow bars represent DMSO control wells and green bars represent non-specific hits. Hit extract RJA 03-398 is identified with a # symbol. Relative light output was calculated by dividing total light output by background light output. (**B**) Extract RJA 03-398 Fractionation.   HEK-hGLP-1R-Luc cells were induced with varying concentrations of fractionated extract RJA 03-398 and light output measured. * $p < 0.05$ compared to an equivalent concentration of DMSO. (**C**) Crude Extract RJA 03-398 and (**D**) Extract RJA 03-398 Fraction B Standard Curves. HEK-pHTS-CRE cells were induced with varying concentrations of Extract RJA 03-398 or Extract RJA 03-398 Fraction B and light output measured. The EC_{50} values were not determined. Data are expressed as means ± SEM, n=3.

Further investigation with the HEK-pHTS-CRE cell line revealed that extract RJA 03-398 was acting independent of the GLP-1 receptor to stimulate luciferase expression and thus light output. As seen in Figure 36C, extract RJA 03-398 also concentration-dependently activated light output in the HEK-pHTS-CRE cell line, which does not express the GLP-1 receptor. The concentration-response curve of extract RJA 03-398 in the HEK-pHTS-CRE cell line also suggests that there may be a cytotoxic compound(s) in the extract (Figure 36C). In addition, fraction B of extract RJA 03-398 was evaluated in the HEK-pHTS-CRE bioassay (Figure 36D). Fraction B concentration-dependently stimulated light output in the HEK-pHTS-CRE bioassay and also displayed decreased light output at high concentrations, potentially due to cytotoxicity (Figure 36D). When comparing the concentration-response curves of crude extract RJA 03-398 and extract RJA 03-398 fraction B, it can be seen that fraction B contains a higher concentration of active compound since the curve is shifted to the left (Figure 36C and 36D). The concentration-response curve for fraction B is also less sporadic than the curve for the crude extract, indicating that the active compound is purer in fraction B (Figure 36C and 36D). EC_{50} values were not determined for extract RJA 03-398 or for fraction B of extract RJA 03-398. Therefore, extract RJA 03-398 acts independent of a receptor to stimulate the cAMP signalling pathway and induce light output.

Further fractionation of extract RJA 03-398 fraction B was performed using C_{18} reverse-phase high-performance liquid chromatography (HPLC), with 4:1 acetonitrile:water as the eluent, to yield the pure compounds, alotaketal A (Figure 37A) and alotaketal B (Figure 37B) (performed by Roberto Forestieri). The structures of alotaketals A and B were elucidated via mass spectrometry and nuclear magnetic resonance (NMR) techniques by Roberto Forestieri. Alotaketals A and B are sesterterpenoids that have an unprecedented alotane carbon skeleton (Figure 37). In order to evaluate
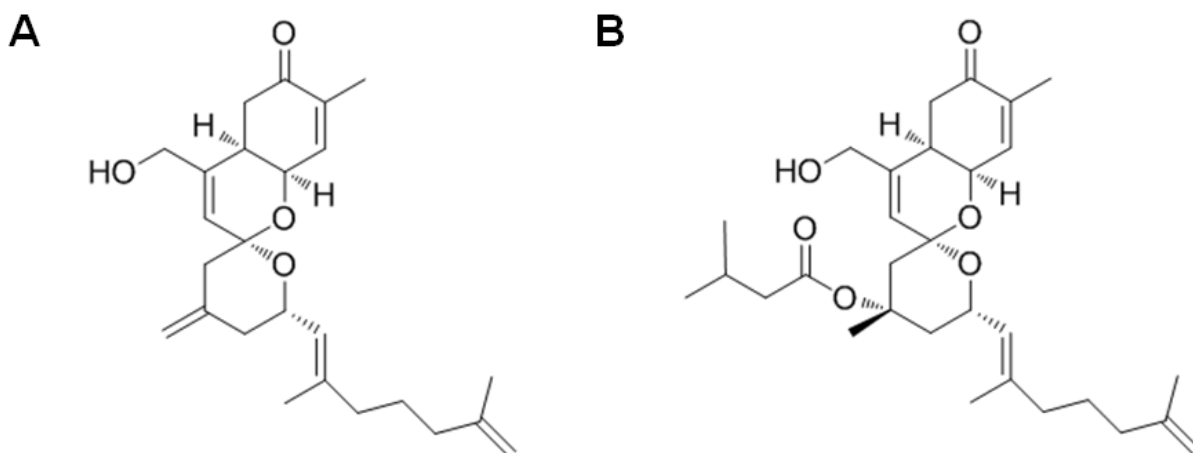
Figure 37. Structures of Alotaketals A and B
(A) Alotaketal A Structure. **(B)** Alotaketal B Structure. The structures of alotaketals A and B were elucidated via mass spectrometry and nuclear magnetic resonance techniques by Roberto Forestieri.

the activity of the alotaketals, a bioassay with the HEK-pHTS-CRE cell line was performed. As seen in Figure 38A, alotaketal A and alotaketal B both concentration-dependently stimulated light output in the HEK-pHTS-CRE bioassay. The EC_{50} value for alotaketal A was determined to be 18 nM, while the EC_{50} value for alotaketal B was determined to be 240 nM (Figure 38A). As alotaketal A is more potent (has a lower EC_{50} value) than alotaketal B in the bioassay, the exocyclic double bond in the alotaketal A structure is likely important for activity. Interestingly, alotaketal A also displays decreased light output at concentrations above ~1 μM, potentially due to cytotoxicity, while alotaketal B does not (Figure 38A). Compared to forskolin, which has an EC_{50} value of 2.9 μM in the HEK-pHTS-CRE bioassay, the alotaketals are much more potent (Figures 19A and 38A). Conversely, forskolin elicits a much greater response in the HEK-pHTS-CRE bioassay compared to the alotaketals, as evidenced by the much larger increase in relative light output (Figures 19A and 38A). The next step was to determine the mechanism of action of the alotaketals in the HEK-pHTS-CRE bioassay with a cAMP assay. As seen in Figure 38B, alotaketal B appears to concentration-dependently increase cAMP levels in HEK-pHTS-CRE cells. However, since the assay was only performed in duplicate, statistical analysis cannot be performed and these preliminary findings have not been confirmed. Further investigations to determine the molecular target of the alotaketals remain to be completed. Thus, alotaketal A and B are novel sesterterpenoids that activate cAMP signalling in a concentration-dependent manner.
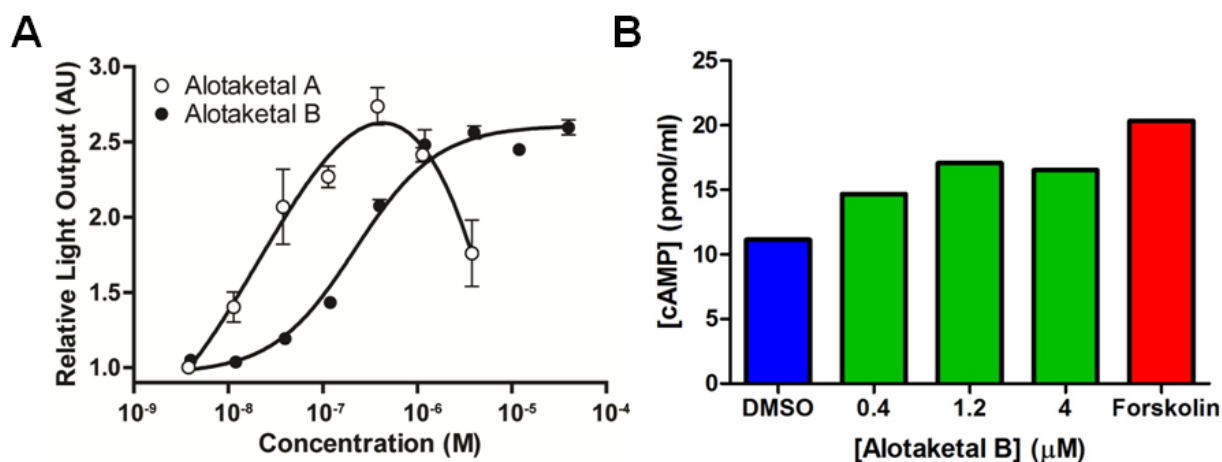
Figure 38.   Characterization of Novel Molecules that Activate cAMP Signalling
(A) Alotaketals A and B Standard Curves. HEK-pHTS-CRE cells were induced with varying concentrations of alotaketals A and B, active compounds isolated from extract RJA 03-398, and light output measured. The EC_{50} values were determined to be 18 nM for alotaketal A and 240 nM for alotaketal B. Relative light output was calculated by dividing total light output by background light output. Data are expressed as means ± SEM, n=3. **(B)** Alotaketal B cAMP Assay. HEK293 cells were induced with varying concentrations of alotaketal B and cAMP levels measured. Forskolin activates adenylyl cyclase to stimulate cAMP signalling and thus acts as a positive control. Data are expressed as means, n=2.

Further chemical examination of the minor terpenoid components of the *Hamigera* sp. extract resulted in the identification of the alotaketal derivatives, alotaketals C, D, E and F (structures not shown). Alotaketals C and D were isolated using the same fractionation procedure described above for the isolation of alotaketals A and B (performed by Roberto Forestieri). As seen in Figure 39A, Alotaketal C and alotaketal D both concentration-dependently increased light output in the HEK-pHTS-CRE bioassay. The EC_{50} values for alotaketals C and D were determined to be 6.3 μm and 320 nM, respectively (Figure 39A). The EC_{50} value of alotaketal D is very similar to that of alotaketal B but less potent than alotaketal A, while alotaketal C is less potent than alotaketals A, B and D (Figures 38A and 39A). Furthermore, alotaketals C and D elicit weaker responses in the HEK-pHTS-CRE bioassay than alotaketals A and B (Figures 38A and 39A). As alotaketal C is less potent (has a lower EC_{50} value) than alotaketal A in the bioassay, the allyl alcohol (which is present in alotaketal A but absent in alotaketal C) is likely very important for activity. In addition, the reduced activity (higher EC_{50} value) of alotaketal D compared to alotaketal A in the bioassay is likely due to the absence of the enone in alotaketal D. The structures of alotaketals B, C and D were determined by Roberto Forestieri using mass spectrometry and NMR techniques. In contrast to alotaketals A, B, C and D, alotaketals E and F were isolated from the marine sponge *Phorbas* sp. from British Columbia by Julie Daoust (University of British Columbia). A sample of *Phorbas* sp. was extracted exhaustively with methanol, evaporated to dryness and chromatographed on a silica gel column with a 100% hexanes to 2:3 hexanes:ethyl acetate gradient (performed by Julie Daoust). The eluent was then subjected to HPLC (3:2 acetonitrile:water) to yield pure alotaketals E and F (performed by Julie Daoust). Alotaketals E and F both stimulate concentration-dependent light output in the HEK-pHTS-CRE bioassay (Figure 39B). The EC_{50} value of alotaketal E was determined to be 6.5 μM, which is comparable to the EC_{50} value of alotaketal C, while the EC_{50} value of alotaketal F was determined to be 100 μM, which is much higher than the EC_{50} values for alotaketals A - E (Figure 39B). In addition, alotaketal E and alotaketal F both induce weaker responses in the HEK-pHTS-CRE bioassay than alotaketals A - D (Figures 38A, 39A and 39B). Similar to alotaketal B, alotaketal E does not contain an exocyclic double bond, likely contributing to the much lower potency (higher EC_{50} value) of alotaketal E compared to alotaketal A in the bioassay. The structure of alotaketal E was determined by Julie Daoust using mass spectrometry and NMR techniques. The structure of alotaketal F remains to be determined. Therefore, alotaketals C, D, E and F are novel alotaketal derivatives that activate the cAMP signalling pathway with varying potencies.
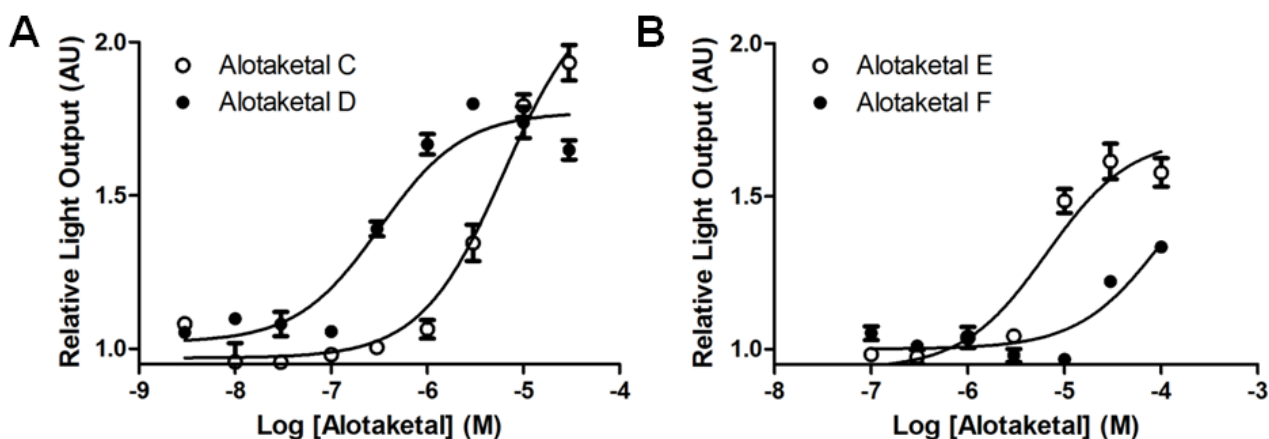
Figure 39.   Characterization of Alotaketal Derivatives in the Bioassay
(A) Alotaketals C and D Standard Curves.   HEK-pHTS-CRE cells were induced with varying concentrations of alotaketals C and D and light output measured.   The EC_{50} values were determined to be 6.3 µM for alotaketal C and 320 nM for alotaketal D.   **(B)** Alotaketals E and F Standard Curves. HEK-pHTS-CRE cells were induced with varying concentrations of alotaketals E and F and light output measured.   The EC_{50} values were determined to be 6.5 µM for alotaketal E and 100 µM for alotaketal F.   Relative light output was calculated by dividing total light output by background light output.   Data are expressed as means ± SEM, n=3.

5.1.2   The Ansellones

The marine sponge *Phorbas* sp. was also investigated in the search for novel sesterterpenoids involved in cAMP signalling.   *Phorbas* sp. was collected via SCUBA in British Columbia by Dr. Andersen's laboratory and a sample of the sponge was immediately extracted with methanol and concentrated *in vacuo* to yield an orange gum.   The orange gum was then fractionated between water and ethyl acetate and the ethyl acetate partition evaporated under reduced pressure (performed by Julie Daoust).   The resulting sample was chromatographed on a silica gel with a 100% hexanes to 3:7 hexanes:ethyl acetate step gradient to yield a pure sample of the novel compound ansellone A (Figure 40A) (performed by Julie Daoust).   Structural elucidation of ansellone A was performed by Julie Daoust with mass spectrometry and NMR techniques.   Ansellone A is a novel sesterterpenoid with an unprecedented tricyclic ansellane carbon skeleton (Figure 40A) and is structurally related to the alotaketals.   As seen in Figure 40B, ansellone A also stimulates cAMP signalling and enhances light output in a concentration-dependent manner in the HEK-pHTS-CRE bioassay (Figure 40B).   The EC_{50} value of ansellone A was determined to be 14 µM.   Ansellone A displays a higher EC_{50} value than alotaketals A, B, C, D and E and a lower EC_{50} value than alotaketal F.   In addition, ansellone A elicits a weaker response in the HEK-pHTS-CRE bioassay compared to alotaketals A - D, but a similar response compared to alotaketals E and F (Figures 38A, 39A, 39B and 40B).   The weaker potency (higher EC_{50} value) of ansellone A compared to alotaketals A - E is likely due to the absence of the spiroketal functionality in ansellone A (which is present in alotaketals A - E).   On the other

hand, the dihydrochromanone moiety, which is present in both the alotaketals and ansellone A, is likely the basic pharmacophore. Finally, compared to forskolin, ansellone A displays a similar EC_{50} value, but elicits a much weaker response in the HEK-pHTS-CRE bioassay (Figures 19A and 40B). Thus, ansellone A is a novel sesterterpenoid related to the alotaketals that is able to induce the cAMP signalling pathway.
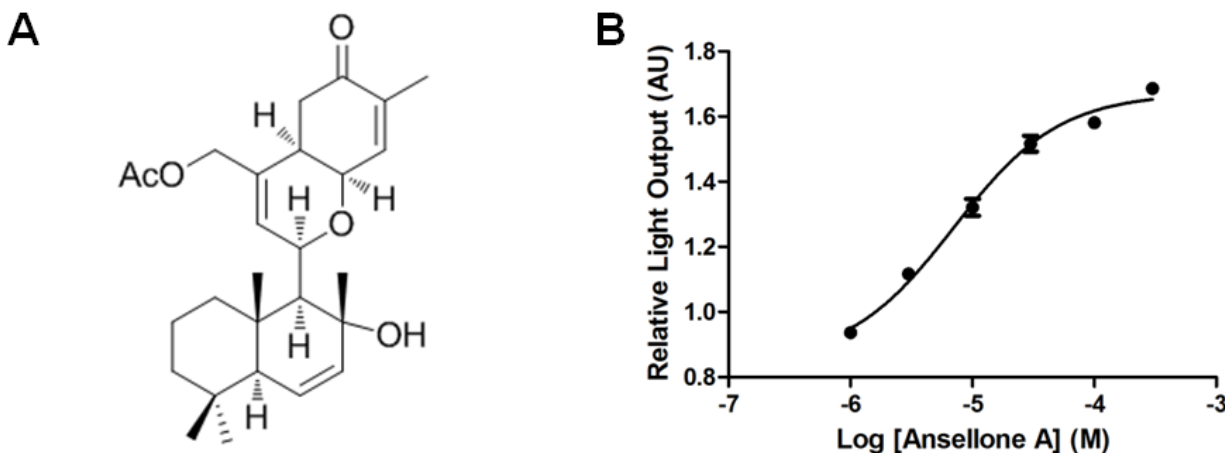
Figure 40. Structure and Characterization of Ansellone A
(A) Ansellone A Structure. The structure of ansellone A was elucidated via mass spectrometry and nuclear magnetic resonance techniques by Julie Daoust. (B) Ansellone A Standard Curve. HEK-pHTS-CRE cells were induced with varying concentrations of ansellone A and light output measured. The EC_{50} value was determined to be 14 μM. Relative light output was calculated by dividing total light output by background light output. Data are expressed as means ± SEM, n=3.

In order to determine if the acetyl moiety of ansellone A is important for function, deacetylated ansellone A (structure not shown) was also tested in the HEK-pHTS-CRE bioassay. Deacetylated ansellone A was produced by hydrolysing ansellone A with lithium hydroxide/water in a 1:1 mixture of tetrahydrofuran:methanol (performed by Julie Daoust). As seen in Figure 41A, deacetylated ansellone A was not active in the HEK-pHTS-CRE bioassay, suggesting that the acetyl moiety of ansellone A is vital for bioactivity. Important to note, the EC_{50} value of ansellone A in this assay was determined to be 38 μM, which is almost 3 fold higher than the previously reported EC_{50} value (14 μM) for ansellone A (Figures 40B and 41A). This substantial difference between EC_{50} values can likely be accounted for by either the inaccuracy of weighing sub-milligram amounts of compound or by incomplete dissolution when solvating the compound. Therefore, the inactivity of deacetylated ansellone A in the HEK-pHTS-CRE bioassay suggests that the acetyl group of ansellone A is essential for bioactivity.
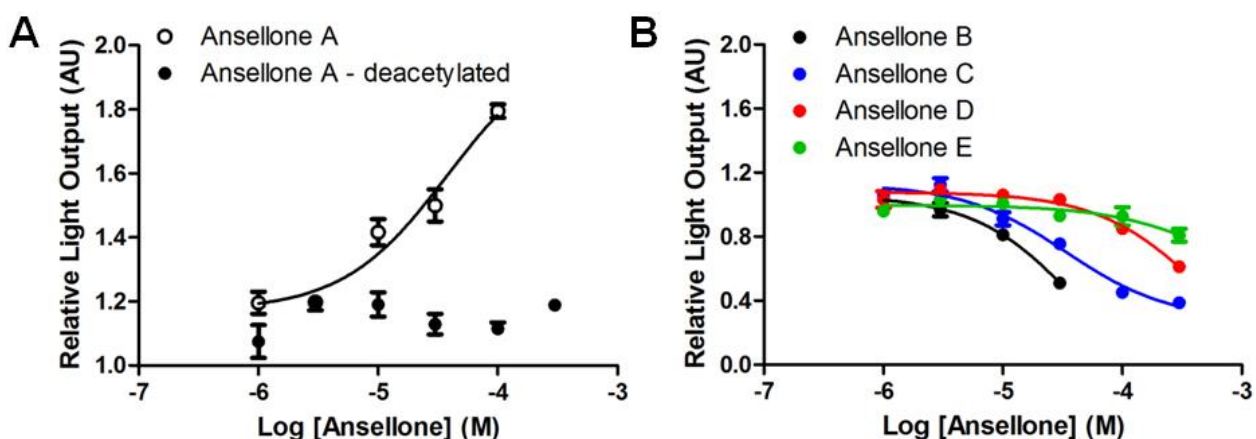
Figure 41. Characterization of Ansellone Derivatives in the Bioassay
(A) Ansellone A and Deacetylated Ansellone A Standard Curves. HEK-pHTS-CRE cells were induced with varying concentrations of ansellone A and deacetylated ansellone A and light output measured. The EC_{50} value was determined to be 38 μM for ansellone A and not determined for deacetylated ansellone A. **(B)** Ansellones B, C, D and E Standard Curves. HEK-pHTS-CRE cells were induced with varying concentrations of ansellones B, C, D and E and light output measured. The EC_{50} values were not determined. Relative light output was calculated by dividing total light output by background light output. Data are expressed as means ± SEM, n=3.

The search for additional sesterterpenoids in *Phorbas* sp. resulted in the isolation of ansellones B - E (structures not shown). As with the isolation of ansellone A, a sample of *Phorbas* sp. was extracted to yield a methanolic extract (performed by Julie Daoust). The methanolic extract was then chromatographed on a silica gel column with a 100% hexanes to 2:3 hexanes:ethyl acetate gradient to yield ansellones A - E (performed by Julie Daoust). Ansellones B, C and D eluted at 4:1 hexanes:ethyl acetate while impure ansellone E eluted at 1:1 hexanes:ethyl acetate. The eluent containing ansellones B, C and D was further fractionated using normal phase HPLC (7:3 hexanes:ethyl acetate) to yield pure ansellones B, C and D, while the eluent containing impure ansellone E was subjected to HPLC (3:2 acetonitrile:water) to yield pure ansellone E (performed by Julie Daoust). As seen in Figure 41B, ansellones B - E did not significantly stimulate cAMP signalling or light output in the HEK-pHTS-CRE bioassay, but rather appeared to be cytotoxic. Since ansellones B - E did not significantly stimulate light output in the HEK-pHTS-CRE bioassay, their EC_{50} values were not determined (Figure 41B). The inactivity of ansellones B and C is likely due to the absence of the dihydrochromanone moiety in both structures, while the inactivity of ansellone D is likely due to the positioning of the oxygen on ring C. Mass spectrometry and NMR techniques were used by Julie Daoust to elucidate the structures of ansellones B - D. The structure of ansellone E remains to be determined. Thus, the marine sponge *Phorbas* sp. contains several inactive sesterterpenoids in addition to biologically active ansellone A.

5.2 Hits That Modulate the Incretin Receptors

As described in the introduction, the modulation of the incretin receptors is an important avenue for the development of drugs to treat diabetes and/or obesity. GIP receptor antagonists have demonstrated beneficial effects in animal models of diabetes and obesity. For example, studies involving GIPR-/- mice, peptidyl and non-peptidyl GIP receptor antagonists, selective K-cell destruction and vaccination against GIP have revealed that GIP receptor blockade results in weight reduction and an improvement in insulin sensitivity. In addition, GLP-1 receptor agonists have been extensively shown to cause weight loss and improve glucose homeostasis in human patients with type 2 diabetes. Thus, the major aim of this thesis was to screen marine invertebrate and bacterial extracts for compounds capable of antagonizing the GIP receptor and/or activating the GLP-1 receptor. After screening over 2000 extracts, extract RJA 03-486 was identified as a putative dual GIP receptor antagonist and GLP-1 receptor agonist hit. The following sections describe the identification, isolation and characterization of the active compound in extract RJA 03-486, halistanol sulphate.

5.2.1 Halistanol Sulphate

5.2.1.1 Characterization of Halistanol Sulphate in the Bioassay

While screening Plate Series 1, extract RJA 03-486 was determined to be a putative GIP receptor antagonist hit as it reduced light output in HEK-hGIPR-Luc cells (Figure 42A; hit extract RJA 03-486 is identified with a # symbol). Extract RJA 03-486 was extracted exhaustively with methanol from an unidentified marine sponge, which was collected by SCUBA in Papua New Guinea by Dr. Andersen's laboratory. Before isolating the active compound in extract RJA 03-486, concentration-response experiments were performed with the crude extract in both the GIP and GLP-1 bioassays (Figures 42B and 42C). As seen in Figure 42B, extract RJA 03-486 (GIPR Antagonist Hit 1, identified with a # symbol) significantly blocked GIP receptor signalling or light output at concentrations of 1X and 5X compared to DMSO controls in the GIP bioassay in the presence of GIP (an extract concentration of 1X corresponds to the concentration of extract used for screening and is equivalent to 12 mg/L). In addition, extract RJA 03-486 inhibits GIP receptor signalling or light output in a concentration-dependent manner and reduces GIP receptor signalling to near background levels (Figure 42B). However, in the GLP-1 bioassay in the presence of GLP-1, extract RJA 03-486 (GIPR Antagonist Hit 1, identified with a # symbol) did not significantly reduce GLP-1 receptor signalling or light output compared to DMSO controls (Figure 42C). These results demonstrated that extract RJA 03-486 significantly inhibits GIP receptor signalling but not GLP-1 receptor signalling,
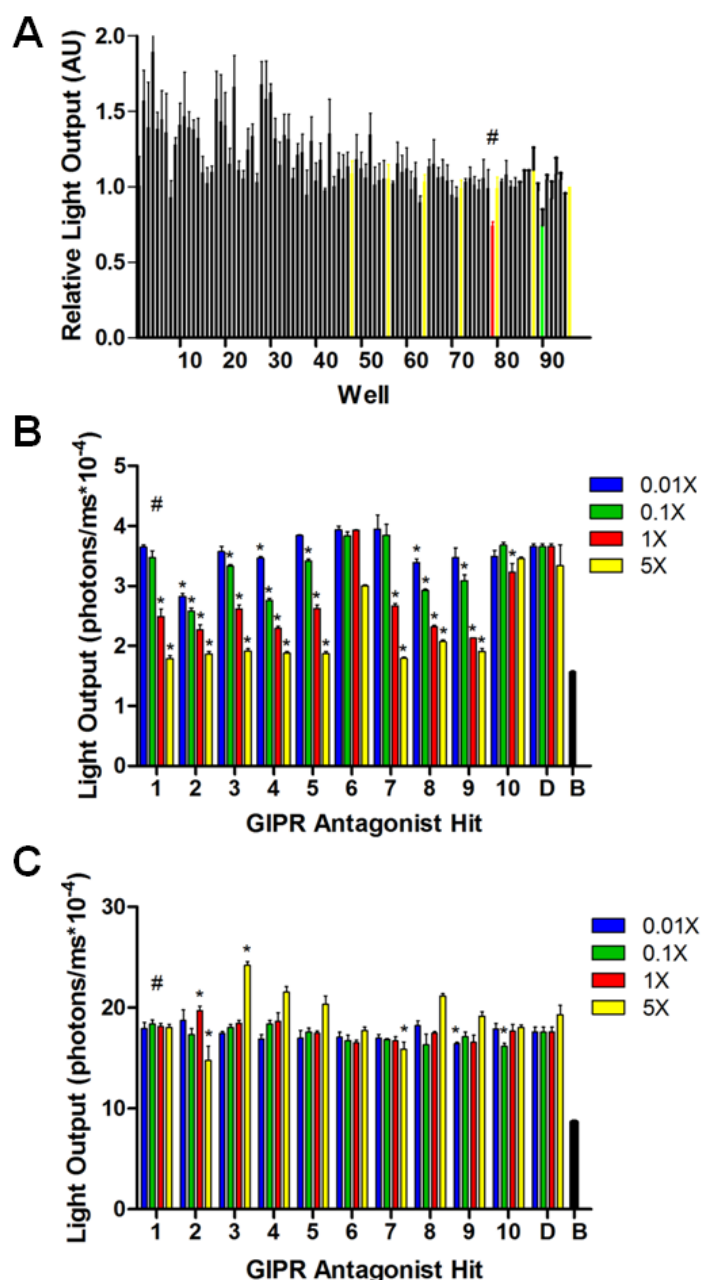
Figure 42.   GIP Receptor Antagonist Hit Identification and Characterization
(**A**) GIP Receptor Allosteric Modulator and Antagonist Screen. HEK-hGIPR-Luc cells were induced with 200 nl of marine invertebrate extract in the presence of 1 nM GIP and light output measured. Yellow bars represent DMSO control wells, green bars represent non-specific hits and red bars represent specific hits.   Relative light output was calculated by dividing total light output by background light output. (**B**) GIP Receptor Antagonist Hits Response in HEK-hGIPR-Luc Cells. HEK-hGIPR-Luc cells were induced with varying concentrations of GIP receptor antagonist hits (1-10) in the presence of 1 nM GIP and light output measured. (**C**) GIP Receptor Antagonist Hits Response in HEK-hGLP-1R-Luc Cells.   HEK-hGLP-1R-Luc cells were induced with varying concentrations of GIP receptor antagonist hits (1-10) in the presence of 10 pM GLP-1 and light output measured. DMSO control wells (D) contained an equivalent concentration of DMSO to the samples in the presence of peptide but absence of hit extract. Background wells (B) did not receive peptide or hit extract. Hit extract RJA 03-486 is identified with a # symbol. * $p < 0.05$ compared to an equivalent concentration of DMSO. Data are expressed as means ± SEM, n=3.

suggesting that extract RJA 03-486 contains a selective GIP receptor antagonist hit compound. The other hit extracts (GIPR Antagonist Hits 2-10) shown in Figures 42B and 42C were eventually ruled out as GIPR antagonist hits, as discussed in Chapter 4. Thus, extract RJA 03-486 was identified as a putative GIP receptor antagonist hit and was of interest for further investigation.

As extract RJA 03-486 was a crude extract containing many compounds, the next step was to isolate and identify the compound acting as a GIP receptor antagonist in the extract. A candidate compound highly abundant in extract RJA 03-486 that had been previously isolated by the Andersen lab, halistanol sulphate (Figure 43), was a candidate for the active compound. The isolation of halistanol sulphate involved partitioning crude extract RJA 03-486 between water and ethyl acetate, followed by *n*-butanol, and evaporating the fractions to dryness (performed by David Williams, University of British Columbia). The *n*-butanol fraction was then subjected to Sephadex LH20 chromatography with 4:1 methanol:dichloromethane as the eluent to yield pure halistanol sulphate (performed by David Williams) (Figure 43). The structure of halistanol sulphate was determined by the Andersen laboratory using mass spectrometry and NMR techniques. As seen in Figure 44A, both halistanol sulphate and crude extract RJA 03-486 significantly inhibited GIP receptor signalling or light output in a concentration-dependent manner compared to DMSO controls in the GIP bioassay in the presence of GIP. In addition, the highest concentration of halistanol sulphate tested (10X) was able to completely block GIP receptor signalling or light output to background levels (Figure 44A). However, in the absence of GIP, neither halistanol sulphate nor crude extract RJA 03-486 significantly inhibited GIP receptor signalling or light output in the GIP bioassay (Figure 44B). The inability of halistanol sulphate to block GIP receptor signalling or light output in the absence of GIP
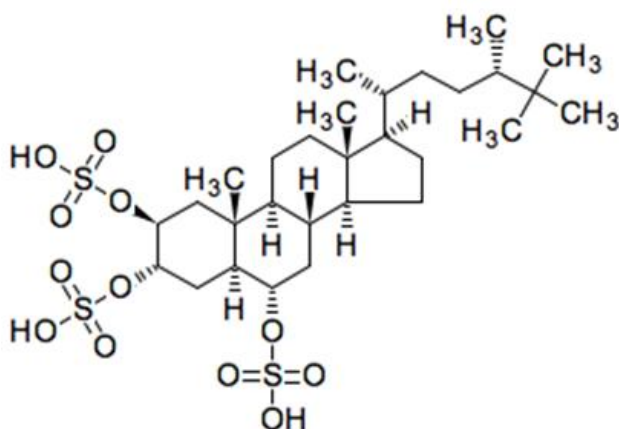
Figure 43.   Structure of Halistanol Sulphate
Halistanol Sulphate Structure.   The structure of halistanol sulphate was elucidated via mass spectrometry and nuclear magnetic resonance techniques by David Williams.
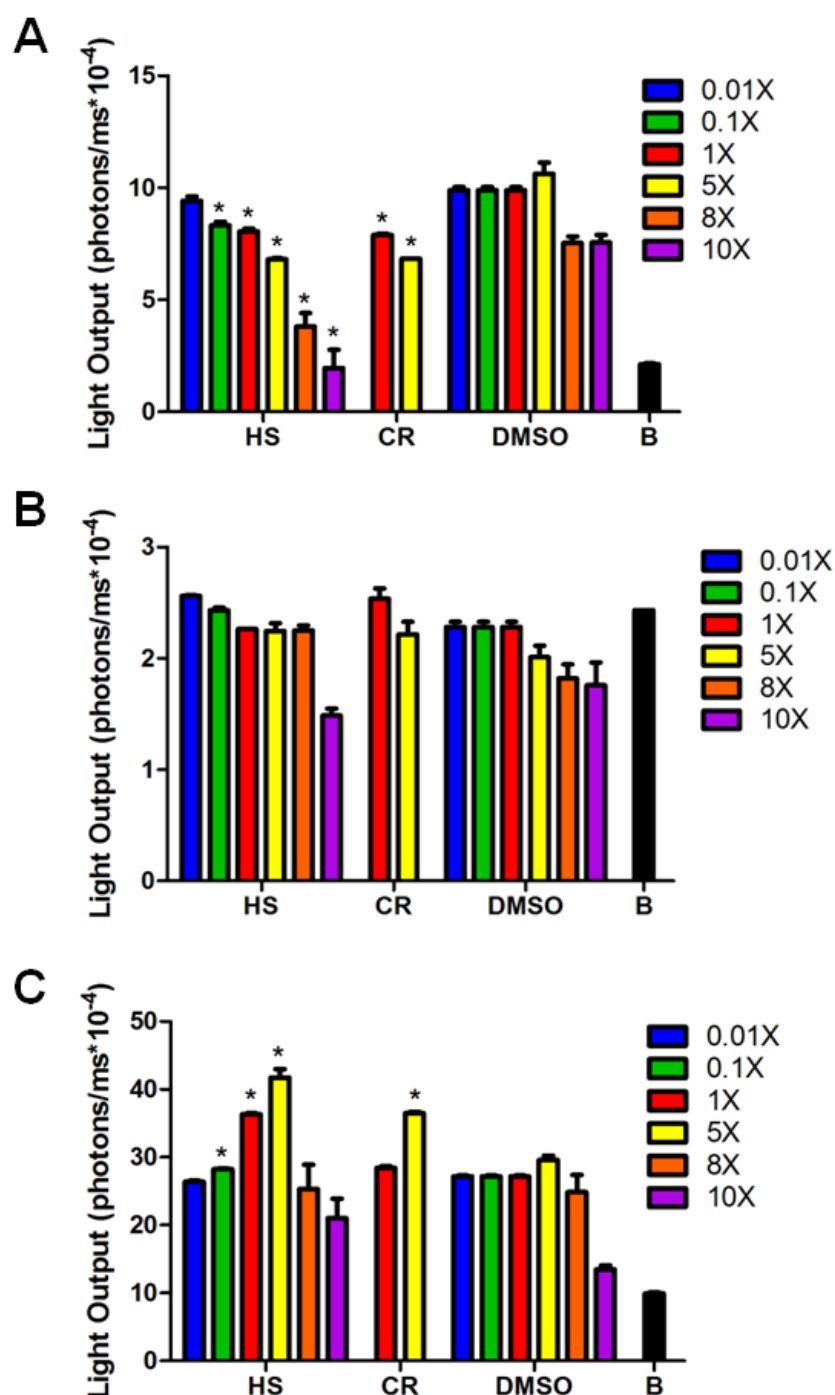
Figure 44. Characterization of Halistanol Sulphate in the Bioassay

(A, B) Halistanol Sulphate Response in HEK-hGIPR-Luc Cells. HEK-hGIPR-Luc cells were induced with varying concentrations of halistanol sulphate (HS, $1X = 16$ µM) and crude extract RJA 03-486 (CR) in the presence **(A)** or absence **(B)** of 1 nM GIP and light output measured. **(C)** Halistanol Sulphate Response in HEK-hGLP-1R-Luc Cells. HEK-hGLP-1R-Luc cells were induced with varying concentrations of halistanol sulphate and crude extract in the presence of 10 pM GLP-1 and light output measured. DMSO control wells contained an equivalent concentration of DMSO to the samples in the absence of hit extract and presence **(A, C)** or absence **(B)** of peptide. Background wells (B) did not receive hit extract or peptide. * $p < 0.05$ compared to equivalent concentration of DMSO. Data are expressed as means ± SEM, n=3.

suggests that halistanol sulphate is indeed an antagonist of the GIP receptor rather than a cytotoxic compound. Furthermore, in the presence of GLP-1 in the GLP-1 bioassay, neither halistanol sulphate nor crude extract RJA 03-486 significantly reduced GLP-1 receptor signalling or light output compared to DMSO controls (Figure 44C). Interestingly, intermediate concentrations of halistanol sulphate significantly stimulated GLP-1 receptor signalling or light output in the GLP-1 bioassay (Figure 44C), suggesting that halistanol sulphate is acting as a dual GIP receptor antagonist/GLP-1 receptor activator. However, high concentrations of halistanol sulphate (5X and 8X) had no effect on GLP-1 receptor signalling (Figure 44C); this finding is yet to be explained and thus requires further investigation. Interestingly, extract RJA 03-486 did not significantly increase light output in the GLP-1 bioassay when originally characterized (Figure 42C), but did significantly increase light output in the GLP-1 bioassay at a concentration of 5X upon subsequent testing (Figure 44C). A possible explanation for this inconsistency is that the composition of compounds in the fresh extract sample was different than the composition of compounds in the extract after multiple freeze/thaw cycles. Finally, the opposing actions of halistanol sulphate on the GIP and GLP-1 receptors provides support that halistanol sulphate is indeed acting on these receptors rather than through a common pathway in the cell lines to alter cellular signalling. Therefore, halistanol sulphate was determined to be the active compound in extract RJA 03-486 and acts as a dual GIP receptor antagonist/GLP-1 receptor agonist in the bioassay.

5.2.1.2 Characterization of Halistanol Sulphate in the Receptor Binding Assay

In order to determine if halistanol sulphate affects the binding of GIP, GLP-1 or GCG to their respective receptors, receptor binding assays were performed. In contrast to the bioassay, which directly measures light output and indirectly measures receptor signalling, the receptor binding assay directly measures the ability of a ligand to bind to a receptor. The ability of halistanol sulphate to block GIP binding to the GIP receptor was first investigated. As seen in Figure 45A, halistanol sulphate displaced [^{125}I]GIP(1-42) binding to the GIP receptor in a concentration-dependent manner. The IC_{50} value for halistanol sulphate in the GIP receptor binding assay was determined to be 590 nM, while the IC_{50} value for GIP was determined to be 3.1 nM (Figure 45A). The dynamic range of halistanol sulphate in the GIP receptor binding assay was determined to be between 10^{-9} and 10^{-4} M, compared to between 10^{-11} and 10^{-5} M for GIP (Figure 45A). Thus, halistanol sulphate displays a broad range of activity in the GIP receptor binding assay, and is only ~200 fold less active at the GIP receptor than GIP itself. The ability of halistanol sulphate to displace [^{125}I]GLP-1(7-36) amide binding to the GLP-1 receptor was then investigated in the GLP-1 receptor binding assay. In contrast to the activity of halistanol sulphate in the GIP receptor binding assay, halistanol sulphate only
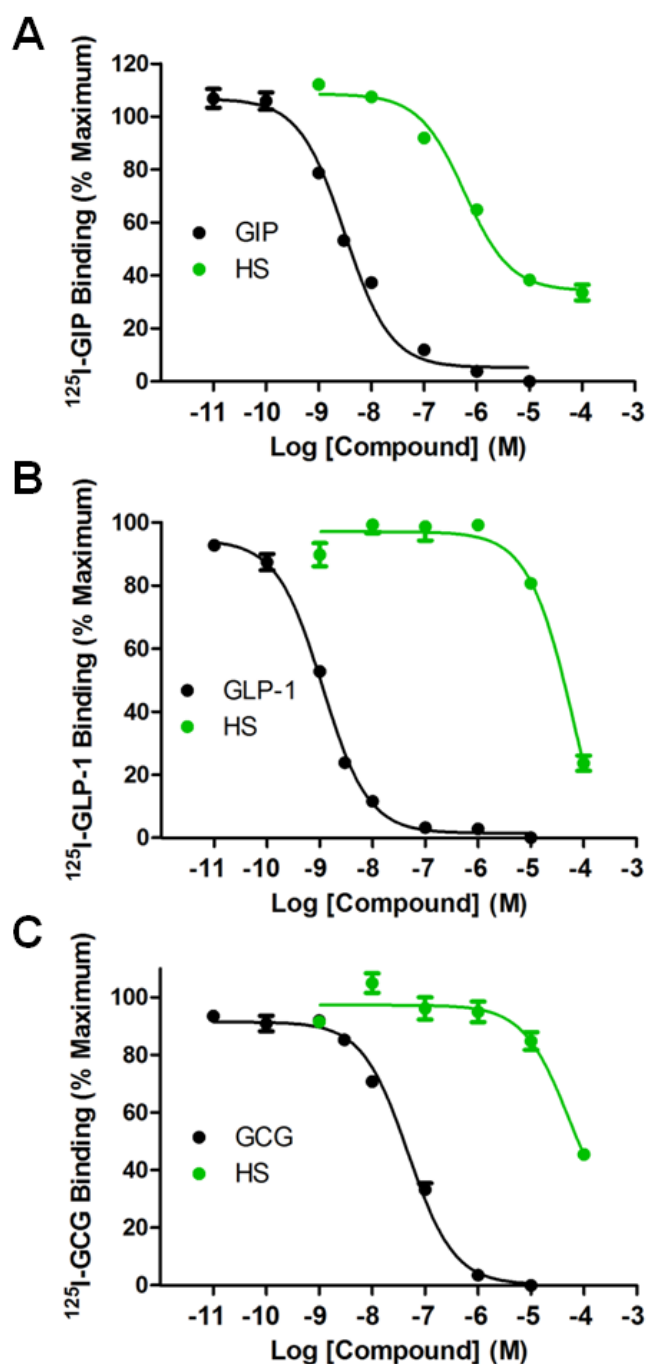
Figure 45.   Characterization of Halistanol Sulphate in the Receptor Binding Assays
(**A**) Characterization of Halistanol Sulphate Binding to the GIP Receptor. Competition of ^{125}I-GIP binding was examined with cold GIP and halistanol sulphate (HS) in HEK-hGIPR-Luc cells. The IC_{50} values were determined to be 3.1 nM for GIP and 590 nM for halistanol sulphate (HS). (**B**) Characterization of Halistanol Sulphate Binding to the GLP-1 Receptor. Competition of ^{125}I-GLP-1 binding was examined with GLP-1 and halistanol sulphate in HEK-hGLP-1R-Luc cells. The IC_{50} values were determined to be 1.1 nM for GLP-1 and 68 μM for halistanol sulphate. (**C**) Characterization of Halistanol Sulphate Binding to the GCG Receptor. Competition of ^{125}I-GCG binding was examined with GCG and halistanol sulphate in HEK-hGCGR-Luc cells. The IC_{50} values were determined to be 48 nM for GCG and 53 μM for halistanol sulphate. Values are expressed as a percentage of maximum specific binding and are means ± SEM, n=3.

blocked $[^{125}I]$GLP-1(7-36) amide binding to the GLP-1 receptor at very high concentrations (10^{-5} and 10^{-4} M) (Figure 45B). The IC_{50} value for halistanol sulphate in the GLP-1 receptor binding assay was determined to be 68 μM, which is ~60,000 fold higher than the IC_{50} value for GLP-1 (1.1 nM) (Figure 45B). In addition, the dynamic range of halistanol sulphate in the GLP-1 receptor binding assay was determined to be between 10^{-6} and 10^{-4} M, compared to between 10^{-11} and 10^{-5} M for GLP-1 (Figure 45B). Finally, a GCG receptor binding assay was also performed in order to evaluate the ability of halistanol sulphate to displace $[^{125}I]$GCG(1-29) binding to the GCG receptor. Similar to the GLP-1 binding assay, halistanol sulphate was only able to displace $[^{125}I]$GCG(1-29) binding to the GCG receptor at very high concentrations (10^{-5} and 10^{-4} M) (Figure 45C). As such, the dynamic range of halistanol sulphate in the GCG receptor binding assay was only between 10^{-6} and 10^{-4} M, compared to between 10^{-10} and 10^{-5} M for GCG (Figure 45C). In addition, the IC_{50} value for halistanol sulphate in the GCG receptor binding assay was determined to be 53 μM, while the IC_{50} value for GCG was determined to be 48 nM (Figure 45C). Thus, halistanol sulphate displays a very narrow range of activity in the GCG receptor binding assay, and is ~1100 fold less active at the GCG receptor than GCG itself. These results are complimentary to the bioassay results, and demonstrate that halistanol sulphate binds strongly to the GIP receptor, but also weakly to the GLP-1 and GCG receptors. Furthermore, the bioassay results demonstrate that halistanol sulphate also modulates both GIP and GLP-1 receptor activity and downstream signalling. Nonetheless, the ability of halistanol sulphate to modulate GCG receptor signalling in the GCG bioassay has not yet been evaluated. Important to note, the active concentrations of halistanol sulphate in the bioassay are very similar to the active concentrations in the receptor binding assay, providing validation for the two techniques. However, the dynamic range for halistanol sulphate in the GIP receptor binding assay (10^{-9} to 10^{-4} M) is much larger than in the GIP bioassay (10^{-7} to 10^{-4} M). In addition, halistanol sulphate completely blocks GIP receptor signalling in the GIP bioassay, but does not completely block $[^{125}I]$GIP(1-42) binding in the GIP receptor binding assay. A potential explanation for this discrepancy is that halistanol sulphate is binding to the GIP receptor at a site other than the orthosteric site, inhibiting receptor signalling but only partially blocking $[^{125}I]$GIP(1-42) binding (likely via a conformational change in the active site). Thus, the receptor binding assay results demonstrate that halistanol sulphate binds predominantly to the GIPR but also to a lesser extent to the GLP-1R and GCGR.

5.2.1.3 Characterization of Halistanol Sulphate via Perifusion

After examining the cell signalling and receptor binding activity of halistanol sulphate, the ability of halistanol sulphate to modulate insulin secretion from perifused mouse islets was next investigated. The perifusion experiment was performed with technical assistance by Betty Hu. As

outlined in Figure 46, the perifusion experiment was designed to evaluate the actions of GIP and halistanol sulphate on insulin secretion. The control perifusion protocol was set up to determine the effects of GIP on insulin secretion in the absence of halistanol sulphate (Figure 46A), while the experimental perifusion protocol was designed to evaluate the effect of halistanol sulphate on GIP induced insulin secretion (Figure 46B). Since halistnaol sulphate has been demonstrated (via bioassays and receptor binding assays) to display antagonistic activity at the GIP receptor, it was expected to inhibit GIP-stimulated insulin secretion but have no effect on insulin secretion in the absence of GIP. Thus, the perifusion experiment was used to supplement the *in vitro* assays and give insight into the ability of halistanol sulphate to modulate physiological activity in an *in vitro* system.
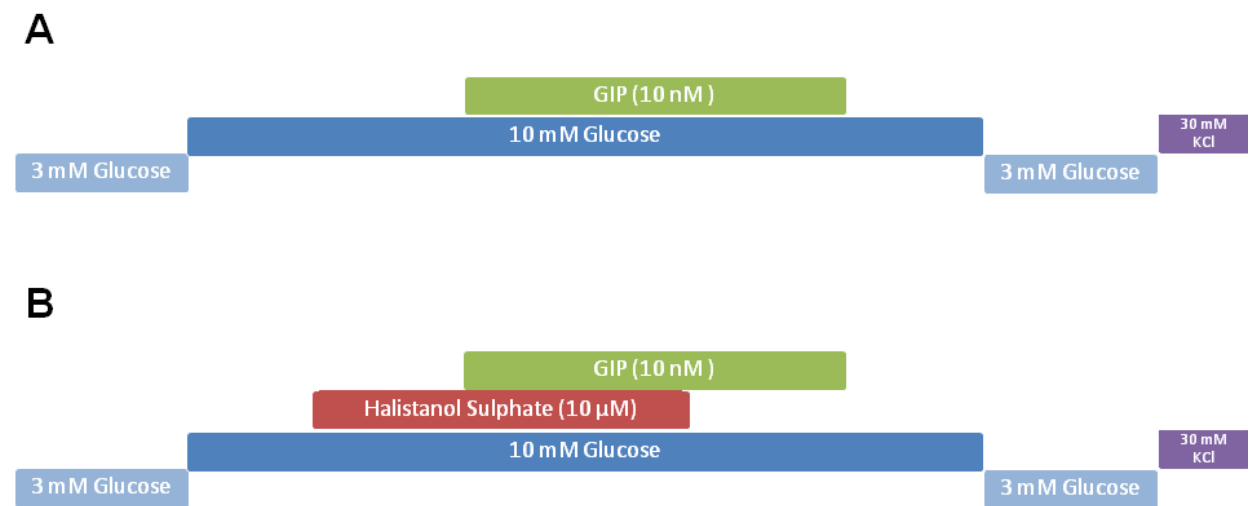
Figure 46. Protocol for Perifusion of Mouse Pancreatic Islets
(A) Control Perifusion Protocol. The control perifusion protocol was designed as a control to reveal the actions of GIP on insulin secretion in the absence of halistanol sulphate. **(B)** Experimental Perifusion Protocol. The experimental perifusion protocol was designed to reveal any modulating actions of halistanol sulphate on GIP-induced insulin secretion. Each protocol lasted 135 minutes, with samples collected every 3 minutes. The perifusion experiment was performed with technical assistance by Betty Hu.

The control perifusion protocol (Figure 46A) was first performed in order to determine the effects of glucose and GIP on insulin secretion from perifused mouse islets in the absence of halistanol sulphate. As seen in Figures 47A and 47C, there was an insignificant trend towards an increase in insulin secretion when the islets were perifused with 10 mM glucose compared to 3 mM glucose. The 10 mM glucose concentration was chosen for the experiment in order to only moderately stimulate insulin secretion and allow for further stimulation with GIP; however, a higher concentration of glucose would be required to significantly stimulate insulin secretion. After stimulating the islets with 10 mM glucose, 10 nM GIP was added to the infusion solution in order to determine the effect of GIP on insulin secretion. As seen in Figures 47A and 47C, GIP significantly

increased insulin secretion from mouse islets in the presence of 10 mM glucose, validating the perifusion system and the quality of the islets. However, after removing GIP from the perifusate, insulin secretion did not significantly decrease, likely due to the lingering effects of GIP (remaining GIP bound to the GIP receptor and the perifusion tubing) (Figures 47A and 47C). The perifusate was then switched from 10 mM glucose to 3 mM glucose, with a large but insignificant decrease in insulin secretion (Figures 47A and 47C). Finally, the islets were stimulated with 30 mM KCl to ensure that the islets were still alive and responsive to stimuli (Figures 47A and 47C). As seen in Figure 47C, KCl did not significantly stimulate insulin secretion, but did display a trend towards an increase in insulin secretion. A larger number of replicates would likely result in a significant increase in insulin secretion. Thus, the control perifusion protocol served to validate the perifusion setup and the responsiveness of the islets, and confirmed that 10 nM GIP significantly stimulates insulin secretion from perifused mouse islets in the absence of halistanol sulphate.

The experimental perifusion protocol (Figure 46B) was then performed in order to evaluate the ability of halistanol sulphate to modulate GIP induced insulin secretion from mouse islets. Similar to the control protocol, there was an insignificant increase in insulin secretion when inducing the islets with 10 mM glucose compared to 3 mM glucose (Figures 47B and 47C). Halistanol sulphate (10 μM) was then tested in the perifusion experiment in the absence of GIP and, as expected, did not significantly alter insulin secretion in the presence of 10 mM glucose (Figures 47B and 47C). After perifusing the islets with 10 μM halistanol sulphate and 10 mM glucose for several minutes, 10 nM GIP was added to the perifusate. The addition of GIP to the perifusate (already containing 10 μM halistanol sulphate and 10 mM glucose) resulted in a significant increase in insulin secretion (Figures 47B and 47C). However, the presence of halistanol sulphate resulted in a significant reduction in GIP induced insulin secretion, as evidenced by the statistically significant difference in insulin release between the experimental perifusion experiment (10 mM glucose, 10 μM halistanol sulphate and 10 nM GIP) and the control perifusion experiment (10 mM glucose and 10 nM GIP) (Figure 47C). As demonstrated in Figure 47C, the GIP stimulated increase in insulin secretion was significantly weaker in the presence of halistanol sulphate (experimental perifusion) compared to in the absence of halistanol sulphate (control perifusion). Furthermore, the removal of 10 μM halistanol sulphate from the perifusate did not result in a significant increase in insulin secretion, likely due to the lingering effects of halistanol sulphate (remaining halistanol sulphate bound to the GIP receptor and the perifusion tubing) (Figures 47B and 47C). As such, the glucose and GIP induced insulin release following the removal of halistanol sulphate from the perifusate (experimental perifusion) was significantly lower than the insulin release from islets never treated with halistanol sulphate (control perifusion) (Figure 47C). This result fits with the previously
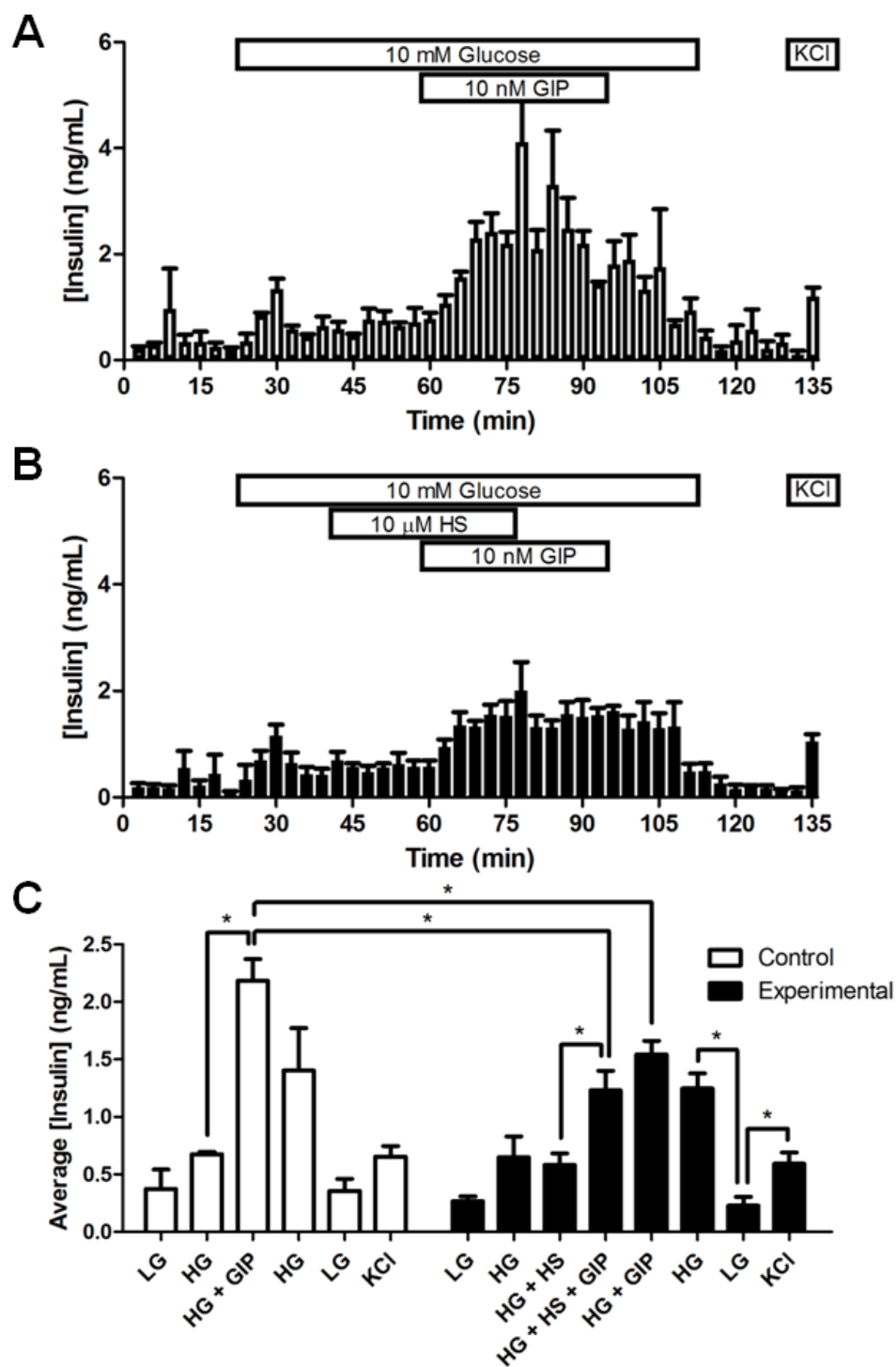
Figure 47. **The Effect of Halistanol Sulphate on GIP-Stimulated Insulin Release From Perifused Mouse Islets**
(A) Control Perifusion Results. **(B)** Experimental Perifusion Results. **(C)** Summary of the Effect of Halistanol Sulphate on GIP Induced Insulin Secretion. Isolated mouse islets were infused with low glucose (LG, 3 mM), high glucose (HG, 10 mM), halistanol sulphate (HS, 10 μM), GIP (10 nM) and/or potassium chloride (KCl, 30 mM) and the insulin content in the effluent determined with an insulin RIA. For 30 minutes prior to infusion, the first 18 minutes of sample collection and the last 27 minutes of sample collection, islets were infused with 3 mM glucose. $*$ $p < 0.05$. Data are expressed as means ± SEM, n=3.

observed lag period that results after the removal of a drug from the perifusion system (Figure 47A). In contrast to the control perifusion experiment, the switch from high glucose to low glucose in the experimental perifusion resulted in a significant decrease in insulin secretion, while stimulation of the islets with KCl resulted in a significant increase in insulin secretion (Figure 47C). Since the same trend exists in the control perifusion experiment (Figure 47C), a larger number of replicates would likely correct these discrepancies. Thus, these results demonstrate that halistanol sulphate significantly blocks GIP induced insulin secretion but does not affect insulin secretion in the absence of GIP, providing further support for the hypothesis that halistanol sulphate is a GIP receptor antagonist. In conclusion, halistanol sulphate displays physiologically relevant activity in mammalian islets in addition to its previously described *in vitro* activity in tumour-derived cell lines.

5.2.1.4 Characterization of Halistanol Sulphate via Perfusion

After examining the effect of halistanol sulphate on insulin secretion in perifused mouse islets, the next step was to evaluate the ability of halistanol sulphate to modulate insulin secretion *ex vivo* from the perfused mouse pancreas. The surgical isolation of the mouse pancreas for perfusion studies was performed by Gary Yang. As shown in Figure 48A, the perfusion experiment was designed to investigate the actions of GIP and halistanol sulphate on insulin secretion. In particular, the experimental perfusion protocol was designed to examine the effect of halistanol sulphate on GIP induced insulin secretion. In contrast, the control perfusion experiment (Figure 48B) was used in order to determine if halistanol sulphate had any effect on GLP-1 induced insulin secretion. As halistanol sulphate acts predominantly as a GIP receptor antagonist (as demonstrated by the bioassays and receptor binding assays), it was expected to reduce GIP-stimulated insulin secretion but have no effect on insulin secretion in the absence of GIP in the experimental perfusion protocol. In addition, as halistanol sulphate activated the GLP-1 receptor in the bioassay and weakly bound to the GLP-1 receptor in the binding assay, it was expected that halistanol sulphate would augment GLP-1 induced insulin secretion. Thus, the perfusion experiments were designed and performed in order to supplement the *in vitro* studies and give insight into the ability of halistanol sulphate to modulate incretin induced insulin secretion in a physiological system.

The experimental perfusion protocol (Figure 48A) was first performed in order to examine the ability of halistanol sulphate to modulate GIP induced insulin secretion from the perfused mouse pancreas. As seen in Figures 49A and 49C, 16.67 mM glucose significantly stimulated insulin secretion compared to basal glucose (4.4 mM), validating the perfusion setup and the health of the pancreata. After stimulating the pancreata for several minutes with 16.67 mM glucose, 10 μM halistanol sulphate was added to the infusion solution in order to determine if halistanol sulphate

A

0.2 nM GIP

Halistanol Sulphate (10 µM)

16.67 mM Glucose

4.4 mM G

B

0.2 nM GLP-1

Halistanol Sulphate (10 µM)

16.67 mM Glucose

4.4 mM G
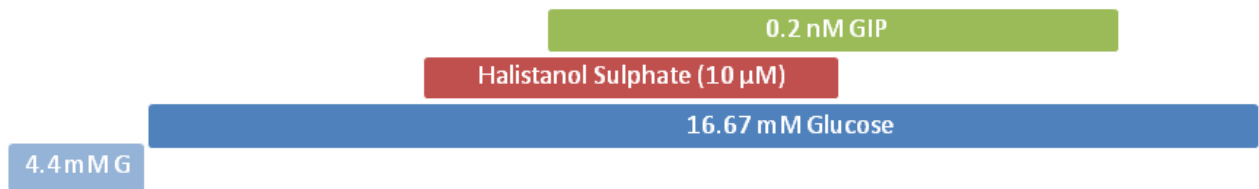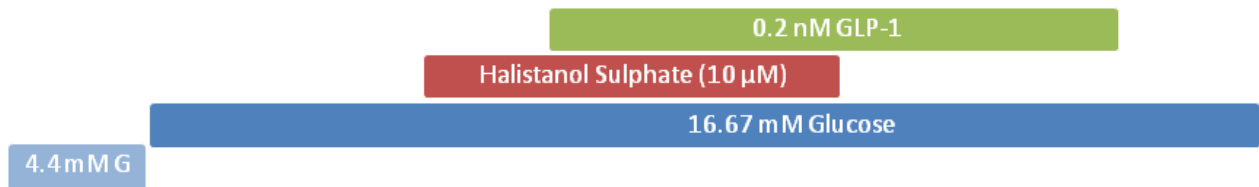
Figure 48.   Protocol for Perfusion of Isolated Mouse Pancreas
(A) Experimental Perfusion Protocol. The experimental perfusion protocol was designed to reveal any modulating actions of halistanol sulphate on GIP-induced insulin secretion.   **(B)** Control Perfusion Protocol.   The control perfusion protocol was designed as a control to reveal any modulating actions of halistanol sulphate on GLP-1-induced insulin secretion. Each protocol lasted 81 minutes, with samples collected every 3 minutes. The surgical isolation of the mouse pancreas for perfusion studies was performed by Gary Yang.

affected insulin secretion in the absence of GIP. Importantly, halistanol sulphate did not significantly alter insulin secretion in the absence of GIP (Figures 49A and 49C). The pancreata were then stimulated with 0.2 nM GIP in addition to 10 µM halistanol sulphate and 16.67 mM glucose. As seen in Figures 49A and 49C, the addition of 0.2 nM GIP to the perfusion solution resulted in significantly stimulated insulin secretion. Similarly, the infusion of 0.2 nM GIP, 10 µM halistanol sulphate and 16.67 mM glucose to the pancreata significantly increased insulin secretion compared to 16.67 mM glucose alone (Figures 49A and 49C). In addition, there was no significant change in insulin secretion once 10 µM halistanol sulphate was removed from the solution and only 0.2 nM GIP and 16.67 mM glucose were infused (Figures 49A and 49C). These results demonstrate that GIP significantly stimulates insulin secretion from the perfused mouse pancreas, validating the well known role of GIP as an insulin secretagogue. Furthermore, halistanol sulphate did not significantly alter GIP induced insulin secretion from the perfused mouse pancreas, suggesting that halistanol sulphate, at the concentration tested, does not act as a GIP receptor antagonist in this model. However, as seen in Figure 49A, there is a trend of increased insulin secretion after removing 10 µM halistanol sulphate from the solution while still in the presence of 0.2 nM GIP and 16.67 mM glucose. This finding suggests that halistanol sulphate may in fact be blocking insulin secretion from

the perfused mouse pancreas in the presence of GIP (acting as a GIP receptor antagonist), but not at a significant level. A potential reason why halistanol sulphate did not significantly alter GIP induced insulin secretion in the perfused mouse pancreas is that the concentration of halistanol sulphate used in the experiment was not high enough to function *ex vivo*. The concentration of halistanol sulphate (10 μM) used for the perfusion was able to strongly block ^{125}I-GIP binding in the GIP receptor binding assay (Figure 45A) and significantly block insulin secretion in the experimental perifusion experiment (Figure 47C) but only moderately inhibit GIP receptor signalling in the bioassay (Figure 44A), and was chosen based on a limited supply of compound. Thus, further studies are warranted to investigate the ability of halistanol sulphate to modulate GIP induced insulin secretion in a physiological system.

Finally, the control perfusion protocol (Figure 48B) was executed in order to investigate the ability of halistanol sulphate to alter GLP-1 induced insulin secretion from the perfused mouse pancreas. Similar to the experimental protocol, the perfusion setup and health of the pancreata were validated by the fact that 16.67 mM glucose significantly stimulated insulin secretion compared to basal glucose (4.4 mM) (Figures 49B and 49D). Furthermore, 10 μM halistanol sulphate did not significantly alter insulin secretion in the absence of GLP-1 (Figures 49B and 49D). In contrast to the experimental protocol, the pancreata were then stimulated with 0.2 nM GLP-1 in the presence of 10 μM halistanol sulphate and 16.67 mM glucose. As seen in Figures 49B and 49D, insulin secretion was significantly stimulated by the addition of 0.2 nM GLP-1 to the perfusion solution. In addition, infusion with 0.2 nM GLP-1, 10 μM halistanol sulphate and 16.67 mM glucose resulted in significantly increased insulin secretion compared to 16.67 mM glucose alone (Figures 49B and 49D). Furthermore, the removal of 10 μM halistanol sulphate from the infusion solution (also containing 0.2 nM GLP-1 and 16.67 mM glucose) did not significantly alter insulin secretion (Figures 49B and 49D). These results validate GLP-1 as an insulin secretagogue by demonstrating that GLP-1 can significantly stimulate insulin secretion from the perfused mouse pancreas. However, GLP-1 induced insulin secretion was not altered by halistanol sulphate in the perfused mouse pancreas, suggesting that halistanol sulphate does not act as a GLP-1 receptor activator in this model, at the concentration used. Nonetheless, there is a trend of decreased insulin secretion following the removal of 10 μM halistanol sulphate from the solution (which still contains 0.2 nM GLP-1 and 16.67 mM glucose) (Figure 49B). This trend suggests that halistanol sulphate may in fact be augmenting insulin secretion from the perfused mouse pancreas in the presence of GLP-1 (acting as a GLP-1 receptor agonist/allosteric modulator), but not to a significant level. As with the experimental protocol, the inability of halistanol sulphate to significantly alter GLP-1 induced insulin secretion may be due to the low concentration of halistanol sulphate used in the experiment. The
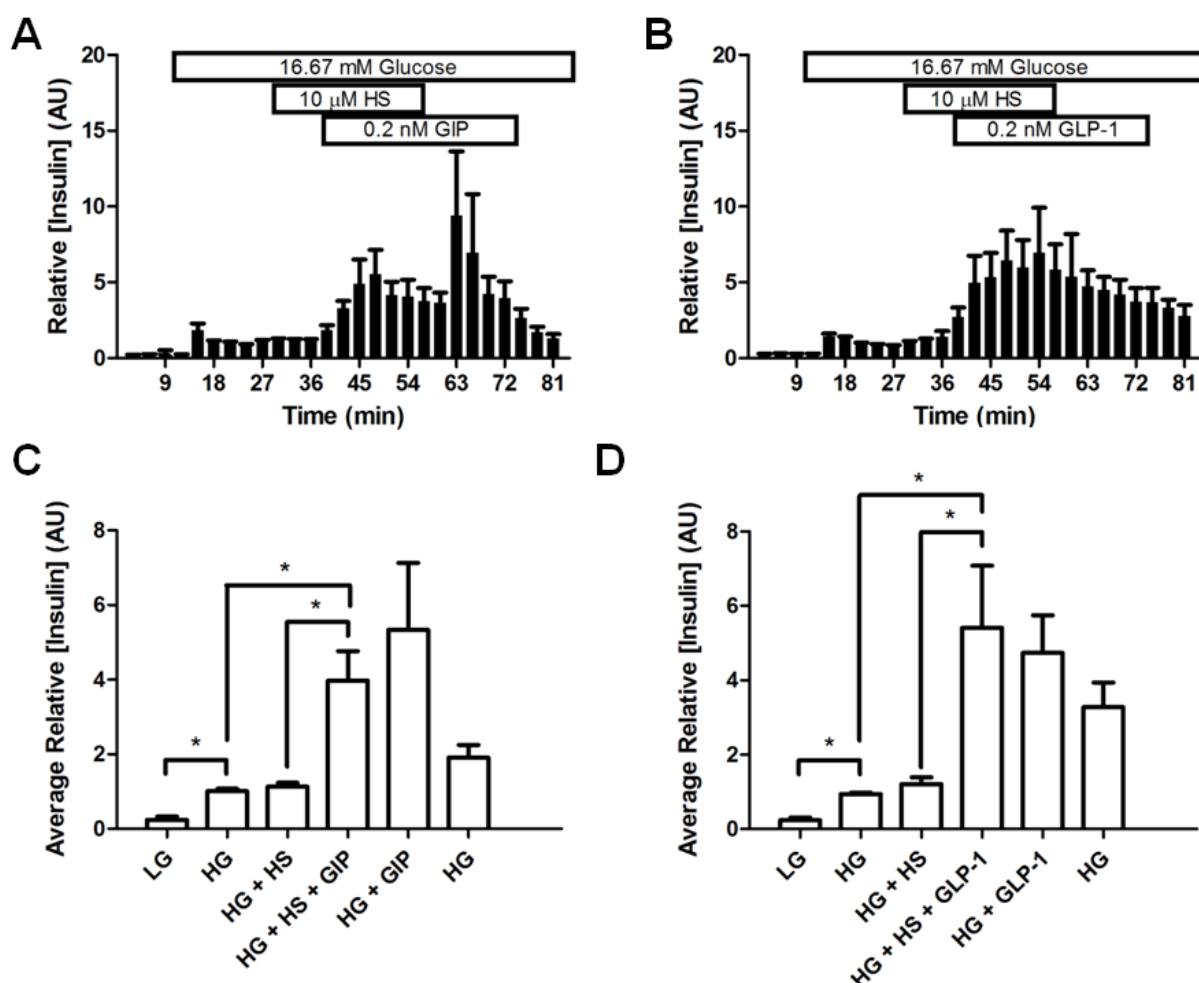
Figure 49.   The Effect of Halistanol Sulphate on Incretin-Stimulated Insulin Release From the Perfused Mouse Pancreas

(A) The Effect of Halistanol Sulphate on GIP-Induced Insulin Secretion.   **(B)** The Effect of Halistanol Sulphate on GLP-1-Induced Insulin Secretion. **(C)** Summary of the Effect of Halistanol Sulphate on GIP Induced Insulin Secretion. **(D)** Summary of the Effect of Halistanol Sulphate on GLP-1 Induced Insulin Secretion. Isolated mouse pancreata were infused with low glucose (LG, 4.4 mM), high glucose (HG, 16.67 mM), halistanol sulphate (HS, 10 μM), GIP (0.2 nM) and/or GLP-1 (0.2 nM) and the insulin content in the effluent determined with an insulin RIA. For 30 minutes prior to infusion and for the first 9 minutes of sample collection, pancreata were equilibrated with 4.4 mM glucose. Relative [insulin] was calculated by subtracting basal insulin levels (in the presence of 4.4 mM glucose) from total insulin levels. * $p < 0.05$. Data are expressed as means ± SEM, n=8.

concentration of halistanol sulphate (10 μM) used for the perfusion was only able to modestly block

^{125}I-GLP-1 binding in the GLP-1 receptor binding assay (Figure 45B) and moderately stimulate GLP-1 receptor signalling in the bioassay (Figure 44B). Thus, the trends in the modulation of insulin secretion by halistanol sulphate match our hypothesis that halistanol sulphate acts as both a GIPR antagonist and a GLP-1 receptor activator; nonetheless, subsequent studies are required to further investigate this possibility.

6   Chapter: Conclusions

6.1   Advantages and Limitations of the Bioassay and the Screening System

In order to screen marine invertebrate and bacterial extracts, several reporter cell lines were developed. As described extensively in Chapters 2 and 3, the reporter cell lines, HEK-hGIPR-Luc, HEK-hGLP-1R-Luc and HEK-hGCGR-Luc, express a receptor of interest (the GIP, GLP-1 or glucagon receptor, respectively) as well as a luciferase gene driven by a cAMP responsive element (Figure 8). As these receptors are all GPCRs that feed into the cAMP signalling pathway, receptor activation leads to an increase in cAMP levels and the production of luciferase (Figure 12). The HEK-pHTS-CRE cell line, which has not been transfected with a receptor plasmid, acts as a negative control cell line as it measures cAMP signalling in the absence of a receptor. Using these reporter cell lines, a functional bioassay was developed. The bioassay involves incubating the reporter cells in the presence of antigen or marine invertebrate/bacterial extract and then adding luciferase substrate and measuring light output. Thus, the bioassay facilitates the detection of GIP, GLP-1 or glucagon receptor activity via the measurement of light output.

The developed bioassay poses many advantages over the typical antigen quantification systems such as the enzyme-linked immunosorbent assay (ELISA) or RIA. One of the major differences of the bioassay compared to other antigen measurement systems is that the bioassay measures biological activity rather than immunoreactivity. While an ELISA or RIA can be tailored to only measure active forms of an antigen (for example, the Millipore GLP-1 (active) ELISA; catalogue number EGLP-35K), it is important to recognize that antigen immunoreactivity does not necessarily correspond with bioactivity. Furthermore, while both the ELISA and RIA are capable of measuring the amount of antigen in a sample, they are not capable of measuring receptor activity via activation by unknown compounds. Moreover, the ELISA and RIA are much more expensive than the bioassay; the cost to run one 96-well plate through the bioassay is under \$25, far less than the \$200 - \$500 cost of testing the equivalent number of samples in an ELISA or RIA. Thus, the bioassay is a cost-effective technique amenable to high-throughput screening, and is far superior to the ELISA and RIA for this purpose. In addition, compared to other reporter systems, such as a green fluorescent protein reporter, the bioassay allows for signal amplification, leading to increased sensitivity and a lower limit of detection. Finally, the reporter system uses a simple output parameter, light output, which can easily and rapidly be measured using a luminometer. Thus, the bioassay possesses many beneficial characteristics that make it an excellent research tool to screen for incretin receptor modulators.

The advantages of using a bioassay to screen for modulators of the GIP, GLP-1 or glucagon receptors have also been recognized by others. Indeed, several other groups have also developed

similar bioassays. Compared to the GLP-1 bioassays developed by Chen et al. and Knudsen et al., which display EC_{50} values of 68 pM and 23 pM, respectively (Chen et al., 2007; Knudsen et al., 2007), our GLP-1 bioassay is more sensitive, with an EC_{50} value of 2.8 pM. Furthermore, our GLP-1 bioassay is much more sensitive than the calcium flux assay described by Multispan, which displays an EC_{50} value of 160 nM (Multispan, 2005b). In addition, commercial GIP and glucagon bioassays are also available from Multispan (Multispan, 2005a; Multispan, 2005c). Compared to the GIP bioassay produced by Multispan, which displays an EC_{50} value of 160 pM (Multispan, 2005a), our GIP bioassay is only slightly less sensitive (displays an EC_{50} value of 560 pM). However, the glucagon bioassay described by Multispan displays an EC_{50} value of 48 pM (Multispan, 2005c), which is less sensitive than our glucagon bioassay (displays an EC_{50} value of 2.5 pM). Finally, the bioassays are not without limitations; the bioassay procedure is time-consuming (2-day procedure) and requires the use of live cells (which require resources and time to maintain in culture, and are susceptible to ills such as contamination and temperature/pH shifts). Another limitation of the bioassay is that it does not distinguish between cytotoxic compounds and compounds that decrease light output by altering cellular signalling. In order to distinguish between these possibilities, a dual luciferase reporter system could be used to normalize light output values; this might involve transfecting the reporter cell lines with a renilla luciferase plasmid driven by a constitutively active promoter in order to control for differences in cell viability. Nonetheless, the bioassays developed in the Kieffer laboratory are valuable research tools that display equal or superior sensitivity to similar bioassays developed by other groups.

As described in Chapter 4, over 2000 extracts (14 marine invertebrate extract 96-well plates and 10 bacterial extract 96-well plates) were tested in each of four screens: the GIP receptor agonist screen, the GIP receptor allosteric modulator and antagonist screen, the GLP-1 receptor agonist screen and the GLP-1 receptor allosteric modulator screen. In these screens, multiple non-specific hits, or compounds that modulate the cAMP signalling pathway independent of the incretin receptors, were identified, while only one specific hit, or compound that modulates the incretin receptors, was identified. In comparable screens, Knudsen et al. screened 250,000 small molecule compounds before identifying a GLP-1 receptor modulator (Knudsen et al., 2007), while Chen et al. screened 48,160 synthetic and natural compounds in order to identify two GLP-1 receptor modulators (Chen et al., 2007). Thus, compared to other high throughput screening projects, our screens have yielded an impressive hit to non-hit ratio. One potential explanation for why our screens yielded a much higher hit to non-hit ratio is that the extracts we screened contained mixtures of several different compounds, effectively allowing us to screen more individual compounds more quickly. However, screening mixtures of multiple compounds also poses a disadvantage; compounds that act as incretin

receptor modulators could be overlooked if they are present in the same extract as a cytotoxic compound or another incretin receptor modulator with an opposing effect. Another explanation for why our screens yielded a higher hit to non-hit ratio is that the extracts that we screened contained a high percentage of biologically active compounds. As described in the introduction, and as demonstrated in the screening results, marine invertebrate extracts generally contain a wide array of biologically active compounds (Cordier et al., 2008). However, our screens revealed that the bacterial extracts were much less active than the marine invertebrate extracts. This difference in activity could be due to inherent differences in biological activity between compounds isolated from marine invertebrates and bacteria, or could be due to the use of a sub-optimal concentration of bacterial extract in the screens. As the hit rate typically rises as the concentration increases and falls as the concentration decreases (due to toxicity of the compounds), an optimal extract concentration is required in order to identify hits without harming the cells. Since cytotoxic effects were not evident in the majority of the wells incubated with bacterial extracts, the bacterial extract concentration used for screening was probably too low rather than too high. Thus, if we were to perform additional screens with bacterial extracts, we would use a higher concentration of bacterial extract in the new screens. In conclusion, our screens for incretin receptor modulators in marine invertebrate and bacterial extract libraries resulted in a good hit to non-hit ratio and led to the identification of an incretin receptor modulator.

As described in Chapter 4, several extracts were originally identified as hits during screening, but were subsequently ruled out after further investigation. The most common reason why hits were ruled out during subsequent testing was that the hits were shown to display activity in the negative control cell line, HEK-pHTS-CRE, when tested at multiple concentrations. A potential explanation for why the extracts did not display activity in the HEK-pHTS-CRE cell line when tested at a single concentration, but displayed activity when tested over several concentrations, is that the cell lines have different sensitivities to cAMP signalling. As such, an extract that was active in the HEK-hGIPR-Luc cell line or the HEK-hGLP-1R-Luc cell line at a specific concentration may only be active in the HEK-pHTS-CRE cell line at a concentration higher or lower than that. These findings solidify the importance of testing hit extracts at multiple concentrations in the HEK-pHTS-CRE cell line in order to eliminate hits that act in a non-specific manner to modulate cAMP signalling. Another less common reason why hits were ruled out during subsequent testing was that fresh aliquots of the hit extracts did not display reproducible activity in the cell line of interest. Possible reasons why the fresh hit extracts did not display reproducible activity are that the concentration of the active compound or of a counter-acting compound in the extract was altered in the original sample due to multiple freeze/thaw cycles. Thus, the inability of the extract to display reproducible

activity may be due to differences in the concentrations of active compounds and counter-acting compounds between the fresh extract sample and the original extract sample. Nonetheless, the majority of hit extracts were reproducible in the cell line of interest, validating that the criteria for determining a hit were stringent enough to identify real hits. Thus, the screening techniques and hit criteria used were able to accurately identify reproducible hits.

6.2   Compounds That Activate cAMP Signalling

As extensively described in Chapter 5, the alotaketals and ansellones were discovered as novel compounds that activate the cAMP signalling pathway. Although these novel molecules are not of interest as therapeutics to treat diabetes or obesity, they still hold value. For example, the alotaketals and ansellones can be used as research tools. Similar to forskolin, the alotaketals and ansellones can be used to stimulate cAMP signalling in cells in order to examine various aspects of the pathway or can be used as tools to investigate other scientific questions. Furthermore, the alotaketals and ansellones also contain unprecedented carbon skeletons that are of interest in organic chemistry and other fields. These novel carbon skeletons can be structurally modified or can be the source of inspiration for the development of novel drugs to treat various diseases. In addition, the novel compounds can offer insight into the biology of the organisms that produce them, in this case, marine sponges. Thus, the discovery of novel compounds involved in cAMP signalling is beneficial to several different scientific disciplines.

Although the alotaketals and ansellones were determined to activate the cAMP signalling pathway, the specific target of these molecules is still not known. As discussed in Chapter 5, alotaketal B displays a trend towards concentration-dependently increasing cAMP concentrations in HEK-pHTS-CRE cells, but this trend cannot be confirmed with statistical analysis since the number of replicates was less than 3 (Figure 38B). In order to confirm these results, a cAMP assay with the alotaketals would need to be repeated with a larger number of replicates. It would also be worthwhile to test the ansellones in the cAMP assay at the same time. Future experiments to determine the mechanism of action of the alotaketals and ansellones include enzymatic assays of adenylyl cyclase and phosphodiesterase and western blots to determine if protein levels of phosphorylated CREB and PKA are altered. Furthermore, additional experiments with alotaketal and ansellone derivatives could be performed in order to further investigate structure-activity relationships, and to determine whether or not the alotaketals and ansellones act on the same target. Therefore, further investigation is required in order to determine the specific target of the alotaketals and ansellones, and to learn more about the structure-activity relationships of these compounds.

6.3   Halistanol Sulphate

After screening over 2000 marine invertebrate and bacterial extracts, extract 03-486 was determined to be a putative GIP receptor antagonist hit.   Crude extract 04-486 displayed a concentration-dependent decrease in light output in the GIP bioassay in the presence of GIP, but not in GLP-1 bioassay in the presence of GLP-1 (Figure 42).   Halistanol sulphate (Figure 43) was isolated as the active compound from extract 03-486, and was shown to concentration-dependently decrease light output in the GIP bioassay in the presence of GIP, but not in the absence of GIP (Figures 44A and 44B).   On the other hand, halistanol sulphate increased activity in the GLP-1 bioassay in the presence of GLP-1, suggesting that halistanol sulphate was also acting as a GLP-1 receptor allosteric modulator or ago-allosteric modulator (Figure 44C).   Halistanol sulphate was then evaluated in the binding assay, and was shown to displace [^{125}I]GIP(1-42) binding from the GIP receptor in a concentration-dependent manner (Figure 45A).   Halistanol sulphate also displaced [^{125}I]GLP-1(7-36) amide binding to the GLP-1 receptor and [^{125}I]GCG(1-29) binding to the GCG receptor, but only at a very high concentration (100 μM) (Figures 45B and 45C).   These *in vitro* studies demonstrated that halistanol sulphate was acting as a GIP receptor antagonist, as well as a GLP-1 receptor agonist/allosteric modulator and potentially as a GCG receptor modulator.

In order to complement the *in vitro* assays performed in the tumour-derived cell lines with halistanol sulphate, perifusion and perfusion experiments were performed in mouse islets and mouse pancreata, respectively.   In mouse islets, halistanol sulphate significantly blocked GIP induced insulin secretion but did not affect insulin secretion in the absence of GIP (Figure 47).   Thus, the perifusion studies provide further support that halistanol sulphate is a GIP receptor antagonist. However, in mouse pancreata, halistanol sulphate did not significantly alter GIP induced insulin secretion (Figure 49C).   Nevertheless, there was a trend towards an increase in insulin secretion after removing halistanol sulphate from the perfusate (which also contained GIP and high glucose) (Figures 49A and 49C).   Similarly, halistanol sulphate did not significantly alter GLP-1 induced insulin secretion from mouse pancreata, but there was a trend towards decreasing insulin secretion following the removal of halistanol sulphate from the perfusate (which also contained GLP-1 and high glucose) (Figures 49B and 49D).   Therefore, the perfusion studies suggest that halistanol may be acting to block GIP-induced insulin secretion and augment GLP-1 induced insulin secretion from the perfused mouse pancreas, but not to significant levels.   As discussed in the results section, the inability of halistanol sulphate to significantly modulate GIP or GLP-1 induced insulin secretion may be due to the low concentration (10 μM) used in the experiment.   Although halistanol sulphate was active in the bioassay, the receptor binding assay and the perifusion experiment at a concentration of 10 μM, this concentration might have been too low to result in significant effects *ex vivo* in the

mouse pancreas. Thus, further experiments are warranted to investigate the ability of halistanol sulphate to modulate GIP and GLP-1 induced insulin secretion in a physiological system.

Although the *in vitro* studies performed in this thesis strongly suggest that halistanol sulphate is acting as a GIP receptor antagonist and a GLP-1 receptor activator, additional experiments would be useful in order to learn more about the mechanism of action of halistanol sulphate. As described above, halistanol sulphate was shown to significantly enhance light output in the GLP-1 bioassay in the presence of GLP-1, suggesting that halistanol sulphate is capable of acting as a GLP-1 receptor allosteric modulator. Interestingly, allosteric modulators of GPCRs have been suggested to act via the stimulation of receptor dimerization (Bai, 2004; Jensen and Spalding, 2004). However, it is unknown whether halistanol sulphate acts as a GLP-1 receptor allosteric modulator or ago-allosteric modulator (functions as both an agonist and an allosteric modulator). In order to determine if halistanol sulphate also displays agonistic activity at the GLP-1 receptor, a GLP-1 bioassay will be performed with halistanol sulphate in the absence of GLP-1. If halistanol sulphate is able to significantly increase light output in the GLP-1 bioassay in the absence of GLP-1, this would suggest that halistanol sulphate is acting as a GLP-1 receptor ago-allosteric modulator. On the other hand, if halistanol sulphate is not able to significantly enhance light output in the GLP-1 bioassay in the absence of GLP-1, this would suggest that halistanol sulphate is acting solely as a GLP-1 receptor allosteric modulator. In addition, the characterization of halistanol sulphate in the GCG receptor bioassay is essential. Although halistanol sulphate was previously shown to block GCG binding to the GCG receptor (Figure 45C), it is unknown whether or not halistanol sulphate modulates GCG receptor signalling. In order to determine if halistanol sulphate modulates GCG receptor activity, and if it acts as a GCG receptor agonist, allosteric modulator or antagonist, GCG bioassays with halistanol sulphate (both in the presence and absence of GCG) will be performed. Furthermore, it is unclear from the performed experiments whether halistanol sulphate mediates its effects by sequestering GIP (so that it is unavailable to interact with the GIP receptor) or by physically binding to the GIP receptor. In order to determine if halistanol sulphate mediates its effects by binding to the GIP receptor, saturation transfer double-difference NMR experiments in the HEK-hGIPR-Luc cell line will be performed. The Andersen laboratory has recently used this approach to show that haplosamate A binds selectively to human cannabinoid receptors, and we will follow the same protocol in our studies (Pereira et al., 2009). Therefore, additional experiments are warranted in order to gain further insight into the mechanism of action of halistanol sulphate.

In order to further investigate the ability of halistanol sulphate to modulate GIP and GLP-1 induced insulin secretion, additional perifusion and perfusion studies need to be performed. In the perifusion studies, the ability of halistanol sulphate to modulate GIP induced insulin secretion was

investigated, but its effects on GLP-1 induced insulin secretion were not examined. Thus, additional perifusion studies could be performed in order to evaluate the ability of halistanol sulphate to modulate GLP-1 induced insulin secretion. Additional perfusion experiments are also warranted in order to provide better insight into the significance of the perfusion data. As seen in Figure 49C, halistanol sulphate did not significantly inhibit GIP induced insulin secretion in the perfusion experiments, even though there was a trend towards an increase in insulin secretion following the removal of halistanol sulphate from the system. However, due to the lack of a proper control protocol, it is impossible to determine whether or not halistanol sulphate partially inhibited GIP induced insulin secretion. Thus, a control perfusion experiment performed in the absence of halistanol sulphate (but presence of the other stimuli) would serve as a better control to compare the experimental perfusion data against. In addition, halistanol sulphate did not significantly enhance GLP-1 induced insulin secretion in the perfusion experiments, even though there was a trend towards a decrease in insulin secretion following the removal of halistanol sulphate from the system. A similar control perfusion protocol performed in the absence of halistanol sulphate (but presence of the other stimuli) could be used to compare the GLP-1 experimental perfusion data against. Furthermore, islets and pancreata from GIPR-/- and GLP-1R-/- mice could be used in the perifusion and perfusion experiments as additional controls to validate that the actions of halistanol sulphate are dependent on the presence of these receptors. Finally, the ability of halistanol sulphate to modulate glucagon secretion could also be investigated in both the perifusion and perfusion experiments. Thus, additional perifusion and perfusion studies are warranted in order to obtain better insight into the significance of the obtained data.

Before proceeding to *in vivo* studies, the next step in drug development is to alter the structure of halistanol sulphate in order to develop a more potent modulator. In drug development, it is important that the potential drug has a high affinity for the receptor(s) of interest, since administering large quantities of a compound can be toxic and can cause unwanted side effects. Thus, the higher the affinity of the molecule for the receptor(s) of interest, in this case the GIP, GLP-1 and GCG receptors, the lower the concentration that needs to be administered and the lower the probability of toxicity and side effects. As such, Chen et al. report that a major limitation of Boc5 (a small molecule GLP-1 receptor agonist) is its relatively weak potency (the EC_{50} value of Boc5 is 2.73 μM and the IC_{50} value is 1.47 μM) (Chen et al., 2007). In addition, Knudsen et al. report that Compound 2 (another small molecule GLP-1 receptor modulator) is not potent enough to use as a drug (the EC_{50} value of Compound 2 is 101 nM) (Knudsen et al., 2007). Similarly, Compound B (a novel small molecule GLP-1 receptor agonist) displays an EC_{50} value of 660 nM and requires structural optimization in order to improve its pharmacokinetic properties and clinical potential

(Sloop et al., 2010). Thus, halistanol sulphate is also likely too weak to use as a therapeutic agent (the IC_{50} values of halistanol sulphate are 590 nM in the GIP binding assay, 68 μM in the GLP-1 binding assay and 53 μM in the GCG binding assay). In order to optimize the structure of halistanol sulphate to develop a more potent drug, the binding mode of halistanol sulphate to the GIP, GLP-1 and GCG receptors will be determine via molecular docking studies (Moitessier et al., 2008). Computer-aided structure-based drug design has aided in the development of many drugs that are now in late-stage clinical trials or have reached the market (Borman, 2005). Once the binding mode of halistanol sulphate is determined, informative structural modifications will be made in order to attempt to develop a more potent modulator. The structural variants will then be tested for activity in the GIP, GLP-1 and GCG bioassays and structure-activity relationships determined. This information will then be used to develop the most potent structural analogue of halistanol sulphate possible. In addition, the structure of halistanol sulphate can be altered in order to generate a compound with an optimal balance of GIP, GLP-1 and GCG receptor activity to create a very potent and highly efficacious triple receptor modulator. Thus, the structural modification of halistanol sulphate to develop a more potent GIP, GLP-1 and GCG receptor modulator is an essential step in drug development.

Ultimately, *in vivo* animal studies will constitute the most significant phase of evaluation of halistanol sulphate. As GIP and GLP-1 modulate insulin and glucagon secretion, we will begin by assessing the effect of halistanol sulphate on insulin, glucagon and glucose levels, both in overnight-fasted and refed 10-12 week old male C57BL/6 mice. Halistanol sulphate will be injected into the intraperitoneal cavity and insulin, glucagon and glucose levels measured in order to assess the effects of halistanol sulphate on physiological levels of GIP and GLP-1. In order to assess the effect of halistanol sulphate on pharmacological levels of GIP and GLP-1, halistanol sulphate will be injected into the intraperitoneal cavity in addition to GIP and GLP-1 and insulin, glucagon and glucose levels measured. Studies will also be performed to test for acute anorectic effects of GIP and GLP-1 receptor modulation by halistanol sulphate. Overnight-fasted C57BL/6 mice will be injected with halistanol sulphate and cumulative food intake and body weight monitored for 24 hours. If effects on food intake and/or body weight are observed, follow-up studies will be performed to more thoroughly assess these parameters, as well as assess water intake, body temperature, energy expenditure and activity levels with metabolic cages at the Centre for Disease Modeling at UBC. Throughout these studies, the general health of all animals will be carefully monitored and the toxicity and side-effect profile of compounds assessed.

In addition to acute studies, chronic studies will also be performed to investigate the physiological effects of halistanol sulphate. As such, halistanol sulphate will be administered once a

day by intraperitoneal injection to 10-12 week old *db/db* mice for 6 weeks. For the duration of the study, including 1 week prior to the start of injections, body weight and blood glucose levels will be measured and plasma samples collected from 6 hour fasted mice twice weekly. At the end of the study, oral glucose tolerance and insulin tolerance tests will be performed on 6 hour fasted mice. Treatments will then cease, but the twice weekly body weight and blood glucose level monitoring and plasma sampling will continue for 6 weeks. Following the 6 week post-injection monitoring period, the oral glucose tolerance and insulin tolerance tests will be repeated. Insulin and glucagon, free fatty acid and triglyceride levels will then be measured from the plasma samples. Additional studies could include measuring β-cell mass, lean to lipid mass ratios by NMR, or hepatic and peripheral insulin sensitivity by hyperinsulinemic/euglycemic clamps. Finally, the above experiments would be repeated with oral administration of the hit compounds if positive results were seen with intraperitoneal injections. If these *in vivo* studies demonstrate promising results, the Centre for Drug Research and Development, a non-profit organization designed to bridge the gap between potential drug discoveries in academia and the development of novel medicines to treat human disease, will be used to aid in the development of halistanol sulphate into a novel therapeutic.

As described above, many additional studies are required in order to more accurately assess the clinical potential of halistanol sulphate as an anti-diabetes/obesity drug. Nonetheless, we have already shown that halistanol sulphate modulates GIP and GLP-1 receptor signalling, GIP, GLP-1 and GCG receptor binding and insulin secretion from mouse islets. In addition, the fact that halistanol sulphate acts as a triple receptor modulator boasts great benefits in that it has the potential to display additive therapeutic effects while counteracting undesirable effects. Furthermore, since halistanol sulphate is a low molecular weight compound, there is a reasonable probability that it could be administered orally, which would greatly improve patient satisfaction and quality of life. However, there are some caveats for the potential use of halistanol sulphate as a diabetes and/or obesity drug. Halistanol sulphate has been shown to exhibit many other biological effects, which could result in a large side-effect profile. For example, halistanol sulphate has been shown to inhibit the activity of pp60[v-src], an oncogenic protein tyrosine kinase (Slate et al., 1994). In addition, halistanol sulphate inhibits the cytopathic effects of HIV-1 in human lymphoblastoid cells (McKee et al., 1994) and demelanizes a pigmented human myeloma cell line (MM418) (Townsend et al., 1992). Furthermore, halistanol sulphate has been shown to exhibit hemolytic activity (Moni et al., 1992) and inhibit the $P2Y_{12}$ receptor, which is involved in platelet aggregation (Yang et al., 2003). Thus, these studies demonstrate that halistanol sulphate displays a wide-range of *in vitro* effects, reducing the clinical potential of halistanol sulphate as a diabetes and obesity drug. However, these studies may not be relevant following the structural modification and optimization of halistanol sulphate to

develop a compound with improved potency and specificity. Finally, since halistanol sulphate has already been well characterized in the literature, it is not of interest to our organic chemistry collaborators. Therefore, the clinical utility of halistanol sulphate may be limited due to its large activity profile, but further studies are still required to determine if these *in vitro* effects are significant *in vivo*.

6.4   GIP Receptor Antagonists vs. GIP Receptor Agonists

As described in detail in the introduction, there is sufficient evidence to suggest that both the activation and inhibition of the GIP receptor are beneficial for the treatment of diabetes and/or obesity. The beneficial outcomes of GIP receptor activation largely stems from the role of GIP in glucose disposal (Kieffer, 2003). However, the therapeutic potential of GIP receptor agonists has been criticized due to the attenuated insulinotropic actions of GIP in subjects with diabetes (Elahi et al., 1994; Holst et al., 1997; Nauck et al., 1993a) and the role of GIP in obesity (Irwin and Flatt, 2009; Irwin et al., 2010; Kieffer, 2003). Nonetheless, the administration of D-Ala^2-GIP(1-42), a DPP-4 resistant GIP analogue, resulted in an enhanced insulinotropic response and improved glucose homeostasis in rodents with compromised GIP receptor expression (Hinke et al., 2002). In addition, near-normalization of blood glucose levels in type 2 diabetic patients results in improved insulin responses to GIP (Hojberg et al., 2009). Moreover, despite GIP being regarded as a pro-obesity hormone, D-Ala^2-GIP(1-30) enhanced insulin secretion and glycemic control in rodents without affecting body weight (Widenmaier et al., 2010). Furthermore, D-Ala^2-GIP(1-30) displayed markedly reduced effects on lipoprotein lipase activity in 3T3-L1 adipocytes compared to GIP(1–42), despite exhibiting equivalent actions *in vitro* on β-cell function and survival (Widenmaier et al., 2010). Thus, GIPR agonists that improve glucose homeostasis without increasing fat accumulation may be beneficial for the treatment of diabetes. Nonetheless, further studies aimed at investigating whether these GIP receptor agonists display comparable properties in humans remain to be completed.

Although the studies described above, as well as other more recent studies, suggest that GIPR agonism may be an effective strategy to treat diabetes (Hinke et al., 2002; Hojberg et al., 2009; Renner et al., 2010; Saxena et al., 2010; Widenmaier et al., 2010), recent human data suggests that this strategy is unlikely to be useful (Chia et al., 2009). The infusion of supraphysiological levels of GIP into patients with type 2 diabetes resulted in worsened postprandial hyperglycemia, likely due to the concomitant increase in glucagon and suppression of GLP-1 (Chia et al., 2009). Thus, GIP receptor antagonism may actually be a more feasible strategy to treat human diabetes and obesity. The evidence for beneficial GIP receptor antagonism is vast and revolves around the concept that

GIP directly links chronic overnutrition to obesity (Miyawaki et al., 2002). For example, GIPR-/- mice are protected from developing both obesity and insulin resistance when placed on a high fat diet (Miyawaki et al., 2002). In addition, multiple studies with Pro^{3}GIP, a putative GIPR antagonist, suggest that GIPR antagonism reverses the obesity and insulin resistance induced in mice by the prolonged consumption of a high-fat diet (Gault et al., 2007; Gault et al., 2005; Gault et al., 2002a; Gault et al., 2003; Irwin et al., 2004; Irwin et al., 2007a; Irwin et al., 2007b; McClean et al., 2008a; McClean et al., 2007; McClean et al., 2008b). Furthermore, selective K-cell destruction in mice results in vastly decreased weight gain, reduced food intake, increased energy expenditure and improved insulin sensitivity compared to wild-type littermates when placed on a high fat diet (Althage et al., 2008). Finally, mice vaccinated with VLP-GIP displayed reduced fat accumulation and weight gain when fed a high fat diet (Fulurija et al., 2008). Importantly, despite the incretin action of GIP, VLP-GIP-treated mice did not show signs of glucose intolerance (Fulurija et al., 2008). Thus, GIP receptor blockade does not appear to significantly impair insulin sensitivity or glucose tolerance, providing further support for the use of GIP receptor antagonists to treat diabetes and obesity. Furthermore, even though mild impairments in glucose homeostasis may result from GIP receptor blockade in some cases (Lewis et al., 2000; Miyawaki et al., 1999), these impairments will likely be outweighed by the anti-obesity benefits of GIP receptor blockade (Kieffer, 2003). Therefore, these studies collectively support the concept that disrupting GIP signalling represents a promising novel therapeutic strategy for the treatment of obesity. Moreover, the fact that a wide range of unique approaches to impair GIP receptor signalling results in strikingly similar beneficial effects strengthens this argument (Irwin and Flatt, 2009). Nonetheless, additional studies are required in order to investigate the clinical potential of GIP receptor blockade in man (Irwin and Flatt, 2009).

Although the evidence supporting GIP receptor antagonism is remarkably strong, there are still some caveats to this approach. The inhibition of GIP receptor signalling interferes with the proper deposition of triglycerides to adipose tissue, which could result in elevated plasma triglyceride levels and an increased risk of coronary heart disease (Kieffer, 2003). Additional detrimental effects of GIP receptor blockade include reduced bone mass and size, reduced β-cell mass and proliferation and a diminished incretin response (Althage et al., 2008; Renner et al., 2010; Xie et al., 2005). Furthermore, GIP receptor antagonism is susceptible to a wide range of side effects due to the broad distribution of the GIP receptor (Kieffer, 2003). In addition, the effects of GIP receptor signalling are not known for all of the tissues expressing the GIP receptor, making it impossible to accurately predict the impact of GIP receptor blockade in these tissues (Kieffer, 2003). Nonetheless, GIPR-/- mice are relatively healthy, supporting the safety of GIP receptor blockade (Miyawaki et al., 2002;

Miyawaki et al., 1999). However, the relative health of GIPR-/- mice may not accurately predict the health consequences of GIP receptor blockade later in life since some compensation to the life-long absence of GIP receptor signalling likely occurred in these mice (Kieffer, 2003). Thus, future studies aimed at evaluating the efficacy of GIP receptor blockade should also include careful side effect profiling.

References

Abrahamsen, N., Nishimura, E., 1995. Regulation of glucagon and glucagon-like peptide-1 receptor messenger ribonucleic acid expression in cultured rat pancreatic islets by glucose, cyclic adenosine 3',5'-monophosphate, and glucocorticoids. Endocrinology. 136, 1572-8.

Abu-Hamdah, R., Rabiee, A., Meneilly, G. S., Shannon, R. P., Andersen, D. K., Elahi, D., 2009. Clinical review: The extrapancreatic effects of glucagon-like peptide-1 and related peptides. J Clin Endocrinol Metab. 94, 1843-52.

Adrian, T. E., Bloom, S. R., Hermansen, K., Iversen, J., 1978. Pancreatic polypeptide, glucagon and insulin secretion from the isolated perfused canine pancreas. Diabetologia. 14, 413-7.

Althage, M. C., Ford, E. L., Wang, S., Tso, P., Polonsky, K. S., Wice, B. M., 2008. Targeted ablation of glucose-dependent insulinotropic polypeptide-producing cells in transgenic mice reduces obesity and insulin resistance induced by a high fat diet. J Biol Chem. 283, 18365-76.

Alumets, J., Hakanson, R., O'Dorisio, T., Sjolund, K., Sundler, F., 1978. Is GIP a glucagon cell constituent? Histochemistry. 58, 253-7.

Amiranoff, B., Vauclin-Jacques, N., Laburthe, M., 1984. Functional GIP receptors in a hamster pancreatic beta cell line, In 111: specific binding and biological effects. Biochem Biophys Res Commun. 123, 671-6.

Amland, P. F., Jorde, R., Aanderud, S., Burhol, P. G., Giercksky, K. E., 1985. Effects of intravenously infused porcine GIP on serum insulin, plasma C-peptide, and pancreatic polypeptide in non-insulin-dependent diabetes in the fasting state. Scand J Gastroenterol. 20, 315-20.

Amori, R. E., Lau, J., Pittas, A. G., 2007. Efficacy and safety of incretin therapy in type 2 diabetes: systematic review and meta-analysis. JAMA. 298, 194-206.

Amylin_Pharmaceuticals, Highlights of Prescribing Information. Vol. 2011, 2010.

Andersen, D. K., Elahi, D., Brown, J. C., Tobin, J. D., Andres, R., 1978. Oral glucose augmentation of insulin secretion. Interactions of gastric inhibitory polypeptide with ambient glucose and insulin levels. J Clin Invest. 62, 152-61.

Asmar, M., Simonsen, L., Madsbad, S., Stallknecht, B., Holst, J. J., Bulow, J., 2010. Glucose-dependent insulinotropic polypeptide may enhance fatty acid re-esterification in subcutaneous abdominal adipose tissue in lean humans. Diabetes. 59, 2160-3.

Augeri, D. J., Robl, J. A., Betebenner, D. A., Magnin, D. R., Khanna, A., Robertson, J. G., Wang, A., Simpkins, L. M., Taunk, P., Huang, Q., Han, S. P., Abboa-Offei, B., Cap, M., Xin, L., Tao, L., Tozzo, E., Welzel, G. E., Egan, D. M., Marcinkeviciene, J., Chang, S. Y., Biller, S. A., Kirby, M. S., Parker, R. A., Hamann, L. G., 2005. Discovery and preclinical profile of Saxagliptin (BMS-477118): a highly potent, long-acting, orally active dipeptidyl peptidase IV inhibitor for the treatment of type 2 diabetes. J Med Chem. 48**,** 5025-37.

Baggio, L., Adatia, F., Bock, T., Brubaker, P. L., Drucker, D. J., 2000a. Sustained expression of exendin-4 does not perturb glucose homeostasis, beta-cell mass, or food intake in metallothionein-preproexendin transgenic mice. J Biol Chem. 275**,** 34471-7.

Baggio, L., Kieffer, T. J., Drucker, D. J., 2000b. Glucagon-like peptide-1, but not glucose-dependent insulinotropic peptide, regulates fasting glycemia and nonenteral glucose clearance in mice. Endocrinology. 141**,** 3703-9.

Baggio, L. L., Drucker, D. J., 2006. Therapeutic approaches to preserve islet mass in type 2 diabetes. Annu Rev Med. 57**,** 265-81.

Baggio, L. L., Drucker, D. J., 2007. Biology of incretins: GLP-1 and GIP. Gastroenterology. 132**,** 2131-57.

Baggio, L. L., Huang, Q., Brown, T. J., Drucker, D. J., 2004a. A recombinant human glucagon-like peptide (GLP)-1-albumin protein (albugon) mimics peptidergic activation of GLP-1 receptor-dependent pathways coupled with satiety, gastrointestinal motility, and glucose homeostasis. Diabetes. 53**,** 2492-500.

Baggio, L. L., Huang, Q., Cao, X., Drucker, D. J., 2008. An albumin-exendin-4 conjugate engages central and peripheral circuits regulating murine energy and glucose homeostasis. Gastroenterology. 134**,** 1137-47.

Baggio, L. L., Kim, J. G., Drucker, D. J., 2004b. Chronic exposure to GLP-1R agonists promotes homologous GLP-1 receptor desensitization in vitro but does not attenuate GLP-1R-dependent glucose homeostasis in vivo. Diabetes. 53 Suppl 3**,** S205-14.

Bai, M., 2004. Dimerization of G-protein-coupled receptors: roles in signal transduction. Cell Signal. 16**,** 175-86.

Baldacchino, V., Oble, S., Decarie, P. O., Bourdeau, I., Hamet, P., Tremblay, J., Lacroix, A., 2005. The Sp transcription factors are involved in the cellular expression of the human glucose-dependent insulinotropic polypeptide receptor gene and overexpressed in adrenals of patients with Cushing's syndrome. J Mol Endocrinol. 35**,** 61-71.

Baron, A. D., Schaeffer, L., Shragg, P., Kolterman, O. G., 1987. Role of hyperglucagonemia in maintenance of increased rates of hepatic glucose output in type II diabetics. Diabetes. 36**,** 274-83.

Beck, B., 1989. Gastric inhibitory polypeptide: a gut hormone with anabolic functions. J Mol Endocrinol. 2**,** 169-74.

Beck, B., Max, J. P., 1986. Direct metabolic effects of gastric inhibitory polypeptide (GIP): dissociation at physiological levels of effects on insulin-stimulated fatty acid and glucose incorporation in rat adipose tissue. Diabetologia. 29**,** 68.

Beinborn, M., Worrall, C. I., McBride, E. W., Kopin, A. S., 2005. A human glucagon-like peptide-1 receptor polymorphism results in reduced agonist responsiveness. Regul Pept. 130**,** 1-6.

Bell, G. I., Sanchez-Pescador, R., Laybourn, P. J., Najarian, R. C., 1983a. Exon duplication and divergence in the human preproglucagon gene. Nature. 304**,** 368-71.

Bell, G. I., Santerre, R. F., Mullenbach, G. T., 1983b. Hamster preproglucagon contains the sequence of glucagon and two related peptides. Nature. 302**,** 716-8.

Berghofer, P., Peterson, R. G., Schneider, K., Fehmann, H. C., Goke, B., 1997. Incretin hormone expression in the gut of diabetic mice and rats. Metabolism. 46**,** 261-7.

Best, J. H., Boye, K. S., Rubin, R. R., Cao, D., Kim, T. H., Peyrot, M., 2009. Improved treatment satisfaction and weight-related quality of life with exenatide once weekly or twice daily. Diabet Med. 26**,** 722-8.

Besterman, H. S., Cook, G. C., Sarson, D. L., Christofides, N. D., Bryant, M. G., Gregor, M., Bloom, S. R., 1979. Gut hormones in tropical malabsorption. Br Med J. 2**,** 1252-5.

Blonde, L., Klein, E. J., Han, J., Zhang, B., Mac, S. M., Poon, T. H., Taylor, K. L., Trautmann, M. E., Kim, D. D., Kendall, D. M., 2006. Interim analysis of the effects of exenatide treatment on A1C, weight and cardiovascular risk factors over 82 weeks in 314 overweight patients with type 2 diabetes. Diabetes Obes Metab. 8**,** 436-47.

Blunt, J. W., Copp, B. R., Munro, M. H., Northcote, P. T., Prinsep, M. R., 2004. Marine natural products. Nat Prod Rep. 21**,** 1-49.

Bohm, S. K., Grady, E. F., Bunnett, N. W., 1997. Regulatory mechanisms that modulate signalling by G-protein-coupled receptors. Biochem J. 322 (Pt 1)**,** 1-18.

Bollag, R. J., Zhong, Q., Phillips, P., Min, L., Zhong, L., Cameron, R., Mulloy, A. L., Rasmussen, H., Qin, F., Ding, K. H., Isales, C. M., 2000. Osteoblast-derived cells express

functional glucose-dependent insulinotropic peptide receptors. Endocrinology. 141, 1228-35.

Borman, S., 2005. Drugs by design. Chem Eng News. 83, 28-30.

Boylan, M. O., Jepeal, L. I., Jarboe, L. A., Wolfe, M. M., 1997. Cell-specific expression of the glucose-dependent insulinotropic polypeptide gene in a mouse neuroendocrine tumor cell line. J Biol Chem. 272, 17438-43.

Boylan, M. O., Jepeal, L. I., Wolfe, M. M., 1999. Structure of the rat glucose-dependent insulinotropic polypeptide receptor gene. Peptides. 20, 219-28.

Brandt, I., Joossens, J., Chen, X., Maes, M. B., Scharpe, S., De Meester, I., Lambeir, A. M., 2005. Inhibition of dipeptidyl-peptidase IV catalyzed peptide truncation by Vildagliptin ((2S)-{[(3-hydroxyadamantan-1-yl)amino]acetyl}-pyrrolidine-2-carbonitrile). Biochem Pharmacol. 70, 134-43.

Brown, J. C., 1971. A gastric inhibitory polypeptide. I. The amino acid composition and the tryptic peptides. Can J Biochem. 49, 255-61.

Brown, J. C., Gastric inhibitory polypeptide (GIP). In: S. Taylor, (Ed.), Endocrinology. Heinemann, London, 1974, pp. 276-84.

Brown, J. C., Dryburgh, J. R., 1971. A gastric inhibitory polypeptide. II. The complete amino acid sequence. Can J Biochem. 49, 867-72.

Brown, J. C., Dryburgh, J. R., Ross, S. A., Dupre, J., 1975. Identification and actions of gastric inhibitory polypeptide. Recent Prog Horm Res. 31, 487-532.

Brown, J. C., Otte, S. C., 1978. Gastrointestinal hormones and the control of insulin secretion. Diabetes. 27, 782-7.

Brubaker, P. L., 2007. Incretin-based therapies: mimetics versus protease inhibitors. Trends Endocrinol Metab. 18, 240-5.

Brubaker, P. L., Drucker, D. J., 2002. Structure-function of the glucagon receptor family of G protein-coupled receptors: the glucagon, GIP, GLP-1, and GLP-2 receptors. Receptors Channels. 8, 179-88.

Brunicardi, F. C., Druck, P., Seymour, N. E., Sun, Y. S., Elahi, D., Andersen, D. K., 1990. Selective neurohormonal interactions in islet cell secretion in the isolated perfused human pancreas. J Surg Res. 48, 273-8.

Buchan, A. M., Ingman-Baker, J., Levy, J., Brown, J. C., 1982. A comparison of the ability of serum and monoclonal antibodies to gastric inhibitory polypeptide to detect

immunoreactive cells in the gastroenteropancreatic system of mammals and reptiles. Histochemistry. 76, 341-9.

Buchan, A. M., Polak, J. M., Capella, C., Solcia, E., Pearse, A. G., 1978. Electronimmunocytochemical evidence for the K cell localization of gastric inhibitory polypeptide (GIP) in man. Histochemistry. 56, 37-44.

Buffa, R., Polak, J. M., Pearse, A. G., Solcia, E., Grimelius, L., Capella, C., 1975. Identification of the intestinal cell storing gastric inhibitory peptide. Histochemistry. 43, 249-55.

Bullock, B. P., Heller, R. S., Habener, J. F., 1996. Tissue distribution of messenger ribonucleic acid encoding the rat glucagon-like peptide-1 receptor. Endocrinology. 137, 2968-78.

Buse, J. B., Henry, R. R., Han, J., Kim, D. D., Fineman, M. S., Baron, A. D., 2004. Effects of exenatide (exendin-4) on glycemic control over 30 weeks in sulfonylurea-treated patients with type 2 diabetes. Diabetes Care. 27, 2628-35.

Buse, J. B., Klonoff, D. C., Nielsen, L. L., Guan, X., Bowlus, C. L., Holcombe, J. H., Maggs, D. G., Wintle, M. E., 2007. Metabolic effects of two years of exenatide treatment on diabetes, obesity, and hepatic biomarkers in patients with type 2 diabetes: an interim analysis of data from the open-label, uncontrolled extension of three double-blind, placebo-controlled trials. Clin Ther. 29, 139-53.

Bush, M. A., Matthews, J. E., De Boever, E. H., Dobbins, R. L., Hodge, R. J., Walker, S. E., Holland, M. C., Gutierrez, M., Stewart, M. W., 2009. Safety, tolerability, pharmacodynamics and pharmacokinetics of albiglutide, a long-acting glucagon-like peptide-1 mimetic, in healthy subjects. Diabetes Obes Metab. 11, 498-505.

Buteau, J., Foisy, S., Joly, E., Prentki, M., 2003. Glucagon-like peptide 1 induces pancreatic beta-cell proliferation via transactivation of the epidermal growth factor receptor. Diabetes. 52, 124-32.

Buteau, J., Roduit, R., Susini, S., Prentki, M., 1999. Glucagon-like peptide-1 promotes DNA synthesis, activates phosphatidylinositol 3-kinase and increases transcription factor pancreatic and duodenal homeobox gene 1 (PDX-1) DNA binding activity in beta (INS-1)-cells. Diabetologia. 42, 856-64.

Buteau, J., Spatz, M. L., Accili, D., 2006. Transcription factor FoxO1 mediates glucagon-like peptide-1 effects on pancreatic beta-cell mass. Diabetes. 55, 1190-6.

Caliceti, P., Veronese, F. M., 2003. Pharmacokinetic and biodistribution properties of poly(ethylene glycol)-protein conjugates. Adv Drug Deliv Rev. 55, 1261-77.

Campos, R. V., Lee, Y. C., Drucker, D. J., 1994. Divergent tissue-specific and developmental expression of receptors for glucagon and glucagon-like peptide-1 in the mouse. Endocrinology. 134**,** 2156-64.

Capella, C., Solcia, E., 1972. The endocrine cells of the pig gastrointestinal mucosa and pancreas. Arch Histol Jpn. 35**,** 1-29.

Capella, C., Solcia, E., Vassallo, G., 1969. Identification of six types of endocrine cells in the gastrointestinal mucosa of the rabbit. Arch Histol Jpn. 30**,** 479-95.

Cataland, S., Crockett, S. E., Brown, J. C., Mazzaferri, E. L., 1974. Gastric inhibitory polypeptide (GIP) stimulation by oral glucose in man. J Clin Endocrinol Metab. 39**,** 223-8.

Chae, S. Y., Choi, Y. G., Son, S., Jung, S. Y., Lee, D. S., Lee, K. C., 2010a. The fatty acid conjugated exendin-4 analogs for type 2 antidiabetic therapeutics. J Control Release. 144**,** 10-6.

Chae, S. Y., Jin, C. H., Shin, J. H., Son, S., Kim, T. H., Lee, S., Youn, Y. S., Byun, Y., Lee, M. S., Lee, K. C., 2010b. Biochemical, pharmaceutical and therapeutic properties of long-acting lithocholic acid derivatized exendin-4 analogs. J Control Release. 142**,** 206-13.

Chang, A. M., Jakobsen, G., Sturis, J., Smith, M. J., Bloem, C. J., An, B., Galecki, A., Halter, J. B., 2003. The GLP-1 derivative NN2211 restores beta-cell sensitivity to glucose in type 2 diabetic patients after a single dose. Diabetes. 52**,** 1786-91.

Chang, C. L., Cai, J. J., Cheng, P. J., Chueh, H. Y., Hsu, S. Y., 2011. Identification of metabolic modifiers that underlie phenotypic variations in energy-balance regulation. Diabetes. 60**,** 726-34.

Chatziioannou, A., Kehagias, D., Mourikis, D., Antoniou, A., Limouris, G., Kaponis, A., Kavatzas, N., Tseleni, S., Vlachos, L., 2001. Imaging and localization of pancreatic insulinomas. Clin Imaging. 25**,** 275-83.

Chen, D., Liao, J., Li, N., Zhou, C., Liu, Q., Wang, G., Zhang, R., Zhang, S., Lin, L., Chen, K., Xie, X., Nan, F., Young, A. A., Wang, M. W., 2007. A nonpeptidic agonist of glucagon-like peptide 1 receptors with efficacy in diabetic db/db mice. Proc Natl Acad Sci U S A. 104**,** 943-8.

Chepurny, O. G., Hussain, M. A., Holz, G. G., 2002. Exendin-4 as a stimulator of rat insulin I gene promoter activity via bZIP/CRE interactions sensitive to serine/threonine protein kinase inhibitor Ro 31-8220. Endocrinology. 143**,** 2303-13.

Chia, C. W., Carlson, O. D., Kim, W., Shin, Y. K., Charles, C. P., Kim, H. S., Melvin, D. L., Egan, J. M., 2009. Exogenous glucose-dependent insulinotropic polypeptide worsens post prandial hyperglycemia in type 2 diabetes. Diabetes. 58**,** 1342-9.

Chia, C. W., Egan, J. M., 2008. Incretin-based therapies in type 2 diabetes mellitus. J Clin Endocrinol Metab. 93**,** 3703-16.

Christ, E., Wild, D., Forrer, F., Brandle, M., Sahli, R., Clerici, T., Gloor, B., Martius, F., Maecke, H., Reubi, J. C., 2009. Glucagon-like peptide-1 receptor imaging for localization of insulinomas. J Clin Endocrinol Metab. 94**,** 4398-405.

Christensen, M., Knop, F. K., 2010. Once-weekly GLP-1 agonists: How do they differ from exenatide and liraglutide? Curr Diab Rep. 10**,** 124-32.

Chu, Z. L., Carroll, C., Alfonso, J., Gutierrez, V., He, H., Lucman, A., Pedraza, M., Mondala, H., Gao, H., Bagnol, D., Chen, R., Jones, R. M., Behan, D. P., Leonard, J., 2008. A role for intestinal endocrine cell-expressed g protein-coupled receptor 119 in glycemic control by enhancing glucagon-like Peptide-1 and glucose-dependent insulinotropic Peptide release. Endocrinology. 149**,** 2038-47.

Chu, Z. L., Jones, R. M., He, H., Carroll, C., Gutierrez, V., Lucman, A., Moloney, M., Gao, H., Mondala, H., Bagnol, D., Unett, D., Liang, Y., Demarest, K., Semple, G., Behan, D. P., Leonard, J., 2007. A role for beta-cell-expressed G protein-coupled receptor 119 in glycemic control by enhancing glucose-dependent insulin release. Endocrinology. 148**,** 2601-9.

Claus, T. H., Pan, C. Q., Buxton, J. M., Yang, L., Reynolds, J. C., Barucci, N., Burns, M., Ortiz, A. A., Roczniak, S., Livingston, J. N., Clairmont, K. B., Whelan, J. P., 2007. Dual-acting peptide with prolonged glucagon-like peptide-1 receptor agonist and glucagon receptor antagonist activity for the treatment of type 2 diabetes. J Endocrinol. 192**,** 371-80.

Cleator, I. G., Gourlay, R. H., 1975. Release of immunoreactive gastric inhibitory polypeptide (IR-GIP) by oral ingestion of food substances. Am J Surg. 130**,** 128-35.

Coopman, K., Huang, Y., Johnston, N., Bradley, S. J., Wilkinson, G. F., Willars, G. B., 2010. Comparative Effects of the Endogenous Agonist GLP-1 7-36 Amide and a Small Molecule Ago-allosteric Agent 'Compound 2' at the GLP-1 Receptor. J Pharmacol Exp Ther. 334**,** 795-808.

Cordier, C., Morton, D., Murrison, S., Nelson, A., O'Leary-Steele, C., 2008. Natural products as an inspiration in the diversity-oriented synthesis of bioactive compound libraries. Nat Prod Rep. 25**,** 719-37.

Creutzfeldt, W., Ebert, R., Willms, B., Frerichs, H., Brown, J. C., 1978. Gastric inhibitory polypeptide (GIP) and insulin in obesity: increased response to stimulation and defective feedback control of serum levels. Diabetologia. 14**,** 15-24.

D'Alessio, D. A., Vogel, R., Prigeon, R., Laschansky, E., Koerker, D., Eng, J., Ensinck, J. W., 1996. Elimination of the action of glucagon-like peptide 1 causes an impairment of glucose tolerance after nutrient ingestion by healthy baboons. J Clin Invest. 97**,** 133-8.

Dall, T. M., Zhang, Y., Chen, Y. J., Quick, W. W., Yang, W. G., Fogli, J., 2010. The economic burden of diabetes. Health Aff (Millwood). 29**,** 297-303.

Day, J. W., Ottaway, N., Patterson, J. T., Gelfanov, V., Smiley, D., Gidda, J., Findeisen, H., Bruemmer, D., Drucker, D. J., Chaudhary, N., Holland, J., Hembree, J., Abplanalp, W., Grant, E., Ruehl, J., Wilson, H., Kirchner, H., Lockie, S. H., Hofmann, S., Woods, S. C., Nogueiras, R., Pfluger, P. T., Perez-Tilve, D., DiMarchi, R., Tschop, M. H., 2009. A new glucagon and GLP-1 co-agonist eliminates obesity in rodents. Nat Chem Biol. 5**,** 749-57.

de Heer, J., Rasmussen, C., Coy, D. H., Holst, J. J., 2008. Glucagon-like peptide-1, but not glucose-dependent insulinotropic peptide, inhibits glucagon secretion via somatostatin (receptor subtype 2) in the perfused rat pancreas. Diabetologia. 51**,** 2263-70.

de Rooij, J., Zwartkruis, F. J., Verheijen, M. H., Cool, R. H., Nijman, S. M., Wittinghofer, A., Bos, J. L., 1998. Epac is a Rap1 guanine-nucleotide-exchange factor directly activated by cyclic AMP. Nature. 396**,** 474-7.

Deacon, C. F., 2005. What do we know about the secretion and degradation of incretin hormones? Regul Pept. 128**,** 117-24.

Deacon, C. F., Johnsen, A. H., Holst, J. J., 1995a. Degradation of glucagon-like peptide-1 by human plasma in vitro yields an N-terminally truncated peptide that is a major endogenous metabolite in vivo. J Clin Endocrinol Metab. 80**,** 952-7.

Deacon, C. F., Knudsen, L. B., Madsen, K., Wiberg, F. C., Jacobsen, O., Holst, J. J., 1998. Dipeptidyl peptidase IV resistant analogues of glucagon-like peptide-1 which have extended metabolic stability and improved biological activity. Diabetologia. 41**,** 271-8.

Deacon, C. F., Nauck, M. A., Toft-Nielsen, M., Pridal, L., Willms, B., Holst, J. J., 1995b. Both subcutaneously and intravenously administered glucagon-like peptide I are rapidly degraded from the NH2-terminus in type II diabetic patients and in healthy subjects. Diabetes. 44**,** 1126-31.

Deacon, C. F., Plamboeck, A., Moller, S., Holst, J. J., 2002. GLP-1-(9-36) amide reduces blood glucose in anesthetized pigs by a mechanism that does not involve insulin secretion. Am J Physiol Endocrinol Metab. 282, E873-9.

Deacon, C. F., Plamboeck, A., Rosenkilde, M. M., de Heer, J., Holst, J. J., 2006. GIP-(3-42) does not antagonize insulinotropic effects of GIP at physiological concentrations. Am J Physiol Endocrinol Metab. 291, E468-75.

Deacon, C. F., Pridal, L., Klarskov, L., Olesen, M., Holst, J. J., 1996. Glucagon-like peptide 1 undergoes differential tissue-specific metabolism in the anesthetized pig. Am J Physiol. 271, E458-64.

DeFronzo, R. A., 1988. Lilly lecture 1987. The triumvirate: beta-cell, muscle, liver. A collusion responsible for NIDDM. Diabetes. 37, 667-87.

Dillon, J. S., Tanizawa, Y., Wheeler, M. B., Leng, X. H., Ligon, B. B., Rabin, D. U., Yoo-Warren, H., Permutt, M. A., Boyd, A. E., 3rd, 1993. Cloning and functional expression of the human glucagon-like peptide-1 (GLP-1) receptor. Endocrinology. 133, 1907-10.

Ding, W. G., Gromada, J., 1997. Protein kinase A-dependent stimulation of exocytosis in mouse pancreatic beta-cells by glucose-dependent insulinotropic polypeptide. Diabetes. 46, 615-21.

Doyle, M. E., Egan, J. M., 2007. Mechanisms of action of glucagon-like peptide 1 in the pancreas. Pharmacol Ther. 113, 546-93.

Drucker, D. J., 2006. The biology of incretin hormones. Cell Metab. 3, 153-65.

Drucker, D. J., 2007a. Dipeptidyl peptidase-4 inhibition and the treatment of type 2 diabetes: preclinical biology and mechanisms of action. Diabetes Care. 30, 1335-43.

Drucker, D. J., 2007b. The role of gut hormones in glucose homeostasis. J Clin Invest. 117, 24-32.

Drucker, D. J., Buse, J. B., Taylor, K., Kendall, D. M., Trautmann, M., Zhuang, D., Porter, L., 2008. Exenatide once weekly versus twice daily for the treatment of type 2 diabetes: a randomised, open-label, non-inferiority study. Lancet. 372, 1240-50.

Drucker, D. J., Sherman, S. I., Gorelick, F. S., Bergenstal, R. M., Sherwin, R. S., Buse, J. B., 2010. Incretin-based therapies for the treatment of type 2 diabetes: evaluation of the risks and benefits. Diabetes Care. 33, 428-33.

Duan, R. D., Erlanson-Albertsson, C., 1992. Gastric inhibitory polypeptide stimulates pancreatic lipase and colipase synthesis in rats. Am J Physiol. 262, G779-84.

Dube, P. E., Brubaker, P. L., 2004. Nutrient, neural and endocrine control of glucagon-like peptide secretion. Horm Metab Res. 36**,** 755-60.

Dunning, B. E., Gerich, J. E., 2007. The role of alpha-cell dysregulation in fasting and postprandial hyperglycemia in type 2 diabetes and therapeutic implications. Endocr Rev. 28**,** 253-83.

Dupre, J., Caussignac, Y., McDonald, T. J., Van Vliet, S., 1991. Stimulation of glucagon secretion by gastric inhibitory polypeptide in patients with hepatic cirrhosis and hyperglucagonemia. J Clin Endocrinol Metab. 72**,** 125-9.

Dupre, J., Ross, S. A., Watson, D., Brown, J. C., 1973. Stimulation of insulin secretion by gastric inhibitory polypeptide in man. J Clin Endocrinol Metab. 37**,** 826-8.

Ebert, R., Nauck, M., Creutzfeldt, W., 1991. Effect of exogenous or endogenous gastric inhibitory polypeptide (GIP) on plasma triglyceride responses in rats. Horm Metab Res. 23**,** 517-21.

Eckel, R. H., Fujimoto, W. Y., Brunzell, J. D., 1979. Gastric inhibitory polypeptide enhanced lipoprotein lipase activity in cultured preadipocytes. Diabetes. 28**,** 1141-2.

Edlund, H., 2002. Pancreatic organogenesis--developmental mechanisms and implications for therapy. Nat Rev Genet. 3**,** 524-32.

Egan, J. M., Margolskee, R. F., 2008. Taste cells of the gut and gastrointestinal chemosensation. Mol Interv. 8**,** 78-81.

Egan, J. M., Montrose-Rafizadeh, C., Wang, Y., Bernier, M., Roth, J., 1994. Glucagon-like peptide-1(7-36) amide (GLP-1) enhances insulin-stimulated glucose metabolism in 3T3-L1 adipocytes: one of several potential extrapancreatic sites of GLP-1 action. Endocrinology. 135**,** 2070-5.

Ehses, J. A., Casilla, V. R., Doty, T., Pospisilik, J. A., Winter, K. D., Demuth, H. U., Pederson, R. A., McIntosh, C. H., 2003. Glucose-dependent insulinotropic polypeptide promotes beta-(INS-1) cell survival via cyclic adenosine monophosphate-mediated caspase-3 inhibition and regulation of p38 mitogen-activated protein kinase. Endocrinology. 144**,** 4433-45.

Ehses, J. A., Lee, S. S., Pederson, R. A., McIntosh, C. H., 2001. A new pathway for glucose-dependent insulinotropic polypeptide (GIP) receptor signaling: evidence for the involvement of phospholipase A2 in GIP-stimulated insulin secretion. J Biol Chem. 276**,** 23667-73.

Ehses, J. A., Pelech, S. L., Pederson, R. A., McIntosh, C. H., 2002. Glucose-dependent insulinotropic polypeptide activates the Raf-Mek1/2-ERK1/2 module via a cyclic AMP/cAMP-dependent protein kinase/Rap1-mediated pathway. J Biol Chem. 277**,** 37088-97.

Eissele, R., Goke, R., Willemer, S., Harthus, H. P., Vermeer, H., Arnold, R., Goke, B., 1992. Glucagon-like peptide-1 cells in the gastrointestinal tract and pancreas of rat, pig and man. Eur J Clin Invest. 22**,** 283-91.

Elahi, D., Andersen, D. K., Brown, J. C., Debas, H. T., Hershcopf, R. J., Raizes, G. S., Tobin, J. D., Andres, R., 1979. Pancreatic alpha- and beta-cell responses to GIP infusion in normal man. Am J Physiol. 237**,** E185-91.

Elahi, D., Egan, J. M., Shannon, R. P., Meneilly, G. S., Khatri, A., Habener, J. F., Andersen, D. K., 2008. GLP-1 (9-36) amide, cleavage product of GLP-1 (7-36) amide, is a glucoregulatory peptide. Obesity (Silver Spring). 16**,** 1501-9.

Elahi, D., McAloon-Dyke, M., Fukagawa, N. K., Meneilly, G. S., Sclater, A. L., Minaker, K. L., Habener, J. F., Andersen, D. K., 1994. The insulinotropic actions of glucose-dependent insulinotropic polypeptide (GIP) and glucagon-like peptide-1 (7-37) in normal and diabetic subjects. Regul Pept. 51**,** 63-74.

Elbrond, B., Jakobsen, G., Larsen, S., Agerso, H., Jensen, L. B., Rolan, P., Sturis, J., Hatorp, V., Zdravkovic, M., 2002. Pharmacokinetics, pharmacodynamics, safety, and tolerability of a single-dose of NN2211, a long-acting glucagon-like peptide 1 derivative, in healthy male subjects. Diabetes Care. 25**,** 1398-404.

Elliott, R. M., Morgan, L. M., Tredger, J. A., Deacon, S., Wright, J., Marks, V., 1993. Glucagon-like peptide-1 (7-36)amide and glucose-dependent insulinotropic polypeptide secretion in response to nutrient ingestion in man: acute post-prandial and 24-h secretion patterns. J Endocrinol. 138**,** 159-66.

Eng, J., Kleinman, W. A., Singh, L., Singh, G., Raufman, J. P., 1992. Isolation and characterization of exendin-4, an exendin-3 analogue, from Heloderma suspectum venom. Further evidence for an exendin receptor on dispersed acini from guinea pig pancreas. J Biol Chem. 267**,** 7402-5.

European_Medicines_Agency, European Public Assessment Report (EPAR) - Galvus. Vol. 2011, 2008.

Faivre, E., Gault, V. A., Thorens, B., Holscher, C., 2011. Glucose-dependent insulinotropic polypeptide receptor knockout mice are impaired in learning, synaptic plasticity, and neurogenesis. J Neurophysiol. 105**,** 1574-80.

Falko, J. M., Crockett, S. E., Cataland, S., Mazzaferri, E. L., 1975. Gastric inhibitory polypeptide (GIP) stimulated by fat ingestion in man. J Clin Endocrinol Metab. 41**,** 260-5.

Fallowfield, L., Atkins, L., Catt, S., Cox, A., Coxon, C., Langridge, C., Morris, R., Price, M., 2006. Patients' preference for administration of endocrine treatments by injection or tablets: results from a study of women with breast cancer. Ann Oncol. 17**,** 205-10.

Faulkner, D. J., 2002. Marine natural products. Nat Prod Rep. 19**,** 1-48.

Fehmann, H. C., Goke, B., 1995. Characterization of GIP(1-30) and GIP(1-42) as stimulators of proinsulin gene transcription. Peptides. 16**,** 1149-52.

Fehmann, H. C., Habener, J. F., 1991a. Functional receptors for the insulinotropic hormone glucagon-like peptide-I(7-37) on a somatostatin secreting cell line. FEBS Lett. 279**,** 335-40.

Fehmann, H. C., Habener, J. F., 1991b. Homologous desensitization of the insulinotropic glucagon-like peptide-I (7-37) receptor on insulinoma (HIT-T15) cells. Endocrinology. 128**,** 2880-8.

Ferdaoussi, M., Abdelli, S., Yang, J. Y., Cornu, M., Niederhauser, G., Favre, D., Widmann, C., Regazzi, R., Thorens, B., Waeber, G., Abderrahmani, A., 2008. Exendin-4 protects beta-cells from interleukin-1 beta-induced apoptosis by interfering with the c-Jun NH2-terminal kinase pathway. Diabetes. 57**,** 1205-15.

Fineman, M. S., Bicsak, T. A., Shen, L. Z., Taylor, K., Gaines, E., Varns, A., Kim, D., Baron, A. D., 2003. Effect on glycemic control of exenatide (synthetic exendin-4) additive to existing metformin and/or sulfonylurea treatment in patients with type 2 diabetes. Diabetes Care. 26**,** 2370-7.

Finkelstein, E. A., Fiebelkorn, I. C., Wang, G., 2003. National medical spending attributable to overweight and obesity: how much, and who's paying? Health Aff (Millwood). Suppl Web Exclusives**,** W3-219-26.

Flatt, P. R., Kwasowski, P., Bailey, C. J., 1989. Stimulation of gastric inhibitory polypeptide release in ob/ob mice by oral administration of sugars and their analogues. J Nutr. 119**,** 1300-3.

Franklin, Z. J., McDonnell, B., Montgomery, I. A., Flatt, P. R., Irwin, N., 2011. Dual modulation of GIP and glucagon action by the low molecular weight compound 4-hydroxybenzoic acid 2-bromobenzylidene hydrazide. Diabetes Obes Metab.

Fraser, I. D., Tavalin, S. J., Lester, L. B., Langeberg, L. K., Westphal, A. M., Dean, R. A., Marrion, N. V., Scott, J. D., 1998. A novel lipid-anchored A-kinase Anchoring Protein facilitates cAMP-responsive membrane events. EMBO J. 17**,** 2261-72.

Freemantle, N., Blonde, L., Duhot, D., Hompesch, M., Eggertsen, R., Hobbs, F. D., Martinez, L., Ross, S., Bolinder, B., Stridde, E., 2005. Availability of inhaled insulin promotes greater perceived acceptance of insulin therapy in patients with type 2 diabetes. Diabetes Care. 28**,** 427-8.

Fujimoto, W. Y., Ensinck, J. W., Merchant, F. W., Williams, R. H., Smith, P. H., Johnson, D. G., 1978. Stimulation by gastric inhibitory polypeptide of insulin and glucagon secretion by rat islet cultures. Proc Soc Exp Biol Med. 157**,** 89-93.

Fujita, Y., Asadi, A., Yang, G. K., Kwok, Y. N., Kieffer, T. J., 2010a. Differential processing of pro-glucose-dependent insulinotropic polypeptide in gut. Am J Physiol Gastrointest Liver Physiol. 298**,** G608-14.

Fujita, Y., Chui, J. W., King, D. S., Zhang, T., Seufert, J., Pownall, S., Cheung, A. T., Kieffer, T. J., 2008. Pax6 and Pdx1 are required for production of glucose-dependent insulinotropic polypeptide in proglucagon-expressing L cells. Am J Physiol Endocrinol Metab. 295**,** E648-57.

Fujita, Y., Wideman, R. D., Asadi, A., Yang, G. K., Baker, R., Webber, T., Zhang, T., Wang, R., Ao, Z., Warnock, G. L., Kwok, Y. N., Kieffer, T. J., 2010b. Glucose-dependent insulinotropic polypeptide (GIP) is expressed in pancreatic islet alpha-cells and promotes insulin secretion. Gastroenterology. 138**,** 1966-1975.

Fujita, Y., Wideman, R. D., Speck, M., Asadi, A., King, D. S., Webber, T. D., Haneda, M., Kieffer, T. J., 2009. Incretin release from gut is acutely enhanced by sugar but not by sweeteners in vivo. Am J Physiol Endocrinol Metab. 296**,** E473-9.

Fulurija, A., Lutz, T. A., Sladko, K., Osto, M., Wielinga, P. Y., Bachmann, M. F., Saudan, P., 2008. Vaccination against GIP for the treatment of obesity. PLoS One. 3**,** e3163.

Furuta, M., Yano, H., Zhou, A., Rouille, Y., Holst, J. J., Carroll, R., Ravazzola, M., Orci, L., Furuta, H., Steiner, D. F., 1997. Defective prohormone processing and altered pancreatic islet morphology in mice lacking active SPC2. Proc Natl Acad Sci U S A. 94**,** 6646-51.

Fushiki, T., Kojima, A., Imoto, T., Inoue, K., Sugimoto, E., 1992. An extract of Gymnema sylvestre leaves and purified gymnemic acid inhibits glucose-stimulated gastric inhibitory peptide secretion in rats. J Nutr. 122, 2367-73.

Gao, Y., Yoon, K. H., Chuang, L. M., Mohan, V., Ning, G., Shah, S., Jang, H. C., Wu, T. J., Johns, D., Northrup, J., Brodows, R., 2009. Efficacy and safety of exenatide in patients of Asian descent with type 2 diabetes inadequately controlled with metformin or metformin and a sulphonylurea. Diabetes Res Clin Pract. 83, 69-76.

Gault, V. A., Hunter, K., Irwin, N., Greer, B., Green, B. D., Harriott, P., O'Harte, F. P., Flatt, P. R., 2007. Characterisation and glucoregulatory actions of a novel acylated form of the (Pro3)GIP receptor antagonist in type 2 diabetes. Biol Chem. 388, 173-9.

Gault, V. A., Irwin, N., Green, B. D., McCluskey, J. T., Greer, B., Bailey, C. J., Harriott, P., O'Harte F, P., Flatt, P. R., 2005. Chemical ablation of gastric inhibitory polypeptide receptor action by daily (Pro3)GIP administration improves glucose tolerance and ameliorates insulin resistance and abnormalities of islet structure in obesity-related diabetes. Diabetes. 54, 2436-46.

Gault, V. A., O'Harte, F. P., Harriott, P., Flatt, P. R., 2002a. Characterization of the cellular and metabolic effects of a novel enzyme-resistant antagonist of glucose-dependent insulinotropic polypeptide. Biochem Biophys Res Commun. 290, 1420-6.

Gault, V. A., O'Harte, F. P., Harriott, P., Mooney, M. H., Green, B. D., Flatt, P. R., 2003. Effects of the novel (Pro3)GIP antagonist and exendin(9-39)amide on GIP- and GLP-1-induced cyclic AMP generation, insulin secretion and postprandial insulin release in obese diabetic (ob/ob) mice: evidence that GIP is the major physiological incretin. Diabetologia. 46, 222-30.

Gault, V. A., Parker, J. C., Harriott, P., Flatt, P. R., O'Harte, F. P., 2002b. Evidence that the major degradation product of glucose-dependent insulinotropic polypeptide, GIP(3-42), is a GIP receptor antagonist in vivo. J Endocrinol. 175, 525-33.

Gedulin, B. R., Nikoulina, S. E., Smith, P. A., Gedulin, G., Nielsen, L. L., Baron, A. D., Parkes, D. G., Young, A. A., 2005. Exenatide (exendin-4) improves insulin sensitivity and {beta}-cell mass in insulin-resistant obese fa/fa Zucker rats independent of glycemia and body weight. Endocrinology. 146, 2069-76.

Gelling, R. W., Coy, D. H., Pederson, R. A., Wheeler, M. B., Hinke, S., Kwan, T., McIntosh, C. H., 1997a. GIP(6-30amide) contains the high affinity binding region of GIP and is a potent inhibitor of GIP1-42 action in vitro. Regul Pept. 69, 151-4.

Gelling, R. W., Wheeler, M. B., Xue, J., Gyomorey, S., Nian, C., Pederson, R. A., McIntosh, C. H., 1997b. Localization of the domains involved in ligand binding and activation of the glucose-dependent insulinotropic polypeptide receptor. Endocrinology. 138, 2640-3.

Getty-Kaushik, L., Song, D. H., Boylan, M. O., Corkey, B. E., Wolfe, M. M., 2006. Glucose-dependent insulinotropic polypeptide modulates adipocyte lipolysis and reesterification. Obesity (Silver Spring). 14, 1124-31.

Glaesner, W., Vick, A. M., Millican, R., Ellis, B., Tschang, S. H., Tian, Y., Bokvist, K., Brenner, M., Koester, A., Porksen, N., Etgen, G., Bumol, T., 2010. Engineering and characterization of the long-acting glucagon-like peptide-1 analogue LY2189265, an Fc fusion protein. Diabetes Metab Res Rev. 26, 287-96.

Goke, R., Fehmann, H. C., Linn, T., Schmidt, H., Krause, M., Eng, J., Goke, B., 1993. Exendin-4 is a high potency agonist and truncated exendin-(9-39)-amide an antagonist at the glucagon-like peptide 1-(7-36)-amide receptor of insulin-secreting beta-cells. J Biol Chem. 268, 19650-5.

Goke, R., Just, R., Lankat-Buttgereit, B., Goke, B., 1994. Glycosylation of the GLP-1 receptor is a prerequisite for regular receptor function. Peptides. 15, 675-81.

Gonzalez-Sanchez, R., Trujillo, X., Trujillo-Hernandez, B., Vasquez, C., Huerta, M., Elizalde, A., 2006. Forskolin versus sodium cromoglycate for prevention of asthma attacks: a single-blinded clinical trial. J Int Med Res. 34, 200-7.

Grace, C. R., Perrin, M. H., Gulyas, J., Digruccio, M. R., Cantle, J. P., Rivier, J. E., Vale, W. W., Riek, R., 2007. Structure of the N-terminal domain of a type B1 G protein-coupled receptor in complex with a peptide ligand. Proc Natl Acad Sci U S A. 104, 4858-63.

Green, B. D., Flatt, P. R., 2007. Incretin hormone mimetics and analogues in diabetes therapeutics. Best Pract Res Clin Endocrinol Metab. 21, 497-516.

Greig, N. H., Holloway, H. W., De Ore, K. A., Jani, D., Wang, Y., Zhou, J., Garant, M. J., Egan, J. M., 1999. Once daily injection of exendin-4 to diabetic mice achieves long-term beneficial effects on blood glucose concentrations. Diabetologia. 42, 45-50.

Gremlich, S., Porret, A., Hani, E. H., Cherif, D., Vionnet, N., Froguel, P., Thorens, B., 1995. Cloning, functional expression, and chromosomal localization of the human pancreatic islet glucose-dependent insulinotropic polypeptide receptor. Diabetes. 44, 1202-8.

Gribble, F. M., Williams, L., Simpson, A. K., Reimann, F., 2003. A novel glucose-sensing mechanism contributing to glucagon-like peptide-1 secretion from the GLUTag cell line. Diabetes. 52, 1147-54.

Gromada, J., Dissing, S., Rorsman, P., 1996. Desensitization of glucagon-like peptide 1 receptors in insulin-secreting beta TC3 cells: role of PKA-independent mechanisms. Br J Pharmacol. 118**,** 769-75.

Gromada, J., Holst, J. J., Rorsman, P., 1998. Cellular regulation of islet hormone secretion by the incretin hormone glucagon-like peptide 1. Pflugers Arch. 435**,** 583-94.

Gromada, J., Rorsman, P., Dissing, S., Wulff, B. S., 1995. Stimulation of cloned human glucagon-like peptide 1 receptor expressed in HEK 293 cells induces cAMP-dependent activation of calcium-induced calcium release. FEBS Lett. 373**,** 182-6.

Gupta, D., Peshavaria, M., Monga, N., Jetton, T. L., Leahy, J. L., 2010. Physiologic and pharmacologic modulation of glucose-dependent insulinotropic polypeptide (GIP) receptor expression in beta-cells by peroxisome proliferator-activated receptor (PPAR)-gamma signaling: possible mechanism for the GIP resistance in type 2 diabetes. Diabetes. 59**,** 1445-50.

Gutniak, M., Orskov, C., Holst, J. J., Ahren, B., Efendic, S., 1992. Antidiabetogenic effect of glucagon-like peptide-1 (7-36)amide in normal subjects and patients with diabetes mellitus. N Engl J Med. 326**,** 1316-22.

Habegger, K. M., Heppner, K. M., Geary, N., Bartness, T. J., DiMarchi, R., Tschop, M. H., 2010. The metabolic actions of glucagon revisited. Nat Rev Endocrinol. 6**,** 689-97.

Hallbrink, M., Holmqvist, T., Olsson, M., Ostenson, C. G., Efendic, S., Langel, U., 2001. Different domains in the third intracellular loop of the GLP-1 receptor are responsible for Galpha(s) and Galpha(i)/Galpha(o) activation. Biochim Biophys Acta. 1546**,** 79-86.

Hansen, A. M., Bodvarsdottir, T. B., Nordestgaard, D. N., Heller, R. S., Gotfredsen, C. F., Maedler, K., Fels, J. J., Holst, J. J., Karlsen, A. E., 2011. Upregulation of alpha cell glucagon-like peptide 1 (GLP-1) in Psammomys obesus-an adaptive response to hyperglycaemia? Diabetologia.

Hansen, L., Deacon, C. F., Orskov, C., Holst, J. J., 1999. Glucagon-like peptide-1-(7-36)amide is transformed to glucagon-like peptide-1-(9-36)amide by dipeptidyl peptidase IV in the capillaries supplying the L cells of the porcine intestine. Endocrinology. 140**,** 5356-63.

Hansotia, T., Baggio, L. L., Delmeire, D., Hinke, S. A., Yamada, Y., Tsukiyama, K., Seino, Y., Holst, J. J., Schuit, F., Drucker, D. J., 2004. Double incretin receptor knockout (DIRKO) mice reveal an essential role for the enteroinsular axis in transducing the glucoregulatory actions of DPP-IV inhibitors. Diabetes. 53**,** 1326-35.

Harada, N., Yamada, Y., Tsukiyama, K., Yamada, C., Nakamura, Y., Mukai, E., Hamasaki, A., Liu, X., Toyoda, K., Seino, Y., Inagaki, N., 2008. A novel GIP receptor splice variant influences GIP sensitivity of pancreatic beta-cells in obese mice. Am J Physiol Endocrinol Metab. 294**,** E61-8.

Hare, K. J., Vilsboll, T., Asmar, M., Deacon, C. F., Knop, F. K., Holst, J. J., 2010. The glucagonostatic and insulinotropic effects of glucagon-like peptide 1 contribute equally to its glucose-lowering action. Diabetes. 59**,** 1765-70.

Harris, M. I., Hadden, W. C., Knowler, W. C., Bennett, P. H., 1987. Prevalence of diabetes and impaired glucose tolerance and plasma glucose levels in U.S. population aged 20-74 yr. Diabetes. 36**,** 523-34.

Hatzichristou, D. G., Apostolidis, A., Tzortzis, V., Ioannides, E., Yannakoyorgos, K., Kalinderis, A., 2000. Sildenafil versus intracavernous injection therapy: efficacy and preference in patients on intracavernous injection for more than 1 year. J Urol. 164**,** 1197-200.

Hauner, H., Glatting, G., Kaminska, D., Pfeiffer, E. F., 1988. Effects of gastric inhibitory polypeptide on glucose and lipid metabolism of isolated rat adipocytes. Ann Nutr Metab. 32**,** 282-8.

Heinrich, G., Gros, P., Habener, J. F., 1984. Glucagon gene sequence. Four of six exons encode separate functional domains of rat pre-proglucagon. J Biol Chem. 259**,** 14082-7.

Heller, R. S., Kieffer, T. J., Habener, J. F., 1996. Point mutations in the first and third intracellular loops of the glucagon-like peptide-1 receptor alter intracellular signaling. Biochem Biophys Res Commun. 223**,** 624-32.

Heller, R. S., Kieffer, T. J., Habener, J. F., 1997. Insulinotropic glucagon-like peptide I receptor expression in glucagon-producing alpha-cells of the rat endocrine pancreas. Diabetes. 46**,** 785-91.

Herbach, N., Goeke, B., Schneider, M., Hermanns, W., Wolf, E., Wanke, R., 2005. Overexpression of a dominant negative GIP receptor in transgenic mice results in disturbed postnatal pancreatic islet and beta-cell development. Regul Pept. 125**,** 103-17.

Herman, G. A., Stevens, C., Van Dyck, K., Bergman, A., Yi, B., De Smet, M., Snyder, K., Hilliard, D., Tanen, M., Tanaka, W., Wang, A. Q., Zeng, W., Musson, D., Winchell, G., Davies, M. J., Ramael, S., Gottesdiener, K. M., Wagner, J. A., 2005. Pharmacokinetics and pharmacodynamics of sitagliptin, an inhibitor of dipeptidyl peptidase IV, in healthy subjects: results from two randomized, double-blind, placebo-controlled studies with single oral doses. Clin Pharmacol Ther. 78**,** 675-88.

Higashimoto, Y., Opara, E. C., Liddle, R. A., 1995. Dietary regulation of glucose-dependent insulinotropic peptide (GIP) gene expression in rat small intestine. Comp Biochem Physiol C Pharmacol Toxicol Endocrinol. 110**,** 207-14.

Hinke, S. A., Gelling, R., Manhart, S., Lynn, F., Pederson, R. A., Kuhn-Wache, K., Rosche, F., Demuth, H. U., Coy, D., McIntosh, C. H., 2003. Structure-activity relationships of glucose-dependent insulinotropic polypeptide (GIP). Biol Chem. 384**,** 403-7.

Hinke, S. A., Gelling, R. W., Pederson, R. A., Manhart, S., Nian, C., Demuth, H. U., McIntosh, C. H., 2002. Dipeptidyl peptidase IV-resistant [D-Ala(2)]glucose-dependent insulinotropic polypeptide (GIP) improves glucose tolerance in normal and obese diabetic rats. Diabetes. 51**,** 652-61.

Hinke, S. A., Manhart, S., Pamir, N., Demuth, H., R, W. G., Pederson, R. A., McIntosh, C. H., 2001. Identification of a bioactive domain in the amino-terminus of glucose-dependent insulinotropic polypeptide (GIP). Biochim Biophys Acta. 1547**,** 143-55.

Hinke, S. A., Pauly, R. P., Ehses, J., Kerridge, P., Demuth, H. U., McIntosh, C. H., Pederson, R. A., 2000. Role of glucose in chronic desensitization of isolated rat islets and mouse insulinoma (betaTC-3) cells to glucose-dependent insulinotropic polypeptide. J Endocrinol. 165**,** 281-91.

Hirasawa, A., Hara, T., Katsuma, S., Adachi, T., Tsujimoto, G., 2008. Free fatty acid receptors and drug discovery. Biol Pharm Bull. 31**,** 1847-51.

Hirasawa, A., Tsumaya, K., Awaji, T., Katsuma, S., Adachi, T., Yamada, M., Sugimoto, Y., Miyazaki, S., Tsujimoto, G., 2005. Free fatty acids regulate gut incretin glucagon-like peptide-1 secretion through GPR120. Nat Med. 11**,** 90-4.

Hojberg, P. V., Vilsboll, T., Rabol, R., Knop, F. K., Bache, M., Krarup, T., Holst, J. J., Madsbad, S., 2009. Four weeks of near-normalisation of blood glucose improves the insulin response to glucagon-like peptide-1 and glucose-dependent insulinotropic polypeptide in patients with type 2 diabetes. Diabetologia. 52**,** 199-207.

Holst, J. J., 2007. The physiology of glucagon-like peptide 1. Physiol Rev. 87**,** 1409-39.

Holst, J. J., Deacon, C. F., 2005. Glucagon-like peptide-1 mediates the therapeutic actions of DPP-IV inhibitors. Diabetologia. 48**,** 612-5.

Holst, J. J., Gromada, J., 2004. Role of incretin hormones in the regulation of insulin secretion in diabetic and nondiabetic humans. Am J Physiol Endocrinol Metab. 287**,** E199-206.

Holst, J. J., Gromada, J., Nauck, M. A., 1997. The pathogenesis of NIDDM involves a defective expression of the GIP receptor. Diabetologia. 40**,** 984-6.

Holst, J. J., Orskov, C., Nielsen, O. V., Schwartz, T. W., 1987. Truncated glucagon-like peptide I, an insulin-releasing hormone from the distal gut. FEBS Lett. 211**,** 169-74.

Holst, J. J., Vilsboll, T., Deacon, C. F., 2009. The incretin system and its role in type 2 diabetes mellitus. Mol Cell Endocrinol. 297**,** 127-36.

Holz, G. G., 2004. Epac: A new cAMP-binding protein in support of glucagon-like peptide-1 receptor-mediated signal transduction in the pancreatic beta-cell. Diabetes. 53**,** 5-13.

Holz, G. G., Kang, G., Harbeck, M., Roe, M. W., Chepurny, O. G., 2006. Cell physiology of cAMP sensor Epac. J Physiol. 577**,** 5-15.

Holz, G. G. t., Kuhtreiber, W. M., Habener, J. F., 1993. Pancreatic beta-cells are rendered glucose-competent by the insulinotropic hormone glucagon-like peptide-1(7-37). Nature. 361**,** 362-5.

Hoo, R. L., Chu, J. Y., Yuan, Y., Yeung, C. M., Chan, K. Y., Chow, B. K., 2010. Functional identification of an intronic promoter of the human glucose-dependent insulinotropic polypeptide gene. Gene. 463**,** 29-40.

Hoy, M., Berggren, P. O., Gromada, J., 2003. Involvement of protein kinase C-epsilon in inositol hexakisphosphate-induced exocytosis in mouse pancreatic beta-cells. J Biol Chem. 278**,** 35168-71.

Huang, C., 2009. Receptor-Fc fusion therapeutics, traps, and MIMETIBODY technology. Curr Opin Biotechnol. 20**,** 692-9.

Hucking, K., Kostic, Z., Pox, C., Ritzel, R., Holst, J. J., Schmiegel, W., Nauck, M. A., 2005. alpha-Glucosidase inhibition (acarbose) fails to enhance secretion of glucagon-like peptide 1 (7-36 amide) and to delay gastric emptying in Type 2 diabetic patients. Diabet Med. 22**,** 470-6.

Hui, H., Nourparvar, A., Zhao, X., Perfetti, R., 2003. Glucagon-like peptide-1 inhibits apoptosis of insulin-secreting cells via a cyclic 5'-adenosine monophosphate-dependent protein kinase A- and a phosphatidylinositol 3-kinase-dependent pathway. Endocrinology. 144**,** 1444-55.

Hupe-Sodmann, K., Goke, R., Goke, B., Thole, H. H., Zimmermann, B., Voigt, K., McGregor, G. P., 1997. Endoproteolysis of glucagon-like peptide (GLP)-1 (7-36) amide by ectopeptidases in RINm5F cells. Peptides. 18**,** 625-32.

Hupe-Sodmann, K., McGregor, G. P., Bridenbaugh, R., Goke, R., Goke, B., Thole, H., Zimmermann, B., Voigt, K., 1995. Characterisation of the processing by human neutral

endopeptidase 24.11 of GLP-1(7-36) amide and comparison of the substrate specificity of the enzyme for other glucagon-like peptides. Regul Pept. 58**,** 149-56.

Iakoubov, R., Izzo, A., Yeung, A., Whiteside, C. I., Brubaker, P. L., 2007. Protein kinase Czeta is required for oleic acid-induced secretion of glucagon-like peptide-1 by intestinal endocrine L cells. Endocrinology. 148**,** 1089-98.

Ichimura, A., Hirasawa, A., Hara, T., Tsujimoto, G., 2009. Free fatty acid receptors act as nutrient sensors to regulate energy homeostasis. Prostaglandins Other Lipid Mediat. 89**,** 82-8.

Inagaki, N., Seino, Y., Takeda, J., Yano, H., Yamada, Y., Bell, G. I., Eddy, R. L., Fukushima, Y., Byers, M. G., Shows, T. B., et al., 1989. Gastric inhibitory polypeptide: structure and chromosomal localization of the human gene. Mol Endocrinol. 3**,** 1014-21.

Ipp, E., Dobbs, R. E., Harris, V., Arimura, A., Vale, W., Unger, R. H., 1977. The effects of gastrin, gastric inhibitory polypeptide, secretin, and the octapeptide of cholecystokinin upon immunoreactive somatostatin release by the perfused canine pancreas. J Clin Invest. 60**,** 1216-9.

Irwin, D. M., 2009. Molecular evolution of mammalian incretin hormone genes. Regul Pept. 155**,** 121-30.

Irwin, N., Flatt, P. R., 2009. Evidence for beneficial effects of compromised gastric inhibitory polypeptide action in obesity-related diabetes and possible therapeutic implications. Diabetologia. 52**,** 1724-31.

Irwin, N., Gault, V., Flatt, P. R., 2010. Therapeutic potential of the original incretin hormone glucose-dependent insulinotropic polypeptide: diabetes, obesity, osteoporosis and Alzheimer's disease? Expert Opin Investig Drugs. 19**,** 1039-48.

Irwin, N., Gault, V. A., Green, B. D., Greer, B., McCluskey, J. T., Harriott, P., O'Harte, F. P., Flatt, P. R., 2004. Effects of short-term chemical ablation of the GIP receptor on insulin secretion, islet morphology and glucose homeostasis in mice. Biol Chem. 385**,** 845-52.

Irwin, N., Hunter, K., Flatt, P. R., 2007a. Comparison of the metabolic effects of GIP receptor antagonism and PYY(3-36) receptor activation in high fat fed mice. Peptides. 28**,** 2192-8.

Irwin, N., McClean, P. L., O'Harte, F. P., Gault, V. A., Harriott, P., Flatt, P. R., 2007b. Early administration of the glucose-dependent insulinotropic polypeptide receptor antagonist (Pro3)GIP prevents the development of diabetes and related metabolic abnormalities associated with genetically inherited obesity in ob/ob mice. Diabetologia. 50**,** 1532-40.

Jackson, R. S., Creemers, J. W., Farooqi, I. S., Raffin-Sanson, M. L., Varro, A., Dockray, G. J., Holst, J. J., Brubaker, P. L., Corvol, P., Polonsky, K. S., Ostrega, D., Becker, K. L., Bertagna, X., Hutton, J. C., White, A., Dattani, M. T., Hussain, K., Middleton, S. J., Nicole, T. M., Milla, P. J., Lindley, K. J., O'Rahilly, S., 2003. Small-intestinal dysfunction accompanies the complex endocrinopathy of human proprotein convertase 1 deficiency. J Clin Invest. 112, 1550-60.

Jang, H. J., Kokrashvili, Z., Theodorakis, M. J., Carlson, O. D., Kim, B. J., Zhou, J., Kim, H. H., Xu, X., Chan, S. L., Juhaszova, M., Bernier, M., Mosinger, B., Margolskee, R. F., Egan, J. M., 2007. Gut-expressed gustducin and taste receptors regulate secretion of glucagon-like peptide-1. Proc Natl Acad Sci U S A. 104, 15069-74.

Jensen, A. A., Spalding, T. A., 2004. Allosteric modulation of G-protein coupled receptors. Eur J Pharm Sci. 21, 407-20.

Jepeal, L. I., Boylan, M. O., Michael Wolfe, M., 2008. GATA-4 upregulates glucose-dependent insulinotropic polypeptide expression in cells of pancreatic and intestinal lineage. Mol Cell Endocrinol. 287, 20-9.

Jepeal, L. I., Boylan, M. O., Wolfe, M. M., 2003. Cell-specific expression of the glucose-dependent insulinotropic polypeptide gene functions through a GATA and an ISL-1 motif in a mouse neuroendocrine tumor cell line. Regul Pept. 113, 139-47.

Jepeal, L. I., Fujitani, Y., Boylan, M. O., Wilson, C. N., Wright, C. V., Wolfe, M. M., 2005. Cell-specific expression of glucose-dependent-insulinotropic polypeptide is regulated by the transcription factor PDX-1. Endocrinology. 146, 383-91.

Jhala, U. S., Canettieri, G., Screaton, R. A., Kulkarni, R. N., Krajewski, S., Reed, J., Walker, J., Lin, X., White, M., Montminy, M., 2003. cAMP promotes pancreatic beta-cell survival via CREB-mediated induction of IRS2. Genes Dev. 17, 1575-80.

Jimeno, J. M., 2002. A clinical armamentarium of marine-derived anti-cancer compounds. Anticancer Drugs. 13 Suppl 1, S15-9.

Jornvall, H., Carlquist, M., Kwauk, S., Otte, S. C., McIntosh, C. H., Brown, J. C., Mutt, V., 1981. Amino acid sequence and heterogeneity of gastric inhibitory polypeptide (GIP). FEBS Lett. 123, 205-10.

Juhl, C. B., Hollingdal, M., Sturis, J., Jakobsen, G., Agerso, H., Veldhuis, J., Porksen, N., Schmitz, O., 2002. Bedtime administration of NN2211, a long-acting GLP-1 derivative, substantially reduces fasting and postprandial glycemia in type 2 diabetes. Diabetes. 51, 424-9.

Kahn, S. E., Hull, R. L., Utzschneider, K. M., 2006. Mechanisms linking obesity to insulin resistance and type 2 diabetes. Nature. 444, 840-6.

Kaneto, H., Suzuma, K., Sharma, A., Bonner-Weir, S., King, G. L., Weir, G. C., 2002. Involvement of protein kinase C beta 2 in c-myc induction by high glucose in pancreatic beta-cells. J Biol Chem. 277, 3680-5.

Kashima, Y., Miki, T., Shibasaki, T., Ozaki, N., Miyazaki, M., Yano, H., Seino, S., 2001. Critical role of cAMP-GEFII--Rim2 complex in incretin-potentiated insulin secretion. J Biol Chem. 276, 46046-53.

Kawasaki, H., Springett, G. M., Mochizuki, N., Toki, S., Nakaya, M., Matsuda, M., Housman, D. E., Graybiel, A. M., 1998. A family of cAMP-binding proteins that directly activate Rap1. Science. 282, 2275-9.

Kieffer, T. J., 2003. GIP or not GIP? That is the question. Trends Pharmacol Sci. 24, 110-2.

Kieffer, T. J., Buchan, A. M., Barker, H., Brown, J. C., Pederson, R. A., 1994. Release of gastric inhibitory polypeptide from cultured canine endocrine cells. Am J Physiol. 267, E489-96.

Kieffer, T. J., Habener, J. F., 1999. The glucagon-like peptides. Endocr Rev. 20, 876-913.

Kieffer, T. J., McIntosh, C. H., Pederson, R. A., 1995. Degradation of glucose-dependent insulinotropic polypeptide and truncated glucagon-like peptide 1 in vitro and in vivo by dipeptidyl peptidase IV. Endocrinology. 136, 3585-96.

Kielgast, U., Asmar, M., Madsbad, S., Holst, J. J., 2010. Effect of glucagon-like peptide-1 on alpha- and beta-cell function in C-peptide-negative type 1 diabetic patients. J Clin Endocrinol Metab. 95, 2492-6.

Kim, B. J., Zhou, J., Martin, B., Carlson, O. D., Maudsley, S., Greig, N. H., Mattson, M. P., Ladenheim, E. E., Wustner, J., Turner, A., Sadeghi, H., Egan, J. M., 2010. Transferrin fusion technology: a novel approach to prolong biological half-life of insulinotropic peptides. J Pharmacol Exp Ther.

Kim, D., Wang, L., Beconi, M., Eiermann, G. J., Fisher, M. H., He, H., Hickey, G. J., Kowalchick, J. E., Leiting, B., Lyons, K., Marsilio, F., McCann, M. E., Patel, R. A., Petrov, A., Scapin, G., Patel, S. B., Roy, R. S., Wu, J. K., Wyvratt, M. J., Zhang, B. B., Zhu, L., Thornberry, N. A., Weber, A. E., 2005a. (2R)-4-oxo-4-[3-(trifluoromethyl)-5,6-dihydro[1,2,4]triazolo[4,3-a]pyrazin -7(8H)-yl]-1-(2,4,5-trifluorophenyl)butan-2-amine: a potent, orally active dipeptidyl peptidase IV inhibitor for the treatment of type 2 diabetes. J Med Chem. 48, 141-51.

Kim, D. M., Chu, S. H., Kim, S., Park, Y. W., Kim, S. S., 2009. Fc fusion to glucagon-like peptide-1 inhibits degradation by human DPP-IV, increasing its half-life in serum and inducing a potent activity for human GLP-1 receptor activation. BMB Rep. 42**,** 212-6.

Kim, J. G., Baggio, L. L., Bridon, D. P., Castaigne, J. P., Robitaille, M. F., Jette, L., Benquet, C., Drucker, D. J., 2003. Development and characterization of a glucagon-like peptide 1-albumin conjugate: the ability to activate the glucagon-like peptide 1 receptor in vivo. Diabetes. 52**,** 751-9.

Kim, M. J., Kang, J. H., Park, Y. G., Ryu, G. R., Ko, S. H., Jeong, I. K., Koh, K. H., Rhie, D. J., Yoon, S. H., Hahn, S. J., Kim, M. S., Jo, Y. H., 2006. Exendin-4 induction of cyclin D1 expression in INS-1 beta-cells: involvement of cAMP-responsive element. J Endocrinol. 188**,** 623-33.

Kim, S. J., Choi, W. S., Han, J. S., Warnock, G., Fedida, D., McIntosh, C. H., 2005b. A novel mechanism for the suppression of a voltage-gated potassium channel by glucose-dependent insulinotropic polypeptide: protein kinase A-dependent endocytosis. J Biol Chem. 280**,** 28692-700.

Kim, S. J., Nian, C., McIntosh, C. H., 2007a. Activation of lipoprotein lipase by glucose-dependent insulinotropic polypeptide in adipocytes. A role for a protein kinase B, LKB1, and AMP-activated protein kinase cascade. J Biol Chem. 282**,** 8557-67.

Kim, S. J., Nian, C., McIntosh, C. H., 2007b. Resistin is a key mediator of glucose-dependent insulinotropic polypeptide (GIP) stimulation of lipoprotein lipase (LPL) activity in adipocytes. J Biol Chem. 282**,** 34139-47.

Kim, S. J., Nian, C., McIntosh, C. H., 2011. Adipocyte expression of the glucose-dependent insulinotropic polypeptide receptor involves gene regulation by PPAR{gamma} and histone acetylation. J Lipid Res. 52**,** 759-70.

Kim, S. J., Nian, C., Widenmaier, S., McIntosh, C. H., 2008. Glucose-dependent insulinotropic polypeptide-mediated up-regulation of beta-cell antiapoptotic Bcl-2 gene expression is coordinated by cyclic AMP (cAMP) response element binding protein (CREB) and cAMP-responsive CREB coactivator 2. Mol Cell Biol. 28**,** 1644-56.

Kim, S. J., Winter, K., Nian, C., Tsuneoka, M., Koda, Y., McIntosh, C. H., 2005c. Glucose-dependent insulinotropic polypeptide (GIP) stimulation of pancreatic beta-cell survival is dependent upon phosphatidylinositol 3-kinase (PI3K)/protein kinase B (PKB) signaling, inactivation of the forkhead transcription factor Foxo1, and down-regulation of bax expression. J Biol Chem. 280**,** 22297-307.

Kim, W., Egan, J. M., 2008. The role of incretins in glucose homeostasis and diabetes treatment. Pharmacol Rev. 60, 470-512.

Kitamura, T., Nakae, J., Kitamura, Y., Kido, Y., Biggs, W. H., 3rd, Wright, C. V., White, M. F., Arden, K. C., Accili, D., 2002. The forkhead transcription factor Foxo1 links insulin signaling to Pdx1 regulation of pancreatic beta cell growth. J Clin Invest. 110, 1839-47.

Klein, R., 1995. Hyperglycemia and microvascular and macrovascular disease in diabetes. Diabetes Care. 18, 258-68.

Klonoff, D. C., Buse, J. B., Nielsen, L. L., Guan, X., Bowlus, C. L., Holcombe, J. H., Wintle, M. E., Maggs, D. G., 2008. Exenatide effects on diabetes, obesity, cardiovascular risk factors and hepatic biomarkers in patients with type 2 diabetes treated for at least 3 years. Curr Med Res Opin. 24, 275-86.

Knapper, J. M., Heath, A., Fletcher, J. M., Morgan, L. M., Marks, V., 1995a. GIP and GLP-1(7-36)amide secretion in response to intraduodenal infusions of nutrients in pigs. Comp Biochem Physiol C Pharmacol Toxicol Endocrinol. 111, 445-50.

Knapper, J. M., Puddicombe, S. M., Morgan, L. M., Fletcher, J. M., 1995b. Investigations into the actions of glucose-dependent insulinotropic polypeptide and glucagon-like peptide-1(7-36)amide on lipoprotein lipase activity in explants of rat adipose tissue. J Nutr. 125, 183-8.

Knoch, K. P., Meisterfeld, R., Kersting, S., Bergert, H., Altkruger, A., Wegbrod, C., Jager, M., Saeger, H. D., Solimena, M., 2006. cAMP-dependent phosphorylation of PTB1 promotes the expression of insulin secretory granule proteins in beta cells. Cell Metab. 3, 123-34.

Knop, F. K., Vilsboll, T., Holst, J. J., 2009. Incretin-based therapy of type 2 diabetes mellitus. Curr Protein Pept Sci. 10, 46-55.

Knudsen, L. B., Kiel, D., Teng, M., Behrens, C., Bhumralkar, D., Kodra, J. T., Holst, J. J., Jeppesen, C. B., Johnson, M. D., de Jong, J. C., Jorgensen, A. S., Kercher, T., Kostrowicki, J., Madsen, P., Olesen, P. H., Petersen, J. S., Poulsen, F., Sidelmann, U. G., Sturis, J., Truesdale, L., May, J., Lau, J., 2007. Small-molecule agonists for the glucagon-like peptide 1 receptor. Proc Natl Acad Sci U S A. 104, 937-42.

Knudsen, L. B., Nielsen, P. F., Huusfeldt, P. O., Johansen, N. L., Madsen, K., Pedersen, F. Z., Thogersen, H., Wilken, M., Agerso, H., 2000. Potent derivatives of glucagon-like peptide-1 with pharmacokinetic properties suitable for once daily administration. J Med Chem. 43, 1664-9.

Kolligs, F., Fehmann, H. C., Goke, R., Goke, B., 1995. Reduction of the incretin effect in rats by the glucagon-like peptide 1 receptor antagonist exendin (9-39) amide. Diabetes. 44, 16-9.

Kolterman, O. G., Kim, D. D., Shen, L., Ruggles, J. A., Nielsen, L. L., Fineman, M. S., Baron, A. D., 2005. Pharmacokinetics, pharmacodynamics, and safety of exenatide in patients with type 2 diabetes mellitus. Am J Health Syst Pharm. 62, 173-81.

Konig, G. M., Kehraus, S., Seibert, S. F., Abdel-Lateff, A., Muller, D., 2006. Natural products from marine organisms and their associated microbes. Chembiochem. 7, 229-38.

Konturek, S. J., Konturek, J., Cieszkowski, M., Ebert, R., Creutzfeldt, W., 1986. Comparison of gastric inhibitory polypeptide and intraduodenal or intravenous fat on gastric acid secretion from vagally innervated and denervated canine stomach. Dig Dis Sci. 31, 49-56.

Krarup, T., 1988. Immunoreactive gastric inhibitory polypeptide. Endocr Rev. 9, 122-34.

Kreymann, B., Williams, G., Ghatei, M. A., Bloom, S. R., 1987. Glucagon-like peptide-1 7-36: a physiological incretin in man. Lancet. 2, 1300-4.

Kubota, A., Yamada, Y., Yasuda, K., Someya, Y., Ihara, Y., Kagimoto, S., Watanabe, R., Kuroe, A., Ishida, H., Seino, Y., 1997. Gastric inhibitory polypeptide activates MAP kinase through the wortmannin-sensitive and -insensitive pathways. Biochem Biophys Res Commun. 235, 171-5.

Kuzio, M., Dryburgh, J. R., Malloy, K. M., Brown, J. C., 1974. Radioimmunoassay for gastric inhibitory polypeptide. Gastroenterology. 66, 357-64.

Lankat-Buttgereit, B., Goke, B., 1997. Cloning and characterization of the 5' flanking sequences (promoter region) of the human GLP-1 receptor gene. Peptides. 18, 617-24.

Larsen, P. J., Tang-Christensen, M., Holst, J. J., Orskov, C., 1997. Distribution of glucagon-like peptide-1 and other preproglucagon-derived peptides in the rat hypothalamus and brainstem. Neuroscience. 77, 257-70.

Lawrence, M. C., Bhatt, H. S., Easom, R. A., 2002. NFAT regulates insulin gene promoter activity in response to synergistic pathways induced by glucose and glucagon-like peptide-1. Diabetes. 51, 691-8.

Lee, D. K., George, S. R., O'Dowd, B. F., 2003. Continued discovery of ligands for G protein-coupled receptors. Life Sci. 74, 293-7.

Leger, R., Thibaudeau, K., Robitaille, M., Quraishi, O., van Wyk, P., Bousquet-Gagnon, N., Carette, J., Castaigne, J. P., Bridon, D. P., 2004. Identification of CJC-1131-albumin bioconjugate as a stable and bioactive GLP-1(7-36) analog. Bioorg Med Chem Lett. 14, 4395-8.

Lester, L. B., Langeberg, L. K., Scott, J. D., 1997. Anchoring of protein kinase A facilitates hormone-mediated insulin secretion. Proc Natl Acad Sci U S A. 94**,** 14942-7.

Lewis, J. T., Dayanandan, B., Habener, J. F., Kieffer, T. J., 2000. Glucose-dependent insulinotropic polypeptide confers early phase insulin release to oral glucose in rats: demonstration by a receptor antagonist. Endocrinology. 141**,** 3710-6.

Li, Y., Cao, X., Li, L. X., Brubaker, P. L., Edlund, H., Drucker, D. J., 2005. beta-Cell Pdx1 expression is essential for the glucoregulatory, proliferative, and cytoprotective actions of glucagon-like peptide-1. Diabetes. 54**,** 482-91.

Light, P. E., Manning Fox, J. E., Riedel, M. J., Wheeler, M. B., 2002. Glucagon-like peptide-1 inhibits pancreatic ATP-sensitive potassium channels via a protein kinase A- and ADP-dependent mechanism. Mol Endocrinol. 16**,** 2135-44.

Liu, Z., Habener, J. F., 2008. Glucagon-like peptide-1 activation of TCF7L2-dependent Wnt signaling enhances pancreatic beta cell proliferation. J Biol Chem. 283**,** 8723-35.

Loganzo, F., Discafani, C. M., Annable, T., Beyer, C., Musto, S., Hari, M., Tan, X., Hardy, C., Hernandez, R., Baxter, M., Singanallore, T., Khafizova, G., Poruchynsky, M. S., Fojo, T., Nieman, J. A., Ayral-Kaloustian, S., Zask, A., Andersen, R. J., Greenberger, L. M., 2003. HTI-286, a synthetic analogue of the tripeptide hemiasterlin, is a potent antimicrotubule agent that circumvents P-glycoprotein-mediated resistance in vitro and in vivo. Cancer Res. 63**,** 1838-45.

Lopez, L. C., Frazier, M. L., Su, C. J., Kumar, A., Saunders, G. F., 1983. Mammalian pancreatic preproglucagon contains three glucagon-related peptides. Proc Natl Acad Sci U S A. 80**,** 5485-9.

Lovshin, J. A., Drucker, D. J., 2009. Incretin-based therapies for type 2 diabetes mellitus. Nat Rev Endocrinol. 5**,** 262-9.

Lu, M., Wheeler, M. B., Leng, X. H., Boyd, A. E., 3rd, 1993. The role of the free cytosolic calcium level in beta-cell signal transduction by gastric inhibitory polypeptide and glucagon-like peptide I(7-37). Endocrinology. 132**,** 94-100.

Lynn, F. C., Pamir, N., Ng, E. H., McIntosh, C. H., Kieffer, T. J., Pederson, R. A., 2001. Defective glucose-dependent insulinotropic polypeptide receptor expression in diabetic fatty Zucker rats. Diabetes. 50**,** 1004-11.

Lyssenko, V., Lupi, R., Marchetti, P., Del Guerra, S., Orho-Melander, M., Almgren, P., Sjogren, M., Ling, C., Eriksson, K. F., Lethagen, A. L., Mancarella, R., Berglund, G., Tuomi, T.,

Nilsson, P., Del Prato, S., Groop, L., 2007. Mechanisms by which common variants in the TCF7L2 gene increase risk of type 2 diabetes. J Clin Invest. 117**,** 2155-63.

Ma, X., Hui, H., Liu, Z., He, G., Hu, J., Meng, J., Guan, L., Luo, X., 2009. Poly-GLP-1, a novel long-lasting glucagon-like peptide-1 polymer, ameliorates hyperglycaemia by improving insulin sensitivity and increasing pancreatic beta-cell proliferation. Diabetes Obes Metab. 11**,** 953-65.

MacDonald, P. E., Sewing, S., Wang, J., Joseph, J. W., Smukler, S. R., Sakellaropoulos, G., Saleh, M. C., Chan, C. B., Tsushima, R. G., Salapatek, A. M., Wheeler, M. B., 2002. Inhibition of Kv2.1 voltage-dependent K+ channels in pancreatic beta-cells enhances glucose-dependent insulin secretion. J Biol Chem. 277**,** 44938-45.

MacDonald, P. E., Wang, X., Xia, F., El-kholy, W., Targonsky, E. D., Tsushima, R. G., Wheeler, M. B., 2003. Antagonism of rat beta-cell voltage-dependent K+ currents by exendin 4 requires dual activation of the cAMP/protein kinase A and phosphatidylinositol 3-kinase signaling pathways. J Biol Chem. 278**,** 52446-53.

MacDonald, P. E., Wheeler, M. B., 2003. Voltage-dependent K(+) channels in pancreatic beta cells: role, regulation and potential as therapeutic targets. Diabetologia. 46**,** 1046-62.

Madsbad, S., Krarup, T., Deacon, C. F., Holst, J. J., 2008. Glucagon-like peptide receptor agonists and dipeptidyl peptidase-4 inhibitors in the treatment of diabetes: a review of clinical trials. Curr Opin Clin Nutr Metab Care. 11**,** 491-9.

Malde, A. K., Srivastava, S. S., Coutinho, E. C., 2007. Understanding interactions of gastric inhibitory polypeptide (GIP) with its G-protein coupled receptor through NMR and molecular modeling. J Pept Sci. 13**,** 287-300.

Manuel, D. G., Schultz, S. E., 2004. Health-related quality of life and health-adjusted life expectancy of people with diabetes in Ontario, Canada, 1996-1997. Diabetes Care. 27**,** 407-14.

Marcadia_Biotech, Marcadia Initiates Phase 1 Clinical Trial of GLP-1/GIP Dual Agonist MAR701. Vol. 2011, 2010.

McClean, P. L., Gault, V. A., Irwin, N., McCluskey, J. T., Flatt, P. R., 2008a. Daily administration of the GIP-R antagonist (Pro3)GIP in streptozotocin-induced diabetes suggests that insulin-dependent mechanisms are critical to anti-obesity-diabetes actions of (Pro3)GIP. Diabetes Obes Metab. 10**,** 336-42.

McClean, P. L., Irwin, N., Cassidy, R. S., Holst, J. J., Gault, V. A., Flatt, P. R., 2007. GIP receptor antagonism reverses obesity, insulin resistance, and associated metabolic

disturbances induced in mice by prolonged consumption of high-fat diet. Am J Physiol Endocrinol Metab. 293**,** E1746-55.

McClean, P. L., Irwin, N., Hunter, K., Gault, V. A., Flatt, P. R., 2008b. (Pro(3))GIP[mPEG]: novel, long-acting, mPEGylated antagonist of gastric inhibitory polypeptide for obesity-diabetes (diabesity) therapy. Br J Pharmacol. 155**,** 690-701.

McDonald, T. F., Pelzer, S., Trautwein, W., Pelzer, D. J., 1994. Regulation and modulation of calcium channels in cardiac, skeletal, and smooth muscle cells. Physiol Rev. 74**,** 365-507.

McIntosh, C. H., 2008. Dipeptidyl peptidase IV inhibitors and diabetes therapy. Front Biosci. 13**,** 1753-73.

McIntosh, C. H., Bremsak, I., Lynn, F. C., Gill, R., Hinke, S. A., Gelling, R., Nian, C., McKnight, G., Jaspers, S., Pederson, R. A., 1999. Glucose-dependent insulinotropic polypeptide stimulation of lipolysis in differentiated 3T3-L1 cells: wortmannin-sensitive inhibition by insulin. Endocrinology. 140**,** 398-404.

McIntosh, C. H., Pederson, R. A., Koop, H., Brown, J. C., 1981. Gastric inhibitory polypeptide stimulated secretion of somatostatinlike immunoreactivity from the stomach: inhibition by acetylcholine or vagal stimulation. Can J Physiol Pharmacol. 59**,** 468-72.

McIntosh, C. H., Widenmaier, S., Kim, S. J., 2009. Glucose-dependent insulinotropic polypeptide (Gastric Inhibitory Polypeptide; GIP). Vitam Horm. 80**,** 409-71.

McIntyre, N., Holdsworth, C. D., Turner, D. S., 1964. New Interpretation of Oral Glucose Tolerance. Lancet. 2**,** 20-1.

McKee, T. C., Cardellina, J. H., 2nd, Riccio, R., D'Auria, M. V., Iorizzi, M., Minale, L., Moran, R. A., Gulakowski, R. J., McMahon, J. B., Buckheit, R. W., Jr., et al., 1994. HIV-inhibitory natural products. 11. Comparative studies of sulfated sterols from marine invertebrates. J Med Chem. 37**,** 793-7.

Meier, J. J., Gallwitz, B., Siepmann, N., Holst, J. J., Deacon, C. F., Schmidt, W. E., Nauck, M. A., 2003. Gastric inhibitory polypeptide (GIP) dose-dependently stimulates glucagon secretion in healthy human subjects at euglycaemia. Diabetologia. 46**,** 798-801.

Meier, J. J., Gethmann, A., Nauck, M. A., Gotze, O., Schmitz, F., Deacon, C. F., Gallwitz, B., Schmidt, W. E., Holst, J. J., 2006. The glucagon-like peptide-1 metabolite GLP-1-(9-36) amide reduces postprandial glycemia independently of gastric emptying and insulin secretion in humans. Am J Physiol Endocrinol Metab. 290**,** E1118-23.

Meier, J. J., Nauck, M. A., 2008. Is secretion of glucagon-like peptide-1 reduced in type 2 diabetes mellitus? Nat Clin Pract Endocrinol Metab. 4**,** 606-7.

Meier, J. J., Nauck, M. A., 2010. Is the diminished incretin effect in type 2 diabetes just an epi-phenomenon of impaired beta-cell function? Diabetes. 59, 1117-25.

Mentlein, R., Gallwitz, B., Schmidt, W. E., 1993. Dipeptidyl-peptidase IV hydrolyses gastric inhibitory polypeptide, glucagon-like peptide-1(7-36)amide, peptide histidine methionine and is responsible for their degradation in human serum. Eur J Biochem. 214, 829-35.

Merkler, D. J., 1994. C-terminal amidated peptides: production by the in vitro enzymatic amidation of glycine-extended peptides and the importance of the amide to bioactivity. Enzyme Microb Technol. 16, 450-6.

Mickel, S. J., 2004. Toward a commercial synthesis of (+)-discodermolide. Curr Opin Drug Discov Devel. 7, 869-81.

Miki, T., Minami, K., Shinozaki, H., Matsumura, K., Saraya, A., Ikeda, H., Yamada, Y., Holst, J. J., Seino, S., 2005. Distinct effects of glucose-dependent insulinotropic polypeptide and glucagon-like peptide-1 on insulin secretion and gut motility. Diabetes. 54, 1056-63.

Miyawaki, K., Yamada, Y., Ban, N., Ihara, Y., Tsukiyama, K., Zhou, H., Fujimoto, S., Oku, A., Tsuda, K., Toyokuni, S., Hiai, H., Mizunoya, W., Fushiki, T., Holst, J. J., Makino, M., Tashita, A., Kobara, Y., Tsubamoto, Y., Jinnouchi, T., Jomori, T., Seino, Y., 2002. Inhibition of gastric inhibitory polypeptide signaling prevents obesity. Nat Med. 8, 738-42.

Miyawaki, K., Yamada, Y., Yano, H., Niwa, H., Ban, N., Ihara, Y., Kubota, A., Fujimoto, S., Kajikawa, M., Kuroe, A., Tsuda, K., Hashimoto, H., Yamashita, T., Jomori, T., Tashiro, F., Miyazaki, J., Seino, Y., 1999. Glucose intolerance caused by a defect in the entero-insular axis: a study in gastric inhibitory polypeptide receptor knockout mice. Proc Natl Acad Sci U S A. 96, 14843-7.

Moens, K., Heimberg, H., Flamez, D., Huypens, P., Quartier, E., Ling, Z., Pipeleers, D., Gremlich, S., Thorens, B., Schuit, F., 1996. Expression and functional activity of glucagon, glucagon-like peptide I, and glucose-dependent insulinotropic peptide receptors in rat pancreatic islet cells. Diabetes. 45, 257-61.

Moitessier, N., Englebienne, P., Lee, D., Lawandi, J., Corbeil, C. R., 2008. Towards the development of universal, fast and highly accurate docking/scoring methods: a long way to go. Br J Pharmacol. 153 Suppl 1, S7-26.

Mojsov, S., Heinrich, G., Wilson, I. B., Ravazzola, M., Orci, L., Habener, J. F., 1986. Preproglucagon gene expression in pancreas and intestine diversifies at the level of post-translational processing. J Biol Chem. 261, 11880-9.

Mojsov, S., Weir, G. C., Habener, J. F., 1987. Insulinotropin: glucagon-like peptide I (7-37) co-encoded in the glucagon gene is a potent stimulator of insulin release in the perfused rat pancreas. J Clin Invest. 79, 616-9.

Moni, R. W., Parsons, P. G., Quinn, R. J., Willis, R. J., 1992. Critical micelle concentration and hemolytic activity--a correlation suggested by the marine sterol, halistanol trisulfate. Biochem Biophys Res Commun. 182, 115-20.

Montrose-Rafizadeh, C., Avdonin, P., Garant, M. J., Rodgers, B. D., Kole, S., Yang, H., Levine, M. A., Schwindinger, W., Bernier, M., 1999. Pancreatic glucagon-like peptide-1 receptor couples to multiple G proteins and activates mitogen-activated protein kinase pathways in Chinese hamster ovary cells. Endocrinology. 140, 1132-40.

Moretto, T. J., Milton, D. R., Ridge, T. D., Macconell, L. A., Okerson, T., Wolka, A. M., Brodows, R. G., 2008. Efficacy and tolerability of exenatide monotherapy over 24 weeks in antidiabetic drug-naive patients with type 2 diabetes: a randomized, double-blind, placebo-controlled, parallel-group study. Clin Ther. 30, 1448-60.

Morgan, L. M., 1979. Immunoassayable gastric inhibitory polypeptide: investigations into its role in carbohydrate metabolism. Ann Clin Biochem. 16, 6-14.

Morgan, L. M., 1996. The metabolic role of GIP: physiology and pathology. Biochem Soc Trans. 24, 585-91.

Mortensen, K., Christensen, L. L., Holst, J. J., Orskov, C., 2003. GLP-1 and GIP are colocalized in a subset of endocrine cells in the small intestine. Regul Pept. 114, 189-96.

Multispan, Multiscreen[TM] Stable Cell Line Human Recombinant GIP Receptor. Vol. 2011, 2005a.

Multispan, Multiscreen[TM] Stable Cell Line Human Recombinant GLP-1 Receptor. Vol. 2011, 2005b.

Multispan, Multiscreen[TM] Stable Cell Line Human Recombinant Glucagon Receptor. Vol. 2011, 2005c.

Nathan, D. M., Schreiber, E., Fogel, H., Mojsov, S., Habener, J. F., 1992. Insulinotropic action of glucagonlike peptide-I-(7-37) in diabetic and nondiabetic subjects. Diabetes Care. 15, 270-6.

Nauck, M., Stockmann, F., Ebert, R., Creutzfeldt, W., 1986a. Reduced incretin effect in type 2 (non-insulin-dependent) diabetes. Diabetologia. 29, 46-52.

Nauck, M. A., 2009. Unraveling the science of incretin biology. Am J Med. 122, S3-S10.

Nauck, M. A., Bartels, E., Orskov, C., Ebert, R., Creutzfeldt, W., 1992. Lack of effect of synthetic human gastric inhibitory polypeptide and glucagon-like peptide 1 [7-36 amide] infused at near-physiological concentrations on pentagastrin-stimulated gastric acid secretion in normal human subjects. Digestion. 52, 214-21.

Nauck, M. A., El-Ouaghlidi, A., 2005. The therapeutic actions of DPP-IV inhibition are not mediated by glucagon-like peptide-1. Diabetologia. 48, 608-11.

Nauck, M. A., Heimesaat, M. M., Behle, K., Holst, J. J., Nauck, M. S., Ritzel, R., Hufner, M., Schmiegel, W. H., 2002. Effects of glucagon-like peptide 1 on counterregulatory hormone responses, cognitive functions, and insulin secretion during hyperinsulinemic, stepped hypoglycemic clamp experiments in healthy volunteers. J Clin Endocrinol Metab. 87, 1239-46.

Nauck, M. A., Heimesaat, M. M., Orskov, C., Holst, J. J., Ebert, R., Creutzfeldt, W., 1993a. Preserved incretin activity of glucagon-like peptide 1 [7-36 amide] but not of synthetic human gastric inhibitory polypeptide in patients with type-2 diabetes mellitus. J Clin Invest. 91, 301-7.

Nauck, M. A., Homberger, E., Siegel, E. G., Allen, R. C., Eaton, R. P., Ebert, R., Creutzfeldt, W., 1986b. Incretin effects of increasing glucose loads in man calculated from venous insulin and C-peptide responses. J Clin Endocrinol Metab. 63, 492-8.

Nauck, M. A., Kleine, N., Orskov, C., Holst, J. J., Willms, B., Creutzfeldt, W., 1993b. Normalization of fasting hyperglycaemia by exogenous glucagon-like peptide 1 (7-36 amide) in type 2 (non-insulin-dependent) diabetic patients. Diabetologia. 36, 741-4.

Nauck, M. A., Meier, J. J., 2010. Individualised incretin-based treatment for type 2 diabetes. Lancet. 376, 393-4.

Nauck, M. A., Ratner, R. E., Kapitza, C., Berria, R., Boldrin, M., Balena, R., 2009. Treatment with the human once-weekly glucagon-like peptide-1 analog taspoglutide in combination with metformin improves glycemic control and lowers body weight in patients with type 2 diabetes inadequately controlled with metformin alone: a double-blind placebo-controlled study. Diabetes Care. 32, 1237-43.

Newman, D. J., Cragg, G. M., Snader, K. M., 2003. Natural products as sources of new drugs over the period 1981-2002. J Nat Prod. 66, 1022-37.

Nie, Y., Nakashima, M., Brubaker, P. L., Li, Q. L., Perfetti, R., Jansen, E., Zambre, Y., Pipeleers, D., Friedman, T. C., 2000. Regulation of pancreatic PC1 and PC2 associated with increased glucagon-like peptide 1 in diabetic rats. J Clin Invest. 105, 955-65.

Nielsen, L. B., Ploug, K. B., Swift, P., Orskov, C., Jansen-Olesen, I., Chiarelli, F., Holst, J. J., Hougaard, P., Porksen, S., Holl, R., de Beaufort, C., Gammeltoft, S., Rorsman, P., Mortensen, H. B., Hansen, L., 2007. Co-localisation of the Kir6.2/SUR1 channel complex with glucagon-like peptide-1 and glucose-dependent insulinotrophic polypeptide expression in human ileal cells and implications for glycaemic control in new onset type 1 diabetes. Eur J Endocrinol. 156**,** 663-71.

Novo_Nordisk, Highlights of Prescribing Information. Vol. 2011, 2010.

Nyberg, J., Anderson, M. F., Meister, B., Alborn, A. M., Strom, A. K., Brederlau, A., Illerskog, A. C., Nilsson, O., Kieffer, T. J., Hietala, M. A., Ricksten, A., Eriksson, P. S., 2005. Glucose-dependent insulinotropic polypeptide is expressed in adult hippocampus and induces progenitor cell proliferation. J Neurosci. 25**,** 1816-25.

O'Dorisio, T. M., Cataland, S., Stevenson, M., Mazzaferri, E. L., 1976. Gastric inhibitory polypeptide (GIP). Intestinal distribution and stimulation by amino acids and medium-chain triglycerides. Am J Dig Dis. 21**,** 761-5.

Oben, J., Morgan, L., Fletcher, J., Marks, V., 1991. Effect of the entero-pancreatic hormones, gastric inhibitory polypeptide and glucagon-like polypeptide-1(7-36) amide, on fatty acid synthesis in explants of rat adipose tissue. J Endocrinol. 130**,** 267-72.

Orskov, C., Holst, J. J., Knuhtsen, S., Baldissera, F. G., Poulsen, S. S., Nielsen, O. V., 1986. Glucagon-like peptides GLP-1 and GLP-2, predicted products of the glucagon gene, are secreted separately from pig small intestine but not pancreas. Endocrinology. 119**,** 1467-75.

Orskov, C., Rabenhoj, L., Wettergren, A., Kofod, H., Holst, J. J., 1994. Tissue and plasma concentrations of amidated and glycine-extended glucagon-like peptide I in humans. Diabetes. 43**,** 535-9.

Orskov, C., Wettergren, A., Holst, J. J., 1993. Biological effects and metabolic rates of glucagonlike peptide-1 7-36 amide and glucagonlike peptide-1 7-37 in healthy subjects are indistinguishable. Diabetes. 42**,** 658-61.

Osterrieder, W., Brum, G., Hescheler, J., Trautwein, W., Flockerzi, V., Hofmann, F., 1982. Injection of subunits of cyclic AMP-dependent protein kinase into cardiac myocytes modulates Ca2+ current. Nature. 298**,** 576-8.

Pan, C. Q., Buxton, J. M., Yung, S. L., Tom, I., Yang, L., Chen, H., MacDougall, M., Bell, A., Claus, T. H., Clairmont, K. B., Whelan, J. P., 2006. Design of a long acting peptide

functioning as both a glucagon-like peptide-1 receptor agonist and a glucagon receptor antagonist. J Biol Chem. 281**,** 12506-15.

Parker, H. E., Habib, A. M., Rogers, G. J., Gribble, F. M., Reimann, F., 2009. Nutrient-dependent secretion of glucose-dependent insulinotropic polypeptide from primary murine K cells. Diabetologia. 52**,** 289-98.

Parker, H. E., Reimann, F., Gribble, F. M., 2010. Molecular mechanisms underlying nutrient-stimulated incretin secretion. Expert Rev Mol Med. 12**,** e1.

Parthier, C., Kleinschmidt, M., Neumann, P., Rudolph, R., Manhart, S., Schlenzig, D., Fanghanel, J., Rahfeld, J. U., Demuth, H. U., Stubbs, M. T., 2007. Crystal structure of the incretin-bound extracellular domain of a G protein-coupled receptor. Proc Natl Acad Sci U S A. 104**,** 13942-7.

Patterson, J. T., Ottaway, N., Gelfanov, V. M., Smiley, D. L., Perez-Tilve, D., Pfluger, P. T., Tschop, M. H., Dimarchi, R. D., 2011. A novel human-based receptor antagonist of sustained action reveals body weight control by endogenous GLP-1. ACS Chem Biol. 6**,** 135-45.

Pauly, R. P., Rosche, F., Wermann, M., McIntosh, C. H., Pederson, R. A., Demuth, H. U., 1996. Investigation of glucose-dependent insulinotropic polypeptide-(1-42) and glucagon-like peptide-1-(7-36) degradation in vitro by dipeptidyl peptidase IV using matrix-assisted laser desorption/ionization-time of flight mass spectrometry. A novel kinetic approach. J Biol Chem. 271**,** 23222-9.

Pederson, R. A., Brown, J. C., 1976. The insulinotropic action of gastric inhibitory polypeptide in the perfused isolated rat pancreas. Endocrinology. 99**,** 780-5.

Pederson, R. A., Brown, J. C., 1978. Interaction of gastric inhibitory polypeptide, glucose, and arginine on insulin and glucagon secretion from the perfused rat pancreas. Endocrinology. 103**,** 610-5.

Pederson, R. A., Schubert, H. E., Brown, J. C., 1975. Gastric inhibitory polypeptide. Its physiologic release and insulinotropic action in the dog. Diabetes. 24**,** 1050-6.

Pereira, A., Pfeifer, T. A., Grigliatti, T. A., Andersen, R. J., 2009. Functional Cell-Based Screening and Saturation Transfer Double-Difference NMR Have Identified Haplosamate A as a Cannabinoid Receptor Agonist. ACS Chem Biol.

Picha, K. M., Cunningham, M. R., Drucker, D. J., Mathur, A., Ort, T., Scully, M., Soderman, A., Spinka-Doms, T., Stojanovic-Susulic, V., Thomas, B. A., O'Neil, K. T., 2008. Protein

engineering strategies for sustained glucagon-like peptide-1 receptor-dependent control of glucose homeostasis. Diabetes. 57**,** 1926-34.

Pilgaard, K., Jensen, C. B., Schou, J. H., Lyssenko, V., Wegner, L., Brons, C., Vilsboll, T., Hansen, T., Madsbad, S., Holst, J. J., Volund, A., Poulsen, P., Groop, L., Pedersen, O., Vaag, A. A., 2009. The T allele of rs7903146 TCF7L2 is associated with impaired insulinotropic action of incretin hormones, reduced 24 h profiles of plasma insulin and glucagon, and increased hepatic glucose production in young healthy men. Diabetologia. 52**,** 1298-307.

Piteau, S., Olver, A., Kim, S. J., Winter, K., Pospisilik, J. A., Lynn, F., Manhart, S., Demuth, H. U., Speck, M., Pederson, R. A., McIntosh, C. H., 2007. Reversal of islet GIP receptor down-regulation and resistance to GIP by reducing hyperglycemia in the Zucker rat. Biochem Biophys Res Commun. 362**,** 1007-12.

Pocai, A., Carrington, P. E., Adams, J. R., Wright, M., Eiermann, G., Zhu, L., Du, X., Petrov, A., Lassman, M. E., Jiang, G., Liu, F., Miller, C., Tota, L. M., Zhou, G., Zhang, X., Sountis, M. M., Santoprete, A., Capito, E., Chicchi, G. G., Thornberry, N., Bianchi, E., Pessi, A., Marsh, D. J., SinhaRoy, R., 2009. Glucagon-like peptide 1/glucagon receptor dual agonism reverses obesity in mice. Diabetes. 58**,** 2258-66.

Polak, J. M., Bloom, S. R., Kuzio, M., Brown, J. C., Pearse, A. G., 1973. Cellular localization of gastric inhibitory polypeptide in the duodenum and jejunum. Gut. 14**,** 284-8.

Porter, D. W., Irwin, N., Flatt, P. R., Holscher, C., Gault, V. A., 2011. Prolonged GIP receptor activation improves cognitive function, hippocampal synaptic plasticity and glucose homeostasis in high-fat fed mice. Eur J Pharmacol. 650**,** 688-93.

Prado, C. L., Pugh-Bernard, A. E., Elghazi, L., Sosa-Pineda, B., Sussel, L., 2004. Ghrelin cells replace insulin-producing beta cells in two mouse models of pancreas development. Proc Natl Acad Sci U S A. 101**,** 2924-9.

Prasadan, K., Koizumi, M., Tulachan, S., Shiota, C., Lath, N., Paredes, J., Guo, P., El-Gohary, Y., Malek, M., Shah, S., Gittes, G. K., 2011. The expression and function of glucose-dependent insulinotropic polypeptide in the embryonic mouse pancreas. Diabetes. 60**,** 548-54.

Ratner, R. E., Maggs, D., Nielsen, L. L., Stonehouse, A. H., Poon, T., Zhang, B., Bicsak, T. A., Brodows, R. G., Kim, D. D., 2006. Long-term effects of exenatide therapy over 82 weeks on glycaemic control and weight in over-weight metformin-treated patients with type 2 diabetes mellitus. Diabetes Obes Metab. 8**,** 419-28.

Reimann, F., Gribble, F. M., 2002. Glucose-sensing in glucagon-like peptide-1-secreting cells. Diabetes. 51**,** 2757-63.

Reimann, F., Habib, A. M., Tolhurst, G., Parker, H. E., Rogers, G. J., Gribble, F. M., 2008. Glucose sensing in L cells: a primary cell study. Cell Metab. 8**,** 532-9.

Renner, S., Fehlings, C., Herbach, N., Hofmann, A., von Waldthausen, D. C., Kessler, B., Ulrichs, K., Chodnevskaja, I., Moskalenko, V., Amselgruber, W., Goke, B., Pfeifer, A., Wanke, R., Wolf, E., 2010. Glucose intolerance and reduced proliferation of pancreatic beta-cells in transgenic pigs with impaired glucose-dependent insulinotropic polypeptide function. Diabetes. 59**,** 1228-38.

Retterstol, K., 2009. Taspoglutide: a long acting human glucagon-like polypeptide-1 analogue. Expert Opin Investig Drugs. 18**,** 1405-11.

Reubi, J. C., Perren, A., Rehmann, R., Waser, B., Christ, E., Callery, M., Goldfine, A. B., Patti, M. E., 2010. Glucagon-like peptide-1 (GLP-1) receptors are not overexpressed in pancreatic islets from patients with severe hyperinsulinaemic hypoglycaemia following gastric bypass. Diabetologia. 53**,** 2641-5.

Reubi, J. C., Waser, B., 2003. Concomitant expression of several peptide receptors in neuroendocrine tumours: molecular basis for in vivo multireceptor tumour targeting. Eur J Nucl Med Mol Imaging. 30**,** 781-93.

Riddle, M. C., Henry, R. R., Poon, T. H., Zhang, B., Mac, S. M., Holcombe, J. H., Kim, D. D., Maggs, D. G., 2006. Exenatide elicits sustained glycaemic control and progressive reduction of body weight in patients with type 2 diabetes inadequately controlled by sulphonylureas with or without metformin. Diabetes Metab Res Rev. 22**,** 483-91.

Rosenstock, J., Reusch, J., Bush, M., Yang, F., Stewart, M., 2009. Potential of albiglutide, a long-acting GLP-1 receptor agonist, in type 2 diabetes: a randomized controlled trial exploring weekly, biweekly, and monthly dosing. Diabetes Care. 32**,** 1880-6.

Ross, S. A., Brown, J. C., Dupre, J., 1977. Hypersecretion of gastric inhibitory polypeptide following oral glucose in diabetes mellitus. Diabetes. 26**,** 525-9.

Ross, S. A., Dupre, J., 1978. Effects of ingestion of triglyceride or galactose on secretion of gastric inhibitory polypeptide and on responses to intravenous glucose in normal and diabetic subjects. Diabetes. 27**,** 327-33.

Rouille, Y., Westermark, G., Martin, S. K., Steiner, D. F., 1994. Proglucagon is processed to glucagon by prohormone convertase PC2 in alpha TC1-6 cells. Proc Natl Acad Sci U S A. 91**,** 3242-6.

Runge, S., Thogersen, H., Madsen, K., Lau, J., Rudolph, R., 2008. Crystal structure of the ligand-bound glucagon-like peptide-1 receptor extracellular domain. J Biol Chem. 283, 11340-7.

Salera, M., Giacomoni, P., Pironi, L., Cornia, G., Capelli, M., Marini, A., Benfenati, F., Miglioli, M., Barbara, L., 1982. Gastric inhibitory polypeptide release after oral glucose: relationship to glucose intolerance, diabetes mellitus, and obesity. J Clin Endocrinol Metab. 55, 329-36.

Salvalaggio, P. R., Deng, S., Ariyan, C. E., Millet, I., Zawalich, W. S., Basadonna, G. P., Rothstein, D. M., 2002. Islet filtration: a simple and rapid new purification procedure that avoids ficoll and improves islet mass and function. Transplantation. 74, 877-9.

Sandberg, E., Ahren, B., Tendler, D., Carlquist, M., Efendic, S., 1986. Potentiation of glucose-induced insulin secretion in the perfused rat pancreas by porcine GIP (gastric inhibitory polypeptide), bovine GIP, and bovine GIP(1-39). Acta Physiol Scand. 127, 323-6.

Sandhu, H., Wiesenthal, S. R., MacDonald, P. E., McCall, R. H., Tchipashvili, V., Rashid, S., Satkunarajah, M., Irwin, D. M., Shi, Z. Q., Brubaker, P. L., Wheeler, M. B., Vranic, M., Efendic, S., Giacca, A., 1999. Glucagon-like peptide 1 increases insulin sensitivity in depancreatized dogs. Diabetes. 48, 1045-53.

Sanofi_Aventis, Once Daily Lixisenatide (AVE 0010) Given as Monotherapy Successfully Meets Phase III Study Endpoints in Diabetes. Vol. 2011, 2010.

Sathananthan, A., Man, C. D., Micheletto, F., Zinsmeister, A. R., Camilleri, M., Giesler, P. D., Laugen, J. M., Toffolo, G., Rizza, R. A., Cobelli, C., Vella, A., 2010. Common Genetic Variation in GLP1R and Insulin Secretion in Response to Exogenous GLP-1 in Nondiabetic Subjects: A pilot study. Diabetes Care. 33, 2074-6.

Sato, A. K., Viswanathan, M., Kent, R. B., Wood, C. R., 2006. Therapeutic peptides: technological advances driving peptides into development. Curr Opin Biotechnol. 17, 638-42.

Saxena, R., Hivert, M. F., Langenberg, C., Tanaka, T., Pankow, J. S., Vollenweider, P., Lyssenko, V., Bouatia-Naji, N., Dupuis, J., Jackson, A. U., Kao, W. H., Li, M., Glazer, N. L., Manning, A. K., Luan, J., Stringham, H. M., Prokopenko, I., Johnson, T., Grarup, N., Boesgaard, T. W., Lecoeur, C., Shrader, P., O'Connell, J., Ingelsson, E., Couper, D. J., Rice, K., Song, K., Andreasen, C. H., Dina, C., Kottgen, A., Le Bacquer, O., Pattou, F., Taneera, J., Steinthorsdottir, V., Rybin, D., Ardlie, K., Sampson, M., Qi, L., van Hoek, M., Weedon, M. N., Aulchenko, Y. S., Voight, B. F., Grallert, H., Balkau, B.,

Bergman, R. N., Bielinski, S. J., Bonnefond, A., Bonnycastle, L. L., Borch-Johnsen, K., Bottcher, Y., Brunner, E., Buchanan, T. A., Bumpstead, S. J., Cavalcanti-Proenca, C., Charpentier, G., Chen, Y. D., Chines, P. S., Collins, F. S., Cornelis, M., G, J. C., Delplanque, J., Doney, A., Egan, J. M., Erdos, M. R., Firmann, M., Forouhi, N. G., Fox, C. S., Goodarzi, M. O., Graessler, J., Hingorani, A., Isomaa, B., Jorgensen, T., Kivimaki, M., Kovacs, P., Krohn, K., Kumari, M., Lauritzen, T., Levy-Marchal, C., Mayor, V., McAteer, J. B., Meyre, D., Mitchell, B. D., Mohlke, K. L., Morken, M. A., Narisu, N., Palmer, C. N., Pakyz, R., Pascoe, L., Payne, F., Pearson, D., Rathmann, W., Sandbaek, A., Sayer, A. A., Scott, L. J., Sharp, S. J., Sijbrands, E., Singleton, A., Siscovick, D. S., Smith, N. L., Sparso, T., Swift, A. J., Syddall, H., Thorleifsson, G., Tonjes, A., Tuomi, T., Tuomilehto, J., Valle, T. T., Waeber, G., Walley, A., Waterworth, D. M., Zeggini, E., Zhao, J. H., Illig, T., Wichmann, H. E., Wilson, J. F., van Duijn, C., Hu, F. B., Morris, A. D., Frayling, T. M., Hattersley, A. T., Thorsteinsdottir, U., Stefansson, K., Nilsson, P., Syvanen, A. C., Shuldiner, A. R., Walker, M., Bornstein, S. R., Schwarz, P., Williams, G. H., Nathan, D. M., Kuusisto, J., Laakso, M., Cooper, C., Marmot, M., Ferrucci, L., Mooser, V., Stumvoll, M., Loos, R. J., Altshuler, D., Psaty, B. M., Rotter, J. I., Boerwinkle, E., Hansen, T., Pedersen, O., Florez, J. C., McCarthy, M. I., Boehnke, M., Barroso, I., Sladek, R., Froguel, P., Meigs, J. B., Groop, L., Wareham, N. J., Watanabe, R. M., 2010. Genetic variation in GIPR influences the glucose and insulin responses to an oral glucose challenge. Nat Genet. 42, 142-8.

Schafer, R., Schatz, H., 1979. Stimulation of (Pro-)insulin biosynthesis and release by gastric inhibitory polypeptide in isolated islets of rat pancreas. Acta Endocrinol (Copenh). 91, 493-500.

Schafer, S. A., Mussig, K., Staiger, H., Machicao, F., Stefan, N., Gallwitz, B., Haring, H. U., Fritsche, A., 2009. A common genetic variant in WFS1 determines impaired glucagon-like peptide-1-induced insulin secretion. Diabetologia. 52, 1075-82.

Schafer, S. A., Tschritter, O., Machicao, F., Thamer, C., Stefan, N., Gallwitz, B., Holst, J. J., Dekker, J. M., t Hart, L. M., Nijpels, G., van Haeften, T. W., Haring, H. U., Fritsche, A., 2007. Impaired glucagon-like peptide-1-induced insulin secretion in carriers of transcription factor 7-like 2 (TCF7L2) gene polymorphisms. Diabetologia. 50, 2443-50.

Schauder, P., Brown, J. C., Frerichs, H., Creutzfeldt, W., 1975. Gastric inhibitory polypeptide: effect on glucose-induced insulin release from isolated rat pancreatic islets in vitro. Diabetologia. 11, 483-4.

Schieldrop, P. J., Gelling, R. W., Elliot, R., Hewitt, J., Kieffer, T. J., McIntosh, C. H., Pederson, R. A., 1996. Isolation of a murine glucose-dependent insulinotropic polypeptide (GIP) cDNA from a tumor cell line (STC6-14) and quantification of glucose-induced increases in GIP mRNA. Biochim Biophys Acta. 1308**,** 111-3.

Schirra, J., Katschinski, M., Weidmann, C., Schafer, T., Wank, U., Arnold, R., Goke, B., 1996. Gastric emptying and release of incretin hormones after glucose ingestion in humans. J Clin Invest. 97**,** 92-103.

Schirra, J., Sturm, K., Leicht, P., Arnold, R., Goke, B., Katschinski, M., 1998. Exendin(9-39)amide is an antagonist of glucagon-like peptide-1(7-36)amide in humans. J Clin Invest. 101**,** 1421-30.

Schmidt, W. E., Siegel, E. G., Kummel, H., Gallwitz, B., Creutzfeldt, W., 1987. Commercially available preparations of porcine glucose-dependent insulinotropic polypeptide (GIP) contain a biologically inactive GIP-fragment and cholecystokinin-33/-39. Endocrinology. 120**,** 835-7.

Scrocchi, L. A., Brown, T. J., MaClusky, N., Brubaker, P. L., Auerbach, A. B., Joyner, A. L., Drucker, D. J., 1996. Glucose intolerance but normal satiety in mice with a null mutation in the glucagon-like peptide 1 receptor gene. Nat Med. 2**,** 1254-8.

Scrocchi, L. A., Hill, M. E., Saleh, J., Perkins, B., Drucker, D. J., 2000. Elimination of glucagon-like peptide 1R signaling does not modify weight gain and islet adaptation in mice with combined disruption of leptin and GLP-1 action. Diabetes. 49**,** 1552-60.

Seamon, K. B., Padgett, W., Daly, J. W., 1981. Forskolin: unique diterpene activator of adenylate cyclase in membranes and in intact cells. Proc Natl Acad Sci U S A. 78**,** 3363-7.

Seino, S., Shibasaki, T., 2005. PKA-dependent and PKA-independent pathways for cAMP-regulated exocytosis. Physiol Rev. 85**,** 1303-42.

Shah, P., Vella, A., Basu, A., Basu, R., Schwenk, W. F., Rizza, R. A., 2000. Lack of suppression of glucagon contributes to postprandial hyperglycemia in subjects with type 2 diabetes mellitus. J Clin Endocrinol Metab. 85**,** 4053-9.

Shu, L., Matveyenko, A. V., Kerr-Conte, J., Cho, J. H., McIntosh, C. H., Maedler, K., 2009. Decreased TCF7L2 protein levels in type 2 diabetes mellitus correlate with downregulation of GIP- and GLP-1 receptors and impaired beta-cell function. Hum Mol Genet. 18**,** 2388-99.

Siegel, E. G., Creutzfeldt, W., 1985. Stimulation of insulin release in isolated rat islets by GIP in physiological concentrations and its relation to islet cyclic AMP content. Diabetologia. 28**,** 857-61.

Simonsen, L., Holst, J. J., Deacon, C. F., 2006. Exendin-4, but not glucagon-like peptide-1, is cleared exclusively by glomerular filtration in anaesthetised pigs. Diabetologia. 49**,** 706-12.

Skoglund, G., Hussain, M. A., Holz, G. G., 2000. Glucagon-like peptide 1 stimulates insulin gene promoter activity by protein kinase A-independent activation of the rat insulin I gene cAMP response element. Diabetes. 49**,** 1156-64.

Slate, D. L., Lee, R. H., Rodriguez, J., Crews, P., 1994. The marine natural product, halistanol trisulfate, inhibits pp60v-src protein tyrosine kinase activity. Biochem Biophys Res Commun. 203**,** 260-4.

Sloop, K. W., Willard, F. S., Brenner, M. B., Ficorilli, J., Valasek, K., Showalter, A. D., Farb, T. B., Cao, J. X., Cox, A. L., Michael, M. D., Gutierrez Sanfeliciano, S. M., Tebbe, M. J., Coghlan, M. J., 2010. Novel Small Molecule Glucagon-like Peptide-1 Receptor Agonist Stimulates Insulin Secretion in Rodents and from Human Islets. Diabetes. 59**,** 3099-107.

Smith, P. H., Merchant, F. W., Johnson, D. G., Fujimoto, W. Y., Williams, R. H., 1977. Immunocytochemical localization of a gastric imhibitory polypeptide-like material within A-cells of the endocrine pancreas. Am J Anat. 149**,** 585-90.

Someya, Y., Inagaki, N., Maekawa, T., Seino, Y., Ishii, S., 1993. Two 3',5'-cyclic-adenosine monophosphate response elements in the promoter region of the human gastric inhibitory polypeptide gene. FEBS Lett. 317**,** 67-73.

Son, S., Chae, S. Y., Kim, C. W., Choi, Y. G., Jung, S. Y., Lee, S., Lee, K. C., 2009. Preparation and structural, biochemical, and pharmaceutical characterizations of bile acid-modified long-acting exendin-4 derivatives. J Med Chem. 52**,** 6889-96.

Sondhi, S., Castellano, J. M., Chong, V. Z., Rogoza, R. M., Skoblenick, K. J., Dyck, B. A., Gabriele, J., Thomas, N., Ki, K., Pristupa, Z. B., Singh, A. N., MacCrimmon, D., Voruganti, P., Foster, J., Mishra, R. K., 2006. cDNA array reveals increased expression of glucose-dependent insulinotropic polypeptide following chronic clozapine treatment: role in atypical antipsychotic drug-induced adverse metabolic effects. Pharmacogenomics J. 6**,** 131-40.

Song, D. H., Getty-Kaushik, L., Tseng, E., Simon, J., Corkey, B. E., Wolfe, M. M., 2007. Glucose-dependent insulinotropic polypeptide enhances adipocyte development and glucose uptake in part through Akt activation. Gastroenterology. 133**,** 1796-805.

Speliotes, E. K., Willer, C. J., Berndt, S. I., Monda, K. L., Thorleifsson, G., Jackson, A. U., Allen, H. L., Lindgren, C. M., Luan, J., Magi, R., Randall, J. C., Vedantam, S., Winkler, T. W., Qi, L., Workalemahu, T., Heid, I. M., Steinthorsdottir, V., Stringham, H. M., Weedon, M. N., Wheeler, E., Wood, A. R., Ferreira, T., Weyant, R. J., Segre, A. V., Estrada, K., Liang, L., Nemesh, J., Park, J. H., Gustafsson, S., Kilpelainen, T. O., Yang, J., Bouatia-Naji, N., Esko, T., Feitosa, M. F., Kutalik, Z., Mangino, M., Raychaudhuri, S., Scherag, A., Smith, A. V., Welch, R., Zhao, J. H., Aben, K. K., Absher, D. M., Amin, N., Dixon, A. L., Fisher, E., Glazer, N. L., Goddard, M. E., Heard-Costa, N. L., Hoesel, V., Hottenga, J. J., Johansson, A., Johnson, T., Ketkar, S., Lamina, C., Li, S., Moffatt, M. F., Myers, R. H., Narisu, N., Perry, J. R., Peters, M. J., Preuss, M., Ripatti, S., Rivadeneira, F., Sandholt, C., Scott, L. J., Timpson, N. J., Tyrer, J. P., van Wingerden, S., Watanabe, R. M., White, C. C., Wiklund, F., Barlassina, C., Chasman, D. I., Cooper, M. N., Jansson, J. O., Lawrence, R. W., Pellikka, N., Prokopenko, I., Shi, J., Thiering, E., Alavere, H., Alibrandi, M. T., Almgren, P., Arnold, A. M., Aspelund, T., Atwood, L. D., Balkau, B., Balmforth, A. J., Bennett, A. J., Ben-Shlomo, Y., Bergman, R. N., Bergmann, S., Biebermann, H., Blakemore, A. I., Boes, T., Bonnycastle, L. L., Bornstein, S. R., Brown, M. J., Buchanan, T. A., Busonero, F., Campbell, H., Cappuccio, F. P., Cavalcanti-Proenca, C., Chen, Y. D., Chen, C. M., Chines, P. S., Clarke, R., Coin, L., Connell, J., Day, I. N., Heijer, M., Duan, J., Ebrahim, S., Elliott, P., Elosua, R., Eiriksdottir, G., Erdos, M. R., Eriksson, J. G., Facheris, M. F., Felix, S. B., Fischer-Posovszky, P., Folsom, A. R., Friedrich, N., Freimer, N. B., Fu, M., Gaget, S., Gejman, P. V., Geus, E. J., Gieger, C., Gjesing, A. P., Goel, A., Goyette, P., Grallert, H., Grassler, J., Greenawalt, D. M., Groves, C. J., Gudnason, V., Guiducci, C., Hartikainen, A. L., Hassanali, N., Hall, A. S., Havulinna, A. S., Hayward, C., Heath, A. C., Hengstenberg, C., Hicks, A. A., Hinney, A., Hofman, A., Homuth, G., Hui, J., Igl, W., Iribarren, C., Isomaa, B., Jacobs, K. B., Jarick, I., Jewell, E., John, U., Jorgensen, T., Jousilahti, P., Jula, A., Kaakinen, M., Kajantie, E., Kaplan, L. M., Kathiresan, S., Kettunen, J., Kinnunen, L., Knowles, J. W., Kolcic, I., Konig, I. R., Koskinen, S., Kovacs, P., Kuusisto, J., Kraft, P., Kvaloy, K., Laitinen, J., Lantieri, O., Lanzani, C., Launer, L. J., Lecoeur, C., Lehtimaki, T., Lettre, G., Liu, J., Lokki, M. L., Lorentzon, M., Luben, R. N., Ludwig, B., Manunta, P., Marek,

D., Marre, M., Martin, N. G., McArdle, W. L., McCarthy, A., McKnight, B., Meitinger, T., Melander, O., Meyre, D., Midthjell, K., Montgomery, G. W., Morken, M. A., Morris, A. P., Mulic, R., Ngwa, J. S., Nelis, M., Neville, M. J., Nyholt, D. R., O'Donnell, C. J., O'Rahilly, S., Ong, K. K., Oostra, B., Pare, G., Parker, A. N., Perola, M., Pichler, I., Pietilainen, K. H., Platou, C. G., Polasek, O., Pouta, A., Rafelt, S., Raitakari, O., Rayner, N. W., Ridderstrale, M., Rief, W., Ruokonen, A., Robertson, N. R., Rzehak, P., Salomaa, V., Sanders, A. R., Sandhu, M. S., Sanna, S., Saramies, J., Savolainen, M. J., Scherag, S., Schipf, S., Schreiber, S., Schunkert, H., Silander, K., Sinisalo, J., Siscovick, D. S., Smit, J. H., Soranzo, N., Sovio, U., Stephens, J., Surakka, I., Swift, A. J., Tammesoo, M. L., Tardif, J. C., Teder-Laving, M., Teslovich, T. M., Thompson, J. R., Thomson, B., Tonjes, A., Tuomi, T., van Meurs, J. B., van Ommen, G. J., Vatin, V., Viikari, J., Visvikis-Siest, S., Vitart, V., Vogel, C. I., Voight, B. F., Waite, L. L., Wallaschofski, H., Walters, G. B., Widen, E., Wiegand, S., Wild, S. H., Willemsen, G., Witte, D. R., Witteman, J. C., Xu, J., Zhang, Q., Zgaga, L., Ziegler, A., Zitting, P., Beilby, J. P., Farooqi, I. S., Hebebrand, J., Huikuri, H. V., James, A. L., Kahonen, M., Levinson, D. F., Macciardi, F., Nieminen, M. S., Ohlsson, C., Palmer, L. J., Ridker, P. M., Stumvoll, M., Beckmann, J. S., Boeing, H., Boerwinkle, E., Boomsma, D. I., Caulfield, M. J., Chanock, S. J., Collins, F. S., Cupples, L. A., Smith, G. D., Erdmann, J., Froguel, P., Gronberg, H., Gyllensten, U., Hall, P., Hansen, T., Harris, T. B., Hattersley, A. T., Hayes, R. B., Heinrich, J., Hu, F. B., Hveem, K., Illig, T., Jarvelin, M. R., Kaprio, J., Karpe, F., Khaw, K. T., Kiemeney, L. A., Krude, H., Laakso, M., Lawlor, D. A., Metspalu, A., Munroe, P. B., Ouwehand, W. H., Pedersen, O., Penninx, B. W., Peters, A., Pramstaller, P. P., Quertermous, T., Reinehr, T., Rissanen, A., Rudan, I., Samani, N. J., Schwarz, P. E., Shuldiner, A. R., Spector, T. D., Tuomilehto, J., Uda, M., Uitterlinden, A., Valle, T. T., Wabitsch, M., Waeber, G., Wareham, N. J., Watkins, H., Wilson, J. F., Wright, A. F., Zillikens, M. C., Chatterjee, N., McCarroll, S. A., Purcell, S., Schadt, E. E., Visscher, P. M., Assimes, T. L., Borecki, I. B., Deloukas, P., Fox, C. S., Groop, L. C., Haritunians, T., Hunter, D. J., Kaplan, R. C., Mohlke, K. L., O'Connell, J. R., Peltonen, L., Schlessinger, D., Strachan, D. P., van Duijn, C. M., Wichmann, H. E., Frayling, T. M., Thorsteinsdottir, U., Abecasis, G. R., Barroso, I., Boehnke, M., Stefansson, K., North, K. E., McCarthy, M. I., Hirschhorn, J. N., Ingelsson, E., Loos, R. J., 2010. Association analyses of 249,796 individuals reveal 18 new loci associated with body mass index. Nat Genet. 42, 937-48.

St Onge, E. L., Miller, S. A., 2010. Albiglutide: a new GLP-1 analog for the treatment of type 2 diabetes. Expert Opin Biol Ther. 10**,** 801-6.

Stoffel, M., Espinosa, R., 3rd, Le Beau, M. M., Bell, G. I., 1993. Human glucagon-like peptide-1 receptor gene. Localization to chromosome band 6p21 by fluorescence in situ hybridization and linkage of a highly polymorphic simple tandem repeat DNA polymorphism to other markers on chromosome 6. Diabetes. 42**,** 1215-8.

Stoffers, D. A., Desai, B. M., DeLeon, D. D., Simmons, R. A., 2003. Neonatal exendin-4 prevents the development of diabetes in the intrauterine growth retarded rat. Diabetes. 52**,** 734-40.

Straub, S. G., Sharp, G. W., 1996. Glucose-dependent insulinotropic polypeptide stimulates insulin secretion via increased cyclic AMP and [Ca2+]1 and a wortmannin-sensitive signalling pathway. Biochem Biophys Res Commun. 224**,** 369-74.

Su, H., He, M., Li, H., Liu, Q., Wang, J., Wang, Y., Gao, W., Zhou, L., Liao, J., Young, A. A., Wang, M. W., 2008. Boc5, a non-peptidic glucagon-like Peptide-1 receptor agonist, invokes sustained glycemic control and weight loss in diabetic mice. PLoS One. 3**,** e2892.

Sun, C., Song, D., Davis-Taber, R. A., Barrett, L. W., Scott, V. E., Richardson, P. L., Pereda-Lopez, A., Uchic, M. E., Solomon, L. R., Lake, M. R., Walter, K. A., Hajduk, P. J., Olejniczak, E. T., 2007. Solution structure and mutational analysis of pituitary adenylate cyclase-activating polypeptide binding to the extracellular domain of PAC1-RS. Proc Natl Acad Sci U S A. 104**,** 7875-80.

Sykes, S., Morgan, L. M., English, J., Marks, V., 1980. Evidence for preferential stimulation of gastric inhibitory polypeptide secretion in the rat by actively transported carbohydrates and their analogues. J Endocrinol. 85**,** 201-7.

Tahrani, A. A., Piya, M. K., Kennedy, A., Barnett, A. H., 2010. Glycaemic control in type 2 diabetes: targets and new therapies. Pharmacol Ther. 125**,** 328-61.

Takeda, J., Seino, Y., Tanaka, K., Fukumoto, H., Kayano, T., Takahashi, H., Mitani, T., Kurono, M., Suzuki, T., Tobe, T., et al., 1987. Sequence of an intestinal cDNA encoding human gastric inhibitory polypeptide precursor. Proc Natl Acad Sci U S A. 84**,** 7005-8.

Teng, M., Johnson, M. D., Thomas, C., Kiel, D., Lakis, J. N., Kercher, T., Aytes, S., Kostrowicki, J., Bhumralkar, D., Truesdale, L., May, J., Sidelman, U., Kodra, J. T., Jorgensen, A. S., Olesen, P. H., de Jong, J. C., Madsen, P., Behrens, C., Pettersson, I., Knudsen, L. B., Holst, J. J., Lau, J., 2007. Small molecule ago-allosteric modulators of

the human glucagon-like peptide-1 (hGLP-1) receptor. Bioorg Med Chem Lett. 17, 5472-8.

Tews, D., Werner, U., Eckel, J., 2008. Enhanced protection against cytokine- and fatty acid-induced apoptosis in pancreatic beta cells by combined treatment with glucagon-like peptide-1 receptor agonists and insulin analogues. Horm Metab Res. 40, 172-80.

Theodorakis, M. J., Carlson, O., Michopoulos, S., Doyle, M. E., Juhaszova, M., Petraki, K., Egan, J. M., 2006. Human duodenal enteroendocrine cells: source of both incretin peptides, GLP-1 and GIP. Am J Physiol Endocrinol Metab. 290, E550-9.

Thorens, B., 1992. Expression cloning of the pancreatic beta cell receptor for the gluco-incretin hormone glucagon-like peptide 1. Proc Natl Acad Sci U S A. 89, 8641-5.

Thorens, B., Deriaz, N., Bosco, D., DeVos, A., Pipeleers, D., Schuit, F., Meda, P., Porret, A., 1996. Protein kinase A-dependent phosphorylation of GLUT2 in pancreatic beta cells. J Biol Chem. 271, 8075-81.

Thorens, B., Porret, A., Buhler, L., Deng, S. P., Morel, P., Widmann, C., 1993. Cloning and functional expression of the human islet GLP-1 receptor. Demonstration that exendin-4 is an agonist and exendin-(9-39) an antagonist of the receptor. Diabetes. 42, 1678-82.

Thorens, B., Widmann, C., Structure and function of the glucagon-like peptide-1 receptor. In: P. J. Lefebvre, (Ed.), Handbook of Experimental Pharmacology Glucagon III. Springer-Verlag, Berlin, 1996, pp. 255-273.

Thorkildsen, C., Neve, S., Larsen, B. D., Meier, E., Petersen, J. S., 2003. Glucagon-like peptide 1 receptor agonist ZP10A increases insulin mRNA expression and prevents diabetic progression in db/db mice. J Pharmacol Exp Ther. 307, 490-6.

Tibaduiza, E. C., Chen, C., Beinborn, M., 2001. A small molecule ligand of the glucagon-like peptide 1 receptor targets its amino-terminal hormone binding domain. J Biol Chem. 276, 37787-93.

Tokuyama, Y., Matsui, K., Egashira, T., Nozaki, O., Ishizuka, T., Kanatsuka, A., 2004. Five missense mutations in glucagon-like peptide 1 receptor gene in Japanese population. Diabetes Res Clin Pract. 66, 63-9.

Tomas, E., Habener, J. F., 2010. Insulin-like actions of glucagon-like peptide-1: a dual receptor hypothesis. Trends Endocrinol Metab. 21, 59-67.

Tomas, E., Stanojevic, V., Habener, J. F., 2011a. GLP-1-derived nonapeptide GLP-1(28-36)amide targets to mitochondria and suppresses glucose production and oxidative stress in isolated mouse hepatocytes. Regul Pept. 167, 177-84.

Tomas, E., Wood, J. A., Stanojevic, V., Habener, J. F., 2011b. Glucagon-like peptide-1(9-36)amide metabolite inhibits weight gain and attenuates diabetes and hepatic steatosis in diet-induced obese mice. Diabetes Obes Metab. 13**,** 26-33.

Tornehave, D., Kristensen, P., Romer, J., Knudsen, L. B., Heller, R. S., 2008. Expression of the GLP-1 receptor in mouse, rat, and human pancreas. J Histochem Cytochem. 56**,** 841-51.

Tourrel, C., Bailbe, D., Lacorne, M., Meile, M. J., Kergoat, M., Portha, B., 2002. Persistent improvement of type 2 diabetes in the Goto-Kakizaki rat model by expansion of the beta-cell mass during the prediabetic period with glucagon-like peptide-1 or exendin-4. Diabetes. 51**,** 1443-52.

Tourrel, C., Bailbe, D., Meile, M. J., Kergoat, M., Portha, B., 2001. Glucagon-like peptide-1 and exendin-4 stimulate beta-cell neogenesis in streptozotocin-treated newborn rats resulting in persistently improved glucose homeostasis at adult age. Diabetes. 50**,** 1562-70.

Townsend, E., Moni, R., Quinn, R., Parsons, P. G., 1992. Reversible depigmentation of human melanoma cells by halistanol trisulphate, a novel marine sterol. Melanoma Res. 1**,** 349-57.

Trumper, A., Trumper, K., Horsch, D., 2002. Mechanisms of mitogenic and anti-apoptotic signaling by glucose-dependent insulinotropic polypeptide in beta(INS-1)-cells. J Endocrinol. 174**,** 233-46.

Trumper, A., Trumper, K., Trusheim, H., Arnold, R., Goke, B., Horsch, D., 2001. Glucose-dependent insulinotropic polypeptide is a growth factor for beta (INS-1) cells by pleiotropic signaling. Mol Endocrinol. 15**,** 1559-70.

Tseng, C. C., Boylan, M. O., Jarboe, L. A., Williams, E. K., Sunday, M. E., Wolfe, M. M., 1995. Glucose-dependent insulinotropic peptide (GIP) gene expression in the rat salivary gland. Mol Cell Endocrinol. 115**,** 13-9.

Tseng, C. C., Jarboe, L. A., Landau, S. B., Williams, E. K., Wolfe, M. M., 1993. Glucose-dependent insulinotropic peptide: structure of the precursor and tissue-specific expression in rat. Proc Natl Acad Sci U S A. 90**,** 1992-6.

Tseng, C. C., Jarboe, L. A., Wolfe, M. M., 1994. Regulation of glucose-dependent insulinotropic peptide gene expression by a glucose meal. Am J Physiol. 266**,** G887-91.

Tseng, C. C., Kieffer, T. J., Jarboe, L. A., Usdin, T. B., Wolfe, M. M., 1996. Postprandial stimulation of insulin release by glucose-dependent insulinotropic polypeptide (GIP). Effect of a specific glucose-dependent insulinotropic polypeptide receptor antagonist in the rat. J Clin Invest. 98**,** 2440-5.

Tseng, C. C., Zhang, X. Y., 1998a. The cysteine of the cytoplasmic tail of glucose-dependent insulinotropic peptide receptor mediates its chronic desensitization and down-regulation. Mol Cell Endocrinol. 139**,** 179-86.

Tseng, C. C., Zhang, X. Y., 1998b. Role of regulator of G protein signaling in desensitization of the glucose-dependent insulinotropic peptide receptor. Endocrinology. 139**,** 4470-5.

Tseng, C. C., Zhang, X. Y., 2000. Role of G protein-coupled receptor kinases in glucose-dependent insulinotropic polypeptide receptor signaling. Endocrinology. 141**,** 947-52.

Tsukiyama, K., Yamada, Y., Yamada, C., Harada, N., Kawasaki, Y., Ogura, M., Bessho, K., Li, M., Amizuka, N., Sato, M., Udagawa, N., Takahashi, N., Tanaka, K., Oiso, Y., Seino, Y., 2006. Gastric inhibitory polypeptide as an endogenous factor promoting new bone formation after food ingestion. Mol Endocrinol. 20**,** 1644-51.

U.S._Food_and_Drug_Administration, FDA Approves New Treatment for Diabetes. Vol. 2011, 2006.

U.S._Food_and_Drug_Administration, FDA Approves New Drug Treatment for Type 2 Diabetes. Vol. 2011, 2009.

Ugleholdt, R., Poulsen, M. L., Holst, P. J., Irminger, J. C., Orskov, C., Pedersen, J., Rosenkilde, M. M., Zhu, X., Steiner, D. F., Holst, J. J., 2006. Prohormone convertase 1/3 is essential for processing of the glucose-dependent insulinotropic polypeptide precursor. J Biol Chem. 281**,** 11050-7.

Ugleholdt, R., Zhu, X., Deacon, C. F., Orskov, C., Steiner, D. F., Holst, J. J., 2004. Impaired intestinal proglucagon processing in mice lacking prohormone convertase 1. Endocrinology. 145**,** 1349-55.

UKPDS, 1995. U.K. prospective diabetes study 16. Overview of 6 years' therapy of type II diabetes: a progressive disease. U.K. Prospective Diabetes Study Group. Diabetes. 44**,** 1249-58.

Unger, R. H., Eisentraut, A. M., 1969. Entero-insular axis. Arch Intern Med. 123**,** 261-6.

Unger, R. H., Orci, L., 1975. The essential role of glucagon in the pathogenesis of diabetes mellitus. Lancet. 1**,** 14-6.

Unger, R. H., Scherer, P. E., 2010. Gluttony, sloth and the metabolic syndrome: a roadmap to lipotoxicity. Trends Endocrinol Metab. 21**,** 345-52.

Unniappan, S., McIntosh, C. H., Demuth, H. U., Heiser, U., Wolf, R., Kieffer, T. J., 2006. Effects of dipeptidyl peptidase IV on the satiety actions of peptide YY. Diabetologia. 49**,** 1915-23.

Usdin, T. B., Mezey, E., Button, D. C., Brownstein, M. J., Bonner, T. I., 1993. Gastric inhibitory polypeptide receptor, a member of the secretin-vasoactive intestinal peptide receptor family, is widely distributed in peripheral organs and the brain. Endocrinology. 133, 2861-70.

Usellini, L., Capella, C., Solcia, E., Buchan, A. M., Brown, J. C., 1984. Ultrastructural localization of gastric inhibitory polypeptide (GIP) in a well characterized endocrine cell of canine duodenal mucosa. Histochemistry. 80, 85-9.

van Eyll, B., Lankat-Buttgereit, B., Bode, H. P., Goke, R., Goke, B., 1994. Signal transduction of the GLP-1-receptor cloned from a human insulinoma. FEBS Lett. 348, 7-13.

Van Ginneken, C., Weyns, A., 2004. A stereological evaluation of secretin and gastric inhibitory peptide-containing mucosal cells of the perinatal small intestine of the pig. J Anat. 205, 267-75.

Varner, A. A., Isenberg, J. I., Elashoff, J. D., Lamers, C. B., Maxwell, V., Shulkes, A. A., 1980. Effect of intravenous lipid on gastric acid secretion stimulated by intravenous amino acids. Gastroenterology. 79, 873-6.

Vassallo, G., Solcia, E., Capella, C., 1969. Light and electron microscopic identification of several types of endocrine cells in the gastrointestinal mucosa of the cat. Z Zellforsch Mikrosk Anat. 98, 333-56.

Vazquez, P., Roncero, I., Blazquez, E., Alvarez, E., 2005. Substitution of the cysteine 438 residue in the cytoplasmic tail of the glucagon-like peptide-1 receptor alters signal transduction activity. J Endocrinol. 185, 35-44.

Verdonk, C. A., Rizza, R. A., Nelson, R. L., Go, V. L., Gerich, J. E., Service, F. J., 1980. Interaction of fat-stimulated gastric inhibitory polypeptide on pancreatic alpha and beta cell function. J Clin Invest. 65, 1119-25.

Verspohl, E. J., 2009. Novel therapeutics for type 2 diabetes: incretin hormone mimetics (glucagon-like peptide-1 receptor agonists) and dipeptidyl peptidase-4 inhibitors. Pharmacol Ther. 124, 113-38.

Villareal, D. T., Robertson, H., Bell, G. I., Patterson, B. W., Tran, H., Wice, B., Polonsky, K. S., 2010. TCF7L2 variant rs7903146 affects the risk of type 2 diabetes by modulating incretin action. Diabetes. 59, 479-85.

Villhauer, E. B., Brinkman, J. A., Naderi, G. B., Burkey, B. F., Dunning, B. E., Prasad, K., Mangold, B. L., Russell, M. E., Hughes, T. E., 2003. 1-[[(3-hydroxy-1-adamantyl)amino]acetyl]-2-cyano-(S)-pyrrolidine: a potent, selective, and orally

bioavailable dipeptidyl peptidase IV inhibitor with antihyperglycemic properties. J Med Chem. 46, 2774-89.

Vilsboll, T., Agerso, H., Krarup, T., Holst, J. J., 2003. Similar elimination rates of glucagon-like peptide-1 in obese type 2 diabetic patients and healthy subjects. J Clin Endocrinol Metab. 88, 220-4.

Vilsboll, T., Krarup, T., Deacon, C. F., Madsbad, S., Holst, J. J., 2001. Reduced postprandial concentrations of intact biologically active glucagon-like peptide 1 in type 2 diabetic patients. Diabetes. 50, 609-13.

Volz, A., Goke, R., Lankat-Buttgereit, B., Fehmann, H. C., Bode, H. P., Goke, B., 1995. Molecular cloning, functional expression, and signal transduction of the GIP-receptor cloned from a human insulinoma. FEBS Lett. 373, 23-9.

Wahl, M. A., Plehn, R. J., Landsbeck, E. A., Verspohl, E. J., Ammon, H. P., 1992. Are ionic fluxes of pancreatic beta cells a target for gastric inhibitory polypeptide? Mol Cell Endocrinol. 90, 117-23.

Wang, M., Matheson, S., Picard, J., Pezzullo, J., 2009. PC-DACTM:Exendin-4 (CJC-1134-PC) Significantly Reduces HbA1c and Body Weight as an Adjunct Therapy to Metformin: Tow Randomized , Double-Blind, Placebo-Controlled, 12 Week, Phase II Studies in Patients with Type 2 Diabetes Mellitus. Diabetes. 58, Abastrct 553-P.

Wang, Q., Brubaker, P. L., 2002. Glucagon-like peptide-1 treatment delays the onset of diabetes in 8 week-old db/db mice. Diabetologia. 45, 1263-73.

Wang, X., Cahill, C. M., Pineyro, M. A., Zhou, J., Doyle, M. E., Egan, J. M., 1999. Glucagon-like peptide-1 regulates the beta cell transcription factor, PDX-1, in insulinoma cells. Endocrinology. 140, 4904-7.

Wang, Y., Montrose-Rafizadeh, C., Adams, L., Raygada, M., Nadiv, O., Egan, J. M., 1996. GIP regulates glucose transporters, hexokinases, and glucose-induced insulin secretion in RIN 1046-38 cells. Mol Cell Endocrinol. 116, 81-7.

Wang, Z., Wang, R. M., Owji, A. A., Smith, D. M., Ghatei, M. A., Bloom, S. R., 1995. Glucagon-like peptide-1 is a physiological incretin in rat. J Clin Invest. 95, 417-21.

Wasada, T., McCorkle, K., Harris, V., Kawai, K., Howard, B., Unger, R. H., 1981. Effect of gastric inhibitory polypeptide on plasma levels of chylomicron triglycerides in dogs. J Clin Invest. 68, 1106-7.

Wei, Y., Mojsov, S., 1995. Tissue-specific expression of the human receptor for glucagon-like peptide-I: brain, heart and pancreatic forms have the same deduced amino acid sequences. FEBS Lett. 358**,** 219-24.

Weir, G. C., Mojsov, S., Hendrick, G. K., Habener, J. F., 1989. Glucagonlike peptide I (7-37) actions on endocrine pancreas. Diabetes. 38**,** 338-42.

Werner, U., Gerlach, M., Hofmann, M., Herling, A. W., 2006. Treatment of obese Zucker diabetic fatty rats with novel GLP-1 receptor agonist AVE0010 improves oral glucose tolerance and glycaemic control without risk of hypoglycemia [Abstract]. Diabetologia. 49 (Suppl 1)**,** 398-9.

Werner, U., Haschke, G., Herling, A. W., Kramer, W., 2010. Pharmacological profile of lixisenatide: A new GLP-1 receptor agonist for the treatment of type 2 diabetes. Regul Pept. in press.

Werner, U., Vanderwalle, B., Kerr Conte, J., Pattou, F., Pruniaux, M., Herling, A. W., 2008. The GLP-1 receptor agonist AVE0010 improves GSIS, prevents lipotoxicity-induced insulin depletion and preserves beta-cell function in human pancreatic islets [Abstract]. Diabetes. 57**,** 3-4.

Wettergren, A., Pridal, L., Wojdemann, M., Holst, J. J., 1998. Amidated and non-amidated glucagon-like peptide-1 (GLP-1): non-pancreatic effects (cephalic phase acid secretion) and stability in plasma in humans. Regul Pept. 77**,** 83-7.

Wheeler, M. B., Gelling, R. W., Hinke, S. A., Tu, B., Pederson, R. A., Lynn, F., Ehses, J., McIntosh, C. H., 1999. Characterization of the carboxyl-terminal domain of the rat glucose-dependent insulinotropic polypeptide (GIP) receptor. A role for serines 426 and 427 in regulating the rate of internalization. J Biol Chem. 274**,** 24593-601.

Wheeler, M. B., Gelling, R. W., McIntosh, C. H., Georgiou, J., Brown, J. C., Pederson, R. A., 1995. Functional expression of the rat pancreatic islet glucose-dependent insulinotropic polypeptide receptor: ligand binding and intracellular signaling properties. Endocrinology. 136**,** 4629-39.

Wicki, A., Wild, D., Storch, D., Seemayer, C., Gotthardt, M., Behe, M., Kneifel, S., Mihatsch, M. J., Reubi, J. C., Macke, H. R., Christofori, G., 2007. [Lys40(Ahx-DTPA-111In)NH2]-Exendin-4 is a highly efficient radiotherapeutic for glucagon-like peptide-1 receptor-targeted therapy for insulinoma. Clin Cancer Res. 13**,** 3696-705.

Wideman, R. D., Kieffer, T. J., 2009. Mining incretin hormone pathways for novel therapies. Trends Endocrinol Metab. 20**,** 280-6.

Wideman, R. D., Yu, I. L., Webber, T. D., Verchere, C. B., Johnson, J. D., Cheung, A. T., Kieffer, T. J., 2006. Improving function and survival of pancreatic islets by endogenous production of glucagon-like peptide 1 (GLP-1). Proc Natl Acad Sci U S A. 103, 13468-73.

Widenmaier, S., Kim, S. J., Yang, G. K., De Los Reyes, T., Nian, C., Asadi, A., Seino, Y., Kieffer, T. J., Kwok, Y. N., McIntosh, C. H., 2010. A GIP receptor agonist exhibits beta-cell anti-apoptotic actions in rat models of diabetes resulting in improved beta-cell function and glycemic control. PLoS One. in press.

Wildhage, I., Trusheim, H., Goke, B., Lankat-Buttgereit, B., 1999. Gene expression of the human glucagon-like peptide-1 receptor is regulated by Sp1 and Sp3. Endocrinology. 140, 624-31.

Wolfe, M. M., Hocking, M. P., Maico, D. G., McGuigan, J. E., 1983. Effects of antibodies to gastric inhibitory peptide on gastric acid secretion and gastrin release in the dog. Gastroenterology. 84, 941-8.

Xie, D., Cheng, H., Hamrick, M., Zhong, Q., Ding, K. H., Correa, D., Williams, S., Mulloy, A., Bollag, W., Bollag, R. J., Runner, R. R., McPherson, J. C., Insogna, K., Isales, C. M., 2005. Glucose-dependent insulinotropic polypeptide receptor knockout mice have altered bone turnover. Bone. 37, 759-69.

Xie, D., Zhong, Q., Ding, K. H., Cheng, H., Williams, S., Correa, D., Bollag, W. B., Bollag, R. J., Insogna, K., Troiano, N., Coady, C., Hamrick, M., Isales, C. M., 2007. Glucose-dependent insulinotropic peptide-overexpressing transgenic mice have increased bone mass. Bone. 40, 1352-60.

Xu, G., Kaneto, H., Laybutt, D. R., Duvivier-Kali, V. F., Trivedi, N., Suzuma, K., King, G. L., Weir, G. C., Bonner-Weir, S., 2007. Downregulation of GLP-1 and GIP receptor expression by hyperglycemia: possible contribution to impaired incretin effects in diabetes. Diabetes. 56, 1551-8.

Xu, G., Stoffers, D. A., Habener, J. F., Bonner-Weir, S., 1999. Exendin-4 stimulates both beta-cell replication and neogenesis, resulting in increased beta-cell mass and improved glucose tolerance in diabetic rats. Diabetes. 48, 2270-6.

Yach, D., Stuckler, D., Brownell, K. D., 2006. Epidemiologic and economic consequences of the global epidemics of obesity and diabetes. Nat Med. 12, 62-6.

Yamada, Y., Hayami, T., Nakamura, K., Kaisaki, P. J., Someya, Y., Wang, C. Z., Seino, S., Seino, Y., 1995. Human gastric inhibitory polypeptide receptor: cloning of the gene (GIPR) and cDNA. Genomics. 29**,** 773-6.

Yang, S. W., Buivich, A., Chan, T. M., Smith, M., Lachowicz, J., Pomponi, S. A., Wright, A. E., Mierzwa, R., Patel, M., Gullo, V., Chu, M., 2003. A new sterol sulfate, Sch 572423, from a marine sponge, Topsentia sp. Bioorg Med Chem Lett. 13**,** 1791-4.

Yip, R. G., Boylan, M. O., Kieffer, T. J., Wolfe, M. M., 1998. Functional GIP receptors are present on adipocytes. Endocrinology. 139**,** 4004-7.

Yip, R. G., Wolfe, M. M., 2000. GIP biology and fat metabolism. Life Sci. 66**,** 91-103.

Youn, Y. S., Jung, J. Y., Oh, S. H., Yoo, S. D., Lee, K. C., 2006. Improved intestinal delivery of salmon calcitonin by Lys18-amine specific PEGylation: stability, permeability, pharmacokinetic behavior and in vivo hypocalcemic efficacy. J Control Release. 114**,** 334-42.

Young, A. A., Gedulin, B. R., Bhavsar, S., Bodkin, N., Jodka, C., Hansen, B., Denaro, M., 1999. Glucose-lowering and insulin-sensitizing actions of exendin-4: studies in obese diabetic (ob/ob, db/db) mice, diabetic fatty Zucker rats, and diabetic rhesus monkeys (Macaca mulatta). Diabetes. 48**,** 1026-34.

Yusta, B., Baggio, L. L., Estall, J. L., Koehler, J. A., Holland, D. P., Li, H., Pipeleers, D., Ling, Z., Drucker, D. J., 2006. GLP-1 receptor activation improves beta cell function and survival following induction of endoplasmic reticulum stress. Cell Metab. 4**,** 391-406.

Zander, M., Madsbad, S., Madsen, J. L., Holst, J. J., 2002. Effect of 6-week course of glucagon-like peptide 1 on glycaemic control, insulin sensitivity, and beta-cell function in type 2 diabetes: a parallel-group study. Lancet. 359**,** 824-30.

Zhong, Q., Itokawa, T., Sridhar, S., Ding, K. H., Xie, D., Kang, B., Bollag, W. B., Bollag, R. J., Hamrick, M., Insogna, K., Isales, C. M., 2007. Effects of glucose-dependent insulinotropic peptide on osteoclast function. Am J Physiol Endocrinol Metab. 292**,** E543-8.

Zhou, J., Cai, Z. H., Li, L., Kou, C., Gao, Y. F., 2009. Preparation and PEGylation of exendin-4 peptide secreted from yeast Pichia pastoris. Eur J Pharm Biopharm.

Zhou, J., Roane, D. S., Xi, X., Bogacka, I., Li, B., Ryan, D. H., Martin, R. J., 2003. Short-term food restriction and refeeding alter expression of genes likely involved in brain glucosensing. Exp Biol Med (Maywood). 228**,** 943-50.

Zhu, X., Zhou, A., Dey, A., Norrbom, C., Carroll, R., Zhang, C., Laurent, V., Lindberg, I., Ugleholdt, R., Holst, J. J., Steiner, D. F., 2002. Disruption of PC1/3 expression in mice causes dwarfism and multiple neuroendocrine peptide processing defects. Proc Natl Acad Sci U S A. 99, 10293-8.

Zinman, B., Hoogwerf, B. J., Duran Garcia, S., Milton, D. R., Giaconia, J. M., Kim, D. D., Trautmann, M. E., Brodows, R. G., 2007. The effect of adding exenatide to a thiazolidinedione in suboptimally controlled type 2 diabetes: a randomized trial. Ann Intern Med. 146, 477-85.